EFFECT OF BOUNDARY FORM ON FINE SAND TRANSPORT IN TWELVE-INCH PIPES

By

A. R. Chamberlain

Department of Civil Engineering

Colorado Agricultural and Mechanical College
Fort Collins, Colorado

June 1955

CER No. 55ARC6

FOREWORD

The work reported herein was conducted under a program receiving financial support from Armco Drainage and Metal Products, Inc., Middletown, Ohio and from the Research Corporation, Santa Monico, California. A. R. Chamberlain was the principal investigator and the studies resulted in a dissertation leading to the degree of Ph D in Irrigation Engineering. In his graduate endeavor, Dr. Chamberlain was supported personally by a scholarship from the Tau Beta Pi Association, Knoxville, Tennessee.

Since the dissertation fully reports and discusses the results of the research, it will serve the additional purpose of a final report to those sponsoring the project and to others interested.

ACKNOWLEDGMENT

The writer wishes to express his appreciation to the faculty members of Colorado Agricultural and Mechanical College, Fort Collins, Colorado, who made up the Committee on Research and Dissertation. Special mention is due Maurice L. Albertson, Director of Fluid Mechanics Research and Professor of Civil Engineering, who was major professor and under whom the research was conducted, and Dean F. Peterson, Jr., Head of Department of Civil Engineering for their continuous support and many ideas during the course of the study. The other committee members are T. H. Evans, Dean of the School of Engineering, Robert Whitney, Professor of Agronomy, Saul Basri, Assistant Professor of Physics, and Robert Butz, Assistant Professor of Mathematics.

Several organizations provided the financial support without which this research would not have been possible. These are:

Armco Drainage and Metal Products, Inc.
Middletown, Ohio,

Research Corporation
Santa Monica, California,

Tau Beta Pi Association
Knoxville, Tennessee.

Others who helped in various respects are, J. R. Barton, Assistant Professor of Civil Engineering, D. L. Bender, and R. J. Garde, Graduate Assistants.

The co-operation of the Hydraulics Laboratory and office personnel, Department of Civil Engineering, helped throughout this study.

ACKNOWLEDGMENT - Continued

Valuable assistance by the wife of the writer, Virginia Chamberlain, in taking data, computation and typing is also gratefully acknowledged.

NOTE BY THE DEAN OF ENGINEERING

This dissertation, by A.R. Chamberlain, is the first produced under the Doctorate program in Engineering, which was the first such program inaugurated at the Colorado A and M College.

TABLE OF CONTENTS

TABLE OF CONTENTS --Continued

LIST OF FIGURES

LIST OF FIGURES --Continued

Chapter I

INTRODUCTION

Sediment has been an important problem for several thousand years. Even the rise and fall of civilizations have sometimes been attributed to the effects of sediment. The sediment-filled canals of the once fertile Tigris and Euphrates rivers region, and the southwestern section of the United States are examples.

Definition of Sediment

Before proceeding further, the term sediment will be defined A dictionary definition is: "Fragmental material transported by, suspended in, or deposited by water or air, or accumulated in beds by other natural agents; any detrital accumulation, such as loess".

Some examples satisfying the definition are: sand being transported by water; sand or snow being carried by wind; and fruits, vegetables or other commercial products being conveyed by some fluid medium. The former, that of sand being transported by water, is the case studied herein.

Sediment Problems

Hydraulic problems involving sediment can arbitrarily be divided into two types. One type is associated with the hydraulics of naturally formed open channels, and the complementary problem is that of transport within rigid boundary conduits. The basic inner mechanism of transport must necessarily be the same in either case. However, the effect of rigid boundaries and the differences in economic considerations separate the water course and rigid channel problems.

In the study and application of sediment mechanics to natural channels the boundary form can seldom be controlled; it is determined by the variables describing the flow, the fluid, and the material being transported. Economic considerations are, in general, directed toward inducing a stable channel at the least possible cost.

Rigid boundary conduits are similar to natural channels in many respects, the most obvious being a pipe in free-flow regime. The difference between them is their relative versatility. Conduits can be designed to flow free, flow full, up and down hills, operate under pressure, and to work under practically any other conditions required by the specific task the boundary must perform.

This dissertation is concerned with rigid boundary conduits.

Economic Application of Rigid Boundary Sediment Transport

One application of rigid boundary sediment transport which has been before the ever-interested eye of the public is gold mining. In the early days of gold mining, water was conveyed to a cradle or other vibratory device, and the less dense unwanted sediment was transported by the water to a spoil area. In recent years essentially the same process is used in dredge or placer mining, except that water is also used to convey ore to the separating equipment.

Another process utilizing sediment mechanics is that of refining oil. Modern refining technology makes use of a fluidized bed of catalytic material. The fluidization process gives rise to a problem in sediment mechanics. In some cases the catalyst also goes through a pipeline recirculation system.

Storm sewers are often required to convey tremendous quantities of sand, rock and detrital material. These sewers usually do not flow full, and hence they are a good example of a rigid conduit with free-flow.

Hydraulic dredging of river channels has been going on for over fifty years. The dredge pumps sediment and water from the river bed or banks and frequently conveys the mixture through pipelines to a spoil area.

Coal and ore transport pipelines operating under pressure are receiving more attention each year. Various United States and European commercial companies have been experimenting with this method for several years.

The food processing industry has been, and is doing more, moving of vegetables, fruits and processing refuse by hydraulic means. Both open and closed conduits are used.

Many more examples of the economic applications of rigid boundary sediment mechanics could be cited. However, the above are sufficient to illustrate possible fields where the results of research are needed and can be applied.

Variables Involved

Variables entering a practical problem include: 1) economic factors, such as a market, 2) physical conditions, topography being an example, 3) mechanics of sediment transport. The latter category is the one of principal interest in this dissertation.

The important variables in the mechanics of transport can be classified into four groups. These are: 1) fluid, 2) flow, 3) sediment, and 4) geometry.

The independent fluid variables are, in most practical application, two in number. They are the dynamic viscosity and the mass density of the fluid. The two fluids used almost exclusively are water and air. There exist many data using these two fluids, under all sorts of combinations of the variables characterizing the fluid. The chemical behavior of the fluid is also sometimes important.

Flow variables differ considerably depending on the problem being examined. The most common are the hydraulic gradient, the mean velocity and local velocity. All of these receive attention in any research or design problem. The yield strength is sometimes important in fluid-sediment systems which exhibit characteristics of plastics.

Sediment variables are mass density, mineralogical composition, chemical activity, shape, texture, and size distribution. All are important. This is an impressive list, most of the items of which have been studied only slightly. Mass density, size distribution and shape have been examined quite closely, and with some success. Mineralogical composition, chemical activity, and texture have been considered by the geologist more than by the engineer.

Geometric variables constitute a description of the boundary within which the sediment-fluid complex is conveyed. For example, one group of length parameters are required in order to specify a trapezoidal channel; a different group is required to specify a circular conduit. In addition to these, however, the boundary needs a local characterization, for example, height of the roughness, frequency of roughness and any other appropriate geometric variable.

Summary of Previous Work

Circular conduits, a special case of rigid boundaries are the only type considered in this dissertation. For centuries engineers have been working to achieve smoother pipes and to reduce mechanical energy losses due to the generation of heat induced by the rough boundaries. In the last half century, however, efforts have been made to introduce artificial roughnesses of a very special type, designed for the job of more effectively transporting a specific sediment. Some of these special roughness types are the prime interest of this dissertation.

Delimitation of Study

Boundary form was the basic variable whose effect on mechanics of sediment transport was studied. Three cases were considered: 1) a geometrically smooth pipe, 2) a corrugated pipe made from steel sheets, and 3) a Hel-Cor type of pipe formed by rollers from coils of steel. All these had a nominal diameter of 12-in.

Clear water was the continuous phase of the sediment-fluid mixture. The pipe was flowing full at all times and only the case of suspended transport was considered. One size of sediment was employed. This sediment was a fine sand with a median sieve diameter of 0.20 mm.

Statement of Problem

Subject to the limitations of the three boundary forms, the one fine-sand sediment, the range of fully-suspended sediment transport, and the pipes flowing full, the problem proposed was that of finding answers to the following questions:

1. What are the interrelationships between boundary form, rate of energy dissipation, discharge of sediment-fluid mixture, and discharge of sediment?
2. What are the effects of the boundary form on the local mechanism of suspended sediment transport?

Answers to question one will give a clear picture of how the boundary form affects the parameters which are important in practical design problems. Question two is a study of the small scale mechanism of sediment transfer, and is important in explaining how the material is transported, thus providing additional information which can lead to development of more efficient artificial boundary roughness.

Chapter II

REVIEW OF LITERATURE

Analysis of the effect of boundary form on the pipeline transport of fine sand by water necessitates reviewing and summarizing earlier work on sediment transport. In order to obtain a clear picture of the interaction of the many variables which might enter the problem, the following review covers a very large number of sediments, velocities and pipes. Two continuous phases, air and water, are reported. Nearly all the papers are concerned with the one-dimensional flow pattern and only qualitative observations are made on the mode of transport. No acceptable theoretical development has been presented for more than a very narrow range of variables.

The review has been divided into several sections. These are: boundary form studies, laminar transport by water, turbulent transport by water, turbulent conveyance by air, installed plants and their design, miscellaneous items and summary. The miscellaneous category covers papers on instrumentation, as an example.

Boundary Form Studies

The papers reviewed in this section cover the effects of rifling on sediment transport, the mechanics of transport in a square pipe, the factors that enter a study of artificial roughness in pipes, some observations on flow over corrugated surfaces, and the effect on the resistance coefficient f of using combinations of artificial roughness.

Howard (27) presented, in 1941, one of the few papers on a large artificial roughness placed in a pipe for the purpose of improving sediment carrying capacity. In order to determine optimum rifling, head loss tests were run on a 4-in. 20-gage steel pipe line, carrying water and 0.39-mm sand from the Pearl River. It was determined that the length of rifling should be 1/3 the pipe length. One of the best riflings consisted of the above length, with 3 riflings spaced at 120 degrees around the pipe and having a pitch of 10 diameters. The roughness height was $D/8$, where D is the pipe diameter.

A similar rifling was installed in a 2-in. pipe and tests made with the same sand. It was hoped that in this manner a design could be made for pipes of 30 to 32 in.

Using the above optimum rifling, head loss tests were made using 0.023-mm silt and 2.48-mm pea gravel.

The conclusion was reached that rifling will increase the efficiency of plants pumping coarse sand and gravel, for the range of velocities customarily used, but will decrease it for silt and clay; i.e., efficiency will be increased for any material large enough to settle and travel along the bottom of the pipe. If the velocity becomes sufficiently high when transporting a given material, the energy loss due to the rifles may overshadow the decrease of energy consumption due to the induced suspended flow, and a decrease in efficiency will result.

The U.S. Corps of Engineers (48) and (49), 1952, reported certain preliminary work in measuring head loss of corrugated pipes. Piezometer taps were placed at various points along the corrugations

of a prototype and a model. It was demonstrated that the actual static pressure did not occur at a unique point on the corrugations for all velocities. However, by comparing resistance coefficients computed with the heads registered by a series of piezometers at identical relative locations with respect to the corrugation to those computed from static tube data, it was concluded the difference was not more than the expected experimental error.

Observations on a sectional model implied the existance of a wavy layer of flow near the corrugations. Examination of velocity profiles indicated the layer exists between the eddies in the corrugations and the established turbulent flow in the center of the pipe.

Ismail (30), published a paper in 1952 on studies conducted in a rectangular pipe 10.5 in. wide and 3.0 in. deep. The conduit was 40 ft long. Sediment was recirculated. Sands having sedimentation diameters of 0.16 mm and 0.10 mm were used. Measurements were made of the discharge, velocity profile, concentration profile and head loss along the conduit.

The analysis of data was based on consideration of the effect of the sediment on f, ϵ_s, ϵ_m, and K, where f is the Darcy-Weisbach resistance coefficient, ϵ_s is the exchange coefficient for sediment, ϵ_m is the exchange coefficient for momentum, and K is the Kármán universal constant. Conclusions were: 1) as C_t increased, K decreased to as low as 0.20 when C_t was 43 gm per litre, 2) $\epsilon_s \propto \epsilon_m$, and 3) that f was not significantly affected by the presence of the sediment until the total load C_t was so great that dunes were formed on the bottom of the pipe.

An independent analysis of the same data by Laursen and Lin, reported in the discussion, led to converse conclusions, i.e., K was not adequately defined to permit reliable conclusions, sediment has little or no effect on the flow, and the proportionality factor in $\epsilon_s \propto \epsilon_m$ is equal to or less than unity.

The U. S. Corps of Engineers (50), summarized in November 1953 the results of tests with clear water flowing through a 5-ft diameter corrugated metal pipe which had the bottom one-fourth of the periphery paved. The paving was accomplished by means of 18-gage steel sheets welded to the pipe and coated with an asphaltic material.

Measurements of f, Re and v_1, led to the conclusions that the resistance coefficient f was decreased and that the values of the local mean velocity v_1 were greater in the lower section of the pipe. The comparison was made with a pipe of the same dimensions not having a paved invert. The Reynolds number is $Re = VD\rho_w/\mu$, where V is the mean velocity in the pipe, ρ_w is the fluid mass density and μ is the dynamic viscosity of the water.

Morris (36) proposed a new concept of flow in rough conduits in 1954. Three basic types of flow: 1) isolated roughness flow, 2) wake-interference flow, and 3) skimming flow were postulated. Corrugated surfaces satisfy the wake-interference type of flow, and the resistance coefficient f is given by

$$f = \left\{ \frac{1}{2 \log_{10} \frac{r_o}{\lambda} + 1.75 + \frac{1}{\sqrt{2}} (2.5 - \zeta)\left(\frac{\beta\lambda}{r_o}\right)} \right\}^2 \qquad (1)$$

where β is a coefficient in $y = \beta\lambda$, and y is the distance from a roughness crest to the breakpoint between wall and core velocity

profiles. The length λ is the longitudinal spacing of the roughness elements and r_o is the radius of the pipe from the pipe axis to roughness crest. The dimensionless function ζ approaches 2.5 as β goes to zero with increasing velocity.

The resistance function

$$\frac{1}{\sqrt{f}} - 2 \log_{10} \frac{r_o}{\lambda}$$

will approach the same constant value 1.75 for all types of roughness elements, with increasing $\frac{Re\sqrt{f}}{r_o/\lambda}$. However, before this value of 1.75 is reached, the resistance coefficient increases with Re .

Vadot (55) published, in 1954, some ideas on the problem of friction loss in pipes. If an artificial roughness is placed on a smooth bottom, formed of similar roughnesses placed in a given manner, the following variables need to be considered: 1) geometric form of roughness, 2) orientation with respect to the wall, 3) orientation with respect to the direction of fluid flow, 4) a characteristic dimension, 5) placement of the roughness pattern with respect to the wall and the flow direction, and 6) a length representing the implantation design.

The U. S. Corps of Engineers (51), 1954, gave some data on the effect of a 50 percent paved invert on f for a 5-ft diameter corrugated pipe. The water carrying capacity was increased 1/3 over the case of no paving. The pipe was flowing full. The hydraulic gradient J was measured at several locations.

The U. S. Corps of Engineers (52), December 1954, reported head loss tests on a 7-ft diameter corrugated pipe. Conclusions were similar to those reported earlier for 5-ft pipes, i.e., f was reduced about 1/8 by paving the lower 1/4 of the pipe periphery, and the high velocities were shifted toward the invert.

Laminar Transport by Water

Sediment transport by laminar flow of water has little application in the field of sand conveyance. However, turbulent flow must reduce to laminar flow for sufficiently small velocities, high viscosities, or small pipe diameter, and herein lies the reason for studying and reporting certain research on the laminar flow transport of sludge.

Clifford (9), 1924, attempted to analyze the flow of sewage sludge by an analogy with the laws of viscous fluid flow. A kinematic viscosity for the sludge was determined by comparing the flow of sludge containing 90 percent moisture to the flow of glycerine. This comparison was made with a tube 5/16 in. in diameter and 5.25 in. long.

Applying the kinematic viscosity determined as given above, theoretical friction losses were computed for an 8-in. line, at Calumet, Illinois, pumping sludges containing 90 percent water. Calculations checked with the measured friction losses.

Hubbel (29) published limited data in 1933 on a sludge line at Dearborn, Michigan. The pipeline was of 8-in. cast-iron and 20,466 ft long. The sludge, obtained by sedimentation of sewage, contained 99.1 percent water. Hazen and Williams coefficients were 140 and 137 at velocities of 3.15 and 4.06 fps.

Caldwell and Babbitt (3), wrote a paper in 1939 on the laminar flow of sludges. Experiments were with 1-in., 2-in., and 3-in. horizontal pipes carrying sewage sludge. It was concluded that clay slurries and sewage sludges behaved as true plastics; and therefore a yield stress and a coefficient of rigidity were necessary to describe the "fluid", in place of the coefficient of viscosity used for a Newtonian fluid.

The yield stress and coefficient of rigidity were independent of the diameter and roughness of the pipe in which they were measured, but did depend on concentration of suspended material, size and character of sediment particles, nature of the continuous phase, temperature, thixotropy, slippage, aggitation and gas content of the sludge.

Turbulent Transport by Water

Study of the papers in this section yields information on turbulent transport, from fully suspended load to bed load. Sediments investigated range from metallic ores to wood pulp and muds. Pipe diameters investigated in the laboratory varied from 1.5 in. to 10 in. Most investigators were concerned with only the one-dimensional behavior of sediment transport, particularly the J-V and f-Re diagrams.

Blatch (6), 1906, appears to have been one of the first to give the problem of sediment transport in pipes the consideration it deserves. Tests were made to determine the head loss along a horizontal pipe 27 ft long with a 1-in. nominal diameter. A 1.0546-in. diameter brass pipe, transporting sands of about 0.60-mm and 0.20-mm median sieve diameter, and specific gravity of 2.64 was studied. Also examined was a 1.0420-in. diameter galvanized iron pipe carrying 0.60-mm sand.

It was demonstrated that, for a given total sediment load, the head loss deviated further and further from the clear water head loss curve as the mean velocity decreased. Defining the "economical velocity" as that at which the head loss due to a given mixture of sand is a minimum, it was concluded the economical velocity for a 1-in. pipe was 3.5 fps. Furthermore, it was observed that there existed a transition in the flow regime between 3.5 and 4.0 fps. The transition increased in length with an increase in grading of the sediment material.

Nevitt (37), 1919, studied the head loss in a 12-in. cast-iron sewage sludge pipe at Toronto, Canada. The test section was 240.5 ft long. Values of Kutters n from 0.0168 to 0.0181, obtained after five years of service with sludge from sedimentation tanks, were found. The sludge was less than 10 days old. Its density was 1.01, moisture content 95.9 percent, ash 49.5 percent, and temperature 54 degrees Fahrenheit.

Gregory (24), 1927 determined the head loss when pumping a slurry through a horizontal 4-in. pipe. Losses due to fittings were also evaluated. The test line was about 250 ft long. The sediment was made up of 70 percent clay (a little sand), 24 percent carbonate of lime, and 6 percent hydrate of magnesia and hydrates of iron oxide. The material ranged from colloidal to microscopic in size and did not settle quickly nor cake in the pipe.

Plotting J versus V, it was found that above a certain velocity the plot agreed with that for clear water, with total loads ranging from 5 to 29 percent by volume. For lower velocities, of a particular total load, the head loss remained constant. The maximum velocity for which J was independent of V, for a constant load, was

named the "critical velocity". It was also the most economical velocity in terms of power consumption.

A Saybolt viscosimeter was used to determine viscosity of the slurry, to be used in Poiseuilles law in a study of the region for which J is independent of V . It was concluded a viscosity measured in this manner has questionable value.

Mikumo, Nishikara, and Takahara (35) wrote a paper in 1933 on their tests of pipeline head loss with copper ore slimes pumped through a 1.5-in. pipe line. The ore had an average specific gravity of 3.5. The median size of the material was 0.0042 in. The equipment consisted of a recirculation system powered by a centrifugal pump. The length of the horizontal test section for measuring pressures was one meter. Methods for the measurement of velocity and concentration are not adequately explained.

Brautlecht and Sethi (7), 1933, presented data on head loss in a horizontal 1-in. pipeline transporting unbleached sulphite pulp. The pulp was screened through a No. 10 flat screen. Concentrations were from 0 to 1.57 percent by bone dry weight. The pipe plugged at a concentration of 3.0 percent. Velocities ranged from 2.0 to 8.8 fps.

Traxler (47), 1937, pointed out that the flow properties of dilute suspensions of clay and other minerals depends to a large extent on particle size, size distribution and shape. It was concluded that there is a simple relationship between concentration of solids and the viscosity of the suspensions.

O'Brien and Folsom (38), 1937, published one of the classic papers on the subject of pipeline sediment transport. They ran a series of tests with 2-in. and 3-in. standard black wrought iron pipe. The pipelines were horizontal. Three sizes of sand were used, ranging from about 0.0065-in. to 0.050-in. median size. A sand and water mixture was circulated, and concentration, hydraulic gradient and mean velocity were measured.

In analyzing these data it was found that the Darcy-Weisbach equation

$$J = f\ V^2/2gD\ , \qquad (2)$$

where g is the gravitational field, was valid for non-homogeneous mixtures as well as for homogeneous fluids.

Two minimum velocities were defined: 1) a "critical velocity", at which the head loss begins to differ appreciably from head loss for clean water in the same pipe, and 2) the velocity of incipient clogging. It was concluded that the critical velocity was a velocity below which a part of the material was transported by rolling along the pipe and as the velocity is decreased, more and more area of the pipe becomes obstructed by rolling sand until conditions of incipient clogging occur. Furthermore, the most efficient velocity for pumping a given total load is the minimum velocity that will move the material through the pipeline, which was independent of sand size for the range reported.

In a discussion of the effects of solids on the turbulent flow, they believed the concentration of material might not be the same

across horizontal surfaces because the particles tend to fall to the lowest point, inducing a double spiral secondary flow, downward at the center and upward along both sides.

Wilhelm, and others (57), 1939, published friction loss data on the pumping of cement rock and filter-gel suspensions. Horizontal pipes 0.75-in., 1.5 in. and 3 in. in diameter, 27 ft long, were tested with water-sediment complex. A reasonable correlation of all these data was obtained on an f-Re diagram by substituting an apparent viscosity, determined with a rotating viscosimeter, for the fluid viscosity.

Howard (28), 1939, studied the head loss in a 4-in. pipe about 30 ft long, the downstream half being the test section, with water-sediment mixtures. Several concentrations and velocities were tested. The sediment was so-called Pearl River Sand. Some tests were run with gravel. The minimum energy loss occurred when a "jerking" motion existed along the bed. Three methods of transport were observed: 1) rolling when velocities are low, 2) by "jerking" at higher velocities, and 3) by all particles being in motion at very high velocities. It was found that f would decrease with an increase in V, and increase with an increase in C_t for a given velocity V.

Durepaire (21), in a discussion of Howard (28), gave conclusions on some tests with water and 0.012-in. Loire River sand pumped through a 52-mm steel pipe. The head loss expressed in feet of mixture was found to be about the same as that for clear water, with concentrations as high as 40 percent by volume. The minimum head loss occurred when deposition was about to begin, and the head loss was never less than that with clear water. For a constant depth of deposit,

the head loss varied as the square of the discharge, whatever the concentration. There was no "jerking" motion, which seemed always to occur for gravity systems.

Danel (14), in a discussion of Howard (28), pointed out that a density gradient in a pipeline could cause a damping of turbulence, just as density variations with height causes the calmness of the atmosphere at sunset.

Caldwell and Babbitt (4) reported in 1941 on extension of the laminar flow tests of 1939, with sewage sludge, to the turbulent regime. New standard black steel pipe 0.5 in., 1 in., 2 in. and 3 in. in diameter was employed. Except for the 0.5-in. pipe, the test reach was 21 ft long, preceded by at least 40 pipe diameters for establishing the flow pattern.

The friction loss was measured for several velocities with each of the eight sludges tested.

In analyzing these data it was found that a diagram of f versus $Re = VD\rho/\mu$ was adequate to solve friction loss problems when the velocity was greater than a certain magnitude. For velocities less than this, the hydraulic gradient deviated appreciably from that for clear water in the same pipe. Another important conclusion was that, for sludges composed of water and suspended material, the viscosity of the dispersion medium is nearly the same as that of water, so that the common hydraulic formulas can be used in evaluating turbulent flow friction losses when pumping sludges.

Wilson (58), proposed an elementary theory in 1942 of pipeline transport of non-colloidal inert solids, assuming that the particle settling velocity relative to the transporting fluid is known. A relationship was written between the work done by the liquid on the particles and the decrease in potential energy of a settling particle. Using the Darcy-Weisbach equation and assuming the energy gradient may be divided into two parts, the result of the energy calculation was the equation

$$J = \frac{fV^2}{2gD} + \frac{\gamma_s - \gamma_w}{\gamma_w} (1 + A_1) \frac{C_t w}{V} \qquad (3)$$

for the hydraulic gradient when sediment is being transported, where γ_s and γ_w are the unit weight of the sediment and water respectively. The fall velocity of the sediment particles is w and A_1 is a constant.

By assuming C_t, W, f, A_1, and D constant, a condition for deposition was derived. The condition is

$$w/\sqrt{JgD/4} = 1,$$

for horizontal pipes.

That actual cases would differ from this, due to non-uniform values of shear over the cross-section, was recognized.

Danel (13), presenting some theoretical considerations in 1948, again put forth the concept of "evening calm" with respect to a flow having a marked density gradient. It was concluded that the amount of energy dissipated in maintaining sediment in suspension was about equal to the decrease in energy dissipation due to damping of the turbulence, i.e, the total head loss for a mixture is approximately the same as that of a fluid of the same average density.

The concept of a plastic film near the wall was postulated for the transport of very fine material. This is the usual laminar sublayer, into which the sediment has diffused until the layer is plastic in character.

Durand (17) reported in 1951 on the hydraulic transport of gravel and pebbles. The material was sieved into categories between the following limits: 2.3 mm - 5.25 mm - 9.9 mm - 15.5 mm - 20 mm - 25 mm. A 104-mm horizontal pipe was used for the tests.

The head loss varied with total load for all the gravels studied, but seemed independent of the mean diameter of the grains. Furthermore, for a given velocity in the range usually found in hydraulic conveying work, the head loss was higher than that for clear water.

A classification of 'sand' sediments was proposed, based on the characteristic plot of head loss versus velocity plot for each class. The classes are: 1) silts and fine sands which follow the Stokes law, 2) coarse sands, and 3) gravels and pebbles that follow the Rittinger law. This classification emphasizes the significance of the parameter w/V .

Durand (18) discussed in 1951 some experimental work on pumping fine ashes from a power plant. The material covered a wide size range, 2 to 100 microns, with a specific gravity of about 2.5. The pipeline was 250 mm in diameter. Total load was as high as 300 grams per litre.

It was felt that due to the heterogeneity of the sediment no precise conclusions could be made until additional data on screened sediments were available.

Tison (46), wrote in 1952 on tests with a chemical plant residue of about 0.05 mm, which was pumped through 1-in. and 2-in. diameter pipes. Concentrations by volume of 15 and 30 percent were used. Head loss was

measured in feet of water because the specific gravity was always less than about 1.15, a negligible error.

The sediment reduced the resistance coefficient f considerably, at least for Reynolds numbers greater than 10,000.

Kestlicher (31), 1952, studied head loss in a 101.6-mm cast-iron pipe 61 m long transporting very fine sediment. Specific gravity of the mixture ranged from 1.00 to 1.28. As in earlier investigations, it was found that the head loss curve corresponded to that of clear water for velocities greater than a value depending on the total load. In this case the asymptotic curve was determined after the tests had been completed, and a very smooth coat of sediment covered the pipe roughnesses. This coating reduced the resistance about to that of a hydrodynamically smooth pipe.

Head (26), 1952, working in the paper engineering field with non-Newtonian fluids of pulp and sulfite, introduced terms to replace the dynamic viscosity which is strictly applicable only for Newtonian fluids. The shear diagram was a straight line with a non-zero intercept for zero shear over the range investigated. This led to defining the physically meaningful "slope viscosity" as the slope of the shear diagram. An "apparent yield stress" was defined as the intercept on the shear diagram when the shear was zero. A "shear criterion" was introduced for non-Newtonian suspensions.

Durand and Condolios (19), presented a very complete paper in 1952 on the hydraulic transport of sediments having a specific gravity of about 2.65. Besides silts, etc., nine categories of sediment, from fine sand to pebbles, were studied in four conduits of 40.6-mm to 250-mm diameter. Total sediment load varied from 50 to 600 grams per litre.

Using a "whistle meter" for discharge measurements, it was reported that for non-deposit regime and concentrations less than 20 percent by volume the manometer reading was not affected by the presence of sand. Also, for fine sands in high velocity flows the presence of the material did not have an appreciable influence on the value of the head loss expressed in terms of clear water, i.e., the presence of the material was not detectable on a metallic manometer.

The head loss for muds in turbulent flow was found to be the same as that of water, if the head was expressed in height of mixture

For analysis of the data on fine sand and coarser material transport, it was found that the Gasterstadt relative head loss $(J - J_e)/J_e$ was a significant variable and related to the transport concentration by

$$(J - J_e)/J_e C_t = \Theta, \tag{4}$$

where Θ was to include V, D, d, etc. It was decided that for sediments having a sieve diameter d greater than 2 mm, with a given velocity V, the head loss is independent of the sediment dimensions. The term J_e is the hydraulic gradient for the pipe transporting clear water under the same V as the corresponding J.

In constructing Θ, it was determined empirically that, for d and D a constant, $\Theta = \Theta(V)$. If D were varied, $\Theta = \Theta(V/\sqrt{gD})$. With both d and D variable, Θ became

$$\Theta = \Theta((V^2/\sqrt{gD})\ (\sqrt{gD}/w))$$

All these data for fine sand or coarser material transported entirely in suspension, by water, were correlated by

$$\Theta = A_2 \left(\sqrt{gD}/V\right)^3 \left(w/\sqrt{gd}\right)^{1.5} ,$$

where A_2 is an empirical constant.

Craven (12), 1952 presented the results of studies at the University of Iowa with 60 ft lengths of 5.55-in. ID and a nominal 2-in. diameter plastic tubes. Tests were run with three grades of uniform quartz sands (0.25 mm , 0.58 mm and 1.62 mm). The slope of the tube could be varied at will.

By dimensional considerations it was demonstrated that the bed-load transport could be adequately described by two dimensional relations. The experiments were designed to determine these functional relationships. The investigation was not sufficiently extensive to attain the original objective, but certain interesting observations were made. It was found that the bed configuration, for each of the sands, evolved through the same pattern but the value of C_t at which a given change occurred was different for each grain size. It seemed that the higher the value of V/w , the greater was the tendency for sediment to be lifted into suspension and the less the tendency for it to travel by dunes.

Ambrose (2), 1952, extending the research of Craven (12), with the same basic equipment, investigated the case of free surface flow in pipes. Two relationships to define the phenomenon of sediment transport were derived by dimensional analysis: a) a transport function relating the discharge to the geometry and to the other characteristics of flow, channel, and sediment, and b) a discharge function relating the discharge to the resistance to flow of the sand bed and pipe wall.

Analysis of these data indicated that the transport function appears to be dependent solely upon the mean geometry. No discernible

effect due to d/D was evident. It was found that the transport reached a maximum value of approximately

$$2.9 \left(\gamma_s / \gamma_w - 1 \right)^{2/5}$$

Deposition would not occur for values of the total load greater than this. The parameter γ_s / γ_w was constant.

The discharge function seemed adequately defined if k/D and Re were neglected (k is an equivalent uniform sand roughness).

Durand (16) reported a somewhat more complete analysis of Durand (19). However, the principal results were the same. The main difference in the two papers is that this 1953 report was published in English.

Turbulent Conveyance by Air

Apparently there has been little exchange of knowledge between the investigators using air and those using water as the continuous phase. Different nomenclature and different names are given to the same parameters and equations with which the hydraulic engineer is familiar. In the following reviews the authors definitions have been very carefully analyzed and put into the more standard symbols of fluid mechanics. The role played by $(J - J_e)/J_e$ should be observed.

Gästerstadt (23), presented in 1924 the results of studies on the pneumatic conveying of wheat in a 3-in. ID pipe. This seems to be the first paper to use the relative pressure drop, $(J - J_e)/J_e$ as a fundamental variable. Measurements were made of the friction losses accompanying transportation of given total loads of wheat at various velocities in horizontal pipelines.

A linear relation, for given velocities, was found between $(J - J_e)/J_e$ and the specific output of grain. The effect of velocity was investigated both theoretically and experimentally by considering w/V. The velocity of an individual grain in the two phase stream was measured by flash photography.

Cramp and Priestley (11) wrote in 1924 on pneumatic grain elevators. Tests were made with No. 1 Manitoba wheat, with the purpose in mind of developing curves of horsepower per ton-hour for various rates of transportation. The acceleration from rest characteristics of wheat, desirable grain-air mixing nozzles, and theoretical efficiencies which could be expected from plants were investigated. Only vertical conveying was studied. These data seem to be somewhat incompletely presented.

Segler (42), 1934, studied the effect of pipe diameter on the horizontal conveying of wheat by air. The pipes ranged from 46 to 420 mm in diameter. A few data were taken with oats, and some on the vertical transport of wheat.

These data for horizontal conveying satisfy a single linear function on a log plot of

$$(J/J_e - 1)1/r \qquad \text{versus} \qquad Re\,(d/D)^2\,(\gamma_s/\gamma_a),$$

where $r = C_t\,(\gamma_s/\gamma_w)$ and ρ_a is the air mass density.

Wood and Bailey (59) published results in 1939 of research with sand and linseed sediments tranported by air in a horizontal brass pipeline 2.9 in. in diameter and 25 ft long.

Observations were on a saltation flow regime. The length of jump decreased with diminished air speed. It was also observed that the hydraulic gradient was steepest at the pipe inlet. The pressure drop due to the grain alone depended on its rate of conveyance but not the grain velocity, indicating decreasing friction between the grain and pipe walls. The hydraulic gradient was found to be a linear function of the ratio of solids to air.

Vogt and White (56), writing in 1949 on work with horizontal and vertical pipes conveying granular solids by gases, followed earlier scientists in using $(J - J_e)/J_e$ as a primary variable. Friction loss data were recorded on a 0.5-in. diameter pipeline carrying 0.0088-in., 0.0138-in. 0.0018-in. and 0.0287-in. diameter sand, 0.0165-in. steel shot, 0.046-in. clover seed and 0.158-in. wheat.

These data, for both horizontal and vertical transport, were represented by the equation

$$J/J_e - 1 = A_3 (D/d)^2 (\rho_a/ \rho_s \quad r/Re)^{A_4}$$

where r is the weight ratio of solids to air flowing, and A_3 and A_4 are functions of

$$\frac{\sqrt{(1/3(\gamma_s - \gamma_a) \quad a d^3)}}{\mu/g^2}$$

The latter parameter was derived from the Stokes law. The effect of particle shape was not investigated but seemed of secondary importance.

Farbar (22) reported in 1949 on some studies of the isothermal flow characteristics of gas-solid mixtures in vertical and horizontal 17-mm diameter pyrex tubes. The sediments were alumina, silica, and catalyst, ranging from 8 to 220 microns in diameter. Air velocities in the approach section were 50 to 150 fps. The ratio of weight of solids to air varied from 0 to 16. Several types of nozzles were used to introduce the sediment into the air stream.

Pressure measurements were made on a 2-ft test section along the 7-ft test pipe. The nozzles were tested for stability of flow in the system, as characterized by pressure surging. Qualitative observations were made on the flow pattern.

The conclusions were mostly qualitative in nature. At low concentrations the solids seemed to travel in clusters following a sinuous path, striking the boundary and deflecting back into the main stream. For high concentrations there was a tendency for the pressure drop to be independent of concentration. It was further concluded that the flow characteristics of gas-solid mixtures in which the particle size distribution covers a wide range differ considerably from mixtures of a narrow size range.

Belden and Kassel (5), 1949, wrote on the vertical conveying of large particles in pipes, by air. Two steel pipes, 0.473 in. and 1.023 in. in diameter were used, preceded by a 20-in. glass section. The catalysts were 0.0379 in. and 0.0764 in. in diameter, with unit weights γ_s of 53.7 and 60.9 pounds per cubic foot respectively. Measurements were made to determine pressure drop as a function of velocity and rate of sediment transport

The pressure drop was divided into a static term and a friction term. The Darcy-Weisbach equation was then arbitrarily generalized to the form

$$\frac{dp_f}{dx} = 2f \frac{(G_a + G_s)V_a}{gD}$$

Where dp_f/dx is the friction pressure drop, V_a the true air velocity and G_i the mass velocity of the respective mixture constituents. Most of these data were represented by the empirical equation

$$f(Re)^{0.2} + 0.049 + 0.22\, G_a G_s/(G_a + G_s)^2$$

with $Re = DG_a/\mu g$.

Hariu and Molstad (25), writing in 1949, reported on the vertical conveying of solids by gas in glass tubes 0.267 in. and 0.532 in. in diameter. Six sediments were used, Ottawa sand of 0.00165 ft and 0.00117 ft diameter, sea sand 0.00090 ft and 0.00070 ft in diameter, a microspheroidal cracking catalyst of 0.00036 ft and a ground cracking catalyst of 0.00036 ft diameter.

The head loss was considered in two parts; that due to the gas alone as if no solids were present, and a solids pressure drop. The solids pressure drop was further divided into a solids static head, a solids friction loss due to particles-pipe contact, and an acceleration drop for some distance above the point of introducing the sediment. Pressure gradients were high in the acceleration zone; the Darcy-Weisbach equation applied beyond it.

In studying sediments having large size ranges, it was felt that some diameter between the average and the largest should be used in calculating the mass-average slip velocity.

Installed Plants and Their Design

The purpose of studying papers on the design of plants and results observed at existing installations is to gain an awareness of the type of problems frequently encountered. The difficulties seem to be: 1) technique of operation, 2) economic feasibility, 3) correct pump design, and 4) energy consumption.

Maltby (34), 1905, reported the results of friction loss investigations on the discharge lines of eight dredges of the Mississippi River Commission. The dredges operated on the portion of the river below the junction of the Mississippi with the Ohio, at Cairo, Illinois. Tests were made from 1896 thru 1905. With the sediment all in suspension, apparently in smooth pipes about 24 in. in diameter, f was found to be about 0.015. Specific conclusions were not presented.

Orrok and Morrison (39), as early as 1921, made estimates on the economic practicability of pumping anthracite and bituminous coal as far as 320 miles. Excluding water costs, all the estimates were equal to or less than 3 mills per ton-mile for pumping 6 million tons per year.

Cramp (10), 1925, set up a design criterion for pneumatic conveyors. Plants were classified as pressure, suction or a combination. The factors to be considered were the pressure differential, the sediment-pipe friction, the air-pipe friction, the force to support the material, the force to support and accelerate the air, and the force to accelerate the material. A very lengthy equation involving all the above factors is

given, for the case of vertical pipes. It is stated that a modification of the equation would be applicable to horizontal lines. Measurements and calculations differed less than 4 percent. Horsepower was computed by assuming isothermal compression.

Lambrette (33) discussed in a general way, in 1935, the pumping of paper pulp, dispersed clays, effluent water, and other solids. A so-called stereophage type pump, suitable for pumping fibrous solids, was described. It is a special centrifugal pump which should not clog easily.

Thoenen (45) discussed in 1936 the advantages and disadvantages of pipeline transportation of sand and gravel. An example of typical pumping performance curves and a list of the characteristics of mixtures are given. Included also are friction losses for fittings and some dredge pipeline data.

Durepaire (20), 1939, in a contribution to the study of sediment pumps, carried out a complete and clear analysis of stability in sediment-water mixture transport lines. Hydraulic gradient was plotted versus discharge of mixture for various arbitrary total loads, giving a typical curve in which there always exists a minimum head loss for each total sediment load. A hypothetical pump characteristic curve was superimposed on the J-V diagram. The stability of the plant operation, which decreases the probability of pipeline clogging, was present for any pump having a Q = constant characteristic, and conversely.

Chatley (8), 1940, discussed the elements of power consumption in the transport of granular solids in suspension. The significant ones are lifting the solid particles, accelerating the grains, sustaining the

grains, friction against the pipe walls, accelerating the fluid, fluid friction and losses at bends and valves.

Sample calculations were presented for a 6-in. pipe 50 ft long transporting 48 tons of grain per hour. Air was used as the fluid. The computations indicated that roughly three times as much horsepower is required for horizontal transport of grains as for vertical conveyance. The major portion of the difference in power seemed to be due to the higher power requirement in the horizontal pipe to accelerate the grains. It was felt that slope is a significant variable in pneumatic transport when it deviates from the vertical.

Soleil and Ballade (44) carried out tests in 1951, reported in 1952, on the Nantes dredging operations. Head loss, rate of material transport and depth of deposit in at 580-mm and 700-mm pipe were measured. The test section was about 100 m long, horizontal and located at the end of the main dredge discharge line.

Conclusions were that the pipe diameter ought to be chosen as large as possible in order that the width of deposit represent a considerable part of the pipe diameter. The larger pipe had the lesser head loss and carried more sediment per cubic foot of discharge than a smaller pipe with equal mixture discharge.

The head loss was very sensitive to sediment size. Material over 0.3 mm affected the head loss, but material less than 0.3 mm diameter did not influence it.

Dougherty (15) made a survey, reported in 1952, on the problems presented by pipe transportation of coal by water. After reviewing the opinions of manufacturers of centrifugal sand pumps, and some

economic studies available in the literature or files of manufacturers, the conclusion was reached that coal could be transported economically in pipelines, especially in large tonnages. Further conclusions were that, before coal pipelines could be built, many more pumping performance data are needed, pumps need more development, data on erosion of pumps are lacking, and data on the most economical linear pumping velocities and pressure drop must be determined for various coal mixtures.

Miscellaneous Items

The reports reviewed below were studied because of their bearing on instrumentation and technique, properties of fluid-sediment systems, stability of concentration profiles, and variables of current importance in open channel sediment work for which there is an analogy in the present study.

Kowalki (32), reported in 1938 on a series of experiments on pumping of an aluminum suspension through an orifice to determine the flow characteristics. A series of photographs shows the path of the powdered aluminum.

The U. S. Corps of Engineers (53), 1941, reported on laboratory investigations of suspended sediment samplers. The following points are relevant to the present study:

1. Comparing a standard nozzle to a rounded-edge type, with 0.45-mm sediment, a variation of the sample intake velocity by ± 10 percent from the ambient velocity caused a sampling error of ± 3 percent. Velocity variation of ± 20 percent gave ± 6 percent concentration error.

2. The standard nozzle, with $V = 5$ fps, had a $\pm$ 3 percent concentration error for a $\pm$ 20 percent error in intake velocity.

3. Various concentrations have little effect on the magnitude of error for a given sampler.

Vanoni (54), 1946, published results on the sediment distribution in an open flume. The purpose of the studies was to investigate the relation between the momentum exchange coefficient ϵ_m and ϵ_s in the diffusion equation. The equation

$$c/c_a = \left(\frac{D' - y}{y} \cdot \frac{a}{D' - a}\right)^{z_1} \qquad (5)$$

was the basis of analysis. This equation is sometimes called the "Rouse equation" and z_1 the "Rouse number". The concentration c_a is at the elevation a above the bed, D' is the depth of flow and y is the distance above the bed that c is measured. The form of the equation was satisfactory but the value of the exponent z_1 was not in quantitative agreement.

Furthermore, suspended load reduced the magnitude of the Kármán K, which characterizes the effectiveness of the turbulence in transferring momentum. This is equivalent to a reduction in ϵ_s, which measures the effectiveness of the diffusion process. The idea that the sediment damps the turbulence was put forth.

Alves (1), 1949, discussed the viscous and turbulent flow of Bingham plastics, pseudoplastics, dilitant suspensions, thixotropic suspensions, and rheopectic suspensions. The characteristics of each

are shown graphically for comparative purposes. Possible methods were advanced by means of which head loss could be measured.

Prandtl (40), 1952, in a section discussing the fluid media, presents the Richardson number R_i as a stability criterion. By definition,

$$R_i = \frac{g/\rho \quad d\rho/dy}{(du/dy)^2} \quad . \tag{6}$$

Sobolewski and Grove (43), 1953, reported data on head loss when pumping fire fighting foam through 0.5-in., 0.75-in. and 1-in. standard black iron pipe. These foams were non-Newtonian systems. Rates of flow varied from 27 to 155 pounds per minute. For each rate of flow the foam specific gravity was varied from 0.1 to 1.0.

Pressure drop was a function of the fluid viscosity for foams having a specific gravity of 0.4 to 1.0. For these foams a laminar lubricating layer existed, if the velocities were not excessively high, resulting in low energy requirements. If the foam had a specific gravity less than 0.2, there was not an excess of liquid to readily form a lubricating layer and it was thought that the pressure drop was a function of the surface tension of the solution, because the pressure drop versus specific gravity curve approached a straight line. A transition existed between specific gravity 0.2 and 0.4.

Summary

The literature is summarized by classes, for simplicity.

Boundary form studies indicate that the number of investigations conducted on the effect of boundary form on sediment transport is very small. The conclusion which can be drawn from these very limited data is that, for sediment large enough to settle rapidly, an artificial roughness will result in less energy expenditure to transport the mixture for some range of mean flow velocities.

The tests carried out to evaluate the effects of artificial roughness, on the fluid mechanics of clear water flow, are of fundamental importance. Such data lay the foundation for the more complex situation which will exist when sediment is present. Corrugated boundaries were investigated in combination with smooth surfaces, and a wavy layer of fluid was present near the corrugated surface. A recent paper postulating three basic types of flow, which are isolated roughness, wake-interference and skimming, is significant. Each type of flow can be associated with the results of a physical boundary shape and spacing on the flow pattern.

Laminar transport by water, has been, for the most part, employed with sludges and slurries. Boundary form hardly enters these problems. The dynamic viscosity of a Newtonian fluid in not adequate to describe the properties of non-Newtonian sludges and similar sediment-laden flows. Solution of problems of friction loss, transition to turbulent flow and clogging reduce to a study of effects of the mixture properties, represented by the slope and intercept of the shear diagram.

The problems of turbulent transport by water are divided by classifying the sediments according to size, i.e., muds and silts, sands, gravels, and pebbles. This implies size is a very significant variable. The friction loss in transporting very fine material is generally accepted to be the same as clear water, if the head loss is computed in terms of the mixture unit weight. Head loss can be expressed in terms of clear water, when transporting sands, with the conclusion that the sediment reduces the energy expended by the continuous phase. Analysis by means of the f-Re diagram has led to various definitions of an apparent viscosity, with no definite conclusions. It is generally believed that the most economical transport velocity corresponds to incipient deposition, for materials small enough to be carried in suspension. A number of criteria for deposition have been advanced. Large particles usually travel by "jumps", i.e., in the saltation regime. The parameters which seem to occur frequently are: Re , $V/\sqrt{gD}$, $w/\sqrt{gd}$, J , C_t , f , ρ_s/ρ_w and w/v .

Turbulent transport by air is centered about the study of vertical conveyance of cereals or fluidization of catalyst beds. A large number of sediments have been studied, with Re, f, and $(J - J_e)/J_e$ as primary variables. Several definitions have been used for Re in an attempt to correlate data. Shape factor for the sediment is believed to be of secondary importance. Head loss is frequently split in parts; that due to the particles, pipe and air, static losses and various others depending on the preference of the investigator. The slip velocity between air and particle is important, and transport is mostly by saltation.

Installed plants and their design indicate there is a very lively interest in sediment transport in pipelines. Plant operation techniques, pump design, new materials to transport and economic studies are receiving support from industry.

The various miscellaneous items reviewed each had only a specific point to illustrate as far as the present study is concerned, thus they do not lead to any general conclusions.

Chapter III

THEORETICAL CONSIDERATIONS

Some insight into the mechanics of fine sand sediment transport, by water in pipelines, can be obtained by certain theoretical considerations. Theoretical analysis employs two complementary methods. One method is based on the fundamental concepts of Newtonian mechanics, i.e., Newton's second law, conservation of matter, and an equation of state. The complementary method is dimensional analysis. Experience plays an important role in selecting the significant variables for dimensional analysis, and organizing certain ones of these variables into products which form dimensionless parameters capable of physical interpretation.

The classical equations of hydrodynamics will be presented and discussed in this chapter, in-so-far as they apply to the problem of pipeline sediment transport. Consideration will also be given to the dissipation of energy by the sand-water system and dimensional analysis of several specific problems.

Local concentrations, local mean velocity and mass density are considered measured over a macroscopic volume of sand-water mixture sufficiently large that they exhibit no appreciable discontinuity because of the two materials present in the system.

It is also quite possible that a suitable solution could be obtained for many of the problems of the mechanics of sediment motion by introducing the tools and concepts of statistical mechanics.

Classical Equations

The classical equations employed in a study of viscous fluids are the Navier-Stokes equation, the continuity equation and the equations of state.

The Navier-Stokes equations are an expression of Newton's law $\underline{F} = d(m\underline{v})/dt$ applied to a fluid continuum. Newton's law of motion for a viscous fluid may be written in the form

$$\rho F_i + \sum_j^3 \partial T_{ij}/\partial x_j = \rho dv_i/dt \ , \ (i = 1, 2, 3) \ , \qquad (7)$$

where the first and second terms on the left represent the i th rectangular component of the volume and surface forces, respectively, in an inertial Cartesian coordinate system (x_1 , x_2 , x_3). T_{ij} is the stress tensor for an isotropic viscous fluid, which may be written in the form,

$$T_{ij} = -p\,\delta_{ij} + \mu\left(\partial v_i/\partial x_j + \partial v_j/\partial x_i - \tfrac{2}{3}\delta_{ij}\sum_k^3 \partial v_k/\partial x_k\right) . \qquad (8)$$

v_i is the i th rectangular component of velocity of a macroscopic element of fluid, δ_{ij}, is the Kronecker delta, and μ is the dynamic viscosity of the fluid.

Substituting Eq 8 into Eq 7 and assuming $\partial\mu/\partial x_i$ is zero,

$$\rho F_i - \frac{\partial p}{\partial x_i} + \mu\sum_j^3 \frac{\partial^2 v_i}{\partial x_j^2} + \tfrac{1}{3}\mu\frac{\partial}{\partial x_i}\sum_j^3 \frac{\partial v_j}{\partial x_j} = \rho\,\frac{dv_i}{dt} \ . \qquad (9)$$

Using vector notation, Eq 9, the Navier-Stokes equation, may be written

$$\rho\underline{F} - \nabla p + \mu\left[\nabla^2\underline{v} + \tfrac{1}{3}\nabla(\nabla\cdot\underline{v})\right] = \rho\,\frac{d\underline{v}}{dt}$$

$$= \rho\left(\frac{\partial \underline{v}}{\partial t} + \underline{v}\cdot\nabla\underline{v}\right) , \qquad (10)$$

Eq 10 will apply to any small macroscopic volume of the sediment-laden flow which is approximately isotropic in character and for which the time rate of change of strain may be linearized. This amounts to saying that the sediment must be, in general, of a size not greater than the very fine sands, and the concentration must be fairly small, say 10 to 15 per cent by volume. The condition of homogeneity cannot, in general, be satisfied throughout the volume of sand-water mixture contained in a large pipeline.

The continuity equation of the sediment-water mixture is

$$\partial \rho / \partial t + \nabla \cdot \rho \underline{v}_m = 0 \ , \tag{11}$$

where $\underline{v}_m$ is the velocity of the mixture, and ρ is the mass density defined by the equation of state

$$\rho = \rho_w + (\rho_s - \rho_w) c \ , \tag{12}$$

where ρ_w and ρ_s are the mass density of water and sediment respectively, and c is the local sediment concentration. This equation is applicable to a pipeline conveying sediment, assuming no sources or sinks exist.

However, the purposes of this dissertation require a continuity relation for the sediment. Eq 11 is not useful because the relation

$$\underline{v}_m = \psi (\underline{v}_s) \tag{13}$$

is usually not known, where $\underline{v}_s$ is the velocity of the sediment.

Continuity Equation for Sediment Concentration Distribution

A continuity equation for the sediment concentration will be derived and then applied to sediment conveyance in a pipeline.

The influx of sediment into an arbitrary but fixed volume is given by

$$-\int_s c\,\underline{v}_s \cdot \hat{n}\, da\ , \tag{14}$$

where $\hat{n}$ is an outward unit vector normal to the element of surface da, and s is the surface bounding τ_o. The time rate of change of sediment in τ is given by

$$\int_\tau \frac{\partial c}{\partial t}\, d\tau\ . \tag{15}$$

Transforming Eq 14 to a volume integral and equating it to Eq 15, one obtains

$$\int_\tau (\partial c/\partial t + \nabla \cdot c\,\underline{v}_s)\, d\tau = 0\ . \tag{16}$$

Since τ is arbitrary it follows that

$$\partial c/\partial t + \nabla \cdot c\,\underline{v}_s = 0\ , \tag{17}$$

which is the desired continuity equation.

In order to apply Eq 17, an expression is needed for $c\underline{v}_s$. Assume that the sediment motion is due to diffusion and transport. Let $\underline{G}$ be a vector which has the direction of the mean sediment motion caused by a concentration gradient and a magnitude equal to the volume of material diffused per unit area per unit time. The transport of the sediment is due to the motion of the mixture and the fall velocity of the sediment. Let $c\,\underline{v}_s'$ represent this transport per unit area. Therefore,

$$c\,\underline{v}_s = c\,\underline{v}_s' + \underline{G}\ . \tag{18}$$

An expression can be derived for $\underline{G}$ in terms of c by means of the Fourier law, which states that for an isotropic medium

$$\underline{G} = -\sum_{i}^{3} \epsilon_i \, \partial c / \partial x_i \, e_i \tag{19}$$

where ϵ_i is an arbitrary function of position. The assumption of isotropy is probably not extremely limiting when fine sediments at low concentrations are considered.

Substituting Eq 19 into Eq 18 and then Eq 18 into Eq 17, one obtains the following diffusion equation for sediment:

$$\partial c / \partial t + \nabla \cdot (c \underline{v}_s' - \sum_{i}^{3} \epsilon_i \partial c / \partial x_i \, \hat{e}_i) = 0 \, . \tag{20}$$

Consider the special case of a horizontal pipe, let e_1, e_2, e_3 be unit vectors, where e_1 is along the axis of the pipe, e_2 is vertically upward and e_3 is normal to e_1 and e_2. Further, assume

$$\begin{aligned} &\underline{v}_s' = v_{s1} \, e_1 + v_{s2} \, e_2 \, , \\ &\partial c / \partial x_3 = 0 \, , \\ &\partial c / \partial t = 0 \, . \end{aligned} \tag{21}$$

Making use of Eq 21, Eq 20 becomes

$$\partial (c v_{s1}' - \epsilon_{x_1} \, \partial c / \partial x_1) / \partial x_1 + \partial (c v_{s2}' - \epsilon_{x_2} \, \partial c / \partial x_2) / \partial x_2 = 0 \tag{22}$$

For the steady flow of mixture,

$$\partial v_{s1} / \partial x = 0 \, , \tag{23}$$

and

$$\partial c/\partial x = 0 \ , \tag{24}$$

hold, and Eq 22 reduces to

$$\partial(cv_{s2}' - \epsilon_{x2} \ \partial c/\partial x_2)/\partial x_2 = 0 \ . \tag{25}$$

Since c , v_{s2}' and x_2 are functions of x_2 only, the partial derivatives in Eq 25 may be replaced by total derivatives. Integrating with respect to y Eq 25 becomes:

$$c \ v_{s2}' - \epsilon_y \ dc/dy = \text{constant}, \tag{26}$$

where x_2 has been replaced by y . In order to put Eq 26 in more meaningful form and evaluate the constant, multiply through by $dxdz$. Thus,

$$(cdxdz)v_2 - (\epsilon_y \ dc/dy) \ dxdz = \text{constant} \ dxdz \ .$$

In the first term, $cdxdz$ is that part of $dxdz$ occupied by the sediment particles. If v_2 were the fall velocity of the sediment, the first term would be the volume of sediment settling downward across $dxdz$ per unit time. The second term is the volume of sediment per unit time diffusing upward through $dxdz$. Setting $v_2 = -w$, the particle fall velocity, and the constant equal to zero,

$$cw + \epsilon_s \ dc/dy = 0 \ , \tag{27}$$

where ϵ_y is associated with the sediment exchange coefficient ϵ_s . Eq 27 is the fundamental equation for the sediment concentration distribution along the vertical diameter of the pipeline in which pronounced secondary circulation does not exist.

In order to apply Eq 27, it is necessary to derive an expression for ϵ_s/w in terms of y. While w varies with sediment concentration and proximity to boundaries, it has often been given a magnitude corresponding to the fall velocity of the median particle sieve diameter. The exchange coefficient ϵ_s is frequently assumed a constant along the vertical direction. However, experiments in Europe, Durand (16), demonstrated that such assumptions are not accurate enough to enable one to solve for the concentration distribution in pipes in the general cases, i.e., for any size sediment, pipe or mean velocity V.

To <u>interpret the continuity equation</u> for the pipe problem, it may be rewritten as

$$-\int_y dy/(\epsilon_s/w) = \int_y (1/c)\,(dc/dy)dy = \ln (c/c_a) \tag{28}$$

or

$$c/c_a = \exp\left(-\int_y \frac{dy}{\epsilon_s/w}\right) \tag{29}$$

where y is measured from the bottom of the pipe and c_a is the local sediment concentration a distance a above the bottom of the pipe. The relative influence of pipe boundary forms on the concentration profile could be determined by comparing plots of ϵ_s/w for various pipes carrying a specific sediment.

Two particular sediment distributions will give an idea of the functional dependency of ϵ_s in an actual case. One case of Eq 29 is $c = c_a$, which implies

$$\int_y \frac{dy}{\epsilon_s/w} = 0\ . \tag{30}$$

This is true when $w/\epsilon_s = 0$, i.e., $w = 0$ and/ or ϵ_s is finite and very large. For example, inert dispersed clay or very small silt particles would give $c = c_a$ because $w \cong 0$. The same result could occur with fine sand, if $\epsilon_s >> w$. This latter case implies a rough boundary and/or a large Reynolds number inducing a large amount of turbulence.

A situation which arises more frequently, with fine sands, is a linear concentration distribution over a vertical diameter of pipeline. According to Durand (16), it occurs for nearly any smooth pipe if the mean velocity is sufficiently high, and w and σ_d are small. The standard deviation of the sediment sieve diameter is σ_d. By calculation it is possible to demonstrate that

$$\epsilon_s/w = A^1 y + A^2 D, \tag{31}$$

for a linear concentration distribution, where A^1 and A^2 are constants. The calculation can be verified by putting Eq 31 into Eq 29, integrating from a to y, using the identity $\ln A = \ln e^{\ln A}$, and carrying out the necessary algebraic operations.

Both of the above concentration distributions are significant because they represent types of profiles that are desirable in transporting sediment. Deposition will not take place until large total loads are present in any pipe boundary which can induce such profiles. Hence, in comparing boundaries satisfying Eq 31, one is essentially looking for a boundary characterized by a large ϵ_s and a small energy dissipation, for a given sediment.

Energy Considerations

The total mechanical energy per unit volume of flow complex may be defined as

$$E = \rho v^2/2 + p + \rho g y \ . \tag{32}$$

With the above definition, an expression for the rate of energy dissipation can be derived. Consider a simply-connected region of space τ fixed with respect to a coordinate system placed at some fixed point along a pipeline. The energy of a unit volume of mixture outside of the surface bounding τ is given by Eq 32. The flow of energy into τ per unit time may be written in the form

$$-\int_S E\, \underline{v}.\underline{n} da = -\int_\tau (\nabla . E\underline{v})\, d\tau \tag{33}$$

The rate of dissipation, i.e., conversion into heat, is

$$\frac{dE_T}{dt} = \frac{d}{dt}\int_\tau E\, d\ = \int_\tau \frac{\partial E}{\partial t}\, d\tau \tag{34}$$

Adding Eqs 33 and 34 and reducing to differential form,

$$\frac{\partial E}{\partial t} + \nabla . E\underline{v} = 0 \tag{35}$$

This is the basic equation for energy considerations.

The energy loss per unit volume due to the sediment is the difference in rate between a homogeneous flow and sediment laden flow. For a homogeneous incompressible fluid, with $\partial\rho/\partial t = 0$, $\nabla . \underline{v} = 0$.

Therefore, with a homogeneous fluid,

$$\partial E/\partial t = - \underline{v} \cdot \nabla E \quad . \tag{36}$$

Expanding Eq 35 for the sediment-laden flow,

$$\partial E/\partial t = -\underline{v} \cdot \nabla E - E \nabla \cdot \underline{v} \quad . \tag{37}$$

Hence, the additional energy expended per unit volume per unit time due to the sediment is

$$\delta E_h = -E(\nabla \cdot \underline{v}) \quad . \tag{38}$$

Substituting Eq 12, Eq 39 may be written as

$$\delta E_h = E \, \nabla \rho / \rho \cdot \underline{v} \quad . \tag{39}$$

From Eq 39 one has the significant conclusion that $\delta E_h = 0$ when $\nabla \rho = 0$, ρ = constant, i.e., a uniform sediment distribution. In detail, any pipeline which is capable of maintaining a uniform sediment distribution can transport sediment without additional energy dissipation per unit volume over that required to transport a liquid of the same average density.

Consider Eq 39 when $\nabla \rho \neq 0$. Substituting Eqs 14 and 32, Eq 39 may be written in the form

$$\delta E_h = \frac{1}{\rho}(p + \frac{\rho}{2} v^2 + \rho gy)(\rho_s - \rho_w) v_2 \frac{\partial c}{\partial y} = -(\frac{p}{\rho} + \frac{v^2}{2} + gy) \cdot (\rho_s - \rho_w) w \frac{dc}{dy} \quad , \tag{40}$$

replacing v_2 by $-w$.

In the analysis of the effect of various boundaries, the desirable boundary, again, would be one such that $dc/dy = 0$. The next most desirable is one corresponding to dc/dy = constant, i.e., a linear concentration profile. But in any case the energy rate is directly proportional to w and dc/dy , and inversely proportional to c . This equation also emphasizes the important role played by $\rho_s - \rho_w$. (compare sand-air and sand-water).

The integral representation is better suited to evaluating the energy dissipated over a length of pipeline. The basic equation is

$$dE_T/dt = \int_\tau \nabla \cdot E\underline{v} \, d\tau \quad . \tag{41}$$

Expanding Eq 41,

$$dE_T/dt = \int_\tau (E\nabla \cdot \underline{v} + \nabla E \cdot \underline{v}) \, d\tau \quad . \tag{42}$$

Substituting Eq 32,

$$dE_T/dt = \int_\tau (v.p\underline{v} + \nabla . \rho gy\underline{v} + \nabla . \rho v^2/2 \, \underline{v}) \, d\tau \tag{43}$$

Eq 43 is applicable whether sediment is present or not. To apply this equation to a pipeline, select a region of length along the pipe, parallel to the direction of the mean flow. Transform the second two integrals of Eq 43 into surface integrals and intergrate over the boundary surface. We find that $dE_T/dt = \int_\tau (\nabla . p\underline{v}) \, d\tau$ for the mean flow. Let s be the surface composing the ends of the region, i.e., the planes normal to the pipe axis. Then

$$\int_{\tau} \nabla \cdot p\underline{v} da = \int_{S} p\underline{v} \cdot n da = \int_{S} pv da \ , \tag{44}$$

$$dE_T/dt = \int_{s_1} pv da - \int_{s_2} pv da \ , \tag{45}$$

where s_1 is the upstream cross-sectional area of the unit pipe length and s_2 the corresponding downstream area.

For a homogeneous fluid, without sediment, retaining the second integral of Eq 44,

$$dE_T/dt = \int (p + \gamma y)\, v da$$

$$= \gamma \int (p/\gamma + y) v da.$$

From Eq 10, $p/\gamma + y$ = constant over a cross-section normal to the direction of the main flow. Therefore,

$$dE_T/dt = (p_1 - p_2)\, Q \ ,$$

which is directly proportional to horsepower, i.e., the classical result.

Comparing the flow characteristics of a homogeneous fluid to those of a sediment-laden fluid, sediment may cause the pressure distribution to be non-hydrostatic, thereby changing the rate of energy dissipation. The effect of this deviation of pressure from the hydrostatic could, conceivably, be negligible when Eq 44 is integrated over a cross-section of the pipeline. The conclusion can be drawn that a sediment-laden fluid might not dissipate more energy per unit time than a homogeneous fluid of the same average unit weight.

Analytical Definition of Total Load

Up to this point in the development, a local mean concentration c , in decimal by volume, has been used. Another definition of concentration is more significant, for example, to a dredge engineer. The dredge engineer needs a concentration which when multiplied by the discharge of mixture will give the cfs of sediment being pumped. The total load C_t defined by

$$C_t Q = G \ , \tag{47}$$

has the necessary property. To evaluate C_t in the laboratory, from concentration profiles, it is necessary to evaluate

$$C_t = (1/Q)\int c v_1 da \tag{48}$$

$$= (1/Q)\int c(y)\ v_1(y,z)\ dydz,$$

wherein time averages are assumed. The integral of Eq 48 is difficult to calculate because of the different functional dependency of c and v_1 .

By installing suitable instrumentation for measuring, C_t can be determined easily. A cross-section is needed at which

$$QC_t = \int c v_1 da = c\int_s v_1 da = cQ$$

or

$$QC_t = \int c v_1 da = v_1 \int_s c da.$$

The former case is desirable.

General Function for Dimensional Considerations

In order to study further the effects of boundary form on fine sand transport in pipes, one can resort to dimensional considerations. Often, when a purely theoretical analysis becomes so complicated as to stall progress, it is possible to extend both analytical and experimental aspects of the problem dimensionally. This section is intended to set up the function from which can stem dimensional analysis of any specific point of the general problem.

Variables entering the study are of four types; those describing the fluid, the sediment, the flow, and the geometry. The significant fluid variables are ρ_w, μ, and γ_w. The sediment can be fully characterized by ρ_s, d, σ_d, γ_s and sf. Flow variables are V, $\underline{v}$, C_t, c, and J. The geometry of the several pipes can be characterized by D and $\emptyset$ (boundary).

Some discussion of the variables is in order. All terms, that have a time associated, are time averaged, i.e., turbulent fluctuations have not been included, as indicated earlier. The reason for this is that existing equipment for water channels is not capable of accurately determining such short duration phenomena. The hydraulic gradient J is an average value characterizing the entire cross-section. It is extremely important to remember that not all the variables listed are independent. This point will be treated in detail as the need arises. The boundary parameter $\emptyset$ is made up of those geometric parameters necessary to describe the boundaries. All considerations are with respect to a horizontal pipe.

A coordinate system satisfying

$$e_i \cdot e_j = \delta_{ij}$$

is assumed. The axis along e_i will correspond to x_1, and v_1 will be along this axis. Let $\underline{r} = \sum_i^3 x_i e_i$.

Bringing the variables together in one functional relationship,

$$\psi(\underline{r}, \rho_w, \mu, \gamma_w, \rho_s, d, \sigma_d, sf, V, \underline{v}, C_t, c, J, D, \emptyset) = 0. \quad (49)$$

From this equation will stem dimensional analysis for the several specific points to be studied.

One should observe in the following development that ψ is a symbol denoting an arbitrary function, and is not the same function throughout the chapter.

One-Dimensional Analysis

The equation

$$J = \psi(\rho_w, \mu, \gamma_w, \rho_s, d, \sigma_d, sf, V, C_t, D, \emptyset)$$

is the starting point for a one-dimensional analysis. Observe that the sediment is sufficiently characterized by ρ_s and d. Therefore,

$$J = \psi(\rho_w, \mu, \gamma_w, \rho_s, d, V, C_t, D, \emptyset). \quad (50)$$

The variables in Eq 50 can be arranged into significant dimensionless groups by selecting ρ_w, V, and D as repeating variables. The resulting function is

$$J = \psi\left(\frac{VD\rho_w}{\mu}, \frac{V}{\sqrt{\frac{\gamma_w}{\rho_w} D}}, \frac{\rho_s}{\rho_w}, \frac{d}{D}, C_t, \frac{\emptyset}{D}\right).$$

For the work reported herein, ρ_s/ρ_w and d/D are constants. Therefore,

$$J = \psi(Re\ ,\ V/\sqrt{gD}\ ,\ C_t\ ,\ \emptyset/D)\ . \tag{51}$$

Eq 51 contains the significant dimensionless groups which form the basis of analysis for specific one-dimensional problems. Of course they can be multiplied or added to one another as desired, and used in conjunction with explicit auxiliary equations.

The resistance problem will be considered first. If sediment were not present, Eq 51 would reduce to

$$J = \psi(Re\ ,\ V/\sqrt{gD}\ ,\ \emptyset/D) \tag{52}$$

Ample evidence by earlier investigators has demonstrated that the form

$$\frac{J}{V^2/2gD} = \psi(Re\ ,\ \emptyset/D)$$

fully represents the data for a homogeneous fluid flowing in pipes.

The expression $J2gD/V^2$ is known as the Darcy-Weisbach resistance coefficient f. Assume a similar solution for the present case. Then

$$f = \psi(Re\ ,\ C_t\ ,\ \emptyset/D)\ . \tag{53}$$

Eq 53 is suitable for a fundamental study of the one-dimensional resistance characteristics of pipes carrying sediment; so long as there are no stationary or quasi-stationary deposits on the bottom of the pipe. If deposits exist, then a new definition is needed for $\emptyset$. In this report

only suspended flow is of interest. Therefore, when C_t is such that $\emptyset = \emptyset(c)$, this fact will be expected to show up as a deviation from Eq 53.

The f-Re diagram, with $\emptyset/D$ and C_t as additional variables, seems the best procedure to use in analyzing these data. A curve for each $\emptyset/D$ can be expected for those data which correspond to $C_t = 0$. Then, as C_t is increased, the effect of C_t can be added as a fourth variable. The $\emptyset/D$ used here is somewhat analagous to the Nikuradse relative smoothness r_o/k for uniform sand grain roughness.

A from of Eq 53, which has been used frequently, results from substituting the definition for f and rewriting the equation in the form

$$J = V^2/2gD\ \psi(Re\ ,\ C_t\ ,\ \emptyset/D)\ .$$

Taking the logarithm of this,

$$\log J = 2\ \log(V/\sqrt{gD}) + \log\ \psi\ . \qquad (54)$$

Study of Eq 54 reveals that, if Re and C_t do not have any influence, a log-log plot of log J versus log $V/\sqrt{gD}$ will be a straight line with an intercept depending on the boundary form, since $\emptyset/D$ is a constant for each. This is exactly the case for turbulent flow in hydrodynamically rough pipes, when $C_t = 0$. Then Eq 54 can be written

$$\log J = 2\ \log\left(V/\sqrt{2gD}\right) + \log\ \psi\ (\emptyset/D) \qquad (55)$$

For rough pipes, the procedure in applying Eq 55 is to make one plot for each $\emptyset/D$, then vary C_t and see if there is any deviation from the

straight lines of $C_t = 0$. While Eq 55 is dimensionless and fundamentally sound, work with $C_t = 0$ is still being presented by most experimenters in the dimensional form log J versus log V . For comparative purposes, the J-V diagram will also be used.

Two of the classic resistance equations for the study of roughness, which can be found in an elementary text on fluid mechanics, are given for reference purposes:

Karman-Prandtl (smooth pipes)

$$1/\sqrt{f} = 2 \log(Re\sqrt{f}) - 0.8 , \tag{56}$$

Karman-Prandtl (rough pipes)

$$1/\sqrt{f} = 2 \log(r_o/k) + 1.74 . \tag{57}$$

Analysis of incipient deposition can be carried out with Eq 51 as a basis. Since D is a constant throughout the study, it is only a dimensional constant in Re and $V/\sqrt{gD}$. As far as studying deposition is concerned, the principal influence of the viscosity μ is its effect on the particle fall velocity. That w need not be considered is evident by noting that d/D , as used in place of w/V , was constant and could be dropped from the beginning. This reduces to Re and $V/\sqrt{gD}$ both being velocity parameters. For convenience (computation for example), the latter parameter is retained. Then Eq 51 becomes

$$J = \psi (V/\sqrt{gD} , C_t , \emptyset/D) . \tag{58}$$

As will be seen later (Fig. 8, chapter VI) for the range of $V/\sqrt{gD}$ studied, C_t is probably not important in $f = \psi (C_t , \emptyset/D)$ until deposition begins.

Using this knowledge, Eq 58 can be written as

$$V/\sqrt{gD} = \psi (C_t , \ \emptyset/D) , \tag{59}$$

which should apply as a deposit is forming as well as when $C_t = 0$.

Let V_L denote the velocity at which deposition begins for a given C_t and $\emptyset/D$. The equation for study of incipient deposition is, therefore,

$$V_L/\sqrt{gD} = \psi (C_t , \ \emptyset/D) . \tag{60}$$

A <u>horsepower function</u> is needed in order to make designs and economic comparisons of the effects of boundary form on sediment transport. For reasons to be pointed out in Chapter VI, the most efficient operation corresponds to operating, for a given J and $V/\sqrt{gD}$, at the C_t of incipient deposition. A fundamental parameter in design is the dimensional form HP, horsepower per unit length of pipe.

By definition,

$$HP = Q \gamma J/550 \tag{61}$$

Assuming $\gamma = \gamma_w$,

$$HP \propto Q \gamma_w J$$

Using Eqs 47, 50, 58, and 60, the equation for studying comparative horsepower, at the point of most efficient operation, is

$$HP = \psi (G , \ \emptyset/D) . \tag{62}$$

This is a dimensional equation. It represents the horsepower per unit length of pipe required to transport G cfs of sediment at the most efficient operating point; what a design or costs engineer needs. However, to complete the study, a plot of Eq 47 ($QC_t = G$) needs to accompany the plot of Eq 62. In this way the amount of water transported, which has to be disposed of, is brought into the analysis. The real significance of these equations will be brought out in Chapter VI.

Analysis of Internal Mechanics

Study of the mechanics of what is happening inside the pipeline, on a local scale, is a somewhat different problem than the one-dimensional analysis. Eq 49, repeated below, is the beginning point for a study of concentration profiles, local deposition, secondary circulation, diffusion coefficient, or the Kármán K.

$$\psi(\underline{r}, \rho_w, \mu, \gamma_w, \rho_s, d, \sigma_d, sf, V, \underline{v}, C_t, c, J, D, \emptyset) = 0 \quad . \tag{49}$$

Significant dimensionless groups can be derived by again using V, ρ_w, and D as repeating variables. The dependent variable will be the local concentration c. The sediment shape factor is constant, and hence unnecessary to retain. Therefore,

$$c = \psi\left(\sum_i x_i/De_i, Re, V/\sqrt{gD}, \sigma_d/D, \rho_s/\rho_w, d/D, \sum_i v_i/Ve_i, C_t, J, \emptyset/D\right) \quad . \tag{63}$$

The parameters σ_d/D, ρ_s/ρ_w and d/D are constants; therefore,

$$c = \psi \left(\sum_i x_i/De_i \ , \ \ Re \ , \ \ V/\sqrt{gD} \ , \ \ \sum_i v_i/Ve_i \ , \ \ C_t \ , \ \ J \ , \ \ \emptyset/D \right).$$

While c is dimensionless, its numerical number will depend on whether it is computed as percent by weight or percent by volume. The parameter c/C_t can be used to eliminate this. A further reason why this latter parameter is meaningful is that all concentration profiles are reduced to a common base.

Application of Eq 51 makes it possible to drop Re or J, which ever seems more convenient.

The two basic forms for specific problems are,

$$c/C_t = \psi \left(\sum_i x_i/De_i \ , \ \ Re \ , \ \ V/\sqrt{gD} \ , \ \ C_t \ , \right.$$

$$\left. \sum_i v_i/Ve_i \ , \ \ \emptyset/D \right) \qquad (64)$$

or

$$c/C_t = \psi \left(\sum_i x_i/De_i \ , \ \ J \ , \ \ V/\sqrt{gD} \ , \ \ C_t \ , \right.$$

$$\left. \sum_i v_i/Ve_i \ , \ \ \emptyset/D \right) \qquad (65)$$

Auxiliary equations can be introduced as necessary.

Analysis of <u>horizontal concentration profiles</u> requires only the z/D part of $\sum_i x_i/De_i$. The $\sum_i v_i/Ve_i$ are extra dependent variables. Eqs 64 and 65 become

$$c/C_t = \psi \left(z/D \ , \ \ Re \ , \ \ V/\sqrt{gD} \ , \ \ C_t \ , \ \ \emptyset/D \right) \ , \qquad (66)$$

and

$$c/C_t = \psi \left(z/D \ , \ \ J \ , \ \ V/\sqrt{gD} \ , \ \ C_t \ , \ \ \emptyset/D \right) \ . \qquad (67)$$

These equations are still very complex. To simplify them, use can be made of the same argument followed in deriving Eq 58. Thus,

$$c/C_t = \Psi(z/D \ , \ V/\sqrt{gD} \ , \ C_t \ , \ \emptyset/D) \ . \tag{68}$$

Eq 68 is fundamental for studying horizontal concentration profiles.

For cases in which secondary circulation was not present in any form, one could expect that c/C_t would not depend on z/D . In such a circumstance the profiles could be reduced to a universal function if C_t was replaced by C' , the arithmetic average concentration over z . Assuming such, the universal profile would be

$$c/C' = 1.0 \ . \tag{69}$$

Vertical concentration profiles can be studied and interpreted by Eq 68, with z/D replaced by y/D . Thus,

$$c/C_t = \Psi(y/D \ , \ V/\sqrt{gD} \ , \ C_t \ , \ \emptyset/D) \ . \tag{70}$$

A simplification such as Eq 69 is not possible in this case. However, there is an excellent possibility for simplication in the variable C_t . For a given y/D , $V/\sqrt{gD}$, and $\emptyset/D$, C_t can be dropped if the standard deviation σ_d of the sediment is very small, or the boundary is very rough. For this case Eq 70 becomes

$$c/C_t = \Psi(y/D \ , \ V/\sqrt{gD} \ , \ \emptyset/D) \ . \tag{71}$$

In presenting data by Eq 70 and 71, the procedure would be to use c/C_t as the ordinate on a c/C_t versus y/D plot. However, physical interpretation is much easier if y/D is the ordinate and c/C_t the abscissa.

The functional equations for such a study are, from Eq 65 and using the arguments for deriving Eq 58,

$$\sum_i v_i/Ve_i = \psi\left(\sum_i x_i/De_i \ , \ V/\sqrt{gD} \ , \ C_t \ , \ \emptyset/D\right) . \qquad (73)$$

These equations are very difficult to treat experimentally. The complications in velocity profile analysis can be visualized by comparing Eq 73 to the two dimensional case, i.e.,

$$v_1/V = \psi\left(y/D \ , \ V/\sqrt{gD} \ , \ C_t \ , \ \emptyset/D\right) . \qquad (74)$$

The functional dependence of the diffusion coefficient ϵ_s is, from Eq 72,

$$\epsilon_s/wD = \psi\left(y/D \ , \ V/\sqrt{gD} \ , \ C_t \ , \ \emptyset/D\right) . \qquad (75)$$

In the theoretical analysis some discussion was given on the type of distribution of ϵ_s that was desirable from the standpoint of economical sediment conveyance lines. In Eq 74 are given the variables which would enter. It is not proposed to study this problem intensively, but only to present the procedure which can be used in later research employing a given sediment.

A logical method to use in analysis of data on the diffusivity coefficient is to construct a dimensionless plot of ϵ_s/wD versus y/D for each $\emptyset/D$. The first step would be to assume $V/\sqrt{gD}$ and C_t secondary. Then, if necessary, introduce $V/\sqrt{gD}$ and subsequently bring in C_t.

Local incipient deposition can be analyzed by means of Eq 70. In studying this problem, the logical procedure is to pick a value of y/D as near to zero as sampling equipment could conveniently take data. Then, for each $\emptyset/D$ to be studied, a plot of

$$c/C_t = \psi\,(C_t\ ,\ \ V/\sqrt{gD}) \tag{72}$$

would be significant, at least for sand sediments in water. This would not apply after much of a bed was formed, however, because $\emptyset/D$ would no longer be constant.

The function, Eq 72, is very important because it indicates the possibilities of an absolute criterion for incipient deposition, a problem so far unanswered and which has made it difficult to bring the results of different scientists together. For $\emptyset/D$, y/D constant, a little thought will lead one to conclude that a plot of c/C_t versus C_t for each $V/\sqrt{gD}$ studied must reach a maximum if σ_d enters the problem (smooth pipe). A maximum of c/C_t need not exist in a rough pipe, but probably a constant value will persist from zero concentration up to incipient deposition. Deposition would be indicated by a rapid decrease of c/C_t with increase in C_t . Using the maximum magnitude, or the departure from a constant magnitude, would constitute an absolute criterion, applicable at least for sands in water and similar problems.

Study of the effect of secondary circulation is actually an analysis of velocity profiles, somewhat beyond the scope of this dissertation. However, because one boundary was tested which did induce pronounced helical flow along the boundaries, the basic equations necessary for an analysis of this problem are presented.

Summary

Summary of theoretical and dimensional considerations can be divided into three sections: 1) theoretical analysis, 2) one-dimensional analysis, and 3) internal mechanics.

Theoretical analysis introduced the classical equations of hydrodynamics, and interpreted them for a sediment-laden flow.

The general continuity equation for sediment distribution in a fluid media was derived. It was found that the special case $cw + \epsilon_s \, dc/dy = 0$ was applicable to pipes. Analysis indicated that a large ϵ_s/w, or ϵ_s/w a linear function of distance from the wall, was most desirable.

Energy considerations on the transport of sediment in suspension led to the conclusion that any change in horsepower over that required to pump a fluid of the same average density was due to the sediment causing the pressure distribution to deviate from the hydrostatic.

One-dimensional analysis can be summarized by giving the fundamental functions derived for each special problem involved in the transport of a single size of sediment through the 12-in. pipes studied.

1. Resistance problem

$$f = \psi(Re, C_t, \phi/D) \qquad \text{Eq 53}$$

$$\log J = 2 \log(V/\sqrt{gD}) + \log \psi(C_t, R_e, \phi/D) \qquad \text{Eq 55}$$

2. Incipient deposition

$$V_L/\sqrt{gD} = \psi(C_t, \phi/D) \qquad \text{Eg 60}$$

3. Horsepower function

$$HP = \psi (G , \ \emptyset/D) \qquad \text{Eq 62}$$

$$C_t = G/Q \qquad \text{Eq 47}$$

Analysis of internal mechanics follows the same pattern as one-dimensional analysis.

1. Horizontal concentration profiles

$$c/C_t = \psi (z/D , \ V/\sqrt{gD} , \ C_t , \ \emptyset/D) \qquad \text{Eq 68}$$

$$c/C' = 1.0 \qquad \text{Eq 69}$$

2. Vertical concentration profiles

$$c/C_t = \psi (y/D , \ V/\sqrt{gD} , \ C_t , \ \emptyset/D) \qquad \text{Eq 70}$$

3. Local incipient deposition

$$c/C_t = \psi (C_t , \ V/\sqrt{gD}) \qquad \text{Eq 72}$$

4. Secondary circulation

$$\sum_i v_i/Ve_i = \psi (\sum_i x_i/Ve_i , \ V/\sqrt{gD} , \ C_t , \ \emptyset/d) \qquad \text{Eq 73}$$

5. Diffusion coefficient

$$\epsilon_s/wD = \psi (y/D , \ V/\sqrt{gD} , \ C_t , \ \emptyset/D) \qquad \text{Eq 75}$$

These equations constitute the basis of the analysis in Chapters VI and VII.

One term which recurs frequently is $V/\sqrt{gD}$. This should not be interpreted as a Froude number. It is a special form of $V^2/2g/D$, employed for convenience throughout the analysis.

Chapter IV

EXPERIMENTAL EQUIPMENT AND PROCEDURE

Study of the effect of pipe boundary on the transport of fine sand was carried out by using 12-in. diameter Hel-Cor, smooth and standard corrugated pipes. The equipment consisted of a continuous recirulation system, sediment sampling devices, velocity and discharge measuring equipment, and a bank of piezometers along the test pipe. One size of sediment was used.

The procedure was to put a fixed volume of sediment into the system and then make measurements of velocity, sediment concentration, discharge of mixture, piezometric head gradient, total sediment load and temperature, for several discharges. The volume of sand in the recirculation system was then changed and the technique repeated, with some variation, from pipe to pipe.

One boundary was tested over the full range of variables before another pipe was installed for investigation.

Experimental Equipment

The experimental equipment was located along the north side of the Hydraulics Laboratory at Colorado A and M College, Fort Collins, Colorado. A jet-pump was built initially to circulate the sediment-water mixture. After discarding the jet-pump principle, an old horizontal centrifugal pump was installed. The three pipes with different boundaries were provided by Armco Drainage and Metal Products, Inc. The sediment was

a natural sand and the discharge of mixture was measured by means of a 10-in. orifice. Total load data were taken at the same orifice. Temperature of the mixture was recorded frequently. Piezometer taps were located at 10-ft intervals along the test section. Velocity data for determining sampling time for local concentration determinations were taken by means of the same instrument used for taking sediment samples.

The first recirculation system was a 100-horsepower motor delivering sediment free water to a 2.5-in. diameter jet discharging vertically into an 8-in. tube, with the jet and pickup submerged in a sediment-laden catch basin at the downstream end of the test pipe. The necessary water to pump through the jet was obtained by putting a screen in such a position that the sediment, and majority of the mixture, remained in the proximity of the jet, but sufficient clear water passed through the screen to operate the jet.

While the principle of the equipment was sound, it was found unsatisfactory in this case because of the high operating head required, impracticability of separating the fine sand from the mixture by screening, too much sediment storage in the system, extreme vibration of the 8-in. pick-up tube, and the excessive noises associated with the operation of the jet.

The recirculation system employed consisted of a 10-cfs horizontal centrifugal pump driven by a 35-horsepower 870-rpm electric motor. The pump discharged vertically into a 12-in. line. The fluid passed through a 10-in. orifice, made a right angle turn to the horizontal and expanded into a 14-in. smooth pipe. Passing through 48 ft of horizontal line, it discharged vertically downward into a 14-in. to 12-in. reducer,

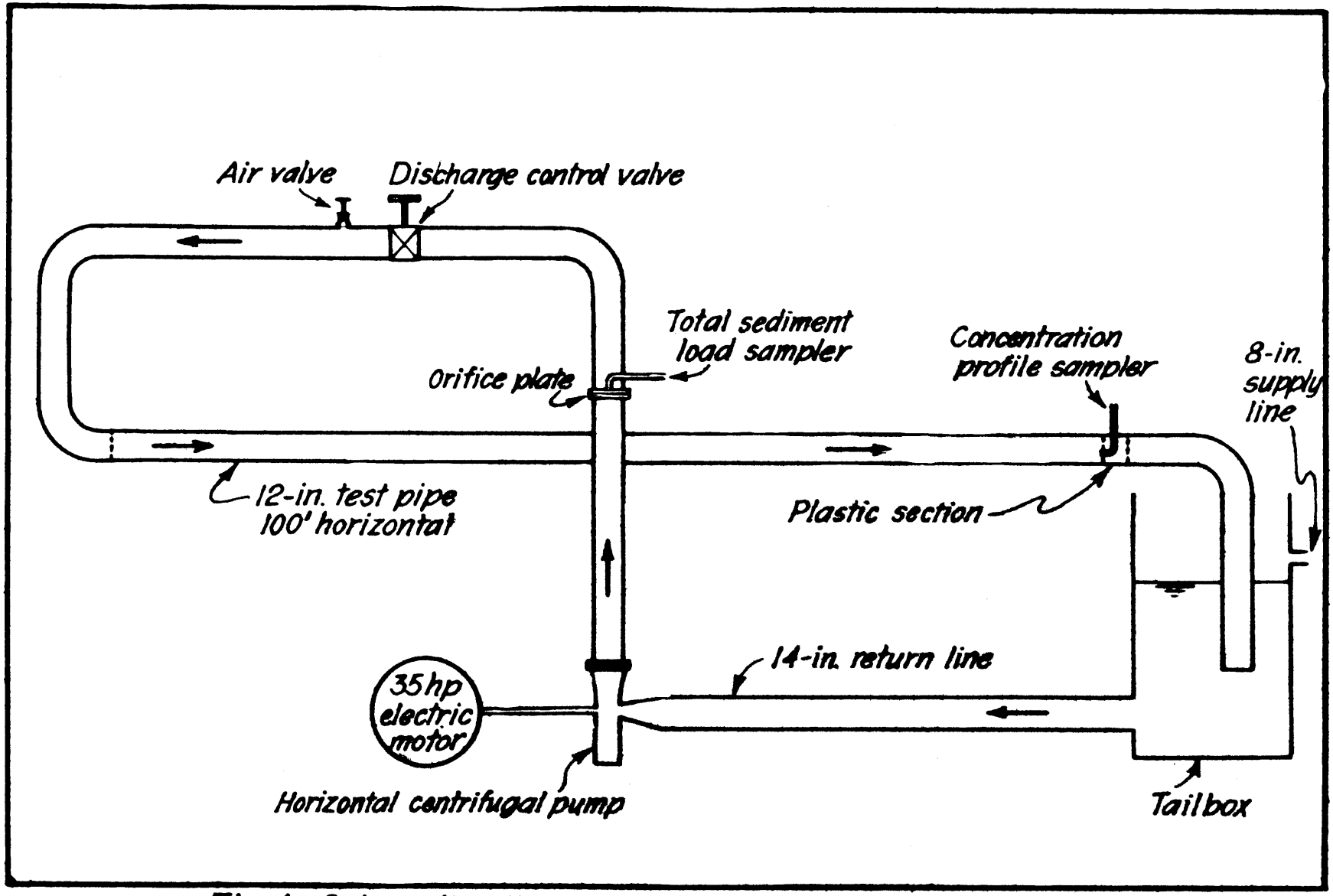

Fig. 1 Schematic diagram of the recirculation system.

and then entered the 100-ft test section. The mixture emptied into a 4-x 4-x 7-ft deep sump at the downstream end of the test pipe.

The fluid traveled from the sump through a horizontal, 40-ft long, 14-in. smooth pipe to the suction side of the pump.

The installation was satisfactory, with two exceptions. The 14-in. smooth return pipe stored large quantities of sediment when low velocities were being used, making it difficult to control the mean transport concentration in the 12-in. test pipes. The other difficulty was that the temperature of the sediment-water complex increased continuously during a run; because of the small volume of fluid being recirculated. The temperature problem was partially controlled by continuously introducing cold water into the pump bearing.

Fig. 1 is a schematic diagram of the recirculation plant that was used for the tests reported herein.

Boundary forms tested were three in number, all nominally 12 in. in diameter. Fig. 2 summarizes the physical characteristics of the pipes. The 12-in. Hel-Cor pipe was zinc coated inside and out. It had a continuous lock seam joint. The corrugations had a pitch, or wave length, of 0.167 ft. The amplitude of the corrugations was $\pm$ 0.0185 ft, measured from the mean elevation. To complete the corrugations, circular arcs with a radius of 0.0370 ft are joined by straight tangent sections. The helix angle, measured from a line drawn along the outer extremity of the pipe parallel to the pipe axis to the tangent of a corrugation, is $11\ \pi/30$ radians.

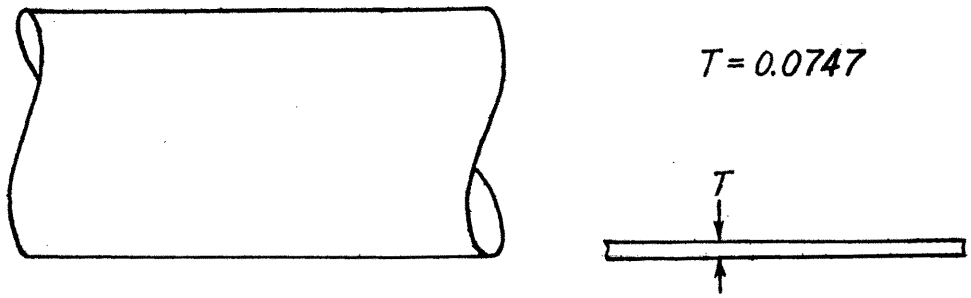

12-in. Smooth Pipe

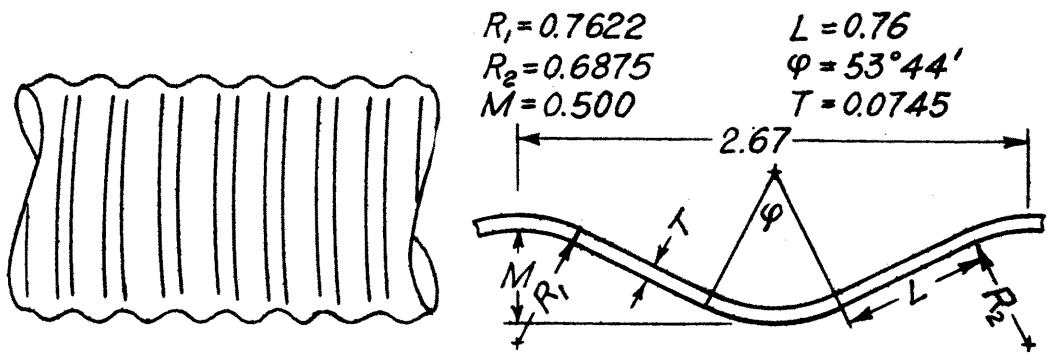

12-in. Standard Corrugated Pipe

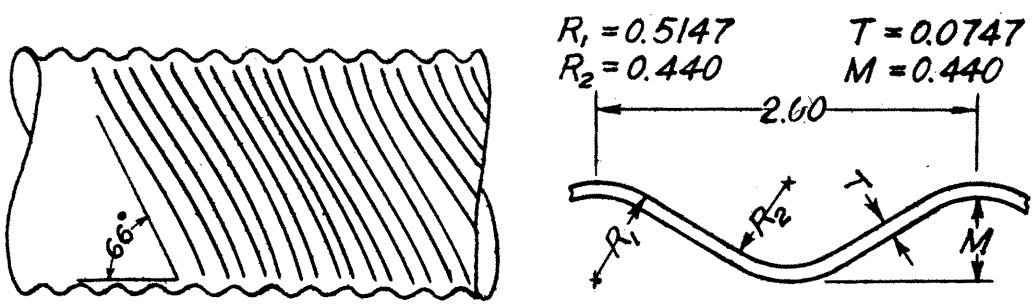

12-in. Hel-Cor Pipe

Note:
All length dimensions are in inches.
Section views are normal to corrugation.

Fig. 2 Details of boundary forms

The 100-ft test length of Hel-Cor pipe had two field weld joints and two victaulic couplings along its length. One victaulic coupling was in the downstream 75 ft of length. The inside clear diameter of the pipe was 12.1 $\pm$ 0.03 in., as measured with inside calipers; this measurement is the average of ten trials.

The 12-in. diameter standard corrugated pipe, also 100 ft long, was zinc coated. It was of close-riveted construction, with all seams soldered on the outside to prevent leakage. The corrugations had a pitch of 0.222 ft along the axis of the pipe. The maximum corrugation amplitude from the mean was 0.0208 ft. The crests and troughs were circular arcs with an included angle of approximately 11 π/30 radians and a radius of 0.0573 ft. Straight tangent sections jointed the circular arcs.

The five 20-ft sections of corrugated pipe were connected by slipping a one-ft long section of corrugated pipe over the joint formed by butting two sections together. This band was then welded to the pipe, making a continous pipeline. The inside clear diameter was 12.1 $\pm$ 0.03 in., measured with inside calipers.

The smooth pipe was of uncoated steel, formed in 20-ft sections by rolls, and had a longitudinal welded seam. The 20-ft sections were field welded to form the 100-ft test pipe. The inside diameter of 12.0 $\pm$ 0.03 in., was an average of ten readings.

Sediment for the tests was obtained from a delta formed in the Lake Loveland Reservoir by a supply canal discharging into the lake. The reservoir is located at Loveland, Colorado. Sieve analysis and fall velocity determinations are given in Chapter V, Preliminary Studies. Brief study under a microscope revealed that about 50 percent of the sand particles

were quartz grains, 40 percent flakes of mica (mostly biotite), and the other 10 percent consisted of a variety of minerals, predominately orthoclase.

Measurement of discharge of the mixture was accomplished by means of a 10-in. diameter sharp-edged orifice located in the 12-in. pump discharge line. It was located about 7 ft downstream from the pump. The mixture discharged vertically upward through the orifice, thus all the sediment present was in suspension.

The taps for measuring the differential head across the orifice were located about 0.10 ft on either side of the plate. They were connected to a water manometer, via some sand traps installed in each line. Measurements could be made to $\pm$ 0.001 ft. The actual accuracy was probably somewhat less due to fluctuations of the water columns.

The orifice calibration curve for clear water was used throughout the duration of the studies. Durand (19) pointed out in 1952 that the presence of the sand has little effect on the calibration curve, for sediment concentrations less than 20 percent by volume, of fine non-cohesive sand. This point is discussed further in Chapter V.

Temperature was determined by a centigrade thermometer partially submerged in the fluid. It was located in the tailbox section.

The piezometer system for recording the hydraulics gradient differed somewhat for each boundary. Taps were installed on the corrugations at the point nearest to the axis of the pipe in every case. Some taps were installed on the troughs of the corrugations of the corrugated pipe in order to check the effect of location.

There were ten taps on the Hel-Cor pipe, spaced at 10-ft intervals starting about twelve diameters from the downstream end of the straight section of test pipe plus diverting pipe, or five diameters upstream from the end of the test pipe. The taps were located on the corrugation troughs, to an observer outside the pipe. The openings into the pipe were 1/16 in. The taps were located on a horizontal plane through the axis of the pipe.

The piezometer taps on the smooth boundary were eight in number. They were spaced at 10-ft intervals, beginning about twelve diameters from the end of the straight pipe. The openings were placed on a horizontal diameter. The orifice had a diameter of 3.64 in. This small hole led to a 0.25-in. brass tube 1 in. long that was soldered to the outside of the pipe wall. Plastic tubes from the manometer bank were connected to the 0.25- in. tubes, via a sand trap to be described later.

Two sets of piezometer taps were placed on the 12-in. standard corrugated pipe. A set of seven taps was located in the corrugation troughs and a set of five taps on the crests. The group of seven taps was used as a base, placed at 10-ft intervals as on the other boundaries. The five piezometer taps were located on the crests nearest to the troughs having taps.

Sand traps were placed at each piezometer station. A 0.5-ft length of 3/16 in. ID Mayon plastic tubing connected each piezometer tap to a sand trap. Each trap was a glass bottle with a volume of about 1/2 pint. The rubber stopper sealing the top of the bottle had three openings;

one for the piezometer tap connection, another for releasing air bubbles, and the third for connection to the manometer bank.

The manometer was made of 14 glass tubes, each 4 ft long. The inside diameter was about 6 mm. The instrument for reading the manometer was a fine wire hairline attached to a T-frame which slid in a groove along the center of the manometer board. Accuracy of reading was of the order of $\pm$ 0.003 ft of water.

A clamping system was devised to facilitate reading the manometer. This device instantaneously clamped all 14 tubes so no fluid could flow -- which permitted rapid reading of the bank of piezometers.

The velocity profile equipment was not satisfactory as first designed. It consisted of two 1/8-in. OD brass tubes, one for recording ambient pressure and the other used as a stagnation tube. One tube was recessed into each side of the sediment concentration sampling tube. The point where the pressure was taken was, for each tube, 0.75 in. from the centerline of the 0.25-in. sampler opening. It was parallel to the direction of the mean velocity. This calibrated, non-standard, pitot tube was not practical to use because a single grain of sand was sufficient to plug it. Furthermore, because the small diameter tube had to be about 3 ft long, the pitot was extremely slow to respond to changes in velocity. The entire apparatus was discarded as impractical for its contemplated application.

The principal function of the velocity profiles was to enable one to compute the desired sampling time (or velocity) at a given location along a diameter of the test section. For reasons to be presented in

Chapter V, extreme accuracy was not necessary. Therefore, the ambient and stagnation pressures necessary for computing the local velocity were measured by approximate means. Ambient pressure was indicated by a 3/16-in. tap in the wall of the smooth plastic section housing the sediment sampler. The 1/4-in. ID opening of the sampler was used to measure the stagnation pressure. A coefficient of velocity, depending on concentration, was determined for each run. Readings were taken from an open piezometer containing clear water.

The sampling equipment to obtain a concentration profile included an intake tube, siphoning and pumping equipment, sampling cones, stop watch, and oven-drying and weighing apparatus. The equipment employed is shown in Fig. 3.

The intake tube extended 5 in. upstream from its support normal to the direction of flow. It was made of 1/2-in. OD by 1/4-in. ID brass tubing. The nozzle section was 4 in. long, tapering to a sharp edge at the inlet.

The sediment samples ordinarily were taken by siphoning. A small horizontal centrifugal pump was used when insufficient piezometric head was available for siphoning. The pump was not used unless absolutely necessary because of its unsteady discharge characteristics.

The samples were collected in one-litre, graduated Imhoff sediment cones.

The stop watch, the oven for drying, and the balance for weighing the samples were standard laboratory equipment.

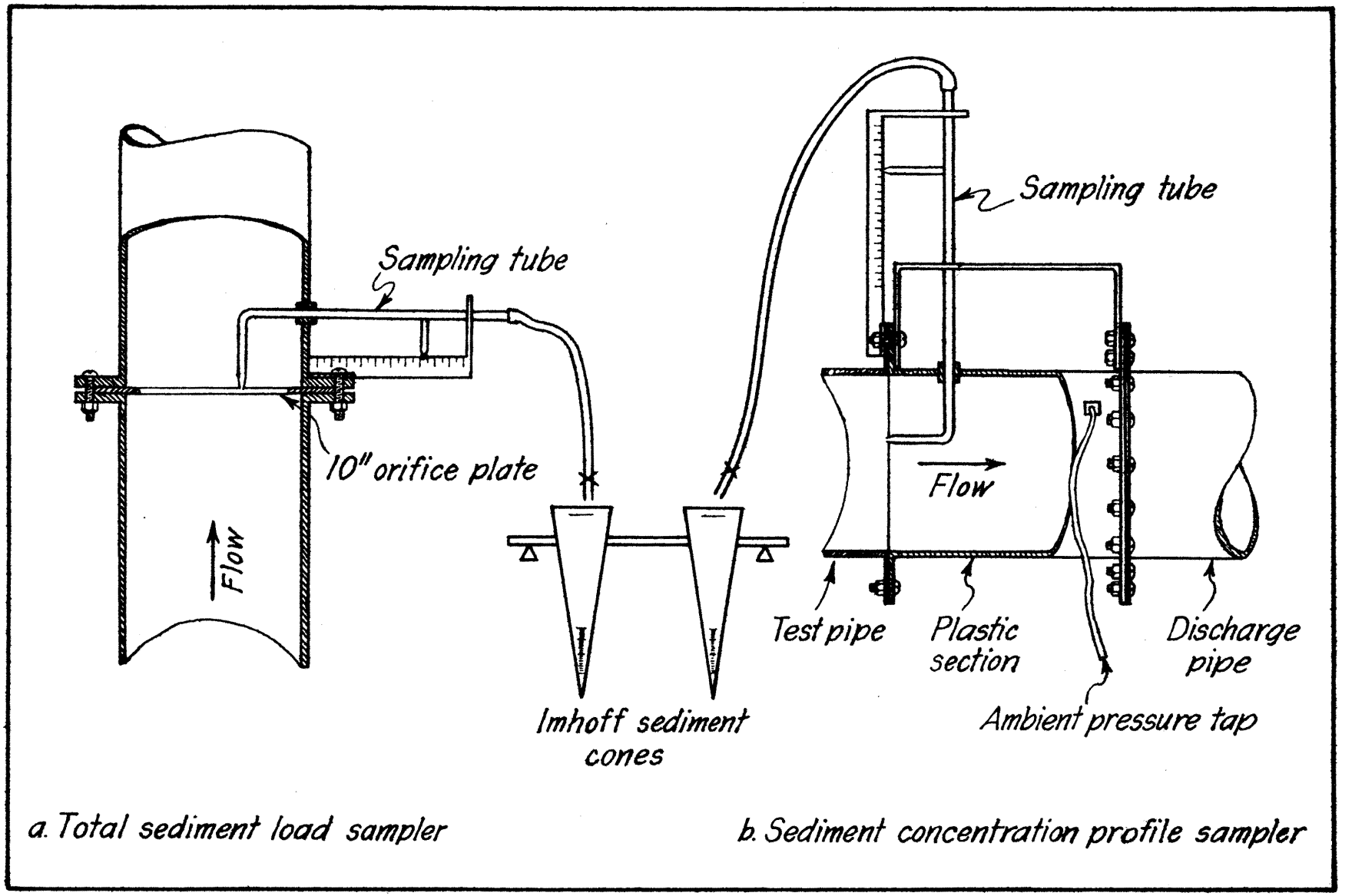

Fig. 3 Schematic diagram of sampling equipment.

Total load sediment samples were taken at the downstream edge of the 10-in. orifice, as illustrated in Fig. 3. The sampling tube had a sharp edge opening 1/4 in. in diameter projecting upstream parallel to the direction of the mean flow.

Samples were taken by siphoning. The rate of sampling was controlled by a pinch clamp on a discharge line made of plastic tubing, and by changing the elevation of the tube outlet. The samples were taken at several locations along two diameters which were at right angles to each other.

Experimental Procedure

The experimental procedure was directed toward collecting data on the mean values of mixture discharge, sediment discharge, energy loss, local mean velocity, and sediment concentration. Additional information required for analysis of the data were periodic sieve analyses of the sediment, velocity and concentration at the total load sampling station, and oven-dry weights of a number of sediment samples.

General operating procedure was to first make a few runs without sediment -- at which time discharge and head loss along the pipeline were recorded. Then a small amount of sediment was added to the system and a range of discharges was repeated -- this time measuring mixture discharge, head loss and total load, and concentration along the vertical and horizontal diameters of the test pipe. After completing such a series, more sediment was added and the process repeated until concentrations were such that deposition occurred. If deposition took place at a given discharge of mixture, that discharge was not used when more sediment was present to the system.

Discharge of mixture was measured with the 10-in. calibrated orifice by reading the manometer four times at ten to fifteen minute intervals during each run.

In determining the hydraulic gradient for a run, all piezometers were clamped simultaneously, read and unclamped. This was repeated four times at roughly fifteen minute intervals for each test. It is believed that repeated readings taken in this manner, and averaged, gave an accurate measure of energy loss.

The manometer was read to $\pm$ 0.003 ft of water, which was sufficiently accurate for determination of the Darcy-Weisbach resistance coefficient.

Total sediment load data were taken for all runs in which there appeared a possibility of deposition. Furthermore, with the smooth pipe, they were taken for every run which had sediment present.

The procedure was first to determine the sampling time required to fill a one-litre sediment cone. Samples were then siphoned at several locations along two normal diameters of the orifice. Five samples were taken at each traverse of a diameter. At least duplicate, and sometimes as many as four, traverses were made along each diameter for each run.

Velocity versus concentration data at the 10-in. orifice were taken in conjunction with the regular runs, on the smooth pipe. During these runs the total load sampler was also used as a stagnation tube. These data were taken for several discharges and sediment concentrations.

Concentration profiles in the 12-in. test pipes were made in the horizontal and vertical directions for each total load. Samples were taken at 0.100-ft intervals along the traverse. To determine the required

time to obtain a 1000-ml sample through a 1/4-in. ID sampler, sampling at the ambient velocity, a velocity profile was first made. This gave a "computed sampling time" for each sampling point. Then samples were taken repeatedly until three samples were obtained such that the average "measured sampling time" was nearly the same as the computed time. Any individual sample for which the measured sampling time differed from the computed by more than 5 percent was rejected.

Siphoning was much easier, faster and more accurate than pumping. The siphon was controlled very closely by a clamp and varying the elevation of the siphon outlet. The pump (of about 1/50 HP) tended to surge.

The samples were collected in 1000-ml cones, tapped three or four times by hand, and left to settle for a few moments. The apparent volume of sediment in ml was then read and recorded. The cones were emptied, washed and drained in readiness for reuse. However, periodically a few samples were retained for oven drying and sieve analysis.

With the Hel-Cor pipes, the first one tested, duplicate concentration profiles were frequently made. This was found unnecessary, and was discontinued when testing the smooth and standard corrugated pipes.

Sediment cone calibration data were obtained by retaining a sample periodically. All of these samples were oven dried and weighed on analytical balances.

A record was kept of the date, the run number, and the position in the concentration profile where each sample was obtained.

A periodic sieve analysis was performed, to determine whether the mean size of the sediment was changing due to recirculation. The samples used for this purpose were picked, essentially at random, from the

ones used in calibrating the sediment cone. Standard shaking procedure was used and the material retained on each sieve was weighed on an analytical balance.

The data for each sieve analysis were plotted on "log-probability" paper. Median size and average standard deviation were taken from this plot for each sample analysed.

Chapter V

PRELIMINARY STUDIES

A number of preliminary studies were conducted before proceeding with the main problem. These preliminary studies were: 1) measurement of the discharge of mixture, 2) determining the sampling time interval, 3) rapid determination of the local sediment concentration 4) description of the one sediment used, 5) method of determining the total sediment load, and 6) effect of piezometer location along corrugations.

Measurement of Discharge of Mixture

Measurement of discharge of the sediment-water mixture hinged on determining whether any of the common rate-of-flow devices used in clear water hydraulics could be applied; or if not, what simple, rapid and economical technique could be used.

Durand (19), employed a special orifice meter in the shape of a whistle. The particular shape apparently was chosen because the devise was usually installed on the end of a pipeline; the whistle-like contraction avoiding separation of the fluid jet from the top of the pipe outlet. Careful calibrations with ashes, fine and course sands, gravels and iron demonstrated that materials had a negligible influence on the clear water calibration curve -- provided that the fine sands were transported at concentrations (in percent by volume) less than 20 percent and no deposition existed at the meter.

For the research reported herein it was assumed that the differential head across a sharp edged orifice plate located in a vertical

section of pipeline would not be materially affected by the presence of fine sand up to concentrations of 15-20 percent. Therefore, all discharge measurements of clear water and the water-sediment mixture were made by using the orifice calibration curve for clear water.

Determining the Sampling Time Interval

Since a sampler with a sharp edge at the opening and a 0.25-in. ID circular intake was to be used, some knowledge of the allowable ratio of intake to ambient velocity was needed, to maintain say a ± 5 percent maximum error or less in sediment concentration. From the Corps of Engineers (53), it was found that, for the particular nozzle used, differences of ± 15 percent in intake velocity from the ambient velocity would result in concentration errors less than ± 5 percent.

Hence, rapid velocity determinations were made at each point in the flow that a point time integrated sample was to be taken. From this velocity the sampling time interval required to fill a one litre sediment cone was calculated. Each sample taken to determine the local concentration was based on a sampling time measured in the above manner. There seems sufficient reason to expect, as far as sampling time is concerned, that concentrations are accurate, in general, to at least ± 5 percent.

Rapid Determination of Local Sediment Concentration

Until recently, about the only technique used to measure concentration was to take the sample of sediment-water mixture, oven dry it, weigh the solids on an analytical balance and calculate concentration; a process often requiring an average time of ten minutes per sample. For

this study it was anticipated that some 12,000 to 15,000 samples would be taken. The above procedure was not practical.

The difficulty was resolved by calibrating a one litre sediment cone. This reduced to determining the actual concentration as a function of the apparent volume of sediment as read with a scale on the cone. A number of samples were oven-dried in order to get the actual concentrations during preliminary testing. The resultant curve looked very promising.

The calibration curve used, Fig. 4, is the result of oven drying more than 140 samples. All samples were taken by one or the other of two persons. The technique used in shaking down the sediment in the cone to obtain a constant voids ratio for each sample was not quite the same for both men. Samples for drying were picked at random, by the man not actually doing the sampling, over a period of about three months.

Studying this calibration curve points out the possibilities of this method for sediment studies. It should be noted that there is a lower limit of concentration beyond which the accuracy is not satisfactory. For some field studies, in which extreme accuracy is not too important, concentrations down to 0.05 percent could be measured satisfactorily. However, in general, oven drying or some alternative method is advisable below 0.10 percent. The technique is probably not applicable to studies involving a large percentage of silt and clay sizes.

Sediment Data

One sediment was used throughout the course of the project. Information as to its source and composition is given in Chapter IV.

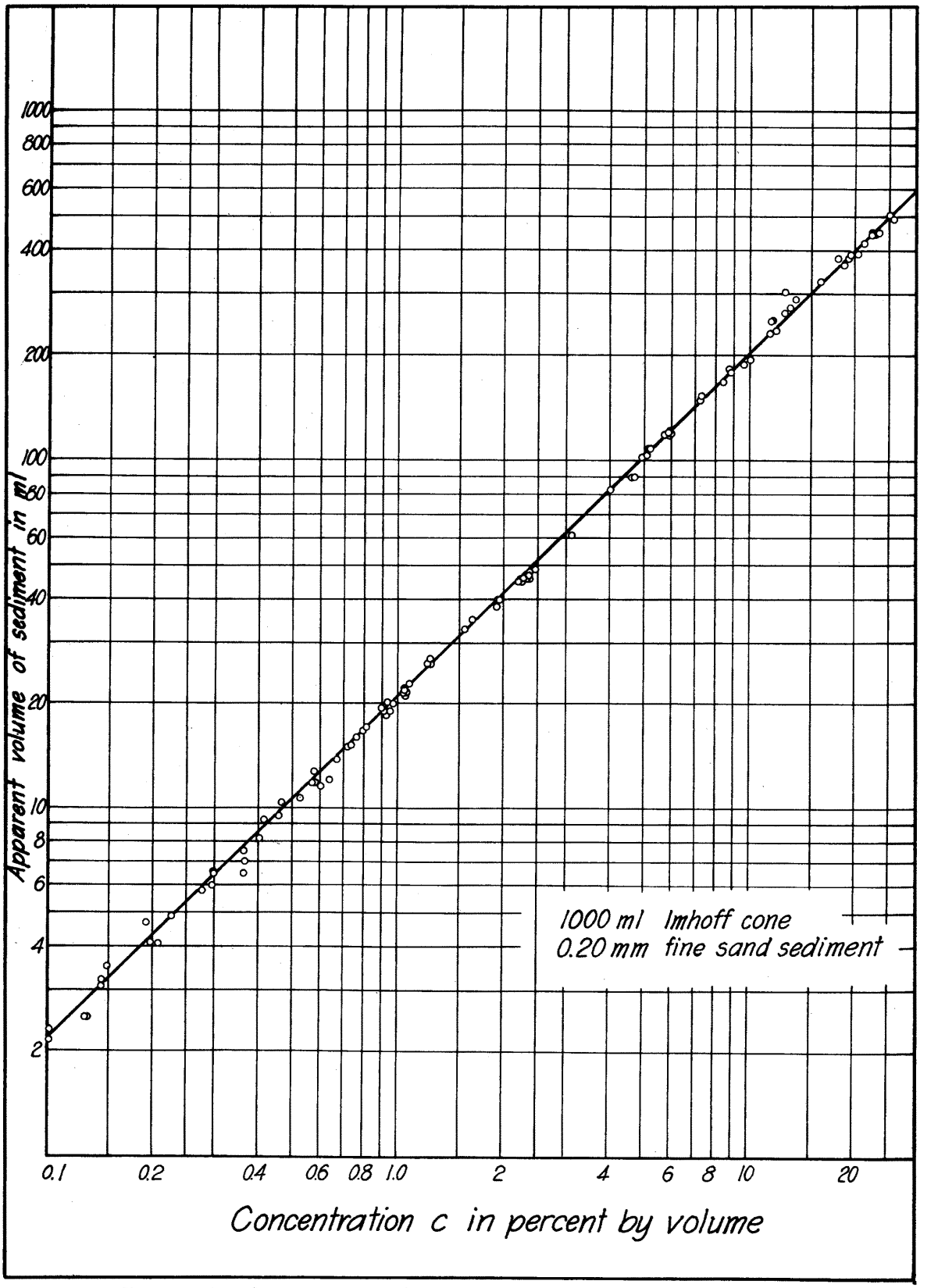

Fig. 4 Sediment cone calibration curve.

The purpose here is to present those data useful in analysis and representing the behavior of the sediment during the testing program.

Representative fall velocity distribution data are given in Fig. 5. These data were obtained from a detailed fall velocity analysis of a sediment sample sent to the Corps of Engineers, Missouri River Division Laboratory, by a cooperating project using the same sediment. The significant point is that the median sieve diameter, to be discussed in the next section, lies slightly beyond the upper limit of applicability of Stokes law. Thus, due to the distribution of sizes present, part of the sediment had fall velocities in the Stokes range and part was outside this range. The latter came close to satisfying the Budryck equation. See Durand (16).

Average median sieve diameter was used as the basic variable for describing the sediment. This variable was particularly convenient because it could be obtained by sieving select samples from those dried for the cone calibration curve. Using these samples, frequently composites, two problems were solved. In the first place, because samples were taken over a time period of several months, a continuous record of change due to abrasion, if any, in the median size was available. Secondly, by proper selection of samples it was possible to determine the difference in median size at the top of the pipe and a point lower on the vertical diameter.

The sieve analyses data were plotted on "log-probability" paper, thus making it possible to rapidly determine the median sieve diameter and the standard deviation of the diameter. A typical analysis is given in Fig. 5. The average median sieve diameter was 0.20 mm and the average standard deviation was 0.051 mm. The average median diameter was computed including

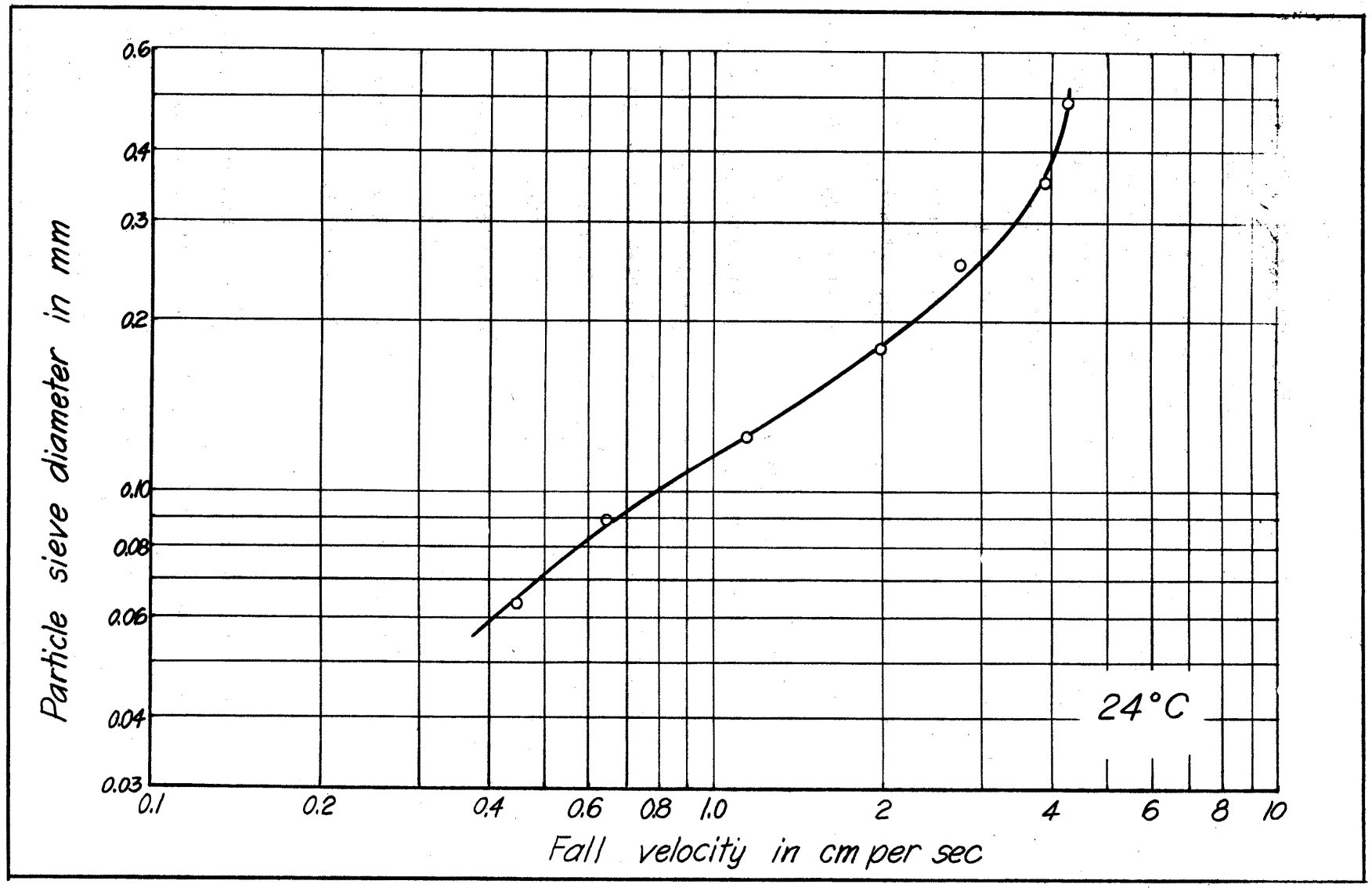

Fig. 5A Fall velocity curve.

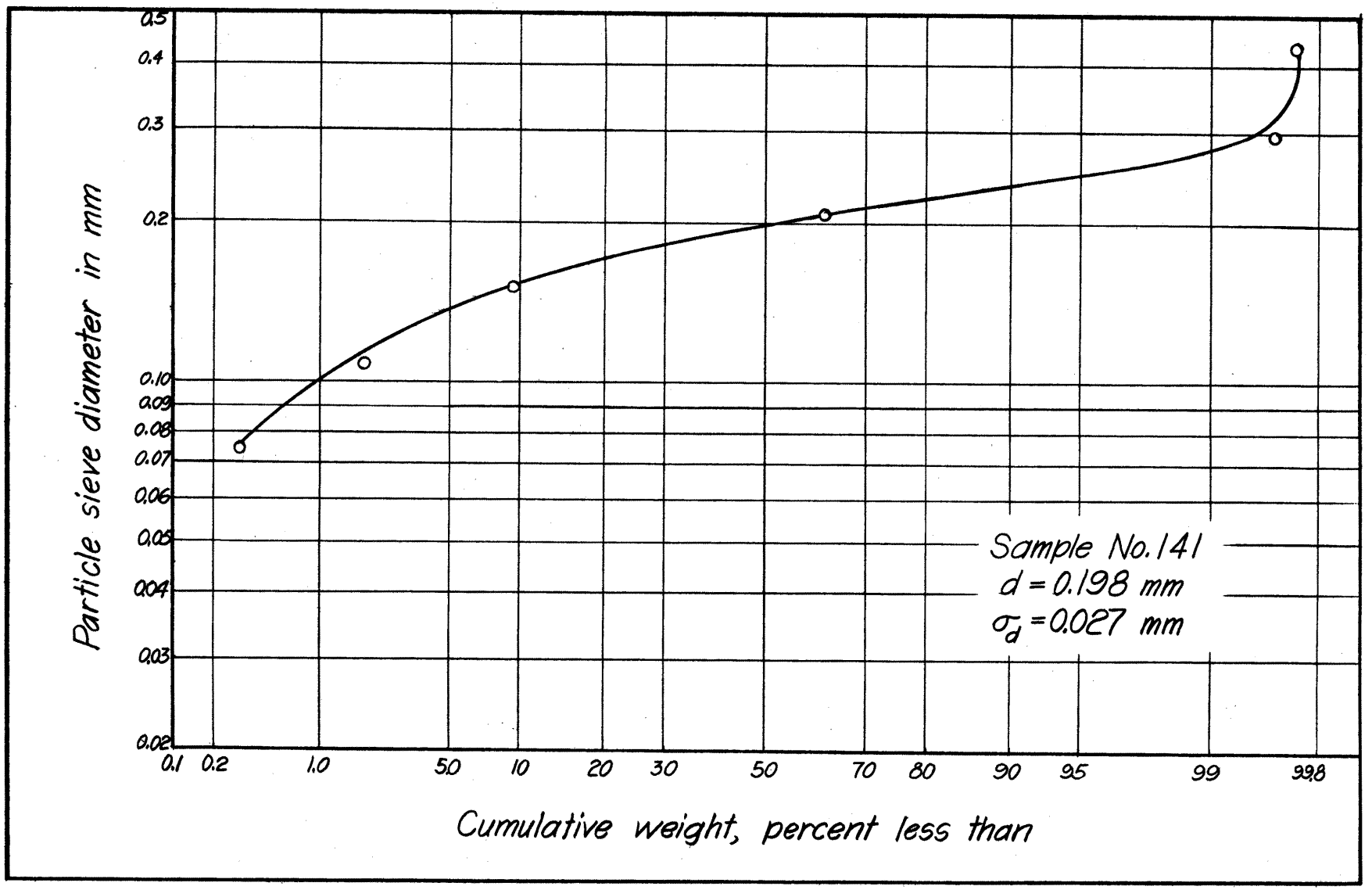

Fig. 5B Sieve analysis curve.

all sieve analyses regardless of the portion of the vertical diameter from which the sediment sample was taken. The median diameter and standard deviation of each analysis are tabulated in the Appendix. The original plots are filed with the Department of Civil Engineering, Colorado A and M College. Arithmetic averages were used in computing average median diameter and average standard deviation.

Maintainance of the median diameter of the sediment was achieved by continuously discharging the somewhat-turbid water and adding new sediment and clear water. The procedure was adequate for this study but probably would not be satisfactory for coarse material, especially if the constituent minerals were soft.

Method of Determining the Total Sediment Load

In evaluating the integral for total sediment load, $C_t = \frac{1}{Q}\int_s cv_1 da$, it is practically a necessity to pick a location for measurement of either c or v_1 , at which at least one of these variables is a constant. An even better location would be that for which $C_t = \frac{(c)\ (v_1)}{Q}\int_s da$. Sampling at an orifice placed in a vertical section of pipe seemed to be the best answer.

The variation of velocity across a 10-in. orifice placed in a vertical 12-in. pipe line was studied. Since only the variation of velocity was of interest, and not its absolute magnitude, special equipment was not developed for the study. One leg of a manometer was connected to the stagnation tap for the orifice plate and the other leg to the 0.25-in. ID sampling tube. Duplicate traverses were made along two diameters for each mixture discharge and sediment discharge. One diameter was parallel to the pump axis, and the other normal to it.

These data are plotted in Fig. 6. The distribution is quite erratic. It is believed this was due to the proximity of the orifice to the pump, a distance of about seven diameters. Another factor was the lack of refinement of the equipment, but neither this nor the presence of sediment could reasonably cause the scatter which is shown.

A study by Kowalki (32) on a similarly oriented orifice, using aluminum particles, gave a practically uniform velocity distribution. The orifice to pipe-diameter ratio was much smaller and the pump was not so close.

The variation of concentration over the 10-in. orifice is also plotted in Fig. 6. The concentration at the edge of the orifice corresponding to the outer rim of the pump impeller is consistently high, and consistently low along the edge normal to it. The concentration is quite uniformly distributed over the core of the jet. The high and low points, mentioned above, average approximately 1.00.

The method used for determination of the total load was

$$C_t = \frac{1}{Q} c \int v_2 da = c \ ,$$

where c was assumed to be near enough constant that it could be taken outside the integral. Furthermore, it was assumed that a sufficient measure of this $C_t = c$ was

$$C_t = \frac{\sum c_i}{n} \ ,$$

where $n \cong 30$, i.e., thirty samples, three at each of ten locations over the orifice cross-section.

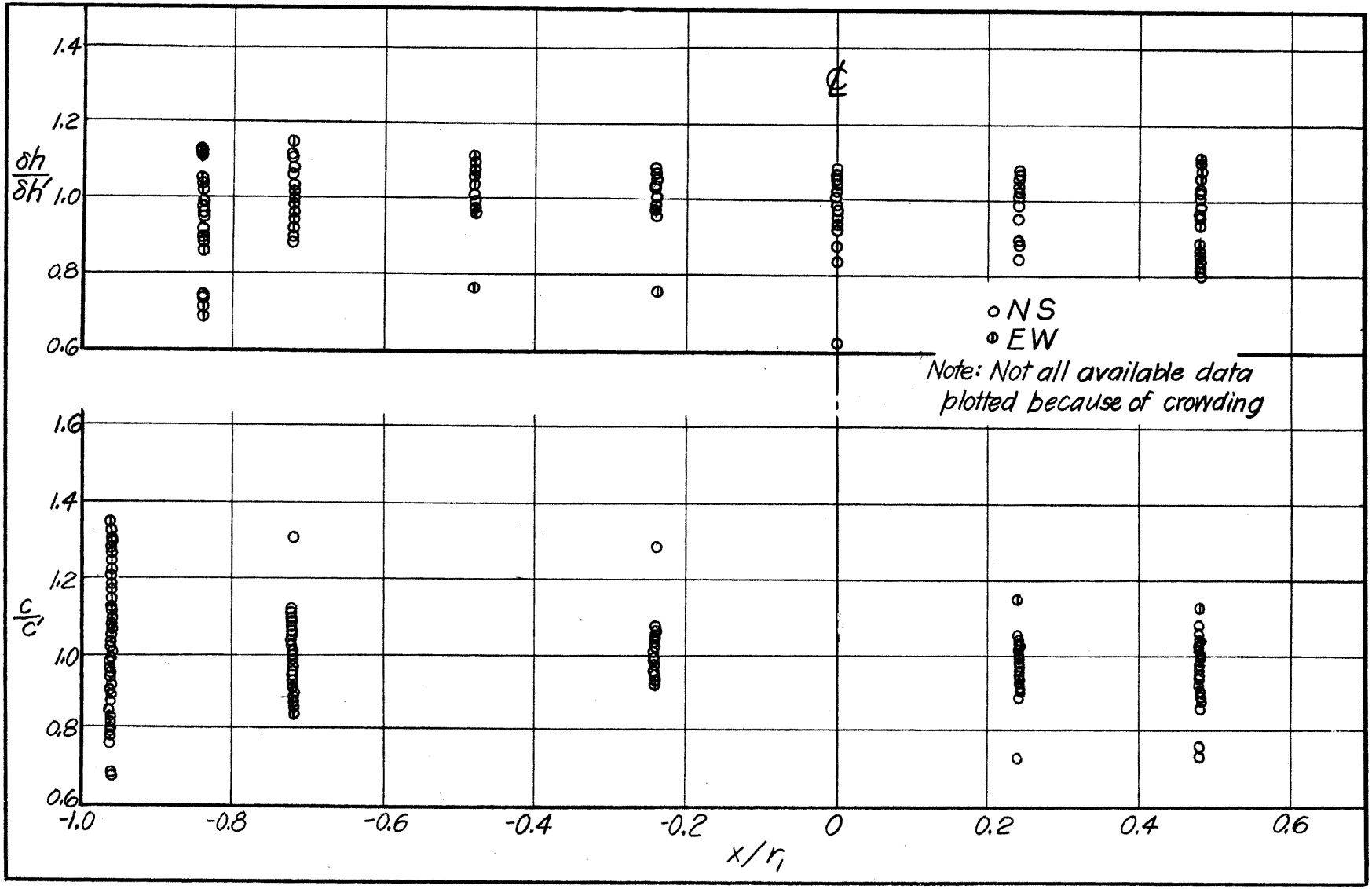

Fig. 6 Velocity and concentration across 10-in. orifice.

Effect of Piezometer Location Along Corrugation

While there seemed no physical reason why the hydraulic gradient as determined from a set of piezometers all located on the crests (observer inside pipe) should differ from a set consistently at some other position, it was believed the matter should be investigated.

The Corps of Engineers (48), reporting on a study of large diameter corrugated pipes, included some information on the deviation in head, from true ambient pressure, at various locations along a corrugation. A hydraulic gradient measured by any consistent piezometer bank seemed to be satisfactory, within ones ability to read the manometer. Sediment was not present during the tests.

Nominal 12-in. close-riveted standard corrugated pipe was used for the tests reported herein. The amplitude of the corrugations was 0.5 in. from crest to trough. A piezometer tap was located at the crest and another at the trough. The difference in head between a crest and nearest trough is given as $\delta\pi$ ft. The hydraulic gradient determined from the crests is called J, and that from the troughs is J_1.

The differential head between a crest and trough $\delta\pi$, is plotted in Fig. 7 as a function of Reynolds number and total load. When sediment was not present $\delta\pi$ appeared to be directly proportional to the Reynolds number of the mean flow. As the concentration increased, however, for a given Re, the $\delta\pi$ in general decreased. A possible explanation can be derived by reasoning that the sediment circulating in the quite stable vortex which exists in the groove between crests caused the vortex to shift slightly in position. This resulted in a different

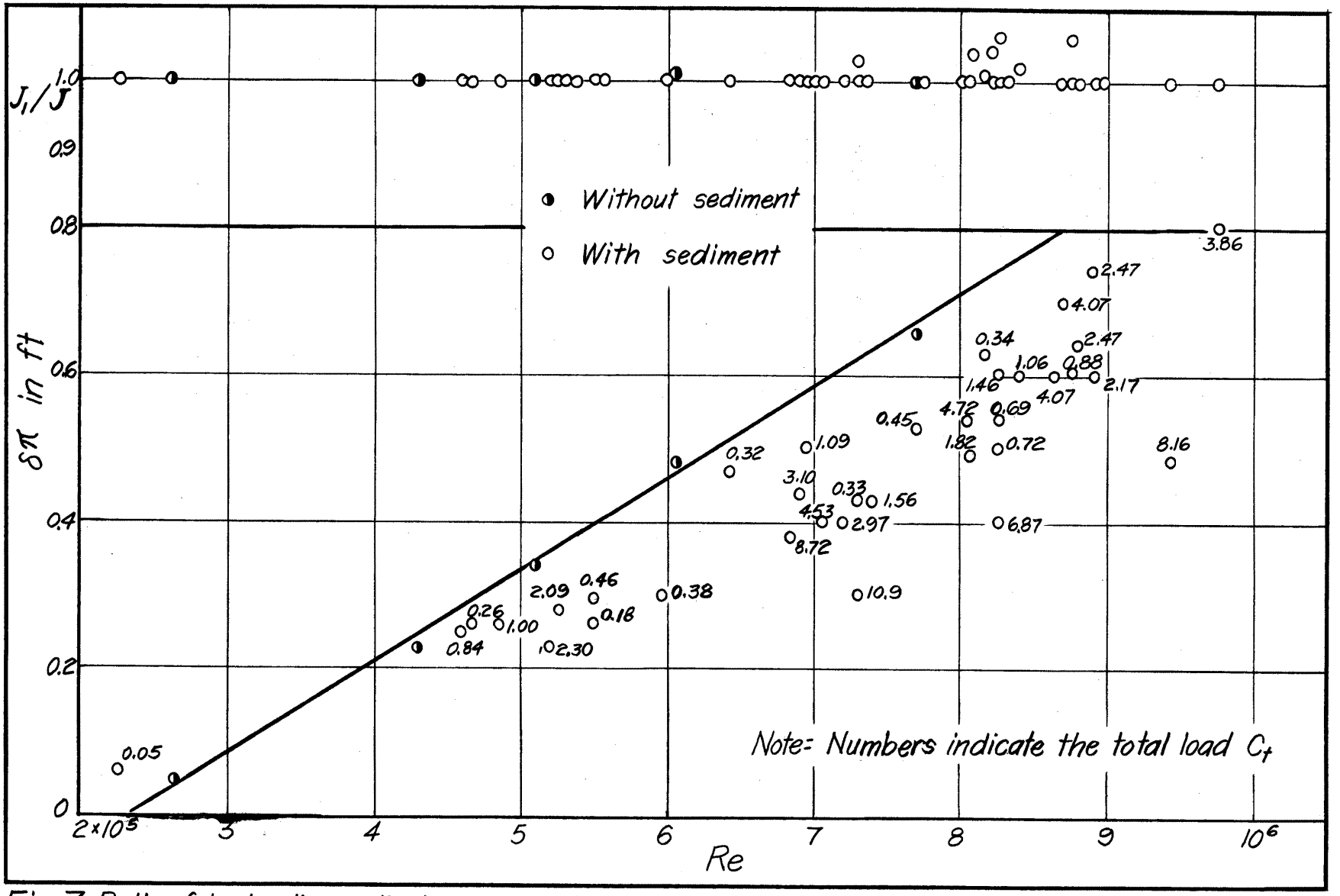

Fig. 7 Ratio of hydraulic gradient on corrugation highs to that of corrugation lows, and average difference in head between highs and lows, versus Reynolds number for 12-in. corrugated pipe.

kinetic head being recorded by the trough piezometer. Another plausible reason for the decrease in $\delta\pi$ is that the angular velocity of the vortex was decreased because of the sediment. That this phenomenon occurs is demonstrated by recalling that, if deposition takes place in the corrugation, the angular velocity of the vortex is reduced to zero.

The effect of the piezometer location on the hydraulic gradient can be evaluated by examining the curve of J_1/J versus Re in Fig. 7. The gradient was not affected significantly, except for a few isolated points. Reviewing the laboratory data revealed that J_1 was based on only two or three piezometers for these points, the piezometric head being so great that the others were off scale. The J set are basic throughout this study, and consist of readings from 4 to 10 piezometer taps on 10 ft centers. Therefore, the deviating points are not given much weight, and it is concluded that the hydraulic gradient as recorded by the corrugation crests gave an accurate measure of the rate of energy dissipation.

Summary

Preliminary studies indicated that a clear water calibration curve for the 10-in. orifice would be used to measure mixture discharge; a considerable error could be made in sampling time without causing undue errors in local concentration measurements; a calibrated sediment cone could be used for rapidly determining local concentration; the total load could be measured at an orifice placed in a vertical pipe; and the error in hydraulic gradient, as determined by any set of piezometers located consistently along the corrugations, was negligible.

Chapter VI

ONE-DIMENSIONAL ANALYSIS

The equations of homogeneous fluid hydraulics were used as a basis in analysis of the one-dimensional characteristics of fine sand transport in 12-in. pipes, and extended to include variables describing the sediment. The one-dimensional study was divided into the following parts: 1) effect of boundary form on hydraulic gradient, 2) resistance coefficient f as a function of the Reynolds number and total load, 3) determination of the total load at which deposition is incipient, and 4) effect of boundary form on horsepower and discharge.

Effect of Boundary Form on Hydraulic Gradient

The hydraulic gradient may be interpreted as the energy loss per unit weight of fluid per unit length traversed along the conduit. Herein rests its importance in hydraulics. Before presenting and discussing the data taken during this study, it is necessary, because of subsequent remarks, to show the region on the J-V diagram in which lie the data of earlier workers and its relation to the present data. The effect of boundary form may then be presented by examining: 1) effect of boundary form for clear water transport, 2) effect of sediment, 3) minimum horsepower for constant total load, and 4) the slope of the J-V curves.

The variation of J with V and C_t is shown schematically in Fig. 8. Most of the field and laboratory work on sands in water, reported in the literature, are in the region A, above the upper shaded horizontal line. The region B is studied in the investigation reported herein.

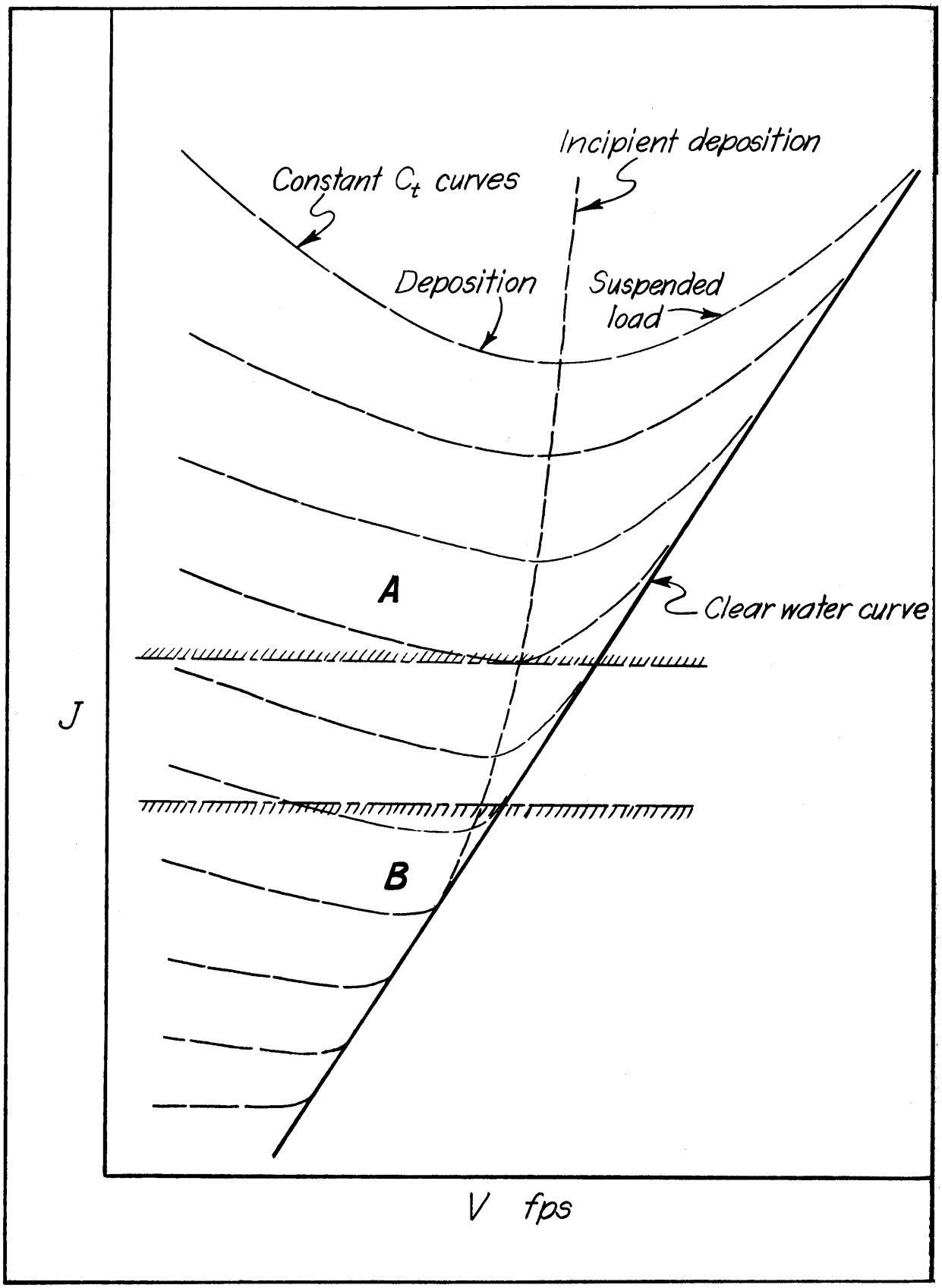

Fig. 8 Qualitative J-V diagram with curves of constant total load.

In many field applications it is desirable to know the minimum rate of energy dissipation required to transport sediment at a given rate. Since horsepower is proportional to the product of J and V, the minimum rate of energy expenditure for a given C_t occurs at the minimums in the C_t curves. A considerable number of data emphasized that this minimum occurred at the point of incipient sediment deposition for any C_t = constant on the J-V diagram.

Summarizing, for minimum energy requirements to transport sediment, it is desirable to have a boundary with J-V curves for clear water as close as possible to the J axis, and large C_t = constant curves intersecting the J axis at small J values.

Effect of boundary form for clear water may be examined by referring to Fig. 9. For a fixed J, the corrugated pipe had the smallest velocity V and the smooth the largest velocity. This could be interpreted as implying that corrugated pipe is the most desirable for conveying fluids which interpretation will be shown later to be true only for special problems.

Since the J-V curves have a slope of two (except the smooth pipe) and horsepower is proportional to the product JV, horsepower versus discharge was least for the smooth and greatest for the corrugated, with Hel-Cor falling between. The artificial roughness had a slightly greater frequency and somewhat smaller amplitude in the Hel-Cor than in the corrugated pipe, but the lesser energy dissipation in Hel-Cor was due to a larger effective conveyance area, because of the helical grooves. A part of the water was conveyed continuously in each helical corrugation.

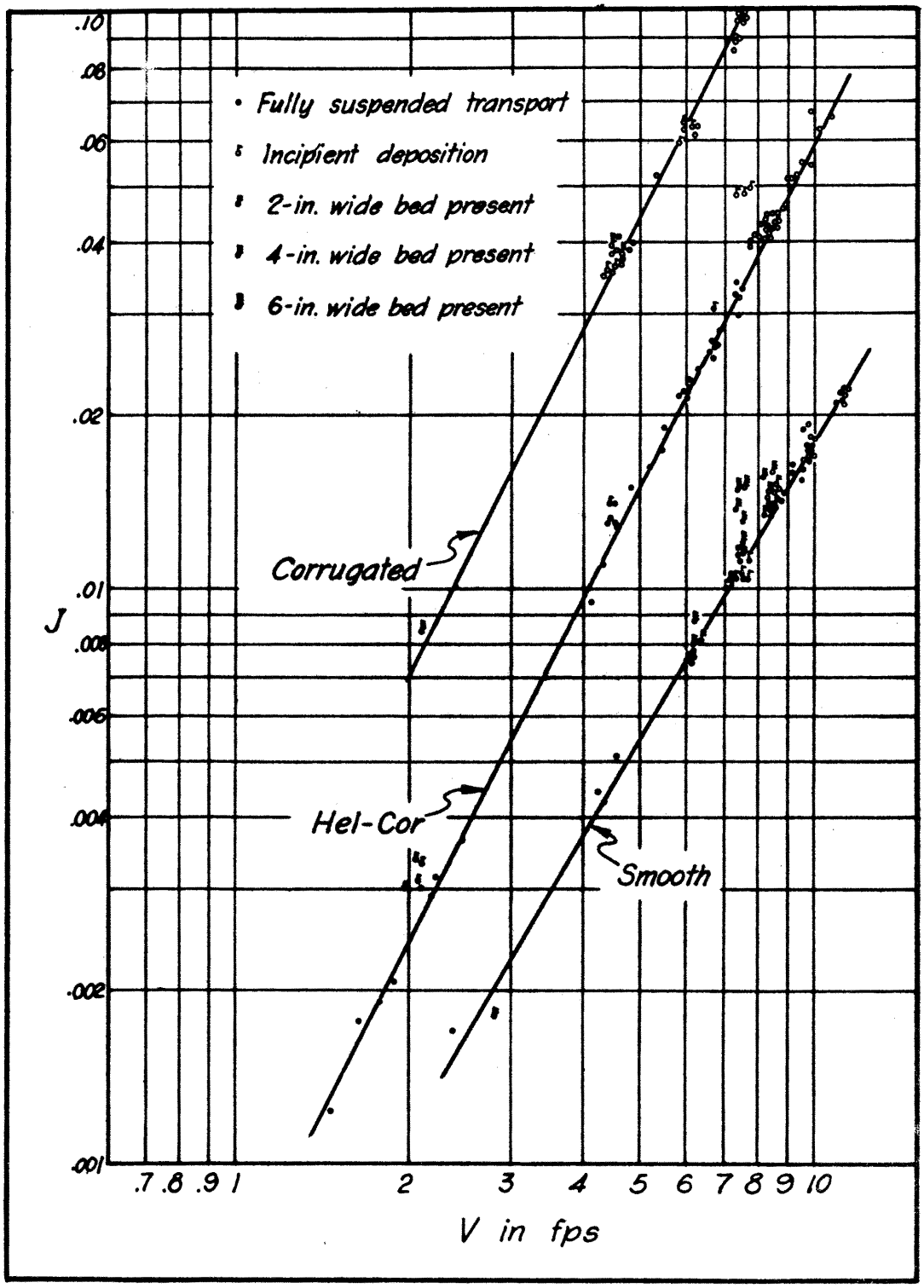

Fig. 9 Variation of hydraulic gradient with velocity and concentration.

The sediment does not have an appreciable influence on horsepower requirements until deposition begins to occur in the pipe. This is what one would expect by extrapolation of earlier work, as was done in presenting Fig. 8. There is a considerable deviation of the data from the clear water curve for smooth and Hel-Cor pipes when deposition occurs, but only a small change for the corrugated pipe. None of these deviations, however, are great enough to enable one to define a minimum in a C_t = constant curve.

The minimum horsepower for a constant total load can not be easily associated with a minimum on the J-V diagram for the data presented, because the minimum of C_t = constant is very near the clear water curve and difficult to define. The data need to be analyzed in a somewhat different manner in order to determine incipient deposition as shown in Fig. 11.

Slope of the J-V curves is worth careful thought. The curves for both the corrugated and Hel-Cor pipes are characterized by a slope of two. However, the smooth pipe definitely has a slope less than two. This implies that the Darcy-Weisbach resistance coefficient f is independent of Reynolds number for corrugated and Hel-Cor, and dependent on Re for the smooth pipe. The significance of this will be pointed out in the section on resistance coefficient.

Resistance Coefficient as a Function of Re and C_t

The dimensional J-V diagrams are important for many field design problems, but do not clarify the fluid mechanics involved. The

resistance coefficient f is more fundamental. It is a drag coefficient capable of representing a given boundary. Dimensional analysis has shown that

$$f = \psi (Re , C_t , \emptyset/D) . \qquad \text{Eq 53}$$

Analysis and discussion of resistance reduces to a study of this equation with the aid of experimental evidence as presented in Fig. 10. The curves of Fig. 10 are drawn in as the best fit consistent with the J-V diagram, for fully suspended sediment transport.

Discussion covers: 1) effect of sediment in fully suspended flow regime, 2) effect of sediment at incipient deposition, 3) comparison of results for smooth pipe with the Kármán-Prandtl resistance equation for turbulent flow in smooth pipes, 4) comparison of results for corrugated and Hel-Cor pipes with the Kármán-Prandtl resistance equation for turbulent flow in rough pipes, and 5) comparison of the results for corrugated pipe with the Morris wake-interference flow concept.

The effect of sediment in fully suspended flow regime seems to be an energy balance phenomenon, because the resistance coefficient does not vary appreciably with total load until deposition begins. This implies that the amount of energy expended in supporting sediment is approximately equal to the decrease in energy transferred to the small energy dissipating eddies by the large scale energy transport eddies -- if there were not a decrease in energy dissipation at some part of a sediment laden flow, then the value of f would continuously increase as C_t increased, because the additional energy dissipated in supporting the sediment increases with C_t .

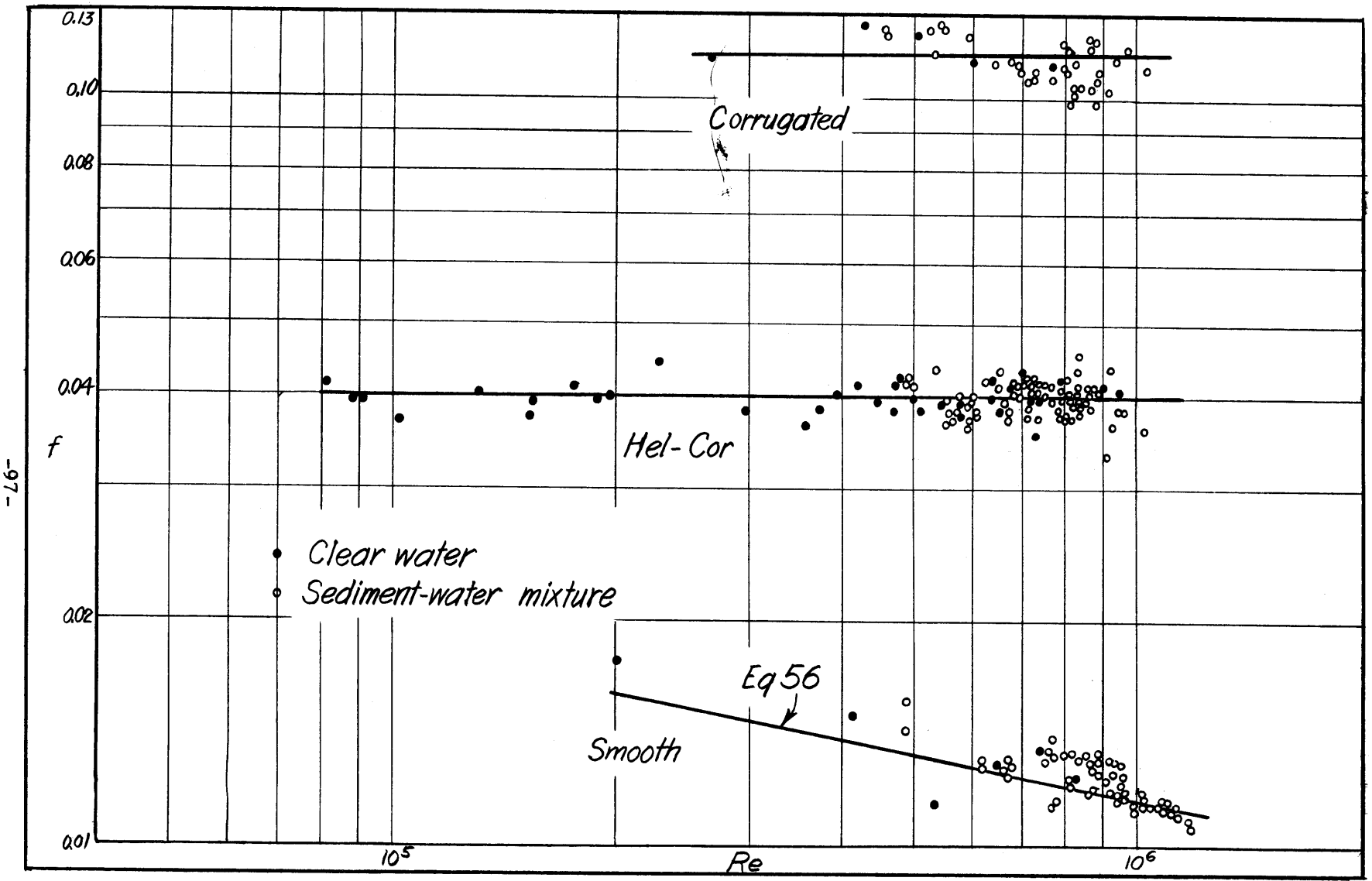

Fig. 10 A Variation of resistance coefficient with Reynolds number — fully suspended transport.

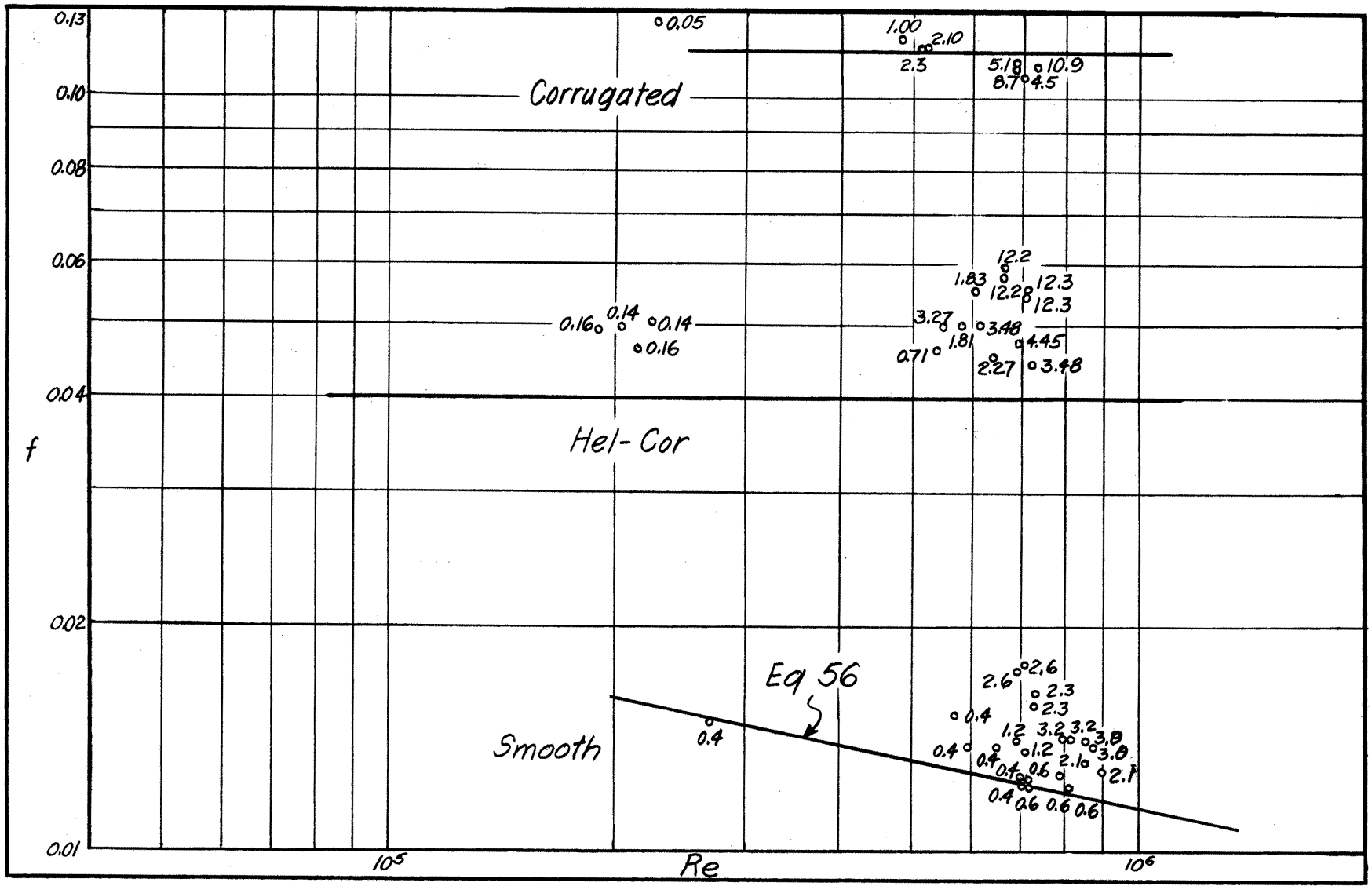

Fig. 10 B Variation of resistance coefficient with Reynolds number— Incipient deposition.

The effect of the sediment at incipient deposition was a change in boundary form. It is significant to note there is a definite increase in f when deposition begins for the smooth and Hel-Cor pipes, but not a noticeable change for the corrugated. The effective boundary of smooth or Hel-Cor is not even approximately that which is implied in the $\emptyset/D$ parameter when deposition is taking place. The concentration profile analysis will yield further information. However, observations through a plastic section in the test pipe contain important information.

A series of unstable dunes formed in the smooth pipe when deposition began to take place. These eliminated $\emptyset/D$ as describing the boundary. In the Hel-Cor it was observed that, for a given mean velocity, the helical motion of the outer shell of mixture became less and less as the total load approached the maximum carrying capacity, i.e., the discharge through the troughs of the artifical roughness was approaching zero. The helical motion was non-existant when deposition was present and the pipe closely resembled a corrugated pipe with small corrugations. The corrugated pipe had comparatively large corrugations and the formation of small dunes did not materially affect $\emptyset/D$; therefore, f did not increase appreciably when deposition began.

Comparison of the results for the smooth pipe with the Kármán-Prandtl resistance equation for turbulent flow in smooth pipes is based on Eq 56,

$$1/\sqrt{f} = 2 \log(Re\sqrt{f}) - 0.8 \ , \qquad \text{Eq 56}$$

The curve for the smooth pipe (see Fig. 10), satisfies this equation as well as one might wish, and can be used as a design equation for the given range of Re .

Comparison of the results for corrugated and Hel-Cor pipes with the Kármán-Prandtl resistance equation for turbulent flow in rough pipes is based on Eq 57,

$$1/\sqrt{f} = 2 \log r_o/k + 1.74 . \qquad \text{Eq 57}$$

The relative smoothness r_o/k, based on Nikuradse sand grain roughness, has been used as a standard in discussing rough pipes. Substitution of $f = 0.115$ and $f = 0.040$ into Eq 57, for the corrugated and Hel-Cor, yields values of r_o/k of 4.03 and 42.6, respectively.

It is interesting to compute an equivalent sand grain diameter from the values of r_o/k. The grain diameter is $k = 0.12$ ft and 0.012 ft for the corrugated and Hel-Cor, respectively. The actual amplitude of the artificial roughness is 0.042 ft and 0.037 ft, respectively. There is very little correlation between k and the physical quantity involved, thus implying that a better roughness parameter is needed for large evenly spaced artificial roughnesses. In this connection the listing of factors which enter, by Vadot (55), should be helpful. See Review of Literature for list.

Comparison of results for corrugated pipe with the Morris wake-interference flow concept for corrugated pipes is based on Eq 1, repeated here for convenience.

$$1/\sqrt{f} = (2 \log r_o/\lambda + 1.75 + (1/\sqrt{2})(2.5 - \varsigma)(\beta\lambda/r_o) \qquad \text{Eq 1}$$

This equation, on a graph of

$$1/\sqrt{f} - 2 \log r_o/\lambda \qquad \text{versus} \qquad \frac{Re\sqrt{f}}{r_o/\lambda} \ ,$$

has an asymptote of 1.75, in close agreement with the Kármán-Prandtl resistance function. An approximate summary curve for corrugated strip roughnesses as a function of the above variables is given in Morris (36). To evaluate the accuracy of this curve, the value of the resistance function, for a given $\frac{Re\sqrt{f}}{r_o/\lambda}$, was computed and compared to that taken from the graph. The computation is below.

Let $Re = 8 \times 10^5$, $f = 0.115$, $r_o = 0.5$ ft and

$= 0.222$ ft. Then

$$\frac{Re\sqrt{f}}{r_o/\lambda} = 12,100 \ .$$

The computed value of $1/\sqrt{f} - 2 \log r_o/\lambda$ is 2.25 and the value from the graph is 2.31.

The close agreement of the curve and experiment, making use of physically measurable quantities, shows the wake-interference concept has considerable merit, and is an improvement over the Nikuradse relative smoothness parameter.

Determination of Total Load at which Deposition is Incipient

As emphasized in the discussion of the J-V curves, the minimum of a C_t = constant curve on the J-V diagram is important in determining the minimum horsepower required for transporting a given total load. The primary purpose of this section is to determine a curve of C_t versus V for which deposition is incipient. Correlation of such a result with a J-V diagram will give the requisite information for efficient design of sediment pumping plants.

A plot was made of C_t versus V on rectangular, log-log and semi-log paper, noting at each plotted point whether the sediment was all in suspension, deposition was incipient, or a bed existed, as observed in the laboratory for each boundary. The object was to plot on a type of paper on which a straight demarcation line could be drawn as separating suspended and deposition regime. Semi-log paper was decided upon, and Fig. 11 is the result. It must be emphasized that the straight line drawn as separating suspended and deposit transport regimes was purely a matter of judgment, i.e an empirical conclusion in every sense of the word. Fig. 12 is a composite of the demarcation lines, on one V scale, as taken from Fig. 11.

A remark on the Hel-Cor pipe will illustrate the latitude one has in constructing an incipient deposition curve. If a bed existed in the pipe before pumping was begun and the discharge was gradually increased to the operating discharge without secondary circulation, transport at incipient deposition would differ considerably from that possible if the secondary circulation were in operation and concentration gradually increased to a maximum for the same operating discharge. In the latter case a helical motion would be aiding suspension but in the former the motion would be one-dimensional.

Personal judgment entered considerably in deciding whether deposition was incipient. Observations were made through a plastic section at the downstream end of the pipe. It was essentially the same problem as deciding in a flume study when the critical tractive force condition exists.

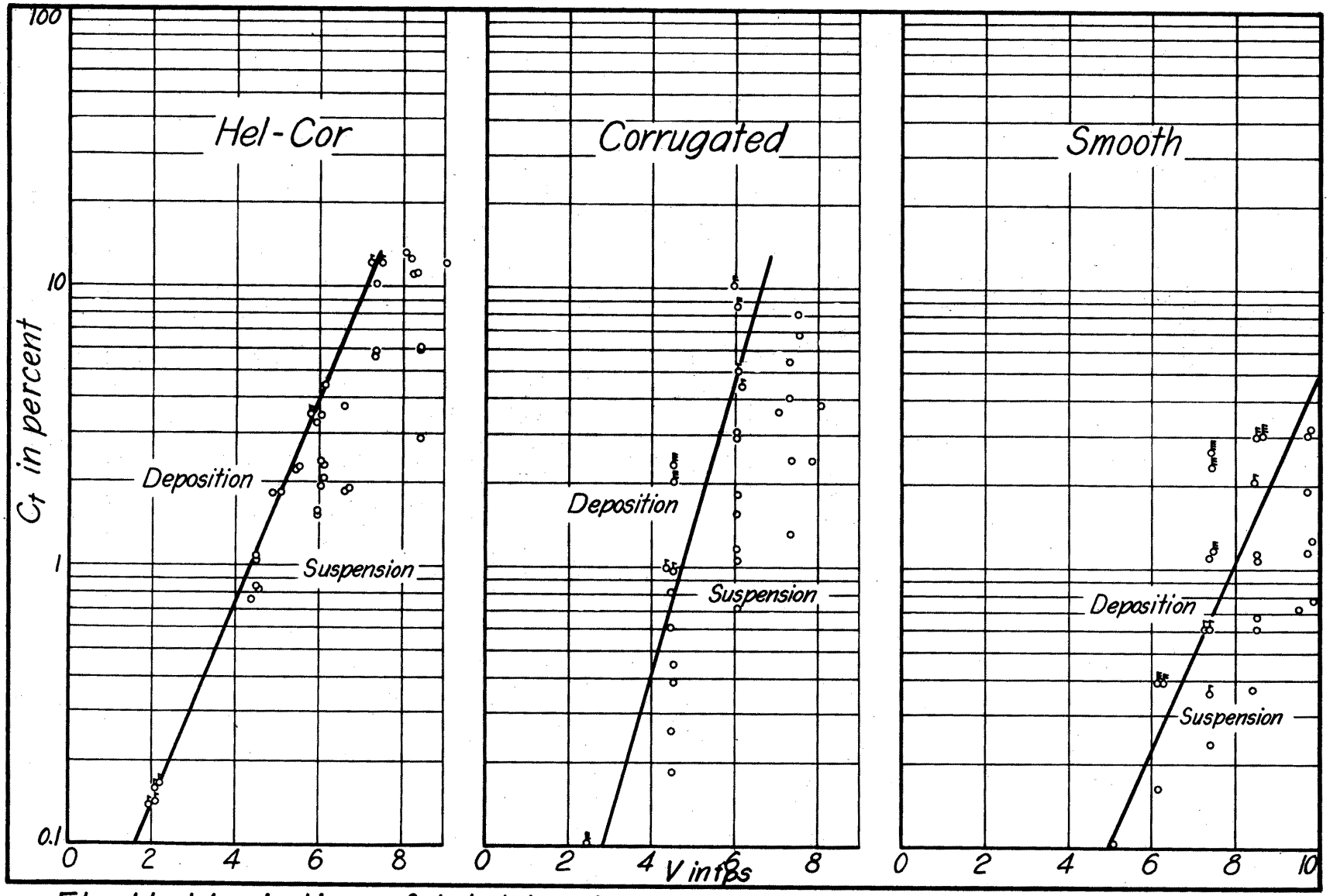

Fig. 11 Variation of total load at incipient deposition with velocity.

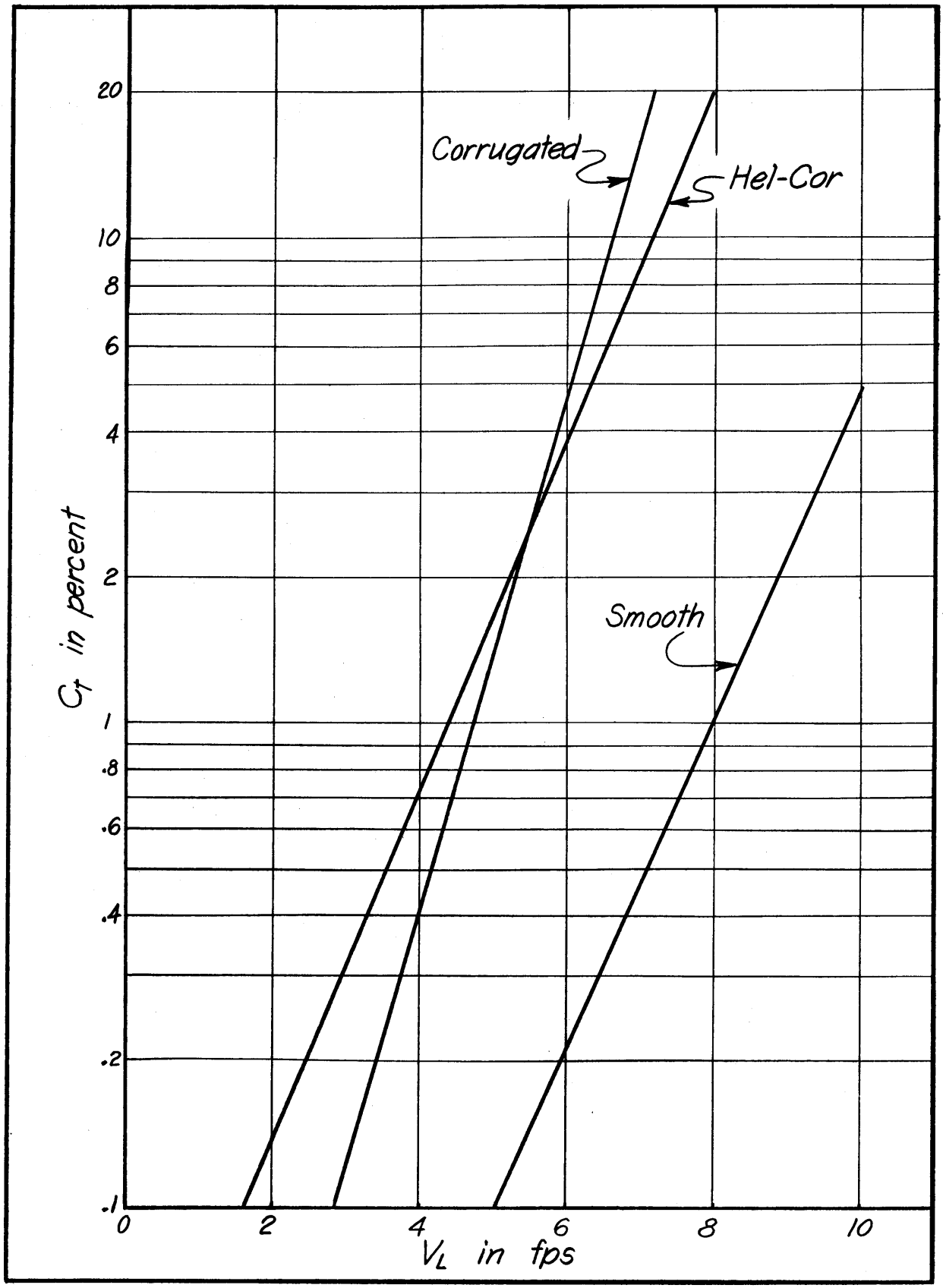

Fig. 12 Comparison of total load curves at incipient deposition.

A significant check on the result discussed above has been found in analyzing the concentration profiles for each pipe. This check will be discussed with the smooth pipe vertical concentration profiles.

Some valuable conclusions can be reached even if the demarcation curves of Fig. 11 were not exact. Dimensional analysis demonstrated the importance of $V/\sqrt{gD}$ in deposition phenomenon. If V_L is used to designate the limiting transport velocity and plots the lines drawn on Fig. 12 in terms of $V_L/\sqrt{gD}$ versus C_t on rectangular coordinates, Fig. 13 results.

For a given boundary (see Fig. 13), the range of C_t for which an observer would probably say deposition was occurring is becoming larger and larger with increasing $V_L/\sqrt{gD}$. This has important ramifications. Horsepower will vary almost entirely with total load for large $V_L/\sqrt{gD}$, assuming operation corresponding to incipient deposition. The importance of this to a dredge operator is that, for a nearly constant mixture discharge, a large range of total loads is possible and still maintain operation near maximum efficiency. Variation of total load occurs when moving the suction line of a dredge from place to place. Furthermore, nearly constant discharge is a desirable feature to have, as discussed later under pump stability.

From the standpoint of sediment mechanics, once $V_L/\sqrt{gD}$ is increased and becomes less dependent on C_t, there is sufficient large-scale eddy transfer energy available to accommodate a rather large range of total load.

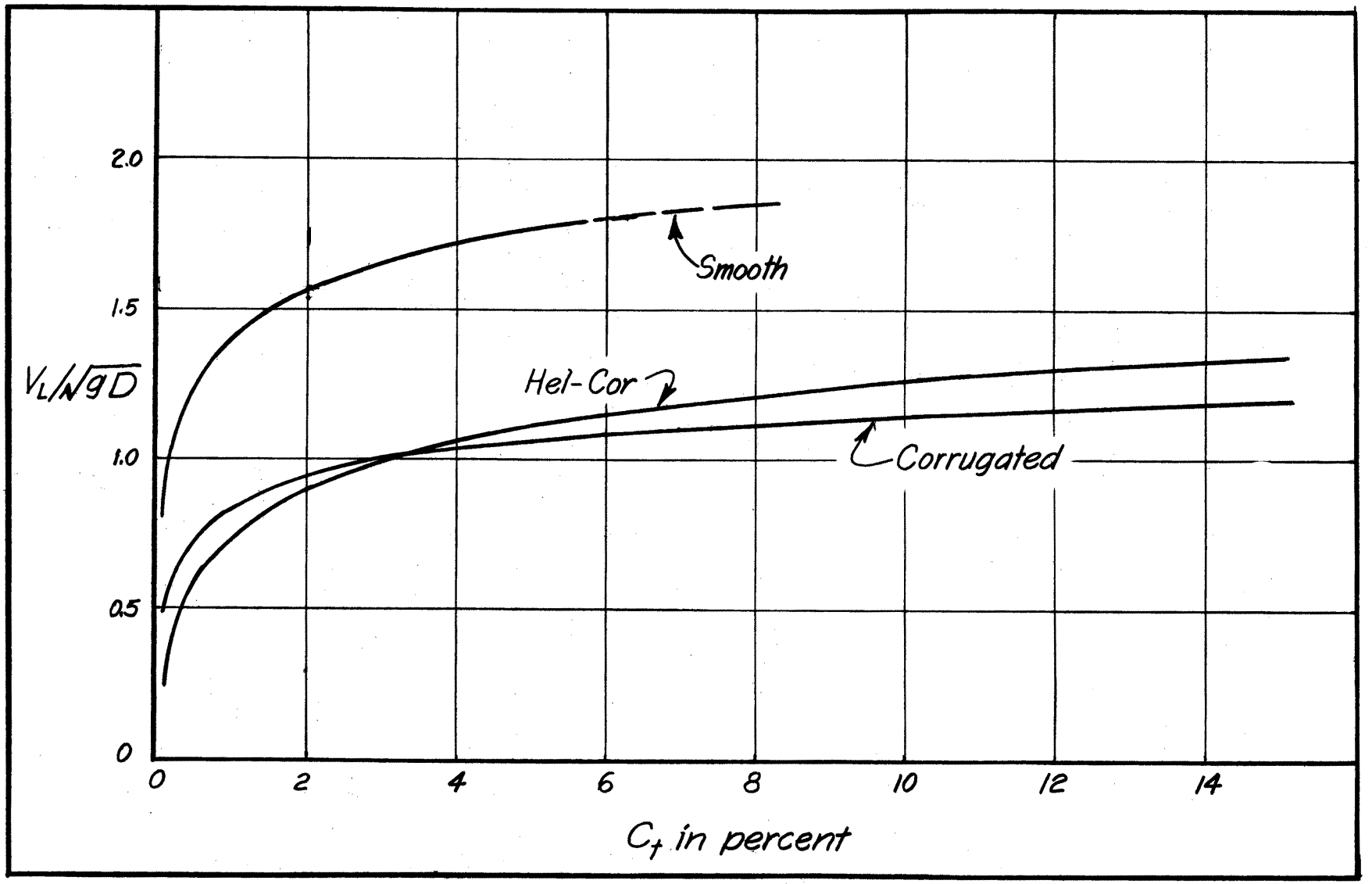

Fig. 13 Variation of limit deposit velocity parameter with total load.

Effect of Boundary Form on Horsepower and Discharge

Design of a sediment pumping installation depends on the limitations and assumptions imposed by the available design data and the equipment available. Most problems involving boundary types are included by: 1) type of pump needed, 2) relative power for a given total load G, 3) relative water required for a given G, 4) comparative sediment discharge for a given horsepower, 5) comparative sediment discharge for a given mixture discharge, and 6) a combination of horsepower and discharge.

Certain limitations and assumptions were imposed in order to make comparative studies of the effects of boundary form on horsepower and mixture discharge characteristics as a function of sediment discharge. The sediment discharge was computed as the product of

$$\left(C_t \pi V_L\right) \left(D^2/4\right),$$

where C_t and V_L are related by the incipient deposition plot. Variation of the mixture unit weight was negligible in calculating horsepower. The equation employed was

$$HP = Q \gamma_w J/550 ,$$

where J corresponds to the clear water value at the velocity V_L. This calculation gives horsepower per ft of pipe. Therefore, results of this calculation are valid only for the most economical operating conditions. It is important to note that this technique is applicable only in the range of velocities such that the minimum value of a constant C_t curve on the J-V diagram lies near the clear water line.

The analysis is strictly applicable only for the sediment used in obtaining these data. However, the curves of Fig. 14 should have at least a qualitative application beyond the range of the data for which they were derived.

The question of type of pump needed for the task of transporting sediment is really a problem in itself. The reason for including a short paragraph on this subject is that the problem of pipelines clogging is often the difference between failure and success of an installation; and correct pump design can be the answer.

Assume a plant operates at velocities on the J-V diagram where a minimum occurs in the C_t curves, as in Fig. 15. Further, suppose a pump with a J-V characteristic curve such as A (constant horsepower) were installed. This curve crosses the C_t line in two places, one in the deposits regime and one in the suspended transport region. Such an operation is unstable because, for the same horsepower, the discharge may oscillate back and forth across the C_t minimum and pipeline clogging may result.

Assume a constant discharge pump with a characteristic curve such as B . Stability is evident and the probability of clogging is materially reduced.

Durepaire (20) gave a very thorough treatment of this subject.

Fig. 14 is helpful in discussing the relative power requirements for a fixed sediment discharge of the three boundaries studied. This type of problem arises in designing a plant which runs continuously. Cost of

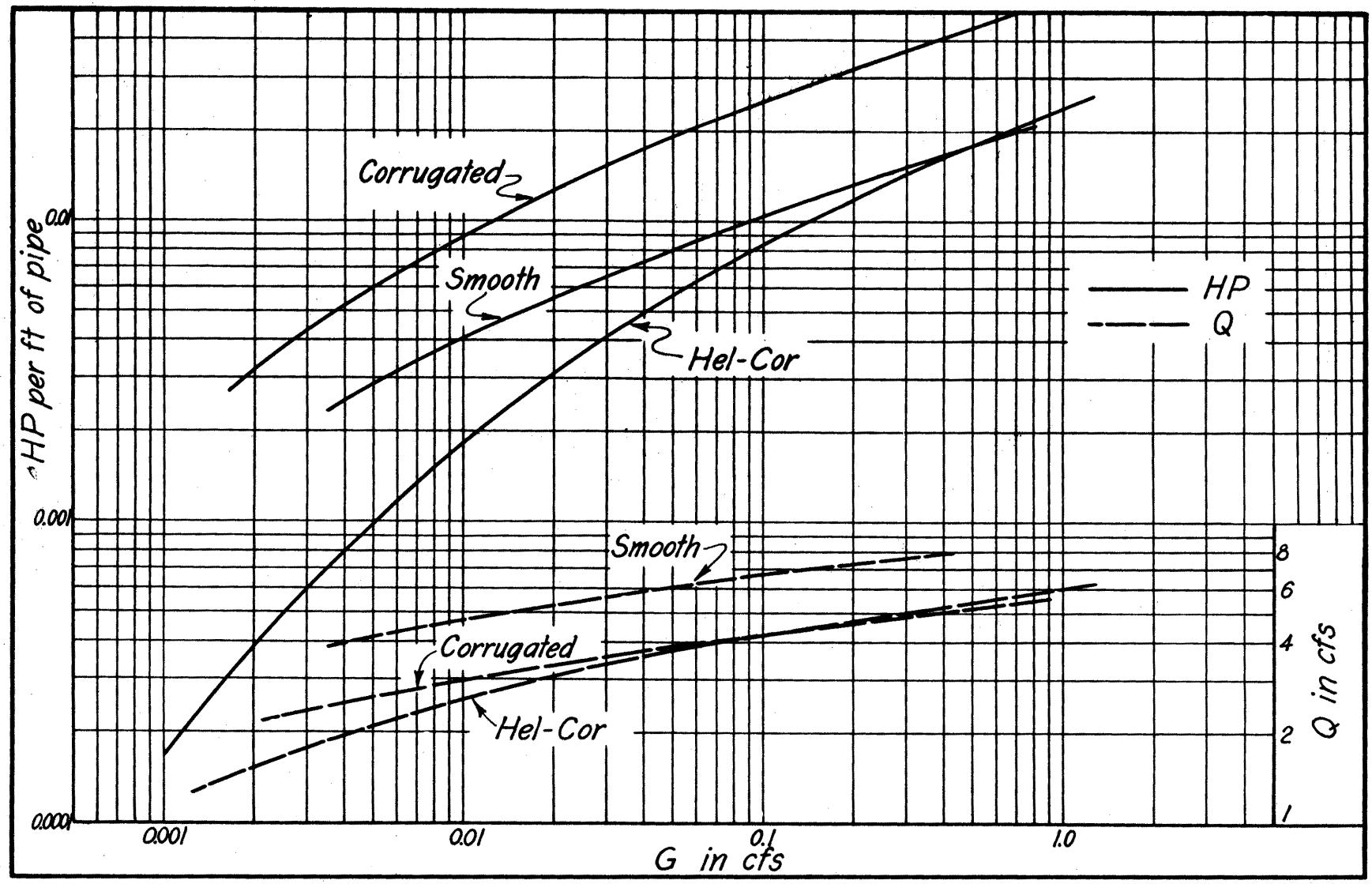

Fig. 14 Variation of horsepower and discharge of mixture with sediment discharge.

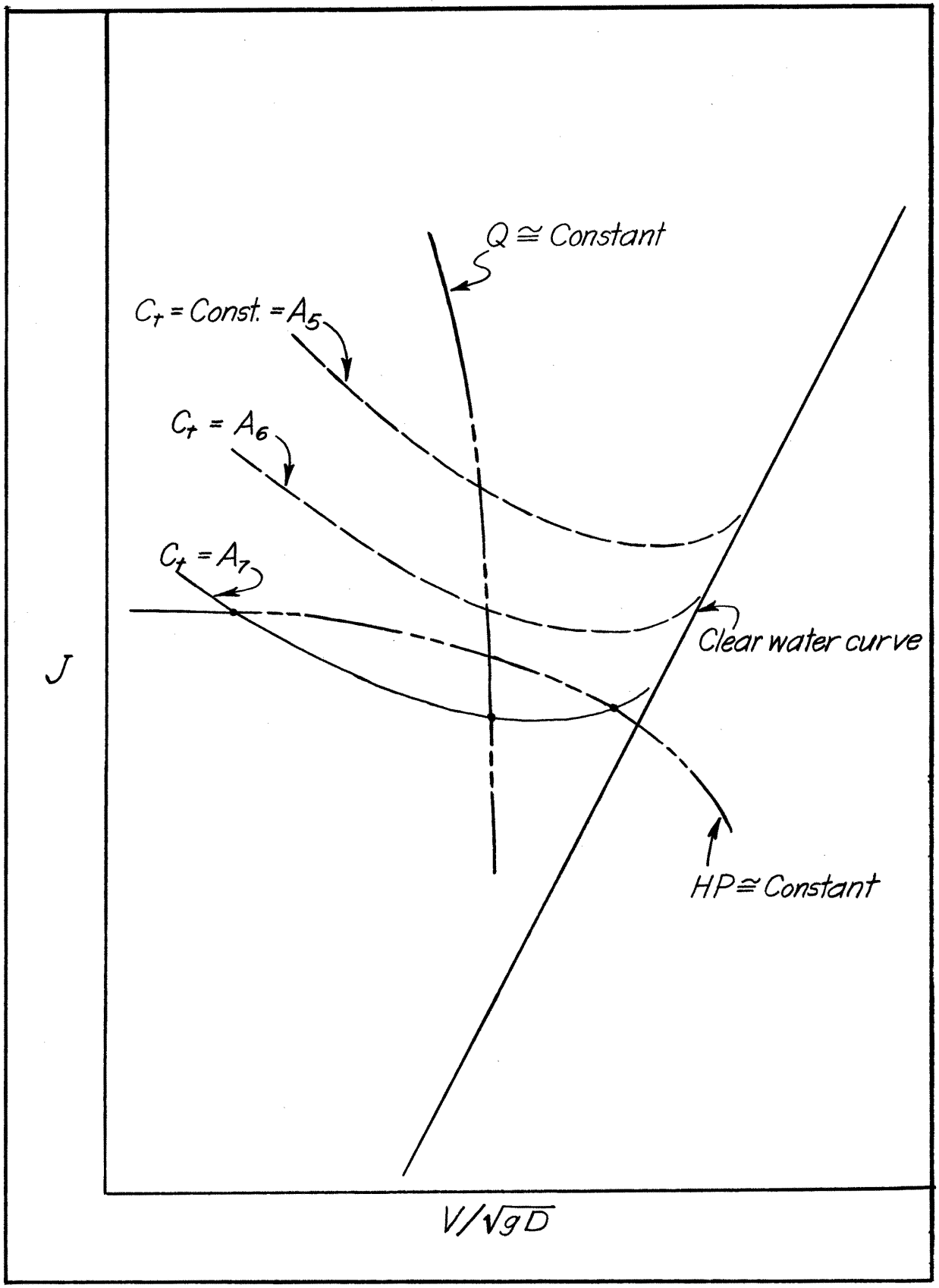

Fig. 15 Comparative stability of operation of sediment pumping units.

power is frequently a major item in such a case. To be more specific, suppose sediment enters a power canal at a constant rate and must not be allowed to enter a set of turbines. Assume further that the amount of water used in the sediment excluding operation is not important. Comparing the boundaries for the above type of problems, the corrugated pipe requires from 250 to 600 percent more power than the Hel-Cor, and 200 to 250 percent more than the smooth. Smooth pipe requires as much as 300 percent more power than Hel-Cor over the low range of total load. This difference continually decreases and at a total sediment load of about one cfs the smooth requires less horsepower than Hel-Cor.

In general, for a given G and assuming Q unimportant, Hel-Cor will be the most economical for $G <$ about 6500 tons per day; for larger G a smooth pipe is desirable.

Problems arise for which the relative water required for a given sediment discharge is the fundamental problem. A typical case could be the construction of a hydraulic fill dam. Disposal of a large volume of water from the top of the fill, once the solids have settled, may be difficult or undesirable. A pipeline is needed which will convey the largest volume of solids for a given amount of mixture.

The broken curves of Fig. 14 indicate that the corrugated and Hel-Cor are about equally efficient for G greater than 0.1 cfs. The smooth pipe discharges about 60 percent more mixture than either of the other pipes for a fixed total sediment load.

It can be concluded that a smooth pipe is not practical for jobs where the amount of water to be wasted must be held to a minimum, and that both corrugated and Hel-Cor give about equally satisfactory results. Power consumption has been ignored in this comparision.

Another design problem for which this study is important is that of excluding sediment from a canal at a given rate. Assume an irrigation system removing sediment from a canal at the rate of 0.5 cfs. A simple calculation, using Fig. 14 and recalling that 1.0 cfs for 28 days corresponds to 55.5 ac-ft, shows that nearly 500 ac-ft of water would be saved for irrigating farm crops by employing Hel-Cor pipe.

It would not be valid to give the water a monetary value and say a fixed amount of money was saved, because a part of the 500 ac-ft might have been lost by canal seepage. Furthermore, a part of the water, if pumped through the smooth pipe, would probably be recovered. The problem of horsepower was not considered.

Other installations can be imagined in which comparative sediment discharge for a given horsepower is being considered. An example would be an operator who already has a motor, and wants to convey a maximum amount of solid material per unit time.

The most evident difference in G for constant horsepower is between the corrugated and Hel-Cor. The Hel-Cor will carry approximately ten times as much sediment per unit time as the corrugated. This is an extremely large difference which can hardly be ignored in field contract jobs because of the significance of the time element. Some contracts are

in terms of a fixed amount of money to deliver a specific amount of solid material not later than a given date. Assuming equivalent working days at the same horsepower for the above two pipes, the Hel-Cor would require only 10 percent as long to finish the job as corrugated. Furthermore, even though horsepower is the same in both cases, since the corrugated would operate 10 times as long, the power bill would be 10 times greater for the corrugated.

The above arguments are also valid when comparing the smooth and Hel-Cor. However, the difference in G decreases with increasing horsepower until HP reaches 0.18. Above this value the smooth pipe transports more per unit time than Hel-Cor. Hel-Cor may convey four times as much sediment per unit time at low horsepower as smooth pipe.

The comparative sediment discharge rate for a given mixture discharge is another important question to be answered. A problem in this category arises quite frequently in irrigated areas. One of the difficulties in the design of stable open channels for irrigation and power is that of preventing sediment from entering in prohibitive amounts. Associated with this is the limited amount of the channel water that can be allocated for aiding the sediment exclusion. Thus, it is imperative to have a pipe boundary, if dredges or similar techniques are used, which will convey the largest amount of sediment for a given mixture discharge.

From Fig. 14 it can be seen that Hel-Cor and corrugated pipes convey about 15 times as much sediment per unit time for a given mixture discharge as smooth pipe. There is not a significant difference between Hel-Cor and corrugated.

In order to gain an idea of what the above savings mean, assume a canal carrying 100 cfs, of which 5 cfs have been used with a smooth pipe to remove sediment. Suppose the system operates four months a year. In these four months the smooth pipe could remove about 5,400 cubic yards of sediment and the other pipes in the order of 80,000 cubic yards. This comparison is tempered by recalling that mention has not been made of the rate at which sediment really needs to be removed from the canal.

A combination of horsepower and discharge will lead to valuable conclusions. Assume a power company has a canal carrying 500 cfs, a maximum of 5 percent of the discharge can be removed in order to keep sediment from entering the turbines and it is known that removing sediment at the rate of 0.05 cfs is necessary. The problem is to determine which boundary will be the most economical as far as operation is concerned; and compare the other pipes to it.

The lower set of curves on Fig. 14 indicates that all the boundaries will satisfy the 5 percent limitation for G = 0.05 cfs. Further use of the curves will give the information given below.

Boundary	Data From Curves			Comparison to Hel-Cor	
	HP x 10^3 / 5.65	G x 10^2	Q	Percent HP	Percent water discharged
Hel-Cor	5.65	0.5	3.75	100	100
Smooth	8.00	0.5	6.05	141	161
Corrugated	19.0	0.5	3.85	337	103

Considering the information above, the Hel-Cor boundary will result in a significant saving over the corrugated and smooth pipes, a problem for which both power and waste water must be kept at a minimum.

Summary

One-dimensional analysis revealed that the sediment has little or no effect on the J-V diagram for clear water, with J in terms of water, until incipient deposition begins. The same conclusion was reached on the f-Re diagram. A plot of the velocity V_L at which deposition begins versus the corresponding total load indicated that V_L became less and less dependent on total load -- occurring for Hel-Cor and corrugated much more rapidly than the smooth. In general, for the velocities used, Hel-Cor carried more sediment at less horsepower than either corrugated or smooth pipe.

Chapter VII

INFLUENCE OF BOUNDARY FORM ON INTERNAL MECHANICS

Analysis of boundary form effects on the internal mechanics of sediment transport by pipes requires sediment concentration profiles in both the horizontal and vertical directions of a cross-sectional normal to the mean flow. Such profiles were obtained for several total sediment loads and a number of mean velocities. To analyze and discuss these profile data, they were subdivided into: 1) horizontal concentration profiles, 2) elementary comparison of vertical concentration profiles, 3) vertical concentration profiles in Hel-Cor pipe, 4) vertical concentration profiles in a smooth pipe, 5) vertical concentration profiles in corrugated pipe, and 6) diffusion coefficient ϵ_s and the Kármán constant κ .

The basic equation for studying concentration profiles is Eq 70,

$$c/C_t = \psi(C_t \ , \ V/\sqrt{gD} \ , \ y/D \ , \ \emptyset/D) \ , \qquad \text{Eq 70}$$

or the same equation with y/D replaced by z/D . Reynolds number or the hydraulic gradient enters some problems.

Analysis of Horizontal Concentration Profiles

Horizontal concentration profiles were obtained and analyzed to determine if there was evidence of a pronounced secondary circulation spiral owing to density gradient and if the Hel-Cor boundary induced transport up the walls of the pipe. The applicable data are summarized in Fig. 16, as a plot of $c/C' = \psi(z/D)$.

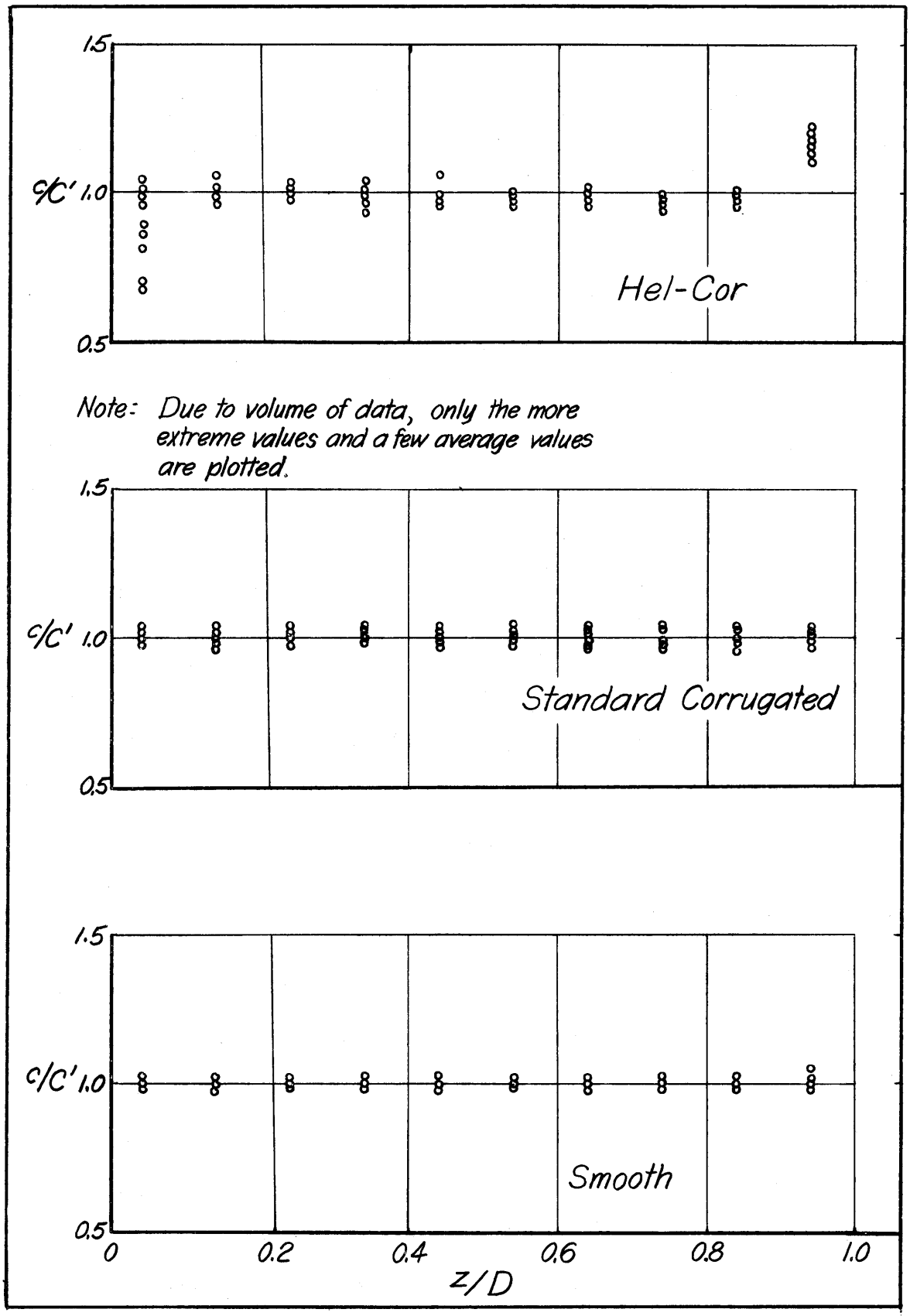

Fig. 16 Comparison of concentrations along horizontal diameter to arithmetic average concentration over profile

Because of the large volume of these data, many of which plotted on top of each other, only the extreme values and a few of the average ones have been plotted. The plot was designed to show variations in concentration across a horizontal diameter, and should not be related to the total load C_t which has previously played such a dominant role. This explains substituting z/D for y/D and c/C' for c/C_t .

For convenience, the discussion of the horizontal profiles was separated into: 1) Hel-Cor, 2) corrugated, 3) smooth, and 4) conclusions.

The Hel-Cor profile (see Fig. 16) had a constantly greater-than-average concentration on the side of the pipe corresponding to that up which material would have a tendency to flow because of the effect of the helix. To clarify this, assume an observer stationed along the centerline of the pipe and looking in the direction of the mean flow. From this point the pipe wall would resemble a right hand screw. Sediment had a tendency to settle to the bottom of the pipe. But if it were carried up the wall, corresponding to turning slightly the right hand screw, the result would be to increase the sediment concentration on the left.

The amount of deficiency of sediment on the opposite side may be shown to depend on the parameter $V/\sqrt{gD}$, as can the amount in excess discussed in the preceding paragraph. Sediment was carried up one side of the pipe when $V/\sqrt{gD}$ was small, but settled away from the boundary before going over the top and reaching the opposite side. The high boundary concentration continued further and further up the wall, as $V/\sqrt{gD}$ increased, until it went completely around the pipe, and a low concentration no longer existed near any portion of the boundary.

A more detailed description will be given when the vertical concentration profiles are discussed. Worth noting at this point is the general uniformity of concentration over the core region.

Standard corrugated pipe had a nearly uniform concentration over the entire horizontal diameter. The maximum deviation from $c/C' = 1.00$ was about $\pm$ 5.5 percent, which was probably experimental since no consistent tendency was observed.

Smooth pipe had the same type of uniform distribution in the horizontal as the corrugated pipe. The variation of concentration from $c/C' = 1.00$ was about $\pm$ 3 percent. The deviation was somewhat smaller than in the corrugated. This was probably because less difficulty was encountered in taking samples in the smooth pipe; in general, the concentrations were less and the sampler operated better.

The principal conclusion is that boundary form has a definite influence on the mechanism of transport. In the Hel-Cor pipe there is a definite helical secondary flow inducing a non-uniform sediment distribution along a horizontal diameter -- but undoubtedly resulting in a more uniform concentration over a cross-section of the pipe. There is no evidence of any secondary motion due to the density gradient along the vertical diameter of corrugated and smooth pipes. Furthermore, as long as there is not a mechanically induced helical flow, or a similar secondary circulation, the horizontal profile is independent of the amount of turbulence generated by roughening the boundaries, insofar as form is concerned. The actual magnitude of the concentration along a horizontal diameter depends on the number of large-scale eddies generated and transporting sediment.

Elementary Comparison of Vertical Profiles

Analysis of the vertical concentration profiles was based on Eq 70,

$$c/C_t = \psi(y/D \ , \ V/\sqrt{gD} \ , \ C_t \ , \ \emptyset/D) \qquad \text{Eq 70}$$

The total load C_t was again a fundamental variable; Fig. 17 is a plot of one typical profile for each pipe, with Re and C_t constant. The purpose of this plot is to show the characteristic form of the concentration profile for each boundary.

Hel-Cor pipe, carrying a fairly high discharge of mixture without deposition, had a nearly constant concentration over the entire section. The high concentration in the vicinity of the boundary may or may not be present, depending on the value of $V/\sqrt{gD}$. In general, for a given C_t , as $V/\sqrt{gD}$ increased the regions of high concentration near the boundary became more pronounced.

Corrugated pipe exhibited a profile that was an exponential function of y/D for low $V/\sqrt{gD}$, and passed to a nearly linear function of y/D for high $V/\sqrt{gD}$, The limit would be $c/C_t = 1.0$, for infinite $V/\sqrt{gD}$. Between these upper and lower limits, on semi-log plots, the typical s-shaped concentration curve of Fig. 17 existed.

Smooth pipe had a comparatively non-uniform concentration profile throughout the range of velocities examined. The roughness of the walls was not sufficient to generate large turbulent eddies capable of transporting sediment; the corrugated pipe was capable of generating.

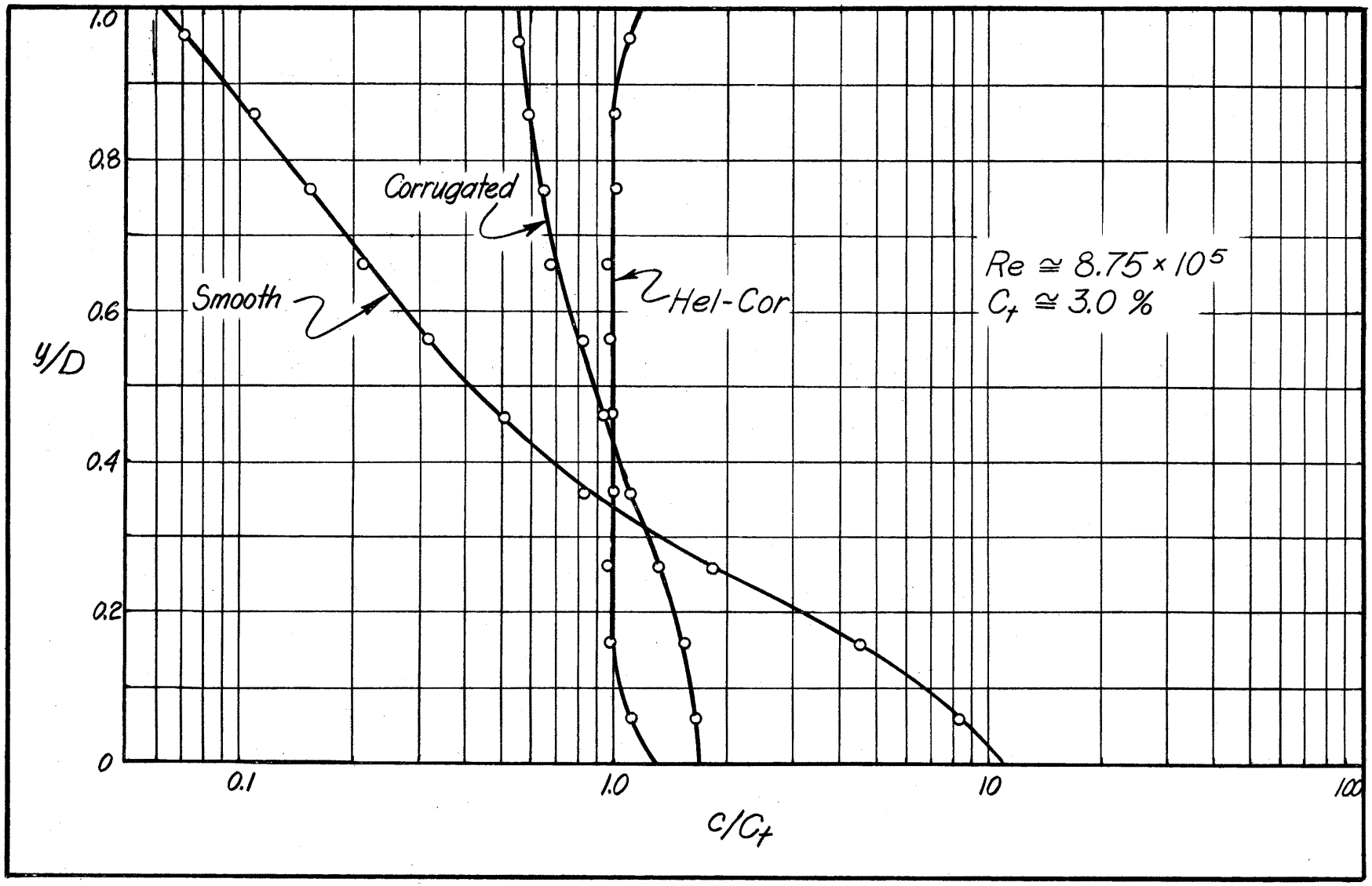

Fig. 17 Comparison of vertical sediment concentration profiles.

Vertical Concentration Profiles in Hel-Cor Pipe

Objectives of this analysis of vertical concentration profiles were to examine the relationship of the parameters in the equation

$$c/C_t = \psi(V/\sqrt{gD}\ ,\ C_t\ ,\ y/D).$$

This is Eq 70 with ϕ/D constant. In order to organize the data for study in terms of Eq 70, they were arranged in groups of nearly constant $V/\sqrt{gD}$ -- that is, one plot for each value of $V/\sqrt{gD}$. See Fig. 18. The C_t for each profile is distinguished by an appropriate symbol. Presentation and discussion are given for several values of $V/\sqrt{gD}$. Some remarks on large eddies and a summary follow.

The limited data for $V/\sqrt{gD} = 0.36$, for incipient deposition, show that there was actually less sediment on the bottom of the pipe than up the side. Deposition occurred for quite low C_t , so low that the "deposit" formed part way up the pipe wall -- where the velocity of the helical shell was about equal to the particle fall velocity.

A value of $V/\sqrt{gD} = 0.79$ is the next lowest given on Fig. 18. In this case there existed a fairly thick shell having a low angular velocity -- hardly sufficient to carry material over a complete circuit from pipe bottom, over the top, and back again. Deposition was about to take place.

The plot for $V/\sqrt{gD} = 0.98$ is nearly identical to the one immediately preceding. The parameter $V/\sqrt{gD}$ had increased but the total load had increased so that deposition was about to begin. Note the nearly uniform concentration distribution characteristic of Hel-Cor just before deposition began.

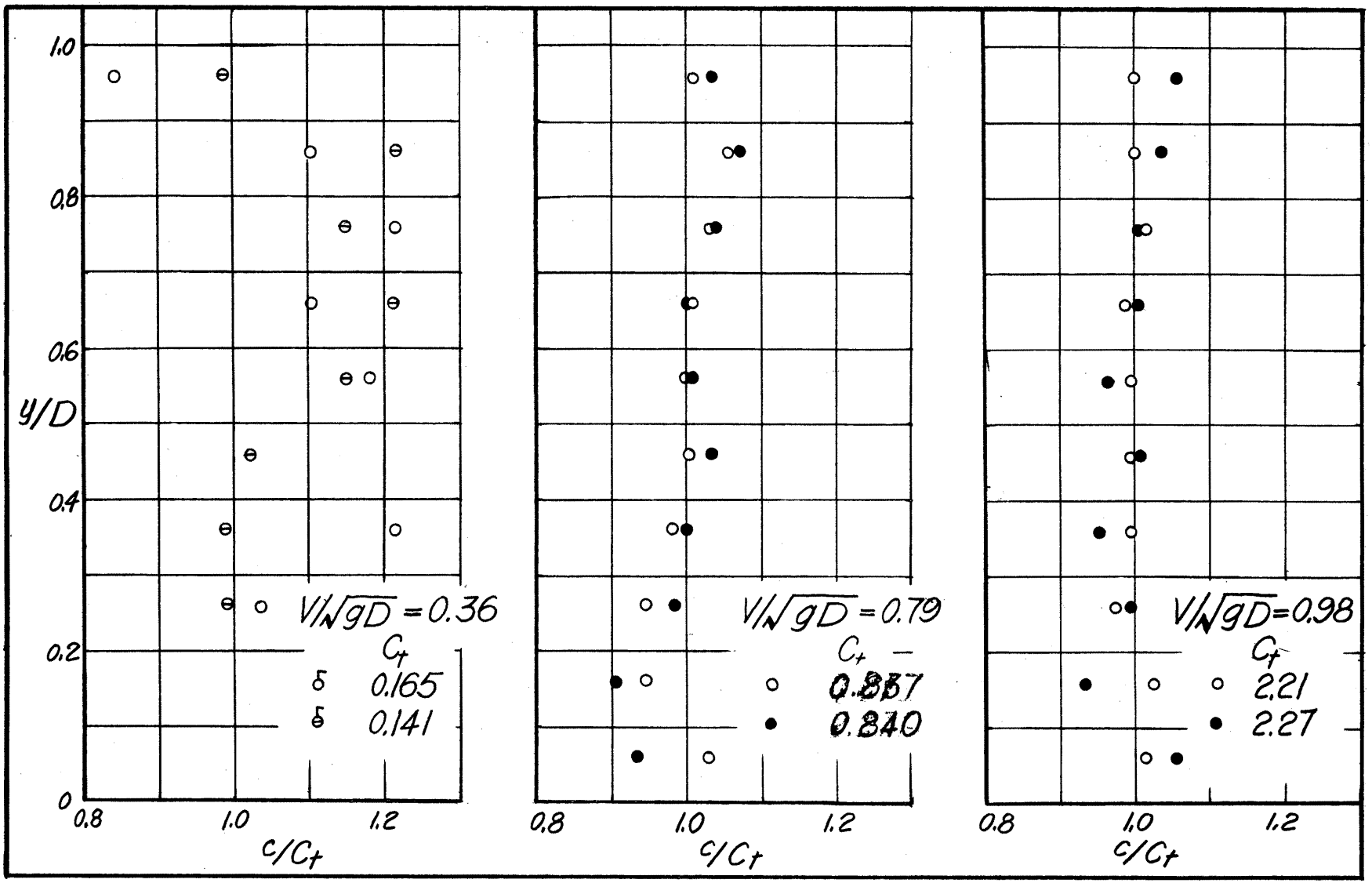

Fig. 18A Variation of vertical concentration profiles with $V/\sqrt{gD}$ for Hel-Cor pipe.

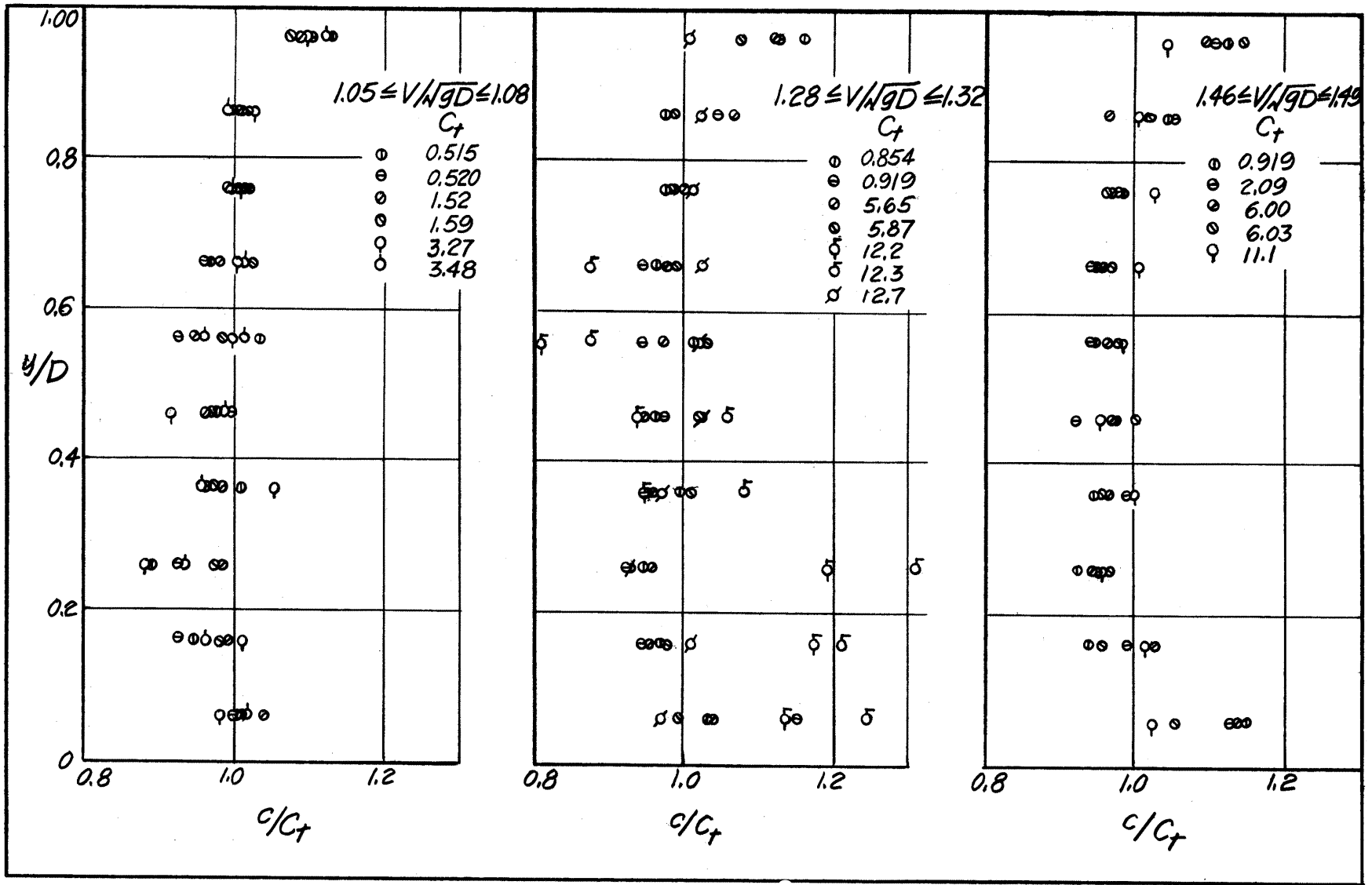

Fig. 18 B Variation of concentration profiles with $V/\sqrt{gD}$ for Hel-Cor pipe —— continued.

When $V/\sqrt{gD} = 1.08$ was reached, material was carried over the top of the pipe before settling into the inner core, even for low concentrations such that the load did not materially slow the rotation of the shell. It is interesting to refer to the horizontal profiles and observe that c/C_t at the wall was about 1.10 to 1.20, and compare this to c/C_t of approximately 1.10 at the top of the pipe. C' is nearly equal to C_t for Hel-Cor.

Data for $V/\sqrt{gD} = 1.30$ are both numerous and informative. The sediment followed a complete path around the pipe for low concentrations. The concentration distribution became more and more uniform as C_t increased, until deposition began. Those data marked with a flag indicate deposition (compare to Fig. 13); which, because of the short c/C_t scale are partial profiles. Comparison of these later data with those for $V/\sqrt{gD} = 0.36$ shows a marked difference in profile form, for the deposition regime. A change also occurred in the flow pattern.

The change in the flow pattern with concentration took place in the following manner. For given $V/\sqrt{gD}$ versus C_t such that $V_L/\sqrt{gD}$ was above the steep part of the $V_L/\sqrt{gD}$ versus C_t curve, and at low C_t, the secondary helical flow along the boundary followed the physical spirals of the pipe walls quite closely. The secondary circulation tended more and more to follow the mean flow as the load increased, and deviated further from the physical boundary helix. The secondary motion was eliminated when the total load increased and deposition began. If C_t increased slightly the profiles somewhat resembled those found in a smooth pipe.

A short note on stability is adequate to explain the incipient deposition point C_t = 12.7 percent when deposition is reported as taking place for C_t less than this. If a bed was present in the pipe the true maximum carrying capacity of the pipe was not reached by gradually increasing $V/\sqrt{gD}$ continuously upward to some point, because the effect of the helical motion did not have a chance to operate. The true maximum was found by increasing $V/\sqrt{gD}$ to a point where all the material was in suspension, the secondary motion was established, and then $V/\sqrt{gD}$ and C_t were regulated until deposition started.

Fig. 19 is a plot of certain profiles depicting the transition from incipient deposition to deposition. The same type of data for $V/\sqrt{gD}$ = 1.17 are also shown on this plot. Shown on Fig. 20 are some profiles in which the helical motion was not present.

Some remarks on large eddies are appropriate. From the section on elementary profile considerations, the Hel-Cor, with the pronounced secondary motion, induced a much more uniform distribution of sediment than a smooth pipe. A similar phenomenon of comparatively constant concentration in the vertical has been observed as "boils", in rivers. These phenomenon are additional evidence to support the idea that secondary circulation and large-scale eddies are the mode by which sediment is transported upward. A smooth pipe, generating only small eddies and no secondary circulation, can not maintain much sediment in suspension. Furthermore, the J-V and f-Re diagrams demonstrated that there is practically no additional energy expended until deposition takes place,

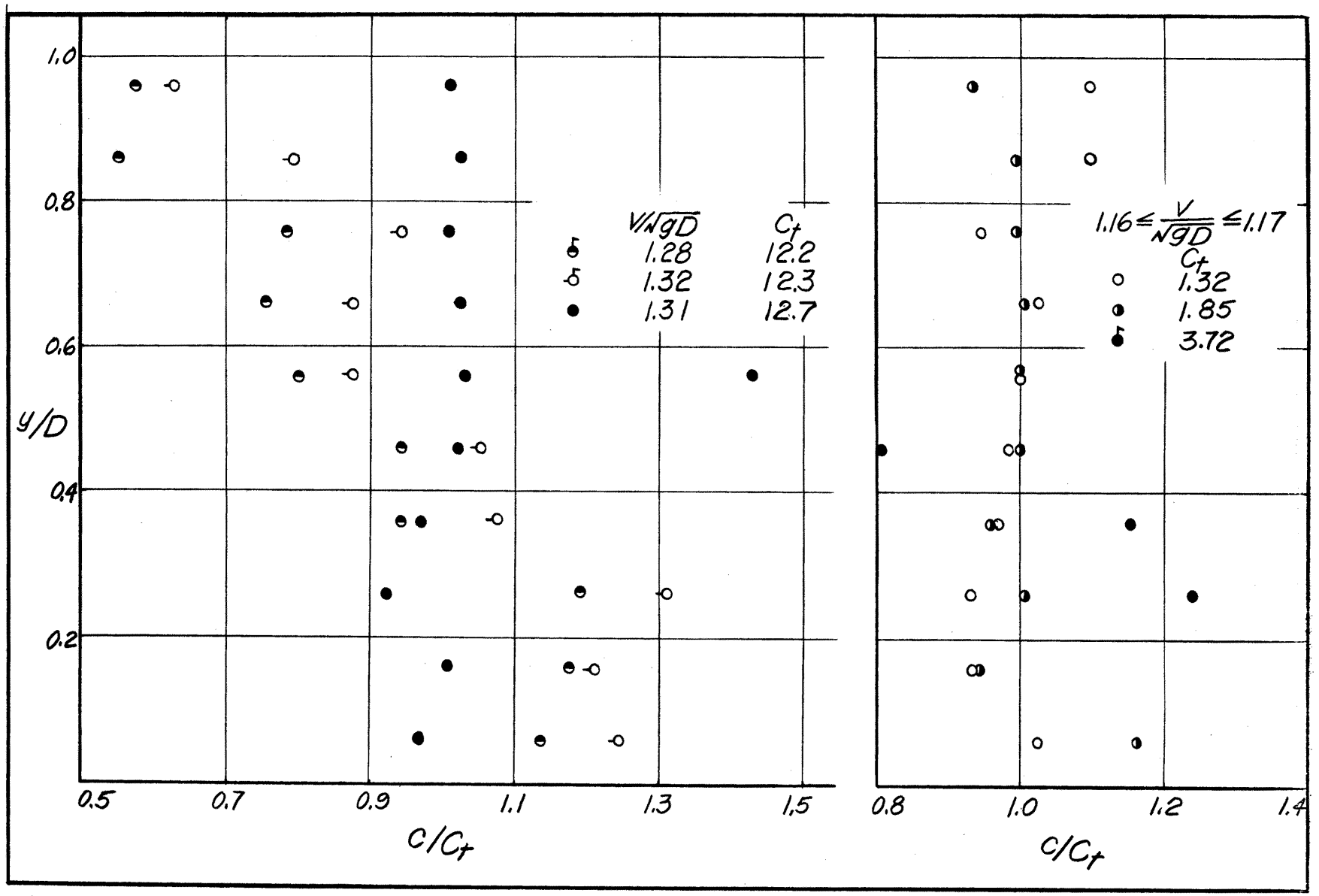

Fig. 19 Effect of damping helical motion on vertical concentration profiles in 12-in. Hel-Cor pipe.

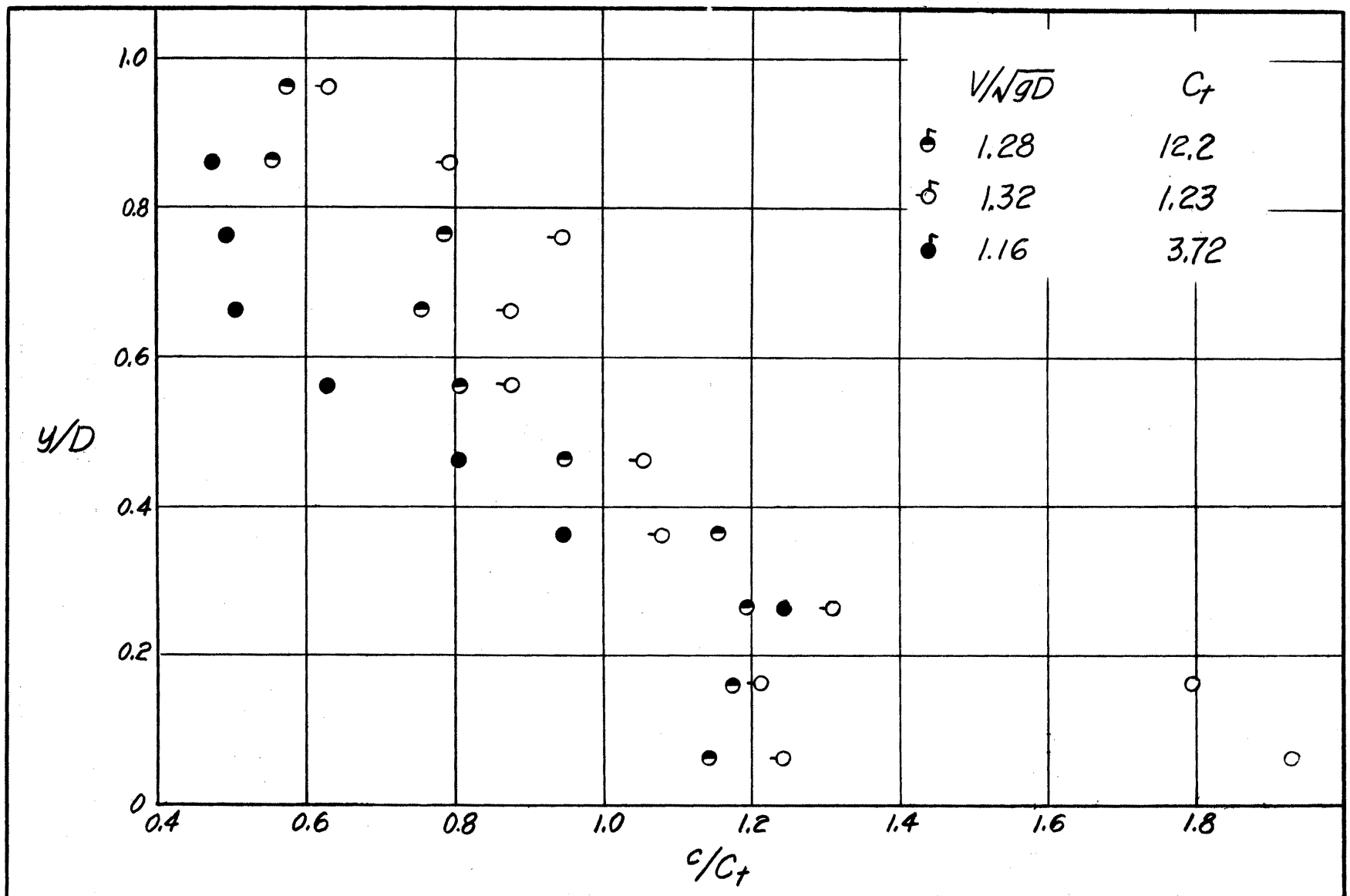

Fig. 20 Effect of eliminating helical motion on vertical concentration profiles in 12-in. Hel-Cor pipe.

which deposition means a change in boundary form. Since the energy expended in supporting the sediment was only a small part of that being dissipated, it is logical to postulate that the energy required to support the sediment is simply transferred to the particles from the large-scale eddies as form drag energy, and not passed on down to the small scale eddies, or energy consumers; thus an energy balance.

The above remarks have further implications. Because the rate of energy transfer to the small-scale turbulent eddies is only slightly reduced, small scale turbulence is damped to only a negligible degree by the presence of the sediment; a very different idea than Vanoni (54), and Danel (13) and (14) seem to have had in mind.

Another deduction is that deposition takes place for a given sediment, having a certain fall velocity, when the particle drag on the large energy transfer eddies is equal to the total mean energy of the eddy. The nearly equivalent C_t at incipient deposition in Hel-Cor and corrugated pipes, for a given $V/\sqrt{gD}$, may be explained from this remark. The Hel-Cor had small frequent corrugations which shed smaller eddies (closer to dissipation rather than energy transfer size) than a corrugated. The Hel-Cor had an additional large-size secondary circulation due to the helical grooves.

With $\underline{V/\sqrt{gD} = 1.48}$, the top and bottom of the pipe had about equal high concentration regions. This means that the sediment was very rapidly circling the entire pheriphery of the pipe. The centrifugal force of the particles was so great compared to the tendency to settle due to gravity that the concentration profile was made up of annular rings.

Following the course of what happened when C_t increased, the high concentration shell gradually disappeared because the energy necessary from the secondary motion was increasing with C_t and the boundary was capable of inducing less and less fluid acceleration as the mass of the shell increased with C_t .

When $V/\sqrt{gD}$ became as large as 1.48 and the flow behavior was as described above, the total load could change over quite large limits without significant deposition occurring. This was not true when $V/\sqrt{gD}$ was so small that sediment was not carried over the top of the pipe.

Summary of the study of Hel-Cor vertical concentration profiles rests on the significant parameter $V/\sqrt{gD}$. The concentration profile, y/D versus c/C_t , took on a given form for each $V/\sqrt{gD}$, that depended somewhat on C_t . Deposition began, for low $V/\sqrt{gD}$, when the fall velocity w was about equal to the vertical component of the angular velocity of the secondary helical motion. For larger $V/\sqrt{gD}$, deposition began when the secondary circulation was reduced to negligible proportions.

Vertical Concentration Profiles in a Smooth Pipe

Study and interpretation of the vertical concentration profiles in smooth pipe was slightly complicated by the fact that the median particle size varied considerably over the cross-section for a sediment with a large standard deviation of sediment diameter. Such a problem does not arise in a boundary inducing a nearly uniform concentration. The effect of the size distribution and Reynolds number will be discussed briefly, with the aid of Fig. 21.

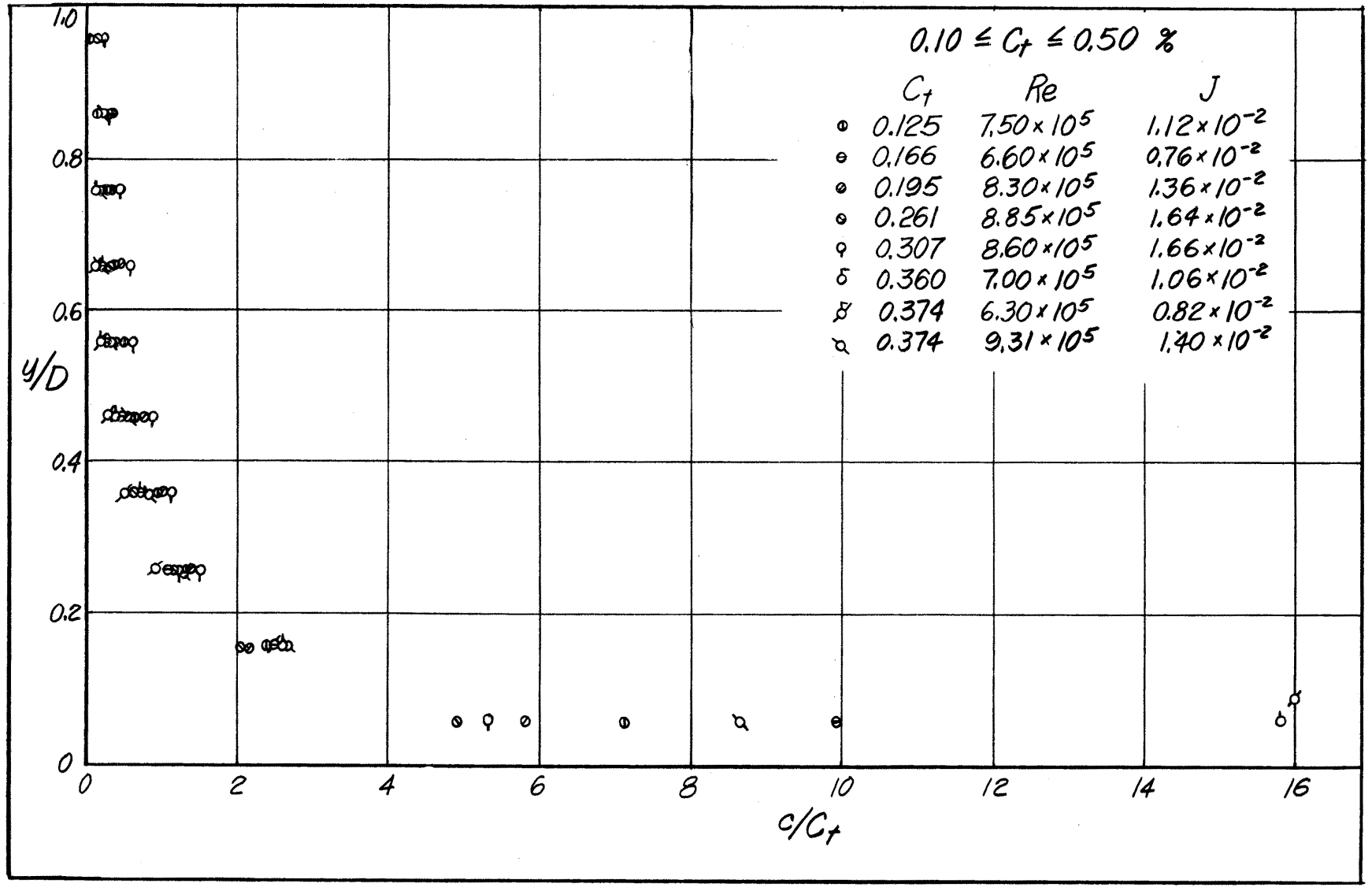

Fig. 21 A Variation of vertical concentration profiles with total load, Reynolds number, and hydraulic gradient—smooth pipe.

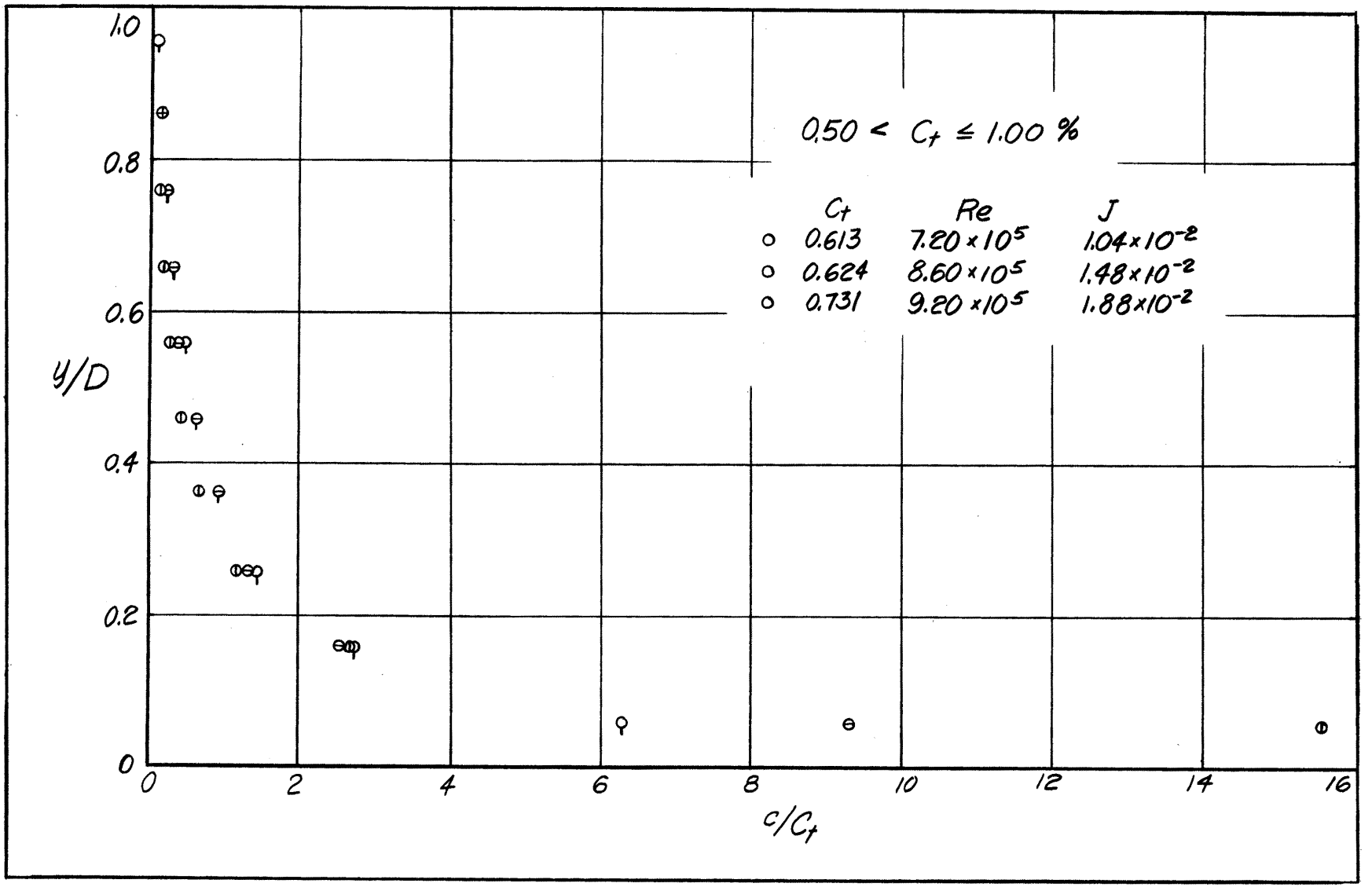

Fig. 21 B Variation of vertical concentration profiles with total load, Reynolds number, and hydraulic gradient — smooth pipe — continued.

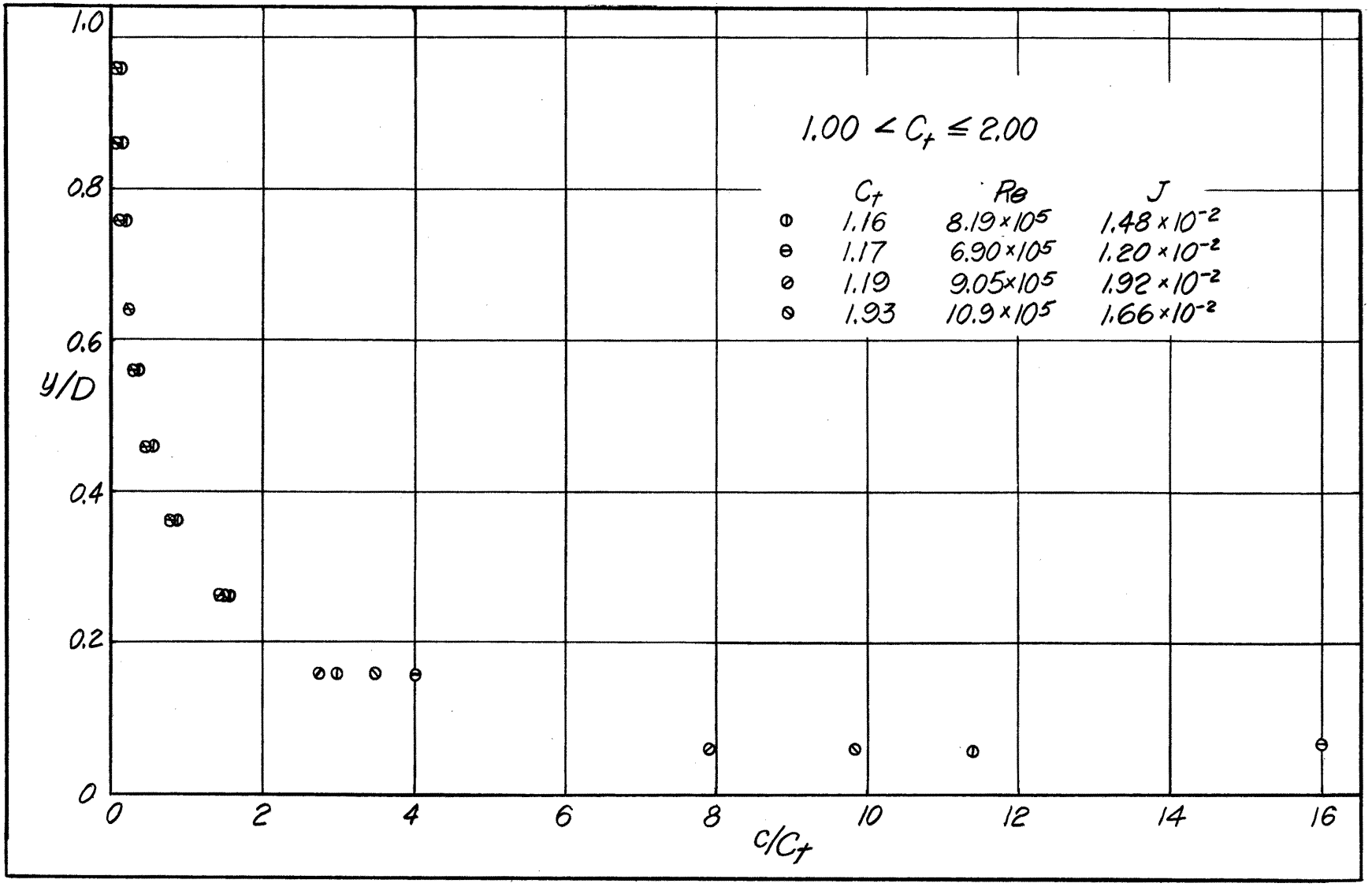

Fig. 21 C Variation of vertical concentration profiles with total load, Reynolds number, and hydraulic gradient — smooth pipe — continued.

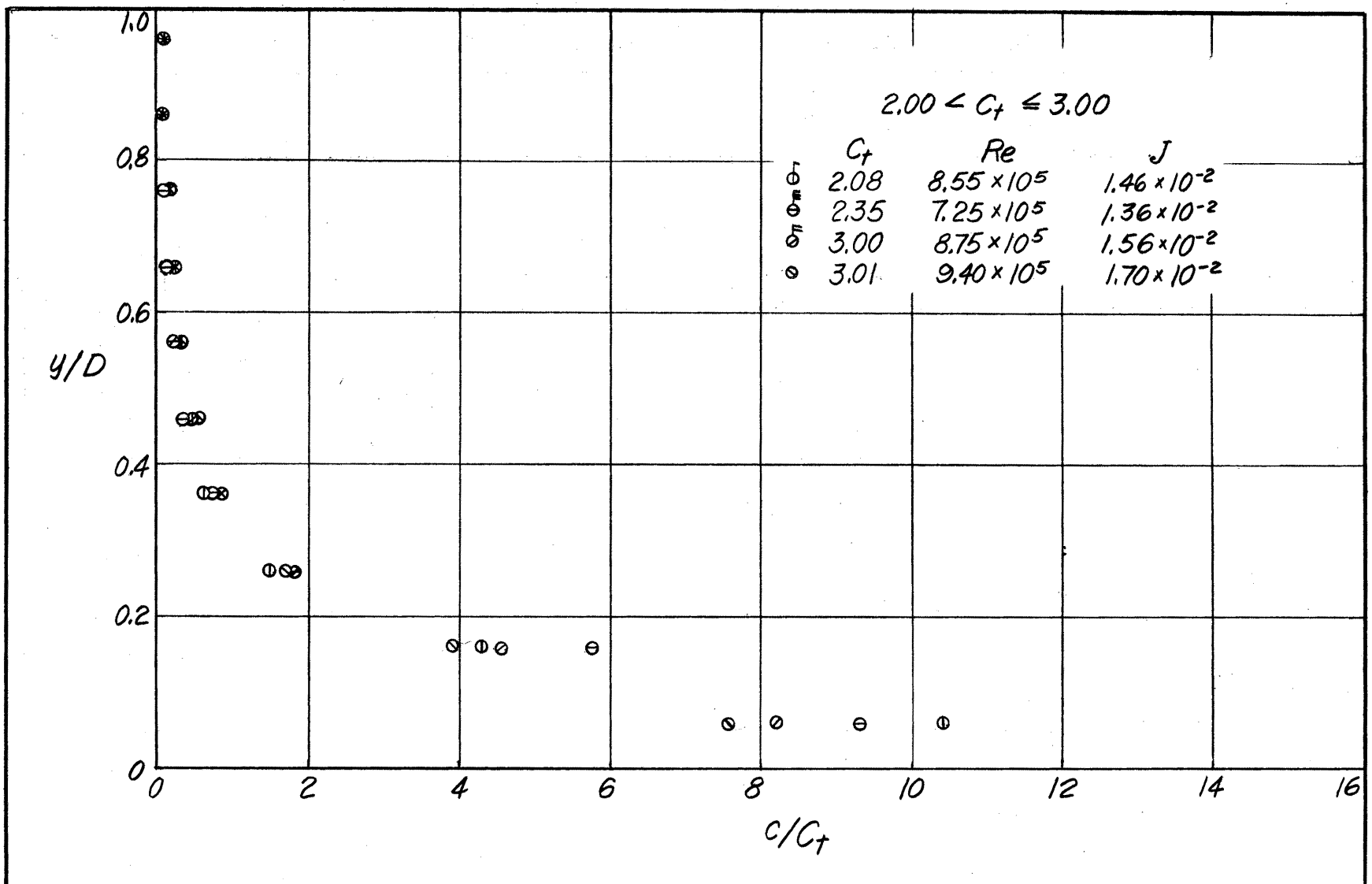

Fig. 21 D Variation of vertical concentration profiles with total load, Reynolds number, and hydraulic gradient — smooth pipe continued.

The primary contribution to sediment transport mechanics stems from

$$c/C_t = \psi(V/\sqrt{gD}\ ,\ C_t\ ,\ y/D)$$

Fig. 22 is a plot of the smooth pipe data in a manner similar to Fig. 18 for Hel-Cor pipes. The salient points to be considered are: 1) form of the profiles, 2) effect of $V/\sqrt{gD}$, 3) absolute criterion for incipient deposition, 4) a practical determination of the total load, and 5) Richardson number.

Effect of size distribution was most pronounced where the slope of the concentration profile was rapidly changing. Fig. 21, separated into intervals of C_t, shows that the slope was changing rapidly at $y/D = 0.2$. This elevation is chosen for subsequent remarks.

The c/C_t increased as C_t increased. This implies that if C_t was doubled for example, with a given $V/\sqrt{gD}$, the concentration would not double over the full profile but would increase near the bottom of the pipe. This occurs when σ_d has a measurable influence.

Careful study of Fig. 21 with Reynolds number as a fourth variable (C_t as the third variable) indicated that the scatter in the lower regions of the concentration profile was not put in order. Another significant parameter had to be considered. The effect of Re and the reasons for dropping it for profile analysis were discussed earlier.

The form of the profiles depended to a marked degree on the total load; unlike Hel-Cor and corrugated which vary only slightly with C_t.

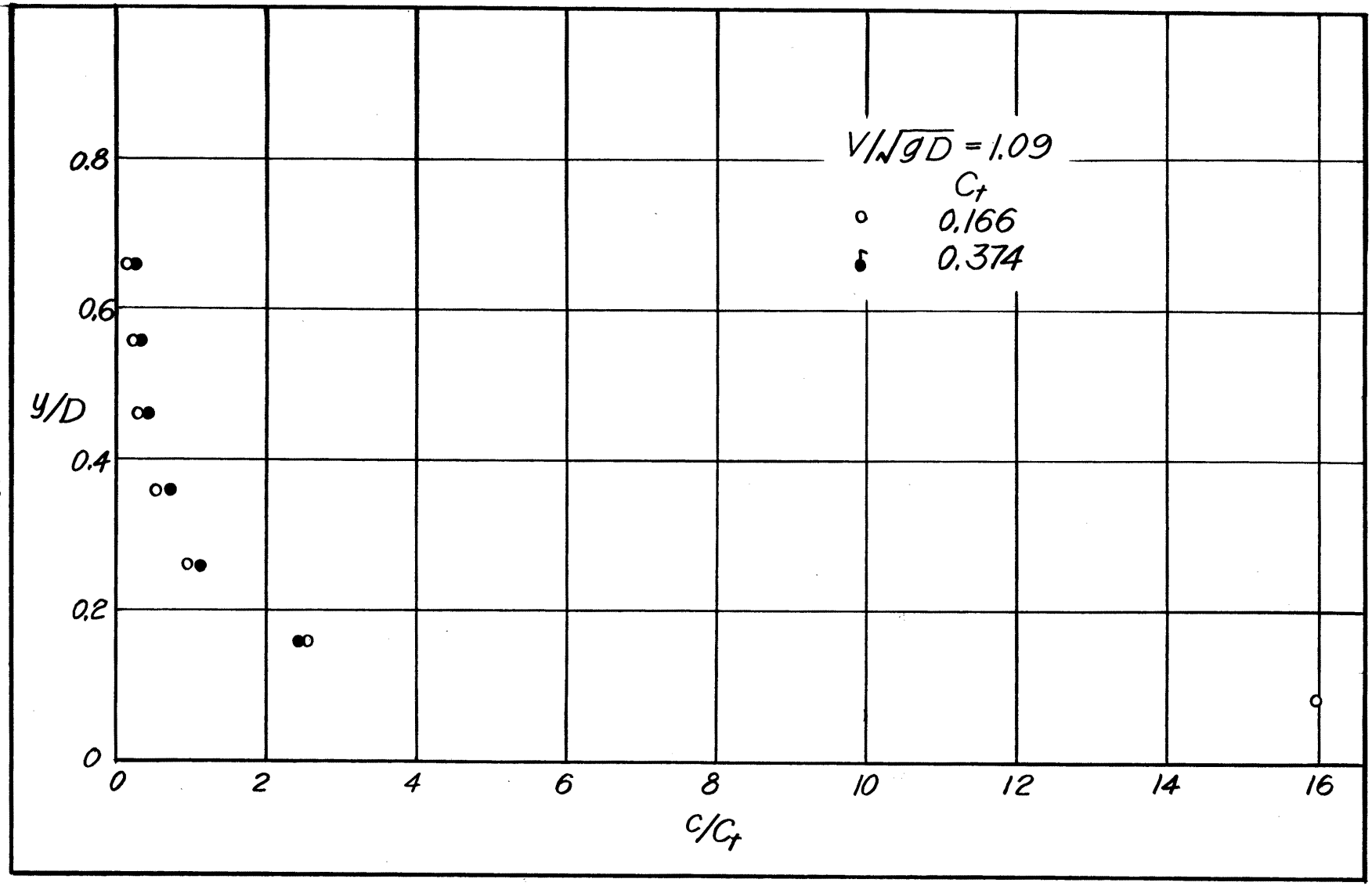

Fig. 22 A Variation of vertical concentration profiles with $V/\sqrt{gD}$ in 12-in smooth pipe.

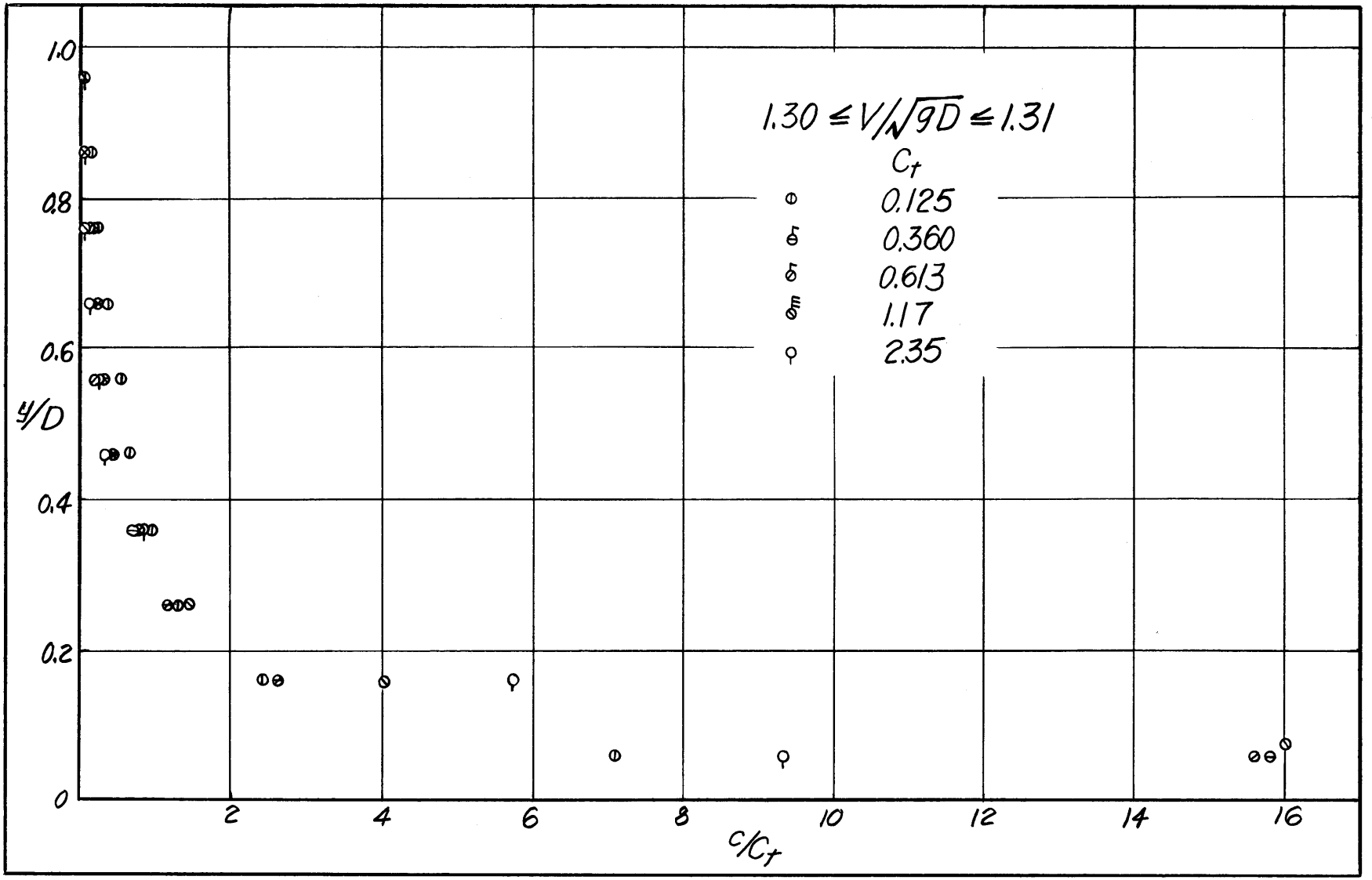

Fig. 22 B Variation of vertical concentration profiles with $V/\sqrt{gD}$ in 12-in. smooth pipe — continued.

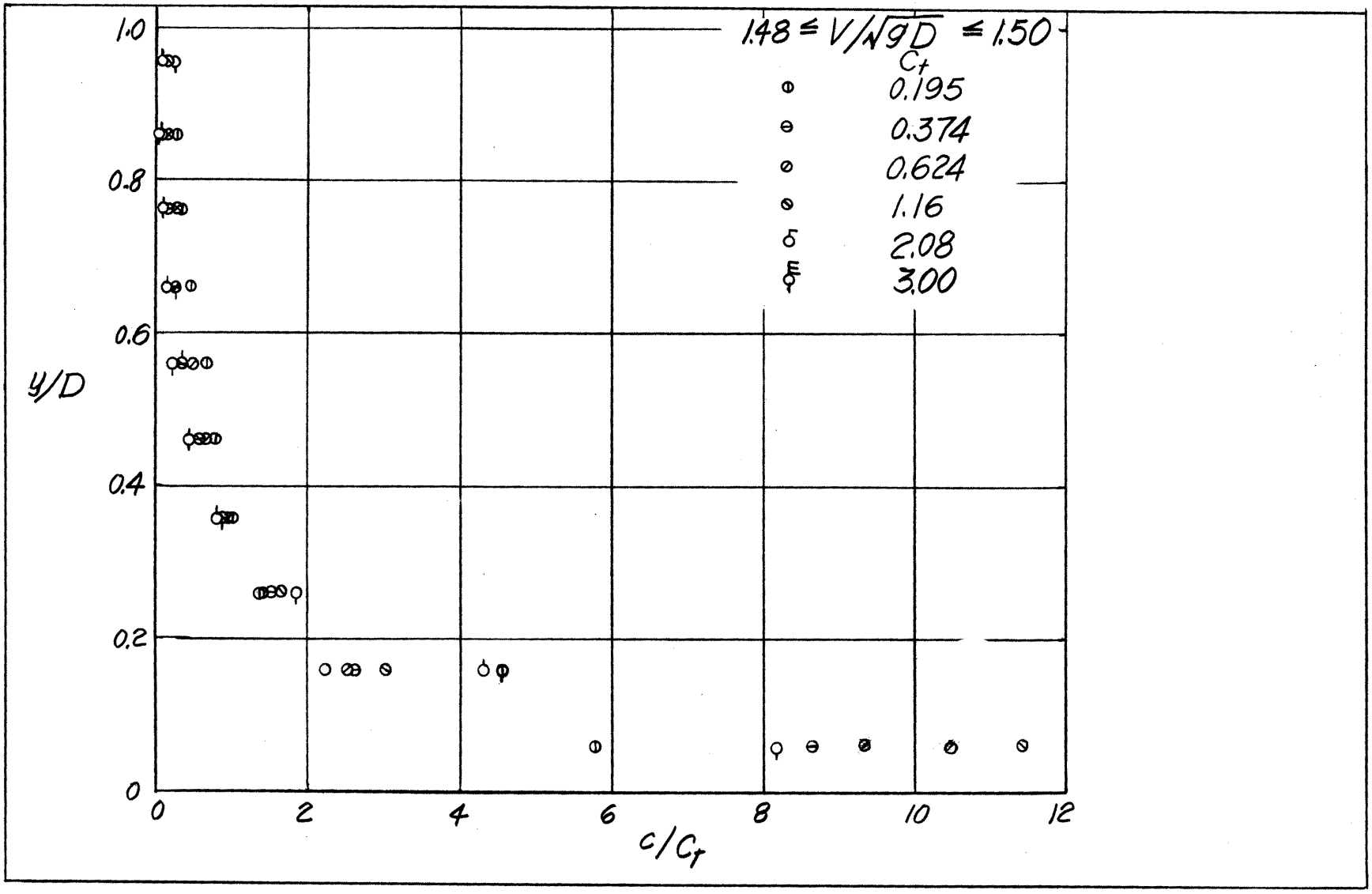

Fig. 22C Variation of vertical concentration profiles with $V/\sqrt{gD}$ in 12-in smooth pipe —continued

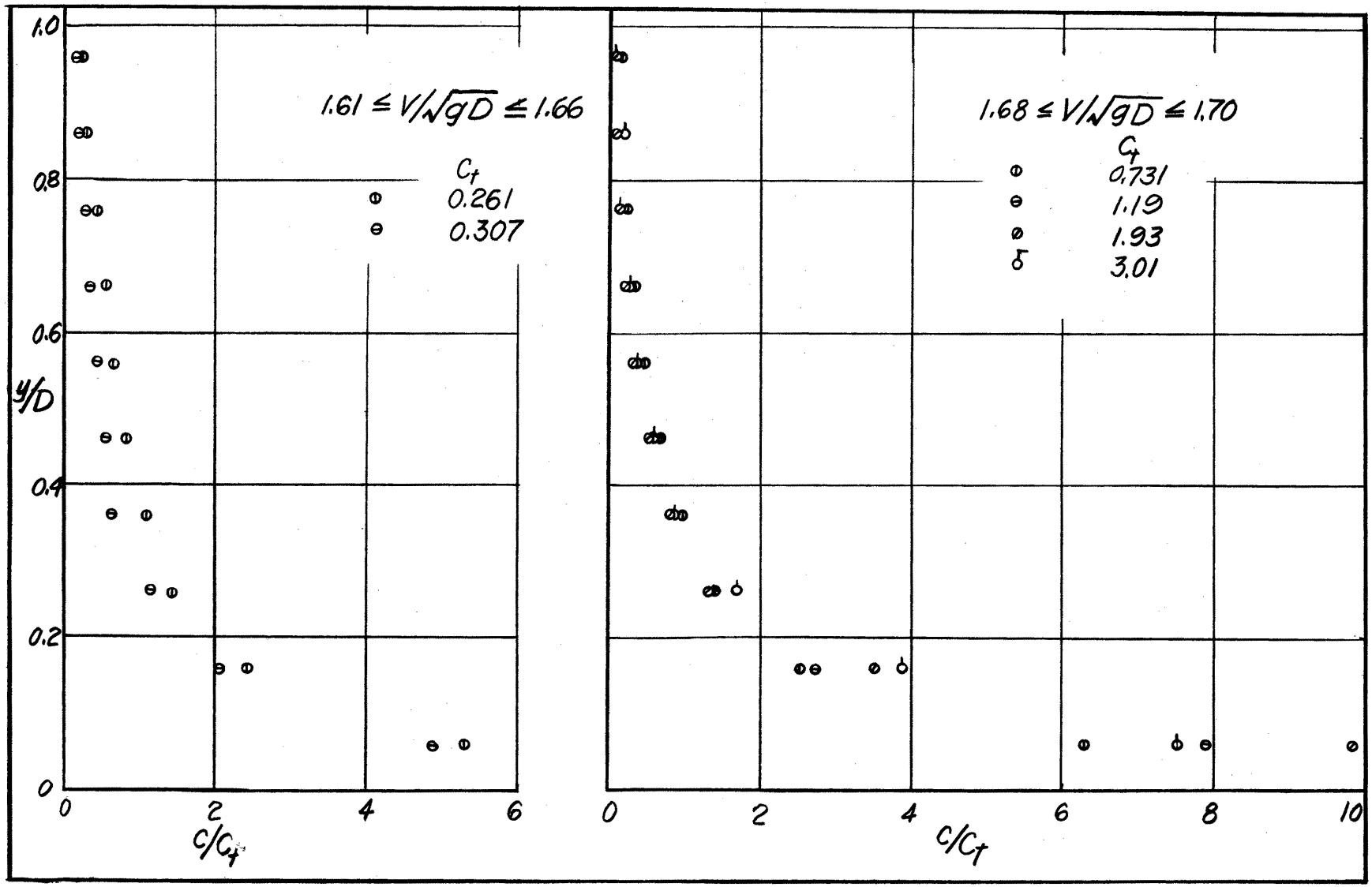

Fig. 22 D Variation of vertical concentration profiles with $V/\sqrt{gD}$ in 12-in. smooth pipe — continued.

A significant difference in the concentration profiles of the three pipes was that a considerable portion of the total load was transported through every small part of the pipe cross-section in Hel-Cor and corrugated, but the top quarter of a smooth pipe carries practically clear water. Conveying clear water is very uneconomical in sediment transport works -- such as in dredging.

The effect of $V/\sqrt{gD}$ was to increase the concentration near the top of the pipe and to decrease it toward the bottom, as $V/\sqrt{gD}$ increased. This is equivalent to saying that as $V/\sqrt{gD}$ increased, the value of c/C_t at the bed, corresponding to deposition, decreased. It is not implied, however, that the local concentration necessary for deposition was less; C_t was much higher when agradation began.

The possibility of developing an absolute criterion for incipient deposition can be seen by considering a plot (see Fig. 23) of C_t versus c/C_t at $y/D = 0.06$ for each $V/\sqrt{gD}$. Data were insufficient for a complete study, but the trend is certainly evident and significant.

The importance of the $V_L/\sqrt{gD}$ versus C_t plot in comparative studies of various pipes for design problems involving horsepower, rate of sediment discharge and excessive water losses points out the need for an evaluation of incipient deposition other than that of visual observation -- which is not the same for any two observers -- to determine incipient deposition. It is proposed that the maximum c/C_t, for a constant $v/\sqrt{gD}$ on a c/C_t versus C_t plot for a given y/D, be used in determining the C_t for incipient agradation.

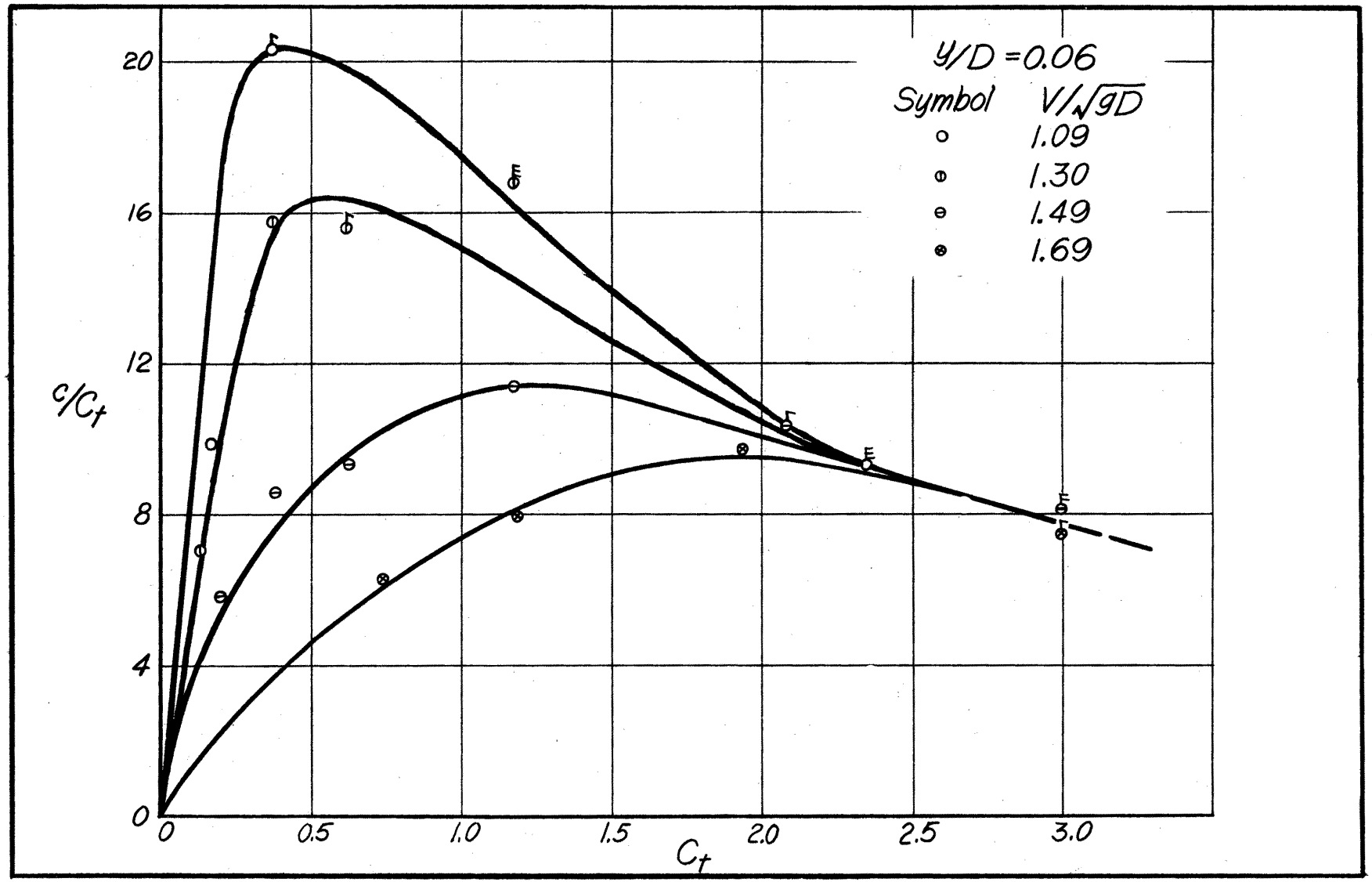

Fig. 23 Absolute criterion for incipient deposition—12-in. smooth pipe.

The magnitude chosen for y/D is not important as long as it is consistent for a complete set of runs in a given pipe and picked somewhere near the bottom of the pipe so that appreciable differences in c/C_t are found.

Sufficient evidence has been presented by earlier investigators to prove that the most economical point for operating a sediment transport line is associated with incipient deposition. Comparing the results of scientists from various parts of the world, in order to evaluate the effect of particle size, pipe diameter, sediment density, etc. on this economical operating point, was practically impossible because the observations of each person were based on personal judgment. The proposed method would eliminate the personal factor.

Fig. 23 demonstrates clearly that, as $V/\sqrt{gD}$ increased, there was an increasingly large range of C_t over which an observer would say deposition was about to begin. The maximum becomes less and less distinct for increasing $V/\sqrt{gD}$.

There are a number of possible applications of an absolute criterion for deposition in flume studies on stable channels, beyond the scope of the present work.

A <u>practical determination of total load</u> C_t for, say dredge operators, is indicated in Fig. 22. A simple and rapid-technique is desirable in order that an operator can maintain maximum efficiency. A single sampling tube located at $y/D = 0.3$ will determine C_t with probably $\pm$ 15 percent maximum error, within the range of velocities and concentrations of these data. Durand (16) presented a plot for 0.18 mm

sediment in a 150 mm pipe which shows essentially the same results for velocities up to about 15 fps.

The Richardson number

$$Ri = \frac{g}{\rho} \frac{d\rho_i}{dy} \Big/ \left(\frac{du}{dy} \right)^2 \qquad \text{Eq 6}$$

could be used for an analysis of the transition from suspended transport to bed load. The lower portion of the concentration profiles, such as used in the derivation of the incipient deposition criterion, show that $d\rho/dy$ will increase with ρ until agradation starts. After a deposit begins to form, $d\rho/dy$ decreases even though ρ continues to increase. Before deposition sets in, dv_1/dy will decrease with concentration, but when a bed begins to form the small ripples will induce sufficient turbulence to increase dv_1/dy.

The end product of the above variations of the individual terms in R_i is that, as C_t increases, R_i will probably increase slightly until deposition begins, and then drop rather sharply.

Vertical Concentration Profiles in a Corrugated Pipe

Concentration profiles in a corrugated pipe are somewhat easier to interprete than those in Hel-Cor and smooth pipes. Fig. 24 has profiles separated into groups of nearly equal Re, with Re, C_t and $V/\sqrt{gD}$ designated by a symbol for each profile. These plots were used to determine the behavior of the profiles as a function of Re. Fig. 25 is a plot similar to Fig. 24 but with constant $V/\sqrt{gD}$ and the symbols

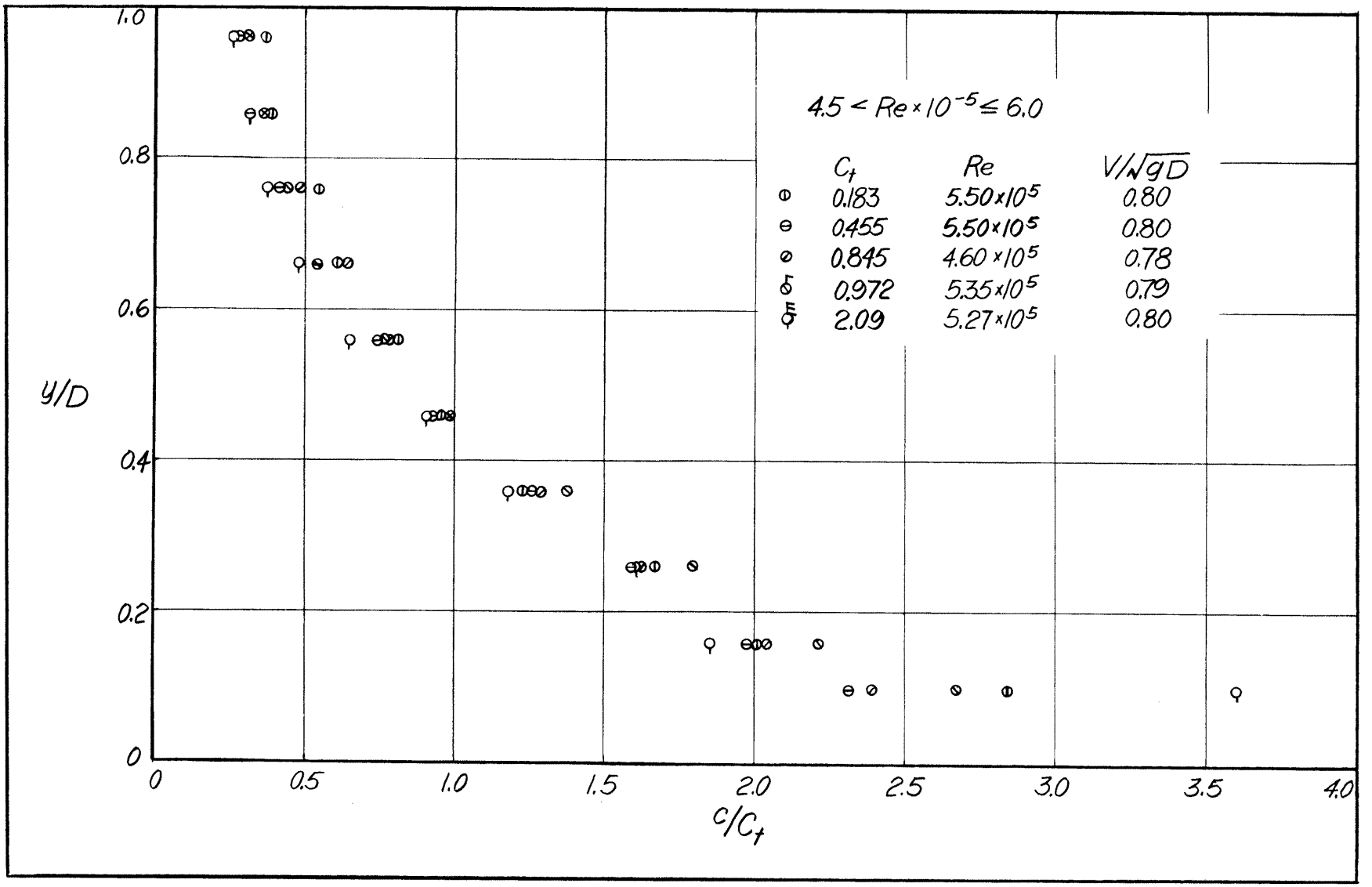

Fig. 24 A Dimensionless vertical concentration profiles — 12-in. standard corrugated pipe.

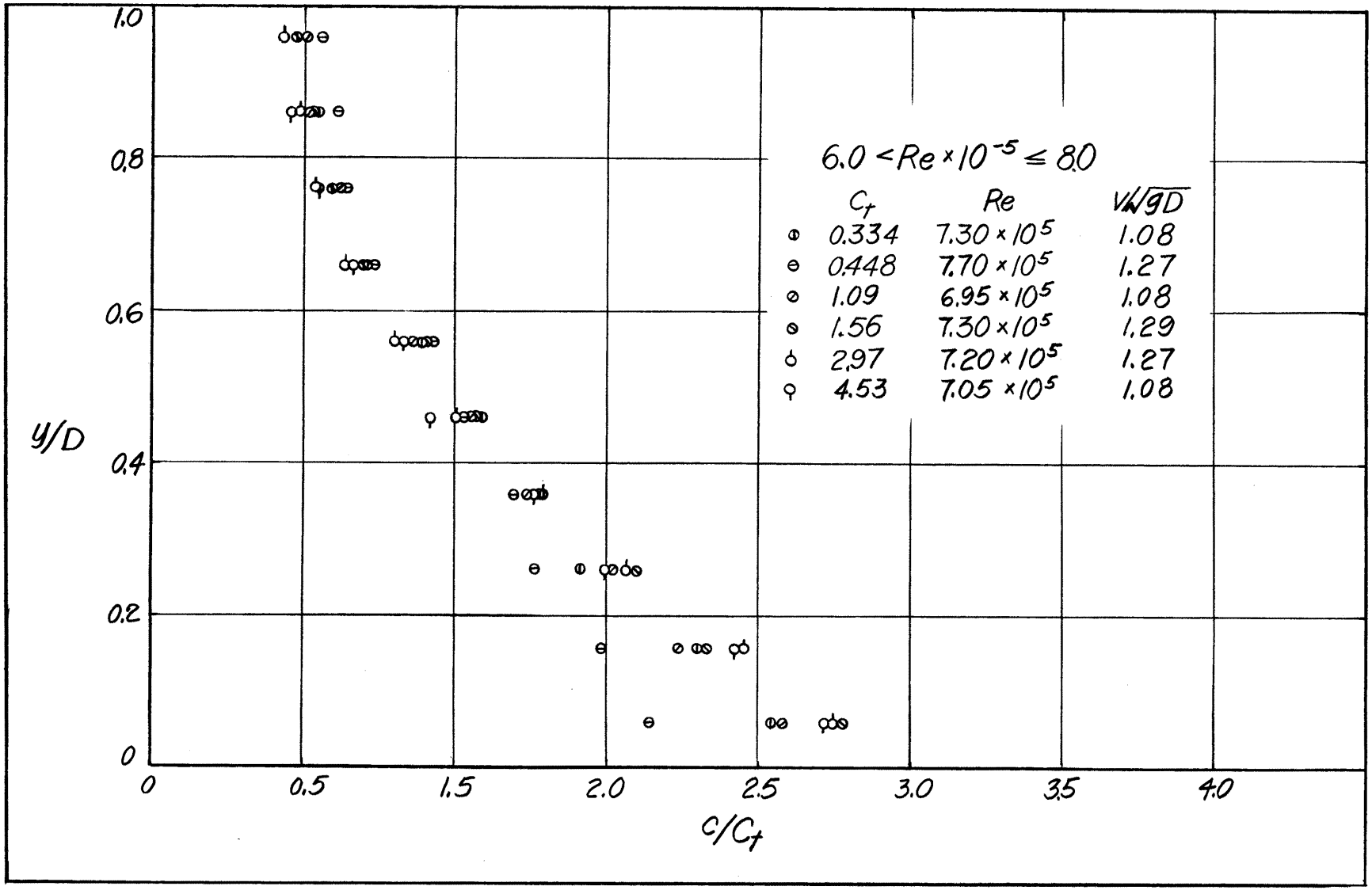

Fig. 24 B Dimensionless vertical concentration profiles—12-in. standard corrugated pipe— continued.

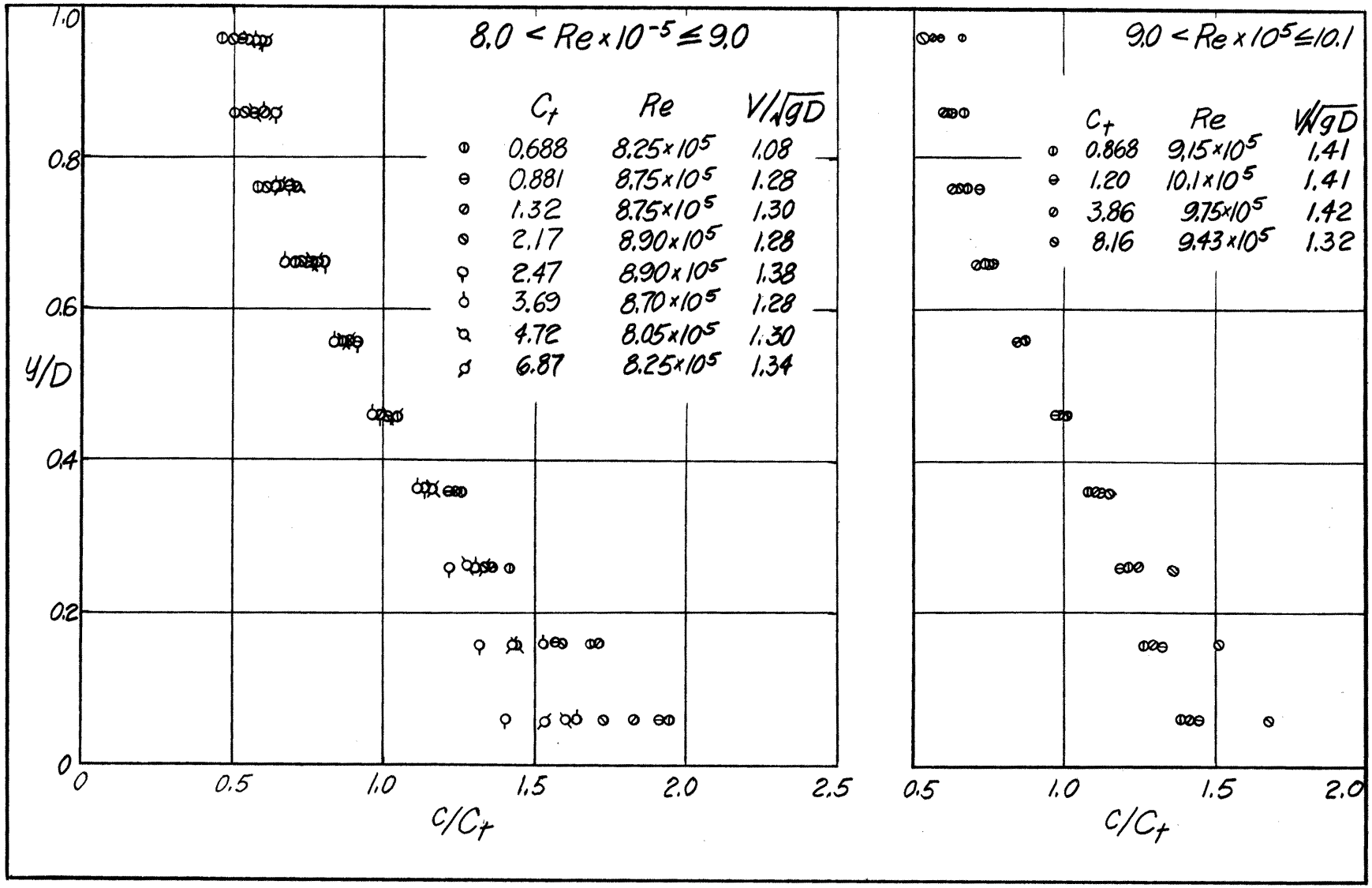

Fig. 24 C Dimensionless vertical concentration profiles — 12-in. standard corrugated pipe — continued.

denoting C_t . This latter figure was employed in evaluating the effect of $V/\sqrt{gD}$ and C_t . Fig. 26 is a composite of all the profiles for corrugated pipe, based on the equation

$$c/C_t = \psi (V/\sqrt{gD} , \quad y/D) .$$

Reynolds number, in Fig. 24, has been used as a third variable to illustrate that it did not seem to be an adequate parameter on which to base the profile analysis. Consideration of the individual Re in each Re interval, in conjunction with the associated C_t and J , did not lead to any consistent conclusions. But if $V/\sqrt{gD}$ is used on this same Fig. 24, a consistent trend is present.

Accordingly, the $V/\sqrt{gD}$ parameter was used as a third variable in Fig. 25, with 5 to 10 fold changes in C_t as a fourth variable. The concentration profile depended to some extent on C_t at small values of $V/\sqrt{gD}$. As $V/\sqrt{gD}$ increased, the dependency of c/C_t on C_t disappeared and became more and more a linear function of elevation.

The main conclusion from the analyis was that the corrugated boundary induced sufficient large scale turbulence, even at quite low velocities, to distribute sediment over the entire cross-section to such an extent that size distribution played a negligible role.

With C_t unimportant, the profiles may be represented by $c/C_t = \psi (y/D , \quad V/\sqrt{gD}$. Fig. 26 is the result of drawing representative curves through each $V/\sqrt{gD}$ plot of Fig. 25. The concentration profile is nearly linear for $V/\sqrt{gD} = 1.40$. This means that if Eq 34,

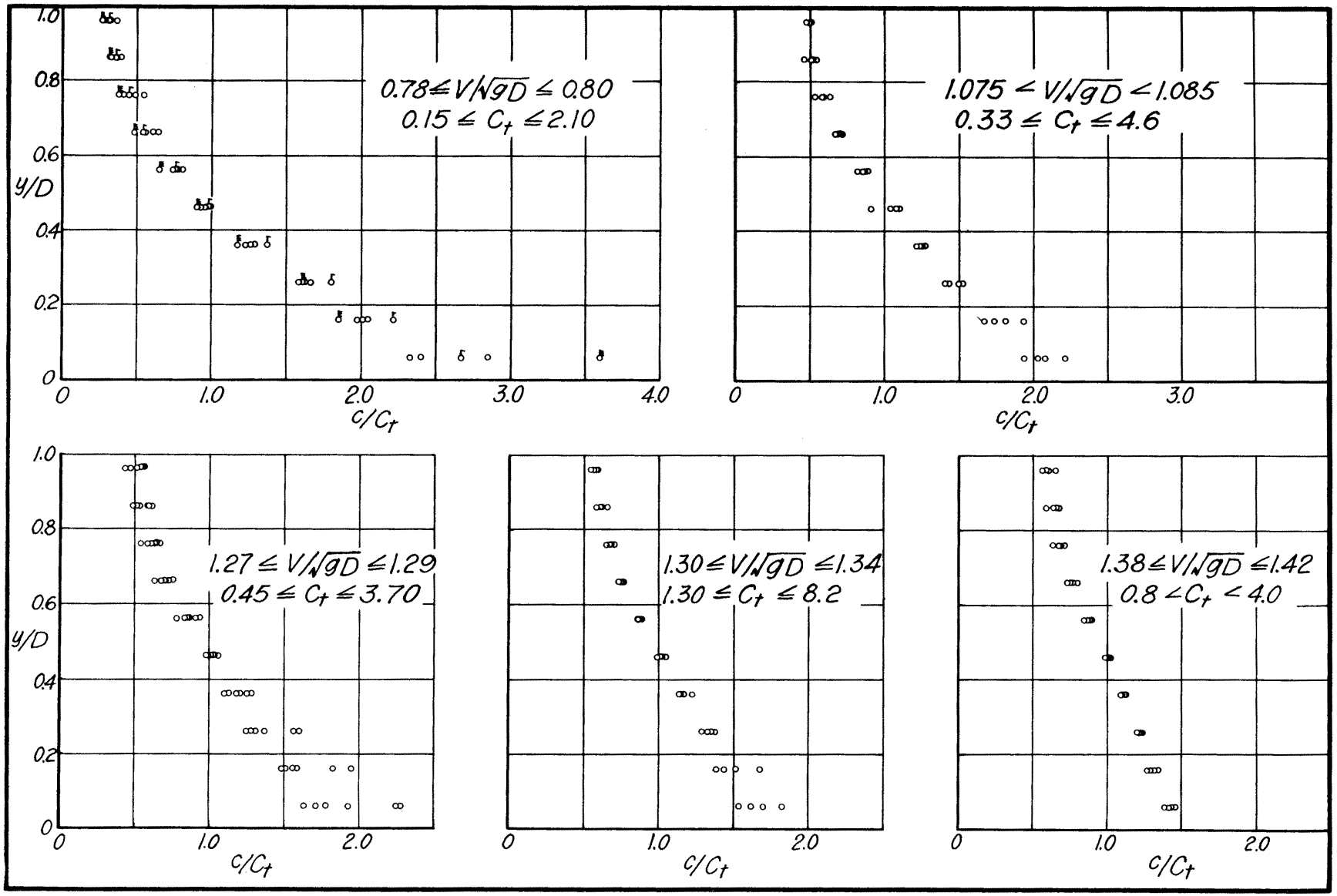

Fig. 25 Vertical Concentration profiles as a function of $V/\sqrt{gD}$ — 12-in corrugated pipe.

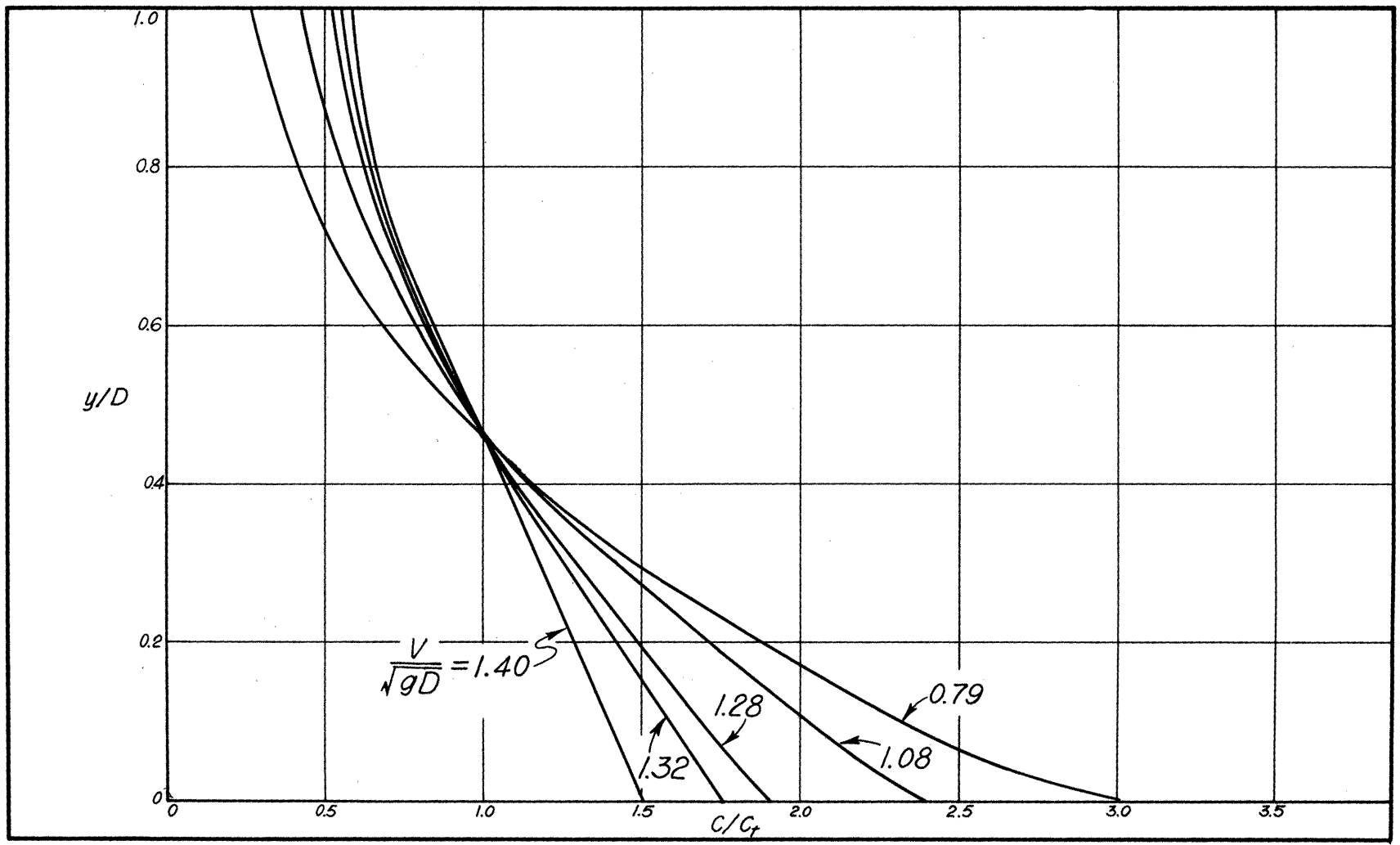

Fig. 26 Composite of vertical concentration profiles – $V/\sqrt{gD}$ as third variable – corrugated pipe.

$cw = -\epsilon_s \, dc/dy$, is applicable then ϵ_s/w is a linear function of distance from the boundary near the crest of the corrugation. A plot of ϵ_s/w versus y/D for $V/\sqrt{gD} = 0.79$ yields a straight line on semi-log paper. This implies that ϵ_s was a constant over the vertical diameter of the pipe. One may conclude that if a boundary is not available which causes pronounced secondary circulation, then the next best type would be a boundary characterized by ϵ_s/w being a linear function of y/D .

Diffusion Coefficient ϵ_s and the Kármán Constant κ

The coefficients ϵ_s and κ are terms which have been receiving considerable attention in recent years, particularly by engineers studying alluvial channels. An analogy exists of course to pipe flow, and the variables, particularly ϵ_s , are applicable in both cases. A detailed study of ϵ_s and κ is beyond the scope of this dissertation; but have been computed and tabulated in an appendix to expedite future research along such lines.

The parameter ϵ_s/w in Eq 34 was determined graphically from plots of the concentration profiles. Data are available for both smooth and corrugated pipes. Since dc/dy was usually zero in the Hel-Cor a tabulation was not possible.

Cursory examination of these data indicated that in the smooth pipe the minimum ϵ_s/w occurred near the lower boundary, increased to a maximum at $y/D = 0.6$ to 0.8 and decreased somewhat as the top of the pipe was approached. The corrugated boundary had a maximum near the top and bottom, and a minimum near the center of the pipe.

The Kármán κ was computed from $z_1 = w/\kappa\, u_* = (w/\kappa V)(\sqrt{8/f})$, in Eq 5. The lower half of the concentration profiles were plotted on log-log paper. The approximate slope was z_1. The constant a was set equal to D/20. Two values of κ were tabulated for the corrugated, κ and κ^1. The former was computed by starting calculations from the crest of the roughness, and the latter from the trough -- assuming an observer inside the pipe.

In the smooth pipe, κ ranged from 0.21 to 0.34. The corrugated boundary had κ values going from 0.34 to 1.33 and κ' from 0.36 to 1.43.

The wide variation and seemingly absurd values are due to concentration and the poor fit of the data to Eq 5.

Summary

The internal mechanics vary, superficially, from pipe to pipe. Hel-Cor had a nearly uniform concentration because of the secondary circulation induced by the helical corrugations. Smooth pipe had a profile comparable to the familiar open channel type. Corrugated pipe maintained a profile intermediate to that of Hel-Cor and smooth. This latter pipe had a fairly large concentration at the top of the pipe and increased in an almost linear manner to the pipe bottom.

An absolute criterion for incipient deposition in pipes is proposed. Very marked differences were apparent in the sediment exchange coefficient and the Kármán κ between smooth and corrugated pipe. Near the

bottom of the pipe, ϵ_s was a minimum in smooth pipe and a maximum in corrugated. The Kármán κ was less than 0.36 for smooth, and ranged to as high as 1.43 in corrugated.

Chapter VIII

SUMMARY AND CONCLUSIONS

Engineering problems involving sediment are many and varied. Pipeline conveyance of fine sediments in suspension was the narrow part of sediment engineering from which the research problem reported in this dissertation was drawn. Presented below are: 1) problem, 2) theoretical considerations, 3) dimensional analysis, 4) equipment, 5) procedure, 6) summary of analysis of data, 7) conclusions, and 8) future studies.

Problem

The problem was to investigate the effect of three artificially roughened boundaries on the energy requirements and mechanics of the horizontal transport of 0.20-mm sand suspended in a water medium. The problem which was studied arose because, within comparatively recent years, pipe manufacturers have been able to economically install artificial roughness in the boundary of pipes. The study took place during the period from September, 1952, to June, 1955. The pipes investigated were nominal 12-in. diameter Hel-Cor, corrugated and smooth, all available commercially.

Theoretical Considerations

Theoretical considerations involved derivation of a general continuity equation in differential form for the spatial distribution of the sediment concentration, and some studies of the rate of energy dissipation on a local and one-dimensional level.

Dimensional Analysis

Dimensional analysis was used to derive functional equations for several special problems. Some of these problems were directed toward determining the effect of boundary form on the parameters which enter the one-dimensional analysis of pipeline resistance. The f-Re diagram, with boundary form and total load as additional variables, played a major role in studying frictional resistance. A function of horsepower, sediment discharge and mixture discharge, as affected by boundary form, was derived for economic and design comparisons at the most efficient operating level of each pipe.

Equations for analysis of the mechanics of the sediment transport process were developed, usually with the ratio of local concentration to total load as the dependent variable. An absolute criterion for incipient deposition was derived.

Equipment

Equipment consisted of the three boundary forms, a pump capable of delivering 10 cfs, an orifice to measure mixture discharge, a sampler for total load determination and a bank of piezometers along the test pipe. Equipment was also installed to measure the local velocity and to obtain samples of the sand-water mixture at any point in a cross-section of the boundary being investigated.

Procedure

The procedure, for each run, was to measure mixture discharge, hydraulic gradient, temperature, total sediment load, and to obtain three

samples of the mixture at each of ten points along a diameter of the pipe. Each sample had a volume of one litre. The hydraulic gradient was measured in feet of clear water per foot of pipeline.

Summary of Analysis of Data

Several important points were brought out by analysis of the data obtained during this investigation on the suspended transport by water of 0.20-mm sand in horizontal 12-in. Hel-Cor, corrugated and smooth pipes.

1. A calibrated sediment cone was found sufficiently accurate for converting the apparent volume of sediment, in one litre samples of the sand-water mixture, to concentration of sediment in percent by volume.

2. A set of piezometers located on the crests of the corrugations of standard corrugated pipe registered the same magnitude of the hydraulic gradient as a set located in the corrugation troughs.

3. An orifice placed in a vertical section of the circulation system was a favorable location for measuring total sediment load.

4. The differential piezometric head, between a corrugation crest and trough on the corrugated pipe, decreased for a given Reynolds number as total load increased.

5. The Darcy-Weisbach resistance coefficient, for a given boundary, was not significantly affected by the presence of fine sand until the total load of sediment increased to a magnitude which caused deposition to take place in the pipe.

6. The resistance coefficient was, in general, increased for Hel-Cor and smooth pipe as deposition began to take place to a marked degree, because the boundary was changing due to the deposits forming on the bottom of the pipe.

7. The Darcy-Weisbach resistance coefficient decreased with increasing Reynolds number and seemed to follow the Kármán-Prandtl resistance equation for turbulent flow in smooth pipes, as long as all the sediment was in suspension.

8. Analysis of the corrugated pipe resistance data by the Morris concept of wake-interference flow, agreed favorably with measurements.

9. The mean velocity, at which deposition started, became less dependent on the magnitude of the total load as velocities were increased. This mean velocity was much higher in the smooth pipe than in the Hel-Cor or corrugated for a fixed total load.

10. The horsepower input required to maintain a certain discharge of sand-water mixture was not materially greater than that necessary to pump the same discharge of water, as long as all the sediment was in suspension. Horsepower was computed in terms of the discharge of mixture, with the unit weight and head loss expressed in feet of water.

11. Defining the point of most efficient operation as the minimum point of a constant total load curve on a J-V diagram and assuming operation at this point, Hel-Cor transported more sediment per unit time for a given horsepower than corrugated, and more than smooth pipe provided the total load was fairly small.

12. Using the above operating point, Hel-Cor required less horsepower for a fixed total sediment load than did corrugated, and usually less than smooth pipe.

13. Hel-Cor and corrugated pipe delivered more sediment for a given mixture discharge than did smooth pipe. The smooth pipe required a higher mixture discharge than Hel-Cor and corrugated in order to maintain the same constant sediment discharge.

14. The horizontal concentration profiles were constant over a horizontal diameter of the corrugated and smooth pipes. The concentration in Hel-Cor pipe deviated considerably from a constant in the vicinity of the wall.

15. The Hel-Cor boundary, which caused pronounced secondary circulation, maintained a more nearly uniform sediment concentration over a cross-section normal to the direction of flow than the smooth and corrugated pipes.

16. The standard deviation of the sediment sieve diameter had a negligible influence on the concentration profiles in Hel-Cor and corrugated pipes, but affected the lower portion of the profiles in the smooth pipes.

17. An absolute criterion for determining incipient deposition was presented.

18. The sediment exchange coefficient ϵ_s had a much different distribution, as a function of distance from the boundary, in a smooth pipe than in a corrugated pipe. The exchange coefficient had little or no meaning in a Hel Cor pipe because the concentration profiles were nearly constant.

19. The Kármán k in the Rouse number z_i was below 0.4 in smooth pipe and ranged from 0.3 to very large values in corrugated, based on an approximate analysis. The concentration profiles deviated considerably from the Rouse equation.

Conclusions

The principal conclusions derived from the experimental data are given below. These conclusions are limited to the transport of a 0.20-mm sand, suspended in water, by 12-in. Hel-Cor, smooth, and corrugated pipes at velocities under 10 fps.

1. Hel-Cor pipe can usually deliver more sediment per unit time with less horsepower than either corrugated or smooth pipe.

2. Secondary circulation induced by continuous helical corrugations is more effective in maintaining a nearly uniform concentration over a pipe cross-section than corrugations placed normal to the direction of the mean flow.

3. Fine sand, traveling in suspension, does not significantly increase the horsepower required to pump the sand-water mixture above that to pump the same discharge of clear water, in a given boundary.

Several conclusions of quite general applicability can be presented. These conclusions are based on theory and experimental evidence, and are valid regardless of boundary form. Assumed to be present is either a fine sand sediment or no sediment at all.

An absolute criterion can be used to determine the total load at which deposition occurs for a given mean velocity. The criterion for incipient deposition is the maximum or rapid decrease (whichever is

applicable) of a c/C_t versus C_t plot for a given distance above the bottom of a pipe and for constant mean velocity. The local concentration at the fixed elevation is c, and C_t is the total load under investigation.

2. The Morris concept of wake-interference flow has merit in studying large, regularly-spaced, artificial roughnesses.

3. Boundary form plays a very important role in determining the diffusion coefficient that will exist in the vicinity of the pipe wall.

Theoretical considerations lead to the conclusions:

1. The energy balance between the rate of energy dissipation required to maintain fine material in suspension and the decrease in the rate the fluid consumes energy seems to take place on the level of large scale energy transport eddies, and not to materially affect the small scale energy consuming turbulent eddies.

2. The difference, if any, between the energy required to transport a sediment laden fluid and an equal discharge of the homogeneous continuous phase is a function of the amount the sediment causes the piezometric head to deviate from a constant over any cross-section normal to the direction of the mean velocity.

Future Studies

It is not difficult to make a long list of sediment transport problems which need to be investigated. Presented below are four of the more general and fundamental studies which the writer believes would yield significant results.

1. A dimensionless function of horsepower, boundary, total load and sediment size (an extension of Fig. 14 in the text), would yield valuable design and economic data for sediment pumping installations.

2. Examination of the J-V diagram (see Fig. 8), with constant total load curves, indicates that with sufficient ingenuity in plotting C_t - J intercepts and $\emptyset/D$ - V intercepts for various sediments and pipes, one could derive a single function involving hydraulic gradient, total load, mixture discharge and boundary form. Such a function would make it possible to develop general sediment transport design criteria for pipes.

3. A study to find an optimum helix angle, frequency of corrugation and amplitude, as a function of sediment size, power consumption and discharge, would lead to a boundary, possible to fabricate commercially, which would transport a maximum amount of sediment per unit time with a minimum of energy input per unit time. Other forms of artificial roughness could also be investigated with the same ultimate objective.

4. Further investigation of the "absolute criterion for incipient deposition", proposed in this dissertation, should make it possible for an observer to eliminate the ambiguity in deciding when deposition is occurring. It would also enable one to define more closely the most efficient operating conditions for a sediment transport plant.

B I B L I O G R A P H Y

BIBLIOGRAPHY

1. Alves, G.E. Flow of non-Newtonian suspensions. Chemical Engineering, 56:107-109, May 1949.

2. Ambrose, H.H. The transportation of sand in pipes: II. Free-surface flow. (In Hydraulics Conference, Iowa City. Proceedings, 5:77-88, 1952. (Iowa. University. Studies in engineering, Bulletin 34, 1953.)

3. Babbitt, H.E., and Caldwell, D.H. Laminar flow of sludges in pipes. Urbana, Illinois. 1939. 58p. (Illinois. University. Engineering Experiment Station. Bulletin series No. 319).

4. Babbitt, H.E., and Caldwell, D.H. Turbulent flow of sludges in pipes. Urbana, Illinois. 1940. 44p. (Illinois. University. Engineering Experiment Station. Bulletin series No. 323).

5. Belden, D.H., and Kassel, L.S. Pressure drops encountered in conveying particles of large diameter in vertical transfer lines. Industrial and Engineering Chemistry, 41:1174-78, June 1949.

6. Blatch, N.S. Discussion:Water filtration at Washington, D.C. American Society of Civil Engineers. Transactions, 57:400-408, 1906.

7. Brautlecht, C.A., and Sethi, J.R. Flow of paper pulps in pipelines. Industrial and Engineering Chemistry, 25:283-288, March 1933.

8. Chatley, Hubert. The pumping of granular solids in fluid suspension. Engineering, 149:230-231, March 1, 1940.

9. Clifford, William. Friction of sewage sludge in pipes. Institution of Sanitary Engineers, London, Transactions, p.59, 1924.
   Cited in Reference 3:52

10. Cramp, William. Pneumatic transport plants. Society of Chemical Industries. Journal, 44:207T-213T, 1925.

11. Cramp, W., and Priestly, A. Pneumatic grain elevators. Engineer, 137:34-36, 64-65, 89-90, 112-113, January 11, 18, 25 and February 1, 1924.

12. Craven, J.P. The transportation of sand in pipes. I. Full pipe flow. (In Hydraulics Conference, Iowa City. Proceedings, 5:67-77, 1953. (Iowa. University. Studies in engineering, Bulletin 34, 1953.))

13. Danel, P.F. Charriage en suspension. International Association of Hydraulic Structures Research. Stockholm, Sweden. 1948. Report of second meeting. Appendix 7:113-145.

14. Danel, P.F. Discussion:Transportation of sand and gravel in a four-inch pipe. American Society of Civil Engineers. Transaction, 104:1372-73, 1939.

15. Dougherty, R.W. A survey on the hydraulic transportation of coal. U.S. Bureau of Mines. Report of investigations, 4799:1-21, July 1951.

16. Durand, R. Basic relationships of the transportation of solids in pipes - experimental research. Minnesota International Hydraulics Convention. Proceedings, 1953:89-103.

17. Durand, R. Transport hydraulique de graviers et galets en conduite. La Houille Blanche, n.s. 6:609-619, Octobre 1951.

18. Durand, R. Transport hydraulique des matériaux solides en conduite. La Houille Blanche, n.s. 6:384-393, Mai-Juin 1951.

19. Durand, R., and Condolios, E. Etude expérimentale du refoulement des matériaux en conduite. Société Hydrotechnique de France. Compte Rendu des 2èmes Journées de l'Hydraulique, 1952:27-55.

20. Durepaire, M.P. Contribution a l'étude du dragage et du refoulement des deblais à l'état de mixture. Extrat des Annales des Ponts et Chaussees, Fasc. II:165-254, Fevrier, 1939.

21. Durepaire, M.P. Discussion:Transportation of sand and gravel in a four-inch pipe. American Society of Civil Engineers. Transactions, 104:1369-70, 1939.

22. Farbar, Leonard. Flow characteristics of solids - gas mixtures in a horizontal and vertical conduit. Industrial and Engineering Chemistry, 4:1184-1191, June 1949.

23. Gästerstadt, M. Die experimentelle Untersuchung des pneumatischen Fordervorganges. Forschungasarbeiten auf dem Gebiete des Ingenieurewesens. n265. 1924. 76p.

24. Gregory, N.B. Pumping clay slurry through a four-inch pipe. Mechanical Engineering, 49:609-616, June 1927.

25. Hariu, O.H., and Molstad, M.C. Pressure drop in vertical tubes in transport of solids by gases. Industrial and Engineering Chemistry, 41:1148-1160, June 1949.

26. Head, V.P. Shear criterion for the hydraulic behavior of paper stocks in pumps, pipes, valves and flowmeters. Tappi, 35:260-266, June 1952.

27. Howard, G.W. Effects of rifling on four-inch pipe transporting solids. American Society of Civil Engineers. Transactions, 106:135-157, 1941.

28. Howard, G.W. Transportation of sand and gravel in a four-inch pipe. American Society of Civil Engineers. Transactions, 104:1334-48, 1939.

29. Hubell, G.E. Dearborn sewage sludge pumped through long pipe line. Engineering News Record, 111:343, September, 1933.

30. Ismail, H.M. Turbulent transfer mechanism and suspended sediment in closed channels. American Society of Civil Engineers, Transactions, 117:409-434, 1952.

31. Kestlicher, D. Pertes de charge dans les conduites alimentées en eau contenant des fines particules solides. Société Hydrotechnique de France. Compte Rendu des 2èmes Journées l'Hydraulique, 1952:139-143.

32. Kowalki, O.L. Manner of liquid flow through a pipe line orifice. Industrial and Engineering Chemistry, 30:216-222, February 1938.

33. Lambrette, A. Transports hydrauliques. Technique Moderne, 27:677-680, Octobre, 1935.

34. Maltby, F.B. Hydraulic dredging on the Mississippi River. American Society of Civil Engineers. Transactions, 54:391-478, 1905.

35. Mikumo, E., Nishihara, T., and Takahara, M. On the hydraulic conveyance of slime pulps. Society of Mechanical Engineers. Japan, Journal, 36:825-831, 1931.

36. Morris, H.N. A new concept of flow in rough conduits. American Society of Civil Engineers. Proceedings, 80:Separate no. 390: 1-18, 1954.

37. Nevitt, T.H. Loss of head in sewage sludge pipe at Toronto, Ontario. Engineering News Record, 82:279, February 6, 1919.

38. O'Brien, M.P., and Folsom, R.G. The transportation of sand in pipe lines. California. University. Publications in engineering 3:343-384, 1937.

39. Orrok, G.A , and Morrison, W.S. Pipeline transportation for anthracite and bituminous coal. Power, 54:699-700, September 1, 1921.

40. Prandtl, Ludwig. Essentials of fluid dynamics. New York, Hafner Publishing Company, 1952. 452p.

41. Rouse, Hunter. Elementary Mechanics of Fluids. New York. John Wiley and Sons, Inc. 1946, 376p.

42. Segler, W. Untersuchungenan Kornergeblasmund grunflagen fur ihren Berechnung. Mannheim, Wiebold Company, 1934. 263p.

43. Sobolewski, E.W., and Grove, C.S. Estimation of pressure drop for foams flowing in closed systems. Report no. 11 on projects no. O.N.R. 248-04, 248-09, 303-00 and 669-07. Syracuse, New York. Syracuse University Research Institue, 1953, 19p.

44. Soleil, G., and Ballade, P. Le transport hydraulique des matériaux dans les travaux publics. Société Hydrotechnique de France. Compte Rendu des 2ème Journées de l'Hydraulique, 1952:9-26.

45. Thoenen, J.R. Sand and gravel excavation. Part 6:Mining Methods. Bureau of Mines. Information circular 6875:211-224, 1936.

46. Tison, L.J. Resultats d'éssais sur le transport de matiéres solides, très fines, dans les conduites. Société Hydrotechnique de France. Compte Rendu des 2ème Journées de l'Hydraulique, 1952; 136-138.

47. Traxler, R.N. Influence of solids on flow properties of dilute suspensions. Paper Trade Journal, 104:151-4, February 25, 1937.

48. U.S. Engineer Department. Bonneville Hydraulic Laboratory. Friction losses in corrugated metal pipe. Portland, Oregon, Corps of Engineers, Oregon District, January, 1952. 10p., 16 pl., processed. (First preliminary report. CWI 828.)

49. U.S. Engineer Department. Bonneville Hydraulic Laboratory. Friction losses in corrugated metal pipe. Portland, Oregon, Corps of Engineers, Oregon, Corps of Engineers, Oregon District, October, 1952. 4p., 17pl., processed. (Supplement to First preliminary report. CWI 828.)

50. U.S. Engineer Department. Bonneville Hydraulic Laboratory. Friction losses in corrugated metal pipe. Portland, Oregon, Corps of Engineers, Oregon District, November 1953. 4p., 6pl., processed. (Memorandum report 2-2. CWI 828.)

51. U.S. Engineer Department. Bonneville Hydraulic Laboratory. Friction losses in corrugated metal pipe. Portland, Oregon, Corps of Engineers, Oregon District. January 1954. 4p., 6pl., processed. (Memorandum report 2-3. CWI 828.)

52. U.S. Engineer Department. Bonneville Hydraulic Laboratory. Friction losses in corrugated metal pipe. Portland, Oregon, Corps of Engineers, Oregon District, December 1954. 4p., 8pl., processed. (Memorandum report 3-1. CWI 828.)

53. U.S. Tennessee Valley Authority, and others. Laboratory investigations of suspended sediment samples. Iowa City, Iowa. St. Paul. U.S. Engineers District Sub Office. November, 1941. 99p. (Report no. 5 of a study of methods used in measurement and analysis of sediment loads in streams.)

54. Vanoni, Vito. Transportation of suspended sediment by water. American Society of Civil Engineers. Transactions, 111:67-133, 1946.

55. Vadot, L. Quelques réflexions sur les pertes de charge. La Houille Blanche, n.s. 9:165-178, December, 1954.

56. Vogt, E.G., and White, R.R. Friction in the flow of suspensions. Industrial and Engineering Chemistry, 40:1731-1738, September, 1948.

57. Wilhelm, R.H., Wroughton, O.M., and Loeffel, W.F. Flow of suspensions through pipes. Industrial and Engineering Chemistry, 31:622-629, May 1939.

58. Wilson, W.E. Mechanics of flow, with non-colloidal inert solids. American Society of Civil Engineers. Transactions, 107:1576-1586, 1942.

59. Wood, W.A., and Bailey, A.J. The horizontal carriage of granular material by an injector driven air stream. Institution of Mechanical Engineers. Proceedings, 142Q:149-173, 1939.

A P P E N D I X

TABLE OF CONTENTS

NOMENCLATURE

The following nomenclature were used in this dissertation. All the symbols were defined where they were first used, and only those used in more than one section are given below. The units are, in general, pound-foot-second (F-L-T). However, the equations are applicable in any system of units if proper cognizance is taken of the appropriate conversion factors.

Symbols	Definition	Unit
a	distance off the channel bed at which c_a is measured	L
c	local sediment concentration in percent by volume	
c_a	local concentration at elevation a in Rouse equation	
d	median sieve diameter of sediment in mm	L
f	Darcy Weisbach resistance coefficient	
g	gravitational acceleration	L/T^2
δh	magnitude of velocity head parameter at position x/r_1	L
$\delta h'$	arithmetic average velocity head parameter; 10-in. orifice	L
k	Nikuradse equivalent uniform sand diameter	L
p	local pressure at some point in the fluid-sediment medium	F/L^2
δp	difference in pressure between two points	F/L^2
r_o	radius of pipe from axis to crest of corrugations	L

NOMENCLATURE --Continued

Symbols	Definition	Unit
r_i	radius of 10-in. diameter orifice	L
t	time coordinate	T
v_i	components of local mean velocity in $\underline{v}$	L/T
$\underline{v}$	velocity vector	L/T
w	fall velocity of particles with median sieve diameter d	L/T
z_i	exponent in Rouse equation	
A_i, A^i	numerical constants	
C_t	total sediment load in percent by volume ($C_tQ = G$)	
C'	average concentration over horizontal diameter, percent by volume	
D	diameter of pipeline	L
E	mechanical energy, defined by $E = p + \rho v^2/2 + \gamma y$	FL/L^3
E_h	mechanical energy being dissipated per unit time	FL/T
E_t	total mechanical energy in a given region	FL
G	total sediment load	L^3/T
HP	horsepower	FL/T
J	hydraulic gradient along pipeline; sediment present or not	
J_e	hydraulic gradient along pipeline for clear water	
Q	discharge of sediment-water mixture	L^3/T
Re	Reynolds number	
T	temperature in °Centigrade degrees	

NOMENCLATURE --Continued

Symbols	Definition	Unit
T_{ij}	stress tensor	FL/L^3
V	mean velocity over cross-section of pipeline	L/T
V_L	velocity at which deposition begins for a given total load	L/T
γ_a	unit weight of air	F/L^3
γ_s	unit weight of sediment	F/L^3
γ_w	unit weight of water	F/L^3
$\delta\pi$	differential head between corrugation crest and nearest trough	L
ϵ_y	exchange coefficient in vertical direction	L^2/T
ϵ_i	diffusion coefficient along e_i coordinate	L^2/T
ϵ_s	exchange coefficient for sediment	L^2/T
ϵ_m	exchange coefficient for momentum	L^2/T
K	Kármán constant in z_1, computed from corrugation crests	
K'	Karman constant in z_1, computed form corrugation troughs	
λ	wave length of corrugations	L
ρ	mass density of mixture	$\frac{FT^2/L}{L^3}$
ρ_a	mass density of air	$\frac{FT^2/L}{L^3}$
ρ_s	mass density of sediment	$\frac{FT^2/L}{L^3}$
ρ_w	mass density of water	$\frac{FT^2/L}{L^3}$
σ_d	standard deviation of sediment sieve diameter	L

Symbol	Definition	Unit
σ_w	standard deviation of sediment fall velocity	L/T
τ	a volume	L^3
φ	group of lengths describing pipe boundary	L
ψ	any functional relation	
δ	incipient deposition	
$\overset{=}{\delta}$	two inch wide bed formed on bottom of pipe	
$\overset{\equiv}{\delta}$	four inch wide bed formed on bottom of pipe	
$\overset{\equiv}{\delta}$	six inch wide bed formed on bottom of pipe	

Mathematical Notation

A rectangular Cartesian coordinate system is assumed.

δ_{ij} Kronecker delta -- $\delta_{ii} = 1$; $\delta_{ij} = 0$, $i \neq j$

e base of Naperian logarithm

e_i unit vectors along coordinate axes

ln denotes logarithm to base e

log denotes logarithm to base 10

$\underline{n}$ unit vector normal to differential area da

$\underline{r}$ position vector

$\underline{A} = \Sigma A_i e_i$ identity

$\underline{A} \cdot \underline{A}$ dot product of two vectors

∇ vector operator; by definition
$\nabla = \Sigma \partial / \partial x_i e_i$

∇^2 scalar operator; by definition
$\nabla = \Sigma \partial^2 / \partial x_i^2$

$\int_\tau \nabla \cdot \underline{A} \, d\tau = \int_s \underline{A} \cdot \underline{n} da$ identity

Abbreviations

Symbol	Definition
cfs	cubic feet per second
fps	feet per second
ft	foot or feet
in.	inch or inches
m	meter
mm	millimeter
C	corrugated pipe (Appendix)
EW	East-West direction
Fig.	Figure
H	Hel-Cor pipe (Appendix)
ID	inside diameter of pipe
No.	number
NS	North-South direction
OD	outside diameter of pipe
S	smooth pipe (Appendix)

DEFINITIONS

Those terms which occur frequently throughout the text are defined below for reference purposes.

1. Load: The sediment being moved by the flow.
2. Suspended load: The material moving in suspension in the fluid medium.
3. Total load: The load of sediment as determined from sampling at an orifice located in a vertical pipe.
4. Incipient deposition: The transition; fully suspended load transport to transport with a permanent bed in the pipeline.
5. Limit deposit velocity: The mean flow velocity at which deposition began for a fixed total load.
6. Sediment size: The median sieve diameter as determined from a sieve analysis.
7. Total mechanical energy: The sum of kinetic and potential energy; thermal energy neglected.
8. Most efficient operating point: The most efficient operating point corresponds to operation of a sediment transport installation with a minimum horsepower input for a fixed total load.

Explanatory notes

1. The letter following a run number denotes the boundary type or form: H for Hel-Cor, C for corrugated and S for smooth. In some cases, a symbol is appended to indicate the bed condition in the pipe as observed through a plastic section at the end of the test pipe. See Nomenclature.

2. The total load C_t is in percent by volume.

3. Each "piezometer reading" is the average of four trials, the piezometers were spaced at 10-ft intervals.

4. Each "piezometer reading for C_t data" is the average of four trials, taken while obtaining the total load sample, during a 1/2-hour interval after the concentration profile was completed.

5. Each "piezometer reading at check station" is the average of four trials taken on the corrugation trough (observer inside the pipe) of the corrugated pipe.

6. "Sampler station (y/D)" is computed from the bottom of the test pipe. The magnitude of D being 1-ft, hence y/D = 0 at the pipe wall for the smooth, and at the crest of corrugations for Hel-Cor and the corrugated pipe (observer inside the pipe).

7. "Average conc. c" is the local sediment concentration of solids to sand-water in percent by volume.

8. "Velocity u" is approximate, measured by the 1/4-in. sampling tube and an ambient pressure tap on the wall of the plastic section.

Boundary Type: Hel-Cor Run No. 1 H Q = 5.20 cfs V = 6.63 fps
Profile Traverse: Vertical C_t = 1.32 percent T = 16.4 °C

Average Piezometer Reading

Piez. No.	4	5	6	7	8	9	10
Piez. reading	8.925	8.714	8.425	8.180	7.945	7.709	7.407
Piez. reading for C_t data							
Piez. reading at check sta.							

Concentration and Velocity Profile Data

Sampler sta (y/D)	0.06	0.16	0.26	0.36	0.46	0.56	0.66	0.76	0.86	0.96
Avg. Conc. (C %)	1.35	1.23	1.23	1.28	1.30	1.32	1.35	1.25	1.45	1.45
Velocity (u fps)	5.95	7.18	8.03	8.93	9.15	9.07	8.60	7.95	6.20	5.84

Boundary Type: Hel-Cor Run No. 2 H Q = 5.20 cfs V = 6.62 fps
Profile Traverse: Vertical C_t = 1.35 percent T = 15.6 °C

Average Piezometer Reading

Piez. No.	4	5	6	7	8	9	10
Piez. reading	8.949	8.736	8.441	8.210	7.975	7.743	7.414
Piez. reading for C_t data							
Piez. reading at check sta.							

Concentration and Velocity Profile Data

Sampler sta (y/D)	0.06	0.16	0.26	0.36	0.46	0.56	0.66	0.76	0.86	0.96
Avg. Conc. (C %)	1.38	1.24	1.33	1.28	1.31	1.33	1.38	1.31	1.53	1.48
Velocity (u fps)	--	7.32	8.38	8.97	9.40	9.25	8.75	8.06	6.76	5.67

Boundary Type: Hel-Cor Run No. 3 H Q = 5.30 cfs V = 6.75 fps
Profile Traverse: Vertical C_t = 1.90 percent T = 15.0 °C

Average Piezometer Reading

Piez. No.	4	5	6	7	8	9	10
Piez. reading	8.931	8.719	8.415	8.190	7.955	7.715	7.419
Piez. reading for C_t data							
Piez. reading at check sta.							

Concentration and Velocity Profile Data

Sampler sta (y/D)	0.06	0.16	0.26	0.36	0.46	0.56	0.66	0.76	0.86	0.96
Avg. Conc. (C %)	1.92	1.80	1.920	1.91	1.900	1.90	1.845	1.90	1.915	2.12
Velocity (u fps)	--	6.95	8.02	8.08	9.15	9.15	8.42	8.03	6.95	6.21

Boundary Type: Hel-Cor Run No. 4 H Q = 5.21 cfs V = 6.63 fps
Profile Traverse: Vertical C_t = 1.85 percent T = 18.4 °C

Average Piezometer Reading

Piez. No.	4	5	6	7	8	9	10
Piez. reading	9.030	8.812	8.510	8.266	8.026	7.780	7.476
Piez. reading for C_t data							
Piez. reading at check sta.							

Concentration and Velocity Profile Data

Sampler sta (y/D)	0.06	0.16	0.26	0.36	0.46	0.56	0.66	0.76	0.86	0.96
Avg. Conc. (C %)	2.150	1.770	1.860	1.780	1.855	1.845	1.860	1.840	1.845	1.73
Velocity (u fps)	6.21	7.62	8.42	9.15	9.50	9.32	9.15	6.90	7.40	5.95

Boundary Type: Hel-Cor Run No. 6 H Q = 6.50 cfs V = 8.28 fps
Profile Traverse: Horizontal C_t = 2.00 percent T = 18.9 °C

Average Piezometer Reading

Piez. No.	4	5	6	7	8	9	10
Piez. reading	---	9.521	9.049	8.650	8.266	7.958	7.398
Piez. reading for C_t data							
Piez. reading at check sta.							

Concentration and Velocity Profile Data

Sampler sta (y/D)	0.06	0.16	0.26	0.36	0.46	0.56	0.66	0.76	0.86	0.96
Avg. Conc. (C %)	2.20	1.94	1.86	1.94	1.93	2.00	1.86	1.97	2.12	2.23
Velocity (u fps)	7.90	9.40	10.10	11.35	11.95	12.00	11.35	10.45	9.31	8.22

Boundary Type: Hel-Cor Run No. 7 H Q = 6.50 cfs V = 8.28 fps
Profile Traverse: Horizontal C_t = 1.83 percent T = 22.5 °C

Average Piezometer Reading

Piez. No.	4	5	6	7	8	9	10
Piez. reading	---	9.571	9.154	8.699	8.316	7.950	7.449
Piez. reading for C_t data							
Piez. reading at check sta.							

Concentration and Velocity Profile Data

Sampler sta (y/D)	0.06	0.16	0.26	0.36	0.46	0.56	0.66	0.76	0.86	0.96
Avg. Conc. (C %)	2.23	1.79	1.79	1.76	1.81	1.79	1.78	1.79	1.79	1.77
Velocity (u fps)	7.90	9.40	10.10	11.35	11.95	12.00	11.35	10.45	9.31	8.22

Boundary Type: Hel-Cor Run No. 8 H Q = 6.60 cfs V = 8.40 fps
Profile Traverse: Vertical C_t = 2.21 percent T = 28.6 °C

Average Piezometer Reading

Piez. No.	4	5	6	7	8	9	10
Piez. reading	9.346	9.009	8.546	8.121	7.730	7.556	6.855
Piez. reading for C_t data							
Piez. reading at check sta.							

Concentration and Velocity Profile Data

Sampler sta (y/D)	0.06	0.16	0.26	0.36	0.46	0.56	0.66	0.76	0.86	0.96
Avg. Conc. (C %)	2.540	2.155	2.150	2.18	2.18	2.19	2.190	2.245	2.23	2.30
Velocity (u fps)	8.26	9.68	10.80	11.40	12.00	12.00	11.40	10.40	9.30	8.45

Boundary Type: Hel-Cor Run No. 9 H Q = 6.50 cfs V = 8.40 fps
Profile Traverse: Horizontal C_t = 2.13 percent T = 29.0 °C

Average Piezometer Reading

Piez. No.	4	5	6	7	8	9	10
Piez. reading	9.322	8.995	8.546	8.115	7.726	7.351	6.850
Piez. reading for C_t data							
Piez. reading at check sta.							

Concentration and Velocity Profile Data

Sampler sta (y/D)	0.06	0.16	0.26	0.36	0.46	0.56	0.66	0.76	0.86	0.96
Avg. Conc. (C %)	2.35	2.15	2.12	2.03	2.06	2.05	2.02	2.18	2.18	2.21
Velocity (u fps)	8.26	9.68	10.80	11.40	12.00	12.00	11.40	10.40	9.30	8.45

Boundary Type: Hel-Cor Run No. 10 H Q = 6.45 cfs V = 8.22 fps
Profile Traverse: Horizontal C_t = 2.87 percent T = 17.5 °C

Average Piezometer Reading

Piez. No.	4	5	6	7	8	9	10
Piez. reading	---	9.288	8.854	8.437	8.041	7.665	7.202
Piez. reading for C_t data							
Piez. reading at check sta.							

Concentration and Velocity Profile Data

Sampler sta (y/D)	0.06	0.16	0.26	0.36	0.46	0.56	0.66	0.76	0.86	0.96
Avg. Conc. (C %)	3.33	2.81	2.71	2.70	2.74	2.70	2.74	2.94	2.71	3.30
Velocity (u fps)										

Boundary Type: Hel-Cor Run No. 11 H Q = 6.45 cfs V = 8.47 fps
Profile Traverse: Horizontal C_t = 2.70 percent T = 20.0 °C

Average Piezometer Reading

Piez. No.	4	5	6	7	8	9	10
Piez. reading	---	9.310	8.898	8.466	8.070	7.691	7.229
Piez. reading for C_t data							
Piez. reading at check sta.							

Concentration and Velocity Profile Data

Sampler sta (y/D)	0.06	0.16	0.26	0.36	0.46	0.56	0.66	0.76	0.86	0.96
Avg. Conc. (C %)	2.84	2.70	2.60	2.64	2.60	2.64	2.64	2.71	2.74	2.85
Velocity (u fps)										

Boundary Type: Hel-Cor Run No. 12 H Q = 6.45 cfs V = 8.22 fps
Profile Traverse: Horizontal C_t = 2.43 percent T = 21.5 °C

Average Piezometer Reading

Piez. No.	4	5	6	7	8	9	10
Piez. reading	---	9.325	8.905	8.480	8.080	7.709	7.244
Piez. reading for C_t data							
Piez. reading at check sta.							

Concentration and Velocity Profile Data

Sampler sta (y/D)	0.06	0.16	0.26	0.36	0.46	0.56	0.66	0.76	0.86	0.96
Avg. Conc. (C %)	2.94	2.48	2.50	2.60	2.63	2.63	2.60	2.68	2.55	2.73
Velocity (u fps)										

Boundary Type: Hel-Cor Run No. 13 H Q = 6.45 cfs V = 8.22 fps
Profile Traverse: Horizontal C_t = 3.17 percent T = 21.3 °C

Average Piezometer Reading

Piez. No.	4	5	6	7	8	9	10
Piez. reading	9.264	8.914	8.496	8.064	7.660	7.283	6.815
Piez. reading for C_t data							
Piez. reading at check sta.							

Concentration and Velocity Profile Data

Sampler sta (y/D)	0.06	0.16	0.26	0.36	0.46	0.56	0.66	0.76	0.86	0.96
Avg. Conc. (C %)	3.49	3.20	3.12	3.14	3.10	3.05	3.12	3.10	3.14	3.28
Velocity (u fps)	8.2	9.21	10.05	10.70	11.50	12.00	11.60	10.75	9.72	8.20

Boundary Type: Hel-Cor Run No. 14 H Q = 6.45 cfs V = 8.22 fps
Profile Traverse: Horizontal C_t = 3.01 percent T = 22.8 °C

Average Piezometer Reading

Piez. No.	4	5	6	7	8	9	10
Piez. reading	9.265	8.921	8.496	8.061	7.658	7.281	6.811
Piez. reading for C_t data							
Piez. reading at check sta.							

Concentration and Velocity Profile Data

Sampler sta (y/D)	0.06	0.16	0.26	0.36	0.46	0.56	0.66	0.76	0.86	0.96
Avg. Conc. (C %)	3.39	2.97	2.91	3.09	3.00	2.85	2.90	2.85	3.00	3.18
Velocity (u fps)										

Boundary Type: Hel-Cor Run No. 15 H δ Q = 1.64 cfs V = 2.09 fps
Profile Traverse: Horizontal C_t = 0.157 percent T = 19.8 °C

Average Piezometer Reading

Piez. No.	4	5	6	7	8	9	10
Piez. reading	----	0.714	0.691	0.659	0.621	0.593	0.554
Piez. reading for C_t data							
Piez. reading at check sta.							

Concentration and Velocity Profile Data

Sampler sta (y/D)	0.06	0.16	0.26	0.36	0.46	0.56	0.66	0.76	0.86	0.96
Avg. Conc. (C %)	0.167	0.162	0.162	0.148	0.162	0.181	0.172	0.167	0.139	0.110
Velocity (u fps)	1.93	2.44	2.79	3.02	3.14	3.11	2.94	2.72	2.44	1.95

Boundary Type: Hel-Cor Run No. 16 H δ Q = 1.55 cfs V = 1.97 fps
Profile Traverse: Horizontal C_t = 0.138 percent T = 24.7 °C

Average Piezometer Reading

Piez. No.	4	5	6	7	8	9	10
Piez. reading	---	7.070	6.890	6.550	6.180	5.890	5.520
Piez. reading for C_t data							
Piez. reading at check sta.							

Concentration and Velocity Profile Data

Sampler sta (y/D)	0.06	0.16	0.26	0.36	0.46	0.56	0.66	0.76	0.86	0.96
Avg. Conc. (C %)	0.167	0.120	0.139	0.182	0.139	0.153	0.134	0.129	0.120	0.096
Velocity (u fps)	1.95	2.44	2.79	3.02	3.14	3.11	2.94	2.72	2.44	1.95

Boundary Type: Hel-Cor Run No. 17 H δ Q = 1.61 cfs V = 2.06 fps
Profile Traverse: Vertical C_t = 0.165 percent T = 25.6 °C

Average Piezometer Reading

Piez. No.	4	5	6	7	8	9	10
Piez. reading	---	7.990	7.962	7.931	7.892	7.865	7.832
Piez. reading for C_t data							
Piez. reading at check sta.							

Concentration and Velocity Profile Data

Sampler sta (y/D)	0.06	0.16	0.26	0.36	0.46	0.56	0.66	0.76	0.86	0.96
Avg. Conc. (C %)	0.125	0.105	0.171	0.200	0.148	0.195	0.181	0.200	0.185	0.139
Velocity (u fps)	1.85	2.33	2.61	2.85	2.96	3.02	2.85	2.56	2.20	1.68

Boundary Type: Hel-Cor Run No. 18 H δ Q = 1.63 cfs V = 2.08 fps
Profile Traverse: Vertical C_t = 0.141 percent T = 26.1 °C

Average Piezometer Reading

Piez. No.	4	5	6	7	8	9	10
Piez. reading	---	8.046	8.024	7.973	7.941	7.924	7.885
Piez. reading for C_t data							
Piez. reading at check sta.							

Concentration and Velocity Profile Data

Sampler sta (y/D)	0.06	0.16	0.26	0.36	0.46	0.56	0.66	0.76	0.86	0.96
Avg. Conc. (C %)	0.064	0.139	0.139	0.144	0.162	0.171	0.120	0.162	0.171	0.139
Velocity (u fps)	1.85	2.33	2.61	2.85	2.96	3.02	2.85	2.56	2.20	1.68

Boundary Type: Hel-Cor Run No. 19 H Q = 4.70 cfs V = 5.98 fps
Profile Traverse: Vertical C_t = 1.59 percent T = 20.0 °C

Average Piezometer Reading

Piez. No.	4	5	6	7	8	9	10
Piez. reading	--	8.701	8.486	8.262	8.036	7.852	7.607
Piez. reading for C_t data							
Piez. reading at check sta.							

Concentration and Velocity Profile Data

Sampler sta (y/D)	0.06	0.16	0.26	0.36	0.46	0.56	0.66	0.76	0.86	0.96
Avg. Conc. (C %)	1.58	1.57	1.55	1.55	1.54	1.56	1.63	1.59	1.62	1.71
Velocity (u fps)	5.29	6.32	7.17	7.80	8.14	8.01	7.58	6.90	5.85	4.87

Boundary Type: Hel-Cor Run No. 20 H Q = 4.70 cfs V = 5.98 fps
Profile Traverse: Vertical C_t = 1.52 percent T = 22.5 °C

Average Piezometer Reading

Piez. No.	4	5	6	7	8	9	10
Piez. reading	--	8,727	8,534	8,282	8,061	7,871	7,632
Piez. reading for C_t data							
Piez. reading at check sta.							

Concentration and Velocity Profile Data

Sampler sta (y/D)	0.06	0.16	0.26	0.36	0.46	0.56	0.66	0.76	0.86	0.96
Avg. Conc. (C %)	1.58	1.51	1.49	1.50	1.47	1.44	1.49	1.505	1.53	1.66
Velocity (u fps)	5.29	6.32	7.17	7.80	8.14	8.01	7.58	6.90	5.85	4.87

Boundary Type: Hel-Cor Run No. 21 H Q = 3.53 cfs V = 4.50 fps
Profile Traverse: Vertical C_t = 0.840 percent T = 27.1 °C

Average Piezometer Reading

Piez. No.	4	5	6	7	8	9	10
Piez. reading	--	8.196	8.065	7.928	7.799	7.680	7.540
Piez. reading for C_t data							
Piez. reading at check sta.							

Concentration and Velocity Profile Data

Sampler sta (y/D)	0.06	0.16	0.26	0.36	0.46	0.56	0.66	0.76	0.86	0.96
Avg. Conc. (C %)	0.785	0.760	0.825	0.840	0.870	0.840	0.840	0.872	0.899	0.870
Velocity (u fps)	5.98	4.81	5.46	5.93	6.18	6.15	5.84	5.24	4.57	3.72

Boundary Type: Hel-Cor Run No. 22 H Q = 3.53 cfs V = 4.50 fps
Profile Traverse: Vertical C_t = 0.837 percent T = 27.7 °C

Average Piezometer Reading

Piez. No.	4	5	6	7	8	9	10
Piez. reading	--	8.141	8.010	7.872	7.741	7.621	7.456
Piez. reading for C_t data							
Piez. reading at check sta.							

Concentration and Velocity Profile Data

Sampler sta (y/D)	0.06	0.16	0.26	0.36	0.46	0.56	0.66	0.76	0.86	0.96
Avg. Conc. (C %)	0.865	0.790	0.790	0.820	0.840	0.830	0.845	0.865	0.885	0.845
Velocity (u fps)	3.98	4.81	5.46	5.93	6.18	6.15	5.84	5.24	4.57	3.72

Boundary Type: Hel-Cor Run No. 23 H Q = 4.80 cfs V = 6.11 fps
Profile Traverse: Horizontal C_t = 1.30 percent T = 26.5 °C

Average Piezometer Reading

Piez. No.	4	5	6	7	8	9	10
Piez. reading	---	8,764	8,537	8,314	8,086	7,887	7,640
Piez. reading for C_t data							
Piez. reading at check sta.							

Concentration and Velocity Profile Data

Sampler sta (y/D)	0.06	0.16	0.26	0.36	0.46	0.56	0.66	0.76	0.86	0.96
Avg. Conc. (C %)	1.41	1.280	1.280	1.24	1.29	1.27	1.31	1.31	1.31	1.28
Velocity (u fps)	5.33	6.35	7.17	7.83	8.10	8.09	7.75	7.05	6.19	5.25

Boundary Type: Hel-Cor Run No. 24 H Q = 4.80 cfs V = 6.11 fps
Profile Traverse: Horizontal C_t = 1.28 percent T = 27.6 °C

Average Piezometer Reading

Piez. No.	4	5	6	7	8	9	10
Piez. reading	--	8,809	8,585	8,349	8,129	7,931	7,685
Piez. reading for C_t data							
Piez. reading at check sta.							

Concentration and Velocity Profile Data

Sampler sta (y/D)	0.06	0.16	0.26	0.36	0.46	0.56	0.66	0.76	0.86	0.96
Avg. Conc. (C %)	1.45	1.26	1.23	1.28	1.29	1.26	1.23	1.29	1.28	1.28
Velocity (u fps)	5.33	6.35	7.17	7.83	8.10	8.09	7.75	7.05	6.19	5.25

Boundary Type: Hel-Cor Run No. 25 H Q = 3.45 cfs V = 4.40 fps
Profile Traverse: Horizontal C_t = 6.756 percent T = 31.8 °C

Average Piezometer Reading

Piez. No.	4	5	6	7	8	9	10
Piez. reading	--	8.155	8.041	7.885	7.754	7.632	7.491
Piez. reading for C_t data							
Piez. reading at check sta.							

Concentration and Velocity Profile Data

Sampler sta (y/D)	0.06	0.16	0.26	0.36	0.46	0.56	0.66	0.76	0.86	0.96
Avg. Conc. (C %)	0.775	0.739	0.740	0.739	0.770	0.741	0.741	0.741	0.719	0.86
Velocity (u fps)	4.01	4.75	5.31	5.83	5.98	5.90	5.51	5.08	4.57	4.01

Boundary Type: Hel-Cor Run No. 26 H δ Q = 3.45 cfs V = 4.40 fps
Profile Traverse: Horizontal C_t = 0.711 percent T = 32.3 °C

Average Piezometer Reading

Piez. No.	4	5	6	7	8	9	10
Piez. reading	--	8,202	8,080	7,908	7,772	7,646	7,501
Piez. reading for C_t data							
Piez. reading at check sta.							

Concentration and Velocity Profile Data

Sampler sta (y/D)	0.06	0.16	0.26	0.36	0.46	0.56	0.66	0.76	0.86	0.96
Avg. Conc. (C %)	0.867	0.695	0.743	0.630	0.740	0.765	0.750	0.705	0.645	0.575
Velocity (u fps)	4.01	4.75	5.31	5.83	5.98	5.90	5.51	5.08	4.57	4.01

Boundary Type: Hel-Cor Run No. 27 H Q = 4.80 cfs V = 6.12 fps
Profile Traverse: Horizontal C_t = 2.06 percent T = 21.1 °C

Average Piezometer Reading

Piez. No.	4	5	6	7	8	9	10
Piez. reading	--	8,711	8,485	8,257	8,020	7,829	7,586
Piez. reading for C_t data							
Piez. reading at check sta.							

Concentration and Velocity Profile Data

Sampler sta (y/D)	0.06	0.16	0.26	0.36	0.46	0.56	0.66	0.76	0.86	0.96
Avg. Conc. (C %)	2.26	1.86	1.94	1.92	1.92	2.20	2.10	2.20	2.00	2.20
Velocity (u fps)	5.22	6.31	7.14	7.80	8.10	8.10	7.69	7.04	6.22	5.18

Boundary Type: Hel-Cor Run No. 28 H Q = 4.75 cfs V = 6.05 fps
Profile Traverse: Horizontal C_t = 1.93 percent T = 22.9 °C

Average Piezometer Reading

Piez. No.	4	5	6	7	8	9	10
Piez. reading	--	8,709	8,485	8,255	8,012	7,826	7,581
Piez. reading for C_t data							
Piez. reading at check sta.							

Concentration and Velocity Profile Data

Sampler sta (y/D)	0.06	0.16	0.26	0.36	0.46	0.56	0.66	0.76	0.86	0.96
Avg. Conc. (C %)	2.26	1.83	1.835	1.84	1.89	1.935	1.90	1.97	1.93	1.90
Velocity (u fps)	5.22	6.31	7.14	7.80	8.10	8.10	7.69	7.04	6.22	5.18

Boundary Type: Hel-Cor Run No. 29 H Q = 3.53 cfs V = 4.50 fps
Profile Traverse: Horizontal C_t = 1.08 percent T = 26.5 °C

Average Piezometer Reading

Piez. No.	4	5	6	7	8	9	10
Piez. reading	--	8,241	8,108	7,971	7,834	7,716	7,537
Piez. reading for C_t data							
Piez. reading at check sta.							

Concentration and Velocity Profile Data

Sampler sta (y/D)	0.06	0.16	0.26	0.36	0.46	0.56	0.66	0.76	0.86	0.96
Avg. Conc. (C %)	1.22	1.05	1.02	1.05	1.07	1.15	1.09	1.13	1.07	0.920
Velocity (u fps)										

Boundary Type: Hel-Cor Run No. 30 H Q = 3.53 cfs V = 4.50 fps
Profile Traverse: Horizontal C_t = 1.08 percent T = 26.7 °C

Average Piezometer Reading

Piez. No.	4	5	6	7	8	9	10
Piez. reading	---	8.240	8.105	7.968	7.832	7.711	7.569
Piez. reading for C_t data							
Piez. reading at check sta.							

Concentration and Velocity Profile Data

Sampler sta (y/D)	0.06	0.16	0.26	0.36	0.46	0.56	0.66	0.76	0.86	0.96
Avg. Conc. (C %)	1.22	1.06	1.03	1.10	1.095	1.130	1.09	1.13	0.985	0.98
Velocity (u fps)										

Boundary Type: Hel-Cor Run No. 31 H Q = 4.82 cfs V = 6.08 fps
Profile Traverse: Horizontal C_t = 0.515 percent T = 19.1 °C

Average Piezometer Reading

Piez. No.	4	5	6	7	8	9	10
Piez. reading	9.189	8.979	8.771	8.547	8.322	8.130	7.885
Piez. reading for C_t data							
Piez. reading at check sta.							

Concentration and Velocity Profile Data

Sampler sta (y/D)	0.06	0.16	0.26	0.36	0.46	0.56	0.66	0.76	0.86	0.96
Avg. Conc. (C %)	0.519	0.490	0.460	0.520	0.502	0.533	0.502	0.525	0.519	0.58
Velocity (u fps)	5.08	6.32	7.25	7.90	8.27	8.22	7.82	7.08	6.16	4.94

Boundary Type: Hel-Cor Run No. 32 H Q = 4.81 cfs V = 6.12 fps
Profile Traverse: Vertical C_t = 0.520 percent T = 20.6 °C

Average Piezometer Reading

Piez. No.	4	5	6	7	8	9	10
Piez. reading	9.167	8.972	8.746	8.524	8.301	8.105	7.864
Piez. reading for C_t data							
Piez. reading at check sta.							

Concentration and Velocity Profile Data

Sampler sta (y/D)	0.06	0.16	0.26	0.36	0.46	0.56	0.66	0.76	0.86	0.96
Avg. Conc. (C %)	0.519	0.482	0.480	0.500	0.519	0.480	0.500	0.529	0.519	0.575
Velocity (u fps)	5.08	6.32	7.25	7.90	8.27	8.22	7.82	7.08	6.16	4.94

Boundary Type: Hel-Cor Run No. 33 H Q = 3.57 cfs V = 4.55 fps
Profile Traverse: Vertical C_t = 0.295 percent T = 24.1 °C
(some air)

Average Piezometer Reading

Piez. No.	4	5	6	7	8	9	10
Piez. reading	8.622	8.478	8.318	8.141	7.970	7.809	7.613
Piez. reading for C_t data							
Piez. reading at check sta.							

Concentration and Velocity Profile Data

Sampler sta (y/D)	0.06	0.16	0.26	0.36	0.46	0.56	0.66	0.76	0.86	0.96
Avg. Conc. (C %)	0.281	0.276	0.258	0.281	0.258	0.305	0.286	0.300	0.315	--
Velocity (u fps)	3.94	5.01	5.68	6.06	6.22	6.22	6.07	5.62	4.89	3.86

Boundary Type: Hel-Cor Run No. 34 H Q = 4.78 cfs V = 6.10 fps
Profile Traverse: Horizontal C_t = 0.564 percent T = 22.0 °C

Average Piezometer Reading

Piez. No.	4	5	6	7	8	9	10
Piez. reading	9.175	8.986	8.765	8.546	8.332	8.135	7.898
Piez. reading for C_t data							
Piez. reading at check sta.							

Concentration and Velocity Profile Data

Sampler sta (y/D)	0.06	0.16	0.26	0.36	0.46	0.56	0.66	0.76	0.86	0.96
Avg. Conc. (C %)	0.632	0.550	0.545	0.585	0.572	0.565	0.560	0.575	0.550	0.560
Velocity (u fps)	5.20	6.22	7.09	7.84	8.22	8.23	7.74	6.96	6.17	4.96

Boundary Type: Hel-Cor Run No. 35 H Q = 4.78 cfs V = 6.10 fps
Profile Traverse: Horizontal C_t = 0.535 percent T = 22.9 °C

Average Piezometer Reading

Piez. No.	4	5	6	7	8	9	10
Piez. reading	9.156	8.970	8.754	8.527	8.316	8.121	7.885
Piez. reading for C_t data							
Piez. reading at check sta.							

Concentration and Velocity Profile Data

Sampler sta (y/D)	0.06	0.16	0.26	0.36	0.46	0.56	0.66	0.76	0.86	0.96
Avg. Conc. (C %)	0.595	0.520	0.500	0.525	0.520	0.565	0.530	0.520	0.560	0.520
Velocity (u fps)	5.20	6.22	7.09	7.84	8.22	8.23	7.74	6.96	6.17	4.96

Boundary Type: Hel-Cor Run No. 36 H Q = 3.43 cfs V = 4.37 fps
Profile Traverse: Horizontal C_t = 0.402 percent T = 24.8 °C
(some air)

Average Piezometer Reading

Piez. No.	4	5	6	7	8	9	10
Piez. reading	8.682	8.502	8.333	8.151	7.981	7.821	7.644
Piez. reading for C_t data							
Piez. reading at check sta.							

Concentration and Velocity Profile Data

Sampler sta (y/D)	0.06	0.16	0.26	0.36	0.46	0.56	0.66	0.76	0.86	0.96
Avg. Conc. (C %)	0.535	0.400	0.415	0.435	0.405	0.385	0.369	0.369	0.325	0.281
Velocity (u fps)										

Boundary Type: Hel-Cor Run No. 37 H Q = 4.73 cfs V = 6.03 fps
Profile Traverse: Horizontal C_t = 2.39 percent T = 28.0 °C

Average Piezometer Reading

Piez. No.	4	5	6	7	8	9	10
Piez. reading	9.225	9.032	8.806	8.566	8.335	8.127	7.877
Piez. reading for C_t data							
Piez. reading at check sta.							

Concentration and Velocity Profile Data

Sampler sta (y/D)	0.06	0.16	0.26	0.36	0.46	0.56	0.66	0.76	0.86	0.96
Avg. Conc. (C %)	2.67	2.27	2.35	2.25	2.37	2.43	2.41	2.45	2.40	2.35
Velocity (u fps)	5.14	6.38	7.18	7.83	8.19	8.16	7.71	7.05	6.22	5.14

Boundary Type: Hel-Cor Run No. 38 H Q = 4.73 cfs V = 6.03 fps
Profile Traverse: Horizontal C_t = 2.36 percent T = 28.8 °C

Average Piezometer Reading

Piez. No.	4	5	6	7	8	9	10
Piez. reading	9.249	9.051	8.824	8.588	8.361	8.153	7.900
Piez. reading for C_t data							
Piez. reading at check sta.							

Concentration and Velocity Profile Data

Sampler sta (y/D)	0.06	0.16	0.26	0.36	0.46	0.56	0.66	0.76	0.86	0.96
Avg. Conc. (C %)	2.70	2.30	2.27	2.33	2.30	2.25	2.36	2.36	2.40	2.30
Velocity (u fps)	5.14	6.38	7.18	7.83	8.19	8.16	7.71	7.05	6.22	5.14

Boundary Type: Hel-Cor Run No. 39 H Q = 4.00 cfs V = 5.10 fps
Profile Traverse: Horizontal C_t = 1.83 percent T = 31.0 °C

Average Piezometer Reading

Piez. No.	4	5	6	7	8	9	10
Piez. reading	8.924	8.625	8.583	8.393	8.175	8.016	7.806
Piez. reading for C_t data							
Piez. reading at check sta.							

Concentration and Velocity Profile Data

Sampler sta (y/D)	0.06	0.16	0.26	0.36	0.46	0.56	0.66	0.76	0.86	0.96
Avg. Conc. (C %)	2.22	1.87	1.84	1.85	1.82	1.68	1.83	1.83	1.81	1.59
Velocity (u fps)	3.78	4.96	5.68	6.22	6.58	6.58	6.22	5.68	4.96	4.40

Boundary Type: Hel-Cor Run No. 40 H Q = 3.82 cfs V = 4.87 fps
Profile Traverse: Horizontal C_t = 1.81 percent T = 31.5 °C

Average Piezometer Reading

Piez. No.	4	5	6	7	8	9	10
Piez. reading	8.896	8.735	8.561	8.371	8.184	8.024	7.822
Piez. reading for C_t data							
Piez. reading at check sta.							

Concentration and Velocity Profile Data

Sampler sta (y/D)	0.06	0.16	0.26	0.36	0.46	0.56	0.66	0.76	0.86	0.96
Avg. Conc. (C %)	2.00	1.82	1.88	1.79	1.83	1.73	1.90	1.85	1.76	1.50
Velocity (u fps)										

Boundary Type: Hel-Cor Run No. 41 H Q = 4.73 cfs V = 6.03 fps
Profile Traverse: Vertical C_t = 3.48 percent T = 24.3 °C

Average Piezometer Reading

Piez. No.	4	5	6	7	8	9	10
Piez. reading	9.504	9.265	8.996	8.716	8.436	8.198	7.894
Piez. reading for C_t data							
Piez. reading at check sta.							

Concentration and Velocity Profile Data

Sampler sta (y/D)	0.06	0.16	0.26	0.36	0.46	0.56	0.66	0.76	0.86	0.96
Avg. Conc. (C %)	3.35	3.35	3.26	3.45	3.31	3.53	3.53	3.45	3.46	3.92
Velocity (u fps)										

Boundary Type: Hel-Cor Run No. 42 H Q = 4.73 cfs V = 5.93 fps
Profile Traverse: Vertical C_t = 3.27 percent T = 25.9 °C

Average Piezometer Reading

Piez. No.	4	5	6	7	8	9	10
Piez. reading	9.530	9.300	9.021	8.739	8.459	8.219	7.920
Piez. reading for C_t data							
Piez. reading at check sta.							

Concentration and Velocity Profile Data

Sampler sta (y/D)	0.06	0.16	0.26	0.36	0.46	0.56	0.66	0.76	0.86	0.96
Avg. Conc. (C %)	3.23	3.30	2.91	3.45	3.00	3.24	3.30	3.28	3.38	3.60
Velocity (u fps)										

Boundary Type: Hel-Cor Run No. 43 H Q = 4.36 cfs V = 5.55 fps
Profile Traverse: Vertical C_t = 2.27 percent T = 29.2 °C

Average Piezometer Reading

Piez. No.	4	5	6	7	8	9	10
Piez. reading	9.225	9.029	8.788	8.550	8.330	8.125	7.884
Piez. reading for C_t data							
Piez. reading at check sta.							

Concentration and Velocity Profile Data

Sampler sta (y/D)	0.06	0.16	0.26	0.36	0.46	0.56	0.66	0.76	0.86	0.96
Avg. Conc. (C %)	2.40	2.12	2.25	2.16	2.29	2.18	2.29	2.28	2.35	2.40
Velocity (u fps)										

Boundary Type: Hel-Cor Run No. 44 H Q = 4.35 cfs V = 5.54 fps
Profile Traverse: Vertical C_t = 2.21 percent T = 29.6 °C

Average Piezometer Reading

Piez. No.	4	5	6	7	8	9	10
Piez. reading	9.226	9.016	8.791	8.566	8.329	8.132	7.874
Piez. reading for C_t data							
Piez. reading at check sta.							

Concentration and Velocity Profile Data

Sampler sta (y/D)	0.06	0.16	0.26	0.36	0.46	0.56	0.66	0.76	0.86	0.96
Avg. Conc. (C %)	2.24	2.27	2.16	2.20	2.20	2.20	2.18	2.24	2.21	2.21
Velocity (u fps)										

Boundary Type: Hel-Cor Run No. 45 H Q = 4.90 cfs V = 6.14 fps
Profile Traverse: C_t = 4.45 percent T = 22.0 °C

Average Piezometer Reading

Piez. No.	4	5	6	7	8	9	10
Piez. reading	9.355	9.098	8.838	8.570	8.287	8.062	7.767
Piez. reading for C_t data	9.300	9.070	8.818	8.550	8.279	8.049	7.769
Piez. reading at check sta.							

Concentration and Velocity Profile Data

Sampler sta (y/D)	0.06	0.16	0.26	0.36	0.46	0.56	0.66	0.76	0.86	0.96
Avg. Conc. (C %)										
Velocity (u fps)										

Boundary Type: Hel-Cor Run No. 46 H δ Q = 3.80 cfs V = 6.60 fps
Profile Traverse: C_t = 3.48 percent T = 26.9 °C

Average Piezometer Reading

Piez. No.	4	5	6	7	8	9	10
Piez. reading							
Piez. reading for C_t data	9.064	8.806	8.522	8.221	7.915	7.635	7.312
Piez. reading at check sta.							

Concentration and Velocity Profile Data

Sampler sta (y/D)	0.06	0.16	0.26	0.36	0.46	0.56	0.66	0.76	0.86	0.96
Avg. Conc. (C %)										
Velocity (u fps)										

Boundary Type: Hel-Cor Run No. 47 H δ Q = 5.10 cfs V = 6.60 fps
Profile Traverse: Vertical C_t = 3.73 percent T = 28.3 °C

Average Piezometer Reading

Piez. No.	4	5	6	7	8	9	10
Piez. reading	9.070	8.811	8.520	8.230	7.915	7.652	7.327
Piez. reading for C_t data							
Piez. reading at check sta.							

Concentration and Velocity Profile Data

Sampler sta (y/D)	0.06	0.16	0.26	0.36	0.46	0.56	0.66	0.76	0.86	0.96
Avg. Conc. (C %)	7.20	6.70	4.63	4.32	2.99	2.35	1.88	1.84	1.78	--
Velocity (u fps)										

Boundary Type: Hel-Cor Run No. 48 H Q = 5.80 cfs V = 7.39 fps
Profile Traverse: C_t = 5.87 percent T = 21.1 °C

Average Piezometer Reading

Piez. No.	4	5	6	7	8	9	10
Piez. reading	9.094	8.825	8.504	8.176	7.846	7.555	7.205
Piez. reading for C_t data	9.119	8.844	8.527	8.199	7.876	7.581	7.232
Piez. reading at check sta.							

Concentration and Velocity Profile Data

Sampler sta (y/D)	0.06	0.16	0.26	0.36	0.46	0.56	0.66	0.76	0.86	0.96
Avg. Conc. (C %)	5.80	5.71	6.63	5.93	5.99	6.03	5.81	5.75	5.80	6.30
Velocity (u fps)										

Boundary Type: Hel-Cor Run No. 49 H Q = 5.80 cfs V = 7.39 fps
Profile Traverse: Vertical C_t = 5.65 percent T = 22.3 °C

Average Piezometer Reading

Piez. No.	4	5	6	7	8	9	10
Piez. reading	9.093	8.815	8.504	8.178	7.850	7.560	7.211
Piez. reading for C_t data	9.119	8.844	8.527	8.199	7.876	7.581	7.232
Piez. reading at check sta.							

Concentration and Velocity Profile Data

Sampler sta (y/D)	0.06	0.16	0.26	0.36	0.46	0.56	0.66	0.76	0.86	0.96
Avg. Conc. (C %)	5.85	5.38	5.40	5.41	5.40	5.49	5.50	5.60	6.03	6.39
Velocity (u fps)										

Boundary Type: Hel-Cor Run No. 50 H Q = 6.60 cfs V = 8.41 fps
Profile Traverse: Vertical C_t = 6.03 percent T = 24.8 °C

Average Piezometer Reading

Piez. No.	4	5	6	7	8	9	10
Piez. reading	--	9.359	8.919	8.461	8.006	7.617	7.131
Piez. reading for C_t data	--	9.366	8.925	8.470	8.033	7.636	7.148
Piez. reading at check sta.							

Concentration and Velocity Profile Data

Sampler sta (y/D)	0.06	0.16	0.26	0.36	0.46	0.56	0.66	0.76	0.86	0.96
Avg. Conc. (C %)	6.35	5.74	5.82	5.75	6.05	5.85	5.85	5.80	6.15	6.90
Velocity (u fps)										

Boundary Type: Hel-Cor Run No. 51 H Q = 6.60 cfs V = 8.41 fps
Profile Traverse: Vertical C_t = 6.00 percent T = 25.5 °C

Average Piezometer Reading

Piez. No.	4	5	6	7	8	9	10
Piez. reading	--	9.371	8.915	8.469	8.022	7.625	7.138
Piez. reading for C_t data	--	9.366	8.925	8.470	8.033	7.636	7.148
Piez. reading at check sta.							

Concentration and Velocity Profile Data

Sampler sta (y/D)	0.06	0.16	0.26	0.36	0.46	0.56	0.66	0.76	0.86	0.96
Avg. Conc. (C %)	6.78	6.15	5.72	5.79	5.85	5.79	5.72	5.82	5.79	5.59
Velocity (u fps)										

Boundary Type: Hel-Cor Run No. 52 H Q = 5.78 cfs V = 7.37 fps
Profile Traverse: C_t =10.3 percent T = 20.0 °C

Average Piezometer Reading

Piez. No.	4	5	6	7	8	9	10
Piez. reading							
Piez. reading for C_t data	9.259	8.945	8.608	8.246	7.877	7.566	7.191
Piez. reading at check sta.							

Concentration and Velocity Profile Data

Sampler sta (y/D)	0.06	0.16	0.26	0.36	0.46	0.56	0.66	0.76	0.86	0.96
Avg. Conc. (C %)										
Velocity (u fps)										

Boundary Type: Hel-Cor Run No. 53 H Q = 6.50 cfs V = 8.32 fps
Profile Traverse: Vertical C_t =11.1 percent T = 23.2 °C

Average Piezometer Reading

Piez. No.	4	5	6	7	8	9	10
Piez. reading		9.196	8.802	8.384	7.956	7.590	7.144
Piez. reading for C_t data		9.194	8.799	8.385	7.956	7.954	7.147
Piez. reading at check sta.							

Concentration and Velocity Profile Data

Sampler sta (y/D)	0.06	0.16	0.26	0.36	0.46	0.56	0.66	0.76	0.86	0.96
Avg. Conc. (C %)	11.40	11.30	10.50	11.10	10.60	10.90	11.50	11.40	11.30	11.60
Velocity (u fps)										

Boundary Type: Hel-Cor Run No. 54 H δ Q = 5.80 cfs V = 7.27 fps
Profile Traverse: Vertical C_t =12.2 percent T = 19.0 °C

Average Piezometer Reading

Piez. No.	4	5	6	7	8	9	10
Piez. reading	--	9.261	8.767	8.294	7.818	7.391	6.887
Piez. reading for C_t data	--	9.264	8.976	8.307	7.820	7.367	6.820
Piez. reading at check sta.							

Concentration and Velocity Profile Data

Sampler sta (y/D)	0.06	0.16	0.26	0.36	0.46	0.56	0.66	0.76	0.86	0.96
Avg. Conc. (C %)	13.90	16.60	16.80	13.30	13.30	10.20	10.70	11.10	7.80	8.10
Velocity (u fps)										

Boundary Type: Hel-Cor Run No. 55 H Q = 6.55 cfs V = 8.20 fps
Profile Traverse: Vertical C_t =12.7 percent T = 22.6 °C

Average Piezometer Reading

Piez. No.	4	5	6	7	8	9	10
Piez. reading	--	9.233	8.809	8.400	7.954	7.576	7.114
Piez. reading for C_t data	--	9.241	8.834	8.405	7.934	7.574	7.110
Piez. reading at check sta.							

Concentration and Velocity Profile Data

Sampler sta (y/D)	0.06	0.16	0.26	0.36	0.46	0.56	0.66	0.76	0.86	0.96
Avg. Conc. (C %)	12.30	12.85	11.70	12.30	13.00	13.10	13.00	12.80	13.00	12.80
Velocity (u fps)										

Boundary Type: Hel-Cor Run No. 56 H δ Q = 5.75 cfs V = 7.52 fps
Profile Traverse: Vertical C_t =12.3 percent T = 21.5 °C

Average Piezometer Reading

Piez. No.	4	5	6	7	8	9	10
Piez. reading	--	9.283	8.776	8.308	7.806	7.348	6.792
Piez. reading for C_t data	--	9.251	8.740	8.330	7.805	7.368	6.837
Piez. reading at check sta.							

Concentration and Velocity Profile Data

Sampler sta (y/D)	0.06	0.16	0.26	0.36	0.46	0.56	0.66	0.76	0.86	0.96
Avg. Conc. (C %)	15.30	14.90	16.10	13.30	13.00	10.80	10.80	11.60	9.80	7.75
Velocity (u fps)										

Boundary Type: Hel-Cor Run No. 57 H Q = 6.35 cfs V = 8.09 fps
Profile Traverse: Horizontal C_t =13.2 percent T = 17.2 °C

Average Piezometer Reading

Piez. No.	4	5	6	7	8	9	10
Piez. reading	--	9.268	8.844	8.405	7.919	7.551	7.071
Piez. reading for C_t data	--	9.236	8.826	8.406	7.967	7.571	7.110
Piez. reading at check sta.							

Concentration and Velocity Profile Data

Sampler sta (y/D)	0.06	0.16	0.26	0.36	0.46	0.56	0.66	0.76	0.86	0.96
Avg. Conc. (C %)	14.40	14.00	13.80	13.60	13.70	13.10	12.40	13.30	11.65	11.65
Velocity (u fps)										

Boundary Type: Hel-Cor Run No. 58 H Q = 7.10 cfs V = 9.05 fps
Profile Traverse: Horizontal C_t =12.2 percent T = 21.2 °C

Average Piezometer Reading

Piez. No.	4	5	6	7	8	9	10
Piez. reading	--	9.650	9.182	8.661	8.127	7.661	7.099
Piez. reading for C_t data	--	9.650	9.188	8.664	8.133	7.665	7.096
Piez. reading at check sta.							

Concentration and Velocity Profile Data

Sampler sta (y/D)	0.06	0.16	0.26	0.36	0.46	0.56	0.66	0.76	0.86	0.96
Avg. Conc. (C %)	13.50	12.20	12.10	11.99	11.80	11.99	12.10	12.00	12.30	12.30
Velocity (u fps)										

Boundary Type: Hel-Cor Run No. 59 H Q = 8.45 cfs V = 10.77 fps
Profile Traverse: C_t =12.2 percent T = 17.8 °C

Average Piezometer Reading

Piez. No.	4	5	6	7	8	9	10
Piez. reading							
Piez. reading for C_t data	--	9.510	8.864	8.204	7.554	6.944	6.230
Piez. reading at check sta.							

Concentration and Velocity Profile Data

Sampler sta (y/D)	0.06	0.16	0.26	0.36	0.46	0.56	0.66	0.76	0.86	0.96
Avg. Conc. (C %)										
Velocity (u fps)										

Boundary Type: Hel-Cor Run No. 60 H Q = 8.00 cfs V = 10.20 fps
Profile Traverse: C_t = 6.25 percent T = 17.0 °C

Average Piezometer Reading

Piez. No.	4	5	6	7	8	9	10
Piez. reading	--	9.285	8.679	8.071	7.481	6.926	6.267
Piez. reading for C_t data							
Piez. reading at check sta.							

Concentration and Velocity Profile Data

Sampler sta (y/D)	0.06	0.16	0.26	0.36	0.46	0.56	0.66	0.76	0.86	0.96
Avg. Conc. (C %)										
Velocity (u fps)										

Boundary Type: Hel-Cor Run No. 61 H Q = 6.93 cfs V = 8.82 fps
Profile Traverse: C_t = 6.25 percent T = 18.9 °C

Average Piezometer Reading

Piez. No.	4	5	6	7	8	9	10
Piez. reading							
Piez. reading for C_t data	--	9.409	8.965	8.506	8.046	7.627	7.125
Piez. reading at check sta.							

Concentration and Velocity Profile Data

Sampler sta (y/D)	0.06	0.16	0.26	0.36	0.46	0.56	0.66	0.76	0.86	0.96
Avg. Conc. (C %)										
Velocity (u fps)										

Boundary Type: Hel-Cor Run No. 62 H Q = 7.00 cfs V = 8.92 fps
Profile Traverse: Vertical C_t = 6.48 percent T = 19.5 °C

Average Piezometer Reading

Piez. No.	4	5	6	7	8	9	10
Piez. reading	--	9.425	8.964	8.499	8.041	7.616	7.117
Piez. reading for C_t data							
Piez. reading at check sta.							

Concentration and Velocity Profile Data

Sampler sta (y/D)	0.06	0.16	0.26	0.36	0.46	0.56	0.66	0.76	0.86	0.96
Avg. Conc. (C %)	7.19	6.30	6.10	6.17	6.30	6.38	6.85	6.25	6.40	6.85
Velocity (u fps)	7.37	8.82	10.05	11.00	11.50	11.50	10.80	9.83	8.61	7.37

Boundary Type: Hel-Cor Run No. 63 H Q = 6.20 cfs V = 7.89 fps
Profile Traverse: Horizontal C_t = 6.74 percent T = 19.8 °C

Average Piezometer Reading

Piez. No.	4	5	6	7	8	9	10
Piez. reading	--	9.156	8.749	8.352	7.949	7.573	7.138
Piez. reading for C_t data	--	9.154	8.747	8.345	7.940	7.566	7.134
Piez. reading at check sta.							

Concentration and Velocity Profile Data

Sampler sta (y/D)	0.06	0.16	0.26	0.36	0.46	0.56	0.66	0.76	0.86	0.96
Avg. Conc. (C %)	7.40	6.75	6.38	6.35	6.50	6.75	6.60	6.85	6.80	7.00
Velocity (u fps)										

Boundary Type: Hel-Cor Run No. 64 H Q = 6.10 cfs V = 7.70 fps
Profile Traverse: Horizontal C_t = 5.37 percent T = 16.1 °C

Average Piezometer Reading

Piez. No.	4	5	6	7	8	9	10
Piez. reading	--	9.204	8.812	8.414	8.005	7.653	7.232
Piez. reading for C_t data	--	9.200	8.807	8.416	8.021	7.663	7.241
Piez. reading at check sta.							

Concentration and Velocity Profile Data

Sampler sta (y/D)	0.06	0.16	0.26	0.36	0.46	0.56	0.66	0.76	0.86	0.96
Avg. Conc. (C %)	5.95	5.34	5.22	5.22	5.28	5.21	5.28	5.40	5.49	5.30
Velocity (u fps)										

Boundary Type: Hel-Cor Run No. 65 H Q = 8.00 cfs V = 10.20 fps
Profile Traverse: Horizontal C_t = 4.44 percent T = 23.5 °C

Average Piezometer Reading

Piez. No.	4	5	6	7	8	9	10
Piez. reading	--	9.349	9.751	8.160	7.587	7.035	6.411
Piez. reading for C_t data							
Piez. reading at check sta.							

Concentration and Velocity Profile Data

Sampler sta (y/D)	0.06	0.16	0.26	0.36	0.46	0.56	0.66	0.76	0.86	0.96
Avg. Conc. (C %)										
Velocity (u fps)	--	--	11.92	12.90	13.55	13.78	13.05	11.80	10.45	8.71

Boundary Type: Hel-Cor Run No. 66 H Q = 6.93 cfs V = 8.82 fps
Profile Traverse: C_t = 4.44 percent T = 18.5 °C

Average Piezometer Reading

Piez. No.	4	5	6	7	8	9	10
Piez. reading							
Piez. reading for C_t data	--	9.563	9.076	8.594	8.112	7.677	7.170
Piez. reading at check sta.							

Concentration and Velocity Profile Data

Sampler sta (y/D)	0.06	0.16	0.26	0.36	0.46	0.56	0.66	0.76	0.86	0.96
Avg. Conc. (C %)										
Velocity (u fps)										

Boundary Type: Hel-Cor Run No. 67 H Q = 6.90 cfs V = 8.80 fps
Profile Traverse: Horizontal C_t = 4.55 percent T = 19.1 °C

Average Piezometer Reading

Piez. No.	4	5	6	7	8	9	10
Piez. reading	--	9.562	9.080	8.600	8.107	7.681	7.172
Piez. reading for C_t data							
Piez. reading at check sta.							

Concentration and Velocity Profile Data

Sampler sta (y/D)	0.06	0.16	0.26	0.36	0.46	0.56	0.66	0.76	0.86	0.96
Avg. Conc. (C %)	3.15	4.61	4.29	4.34	4.40	4.30	4.50	4.65	4.70	4.60
Velocity (u fps)	7.48	9.23	10.47	11.62	12.04	12.04	11.60	10.45	8.97	7.65

Boundary Type: Hel-Cor Run No. 68 H Q = 5.95 cfs V = 7.64 fps
Profile Traverse: Horizontal C_t = 4.40 percent T = 22.0 °C

Average Piezometer Reading

Piez. No.	4	5	6	7	8	9	10
Piez. reading	--	9.102	8.722	8.344	7.964	7.611	7.208
Piez. reading for C_t data	--	9.092	8.715	8.335	7.957	7.608	7.203
Piez. reading at check sta.							

Concentration and Velocity Profile Data

Sampler sta (y/D)	0.06	0.16	0.26	0.36	0.46	0.56	0.66	0.76	0.86	0.96
Avg. Conc. (C %)	5.15	4.20	4.32	4.15	4.31	4.31	4.29	4.41	4.45	4.40
Velocity (u fps)	6.81	8.15	9.35	10.50	10.63	10.63	10.28	9.30	8.03	6.83

Boundary Type: Hel-Cor Run No. 69 H Q = 8.80 cfs V = 10.05 fps
Profile Traverse: Horizontal C_t = 1.98 percent T = 18.7 °C

Average Piezometer Reading

Piez. No.	4	5	6	7	8	9	10
Piez. reading							
Piez. reading for C_t data							
Piez. reading at check sta.							

Concentration and Velocity Profile Data

Sampler sta (y/D)	0.06	0.16	0.26	0.36	0.46	0.56	0.66	0.76	0.86	0.96
Avg. Conc. (C %)										
Velocity (u fps)										

Boundary Type: Hel-Cor Run No. 70 H Q = 5.85 cfs V = 7.45 fps
Profile Traverse: Horizontal C_t = 2.13 percent T = 20.5 °C

Average Piezometer Reading

Piez. No.	4	5	6	7	8	9	10
Piez. reading	--	9.494	9.129	8.774	8.424	8.108	7.705
Piez. reading for C_t data	--	9.502	9.137	8.781	8.435	8.099	7.719
Piez. reading at check sta.							

Concentration and Velocity Profile Data

Sampler sta (y/D)	0.06	0.16	0.26	0.36	0.46	0.56	0.66	0.76	0.86	0.96
Avg. Conc. (C %)	2.46	2.15	1.97	1.95	2.05	2.19	2.10	2.05	2.23	2.20
Velocity (u fps)	6.05	7.00	8.12	8.81	9.32	9.32	8.81	7.89	7.08	6.05

Boundary Type: Hel-Cor Run No. 71 H Q = 5.90 cfs V = 7.52 fps
Profile Traverse: Horizontal C_t = 2.09 percent T = 21.5 °C

Average Piezometer Reading

Piez. No.	4	5	6	7	8	9	10
Piez. reading	--	9.480	9.118	8.763	8.421	8.084	7.711
Piez. reading for C_t data	--	9.502	9.137	8.781	8.435	8.099	7.719
Piez. reading at check sta.							

Concentration and Velocity Profile Data

Sampler sta (y/D)	0.06	0.16	0.26	0.36	0.46	0.56	0.66	0.76	0.86	0.96
Avg. Conc. (C %)	2.37	2.04	1.94	2.04	1.97	1.97	2.16	2.10	2.15	2.16
Velocity (u fps)	6.05	7.00	8.12	8.81	9.32	9.32	8.81	7.89	7.08	6.05

Boundary Type: Hel-Cor Run No. 72 H Q = 6.73 cfs V = 8.58 fps
Profile Traverse: Horizontal C_t = 1.80 percent T = 21.4 °C

Average Piezometer Reading

Piez. No.	4	5	6	7	8	9	10
Piez. reading	--	9.218	8.754	8.301	7.862	7.430	6.949
Piez. reading for C_t data	--	9.229	8.767	8.310	7.871	7.442	6.964
Piez. reading at check sta.							

Concentration and Velocity Profile Data

Sampler sta (y/D)	0.06	0.16	0.26	0.36	0.46	0.56	0.66	0.76	0.86	0.96
Avg. Conc. (C %)	1.96	1.71	1.69	1.80	1.75	1.75	1.75	1.76	1.86	1.97
Velocity (u fps)	6.55	8.94	10.10	11.20	11.70	11.80	11.20	10.10	8.99	7.57

Boundary Type: Hel-Cor Run No. 73 H Q = 6.75 cfs V = 8.48 fps
Profile Traverse: Vertical C_t = 2.09 percent T = 23.3 °C

Average Piezometer Reading

Piez. No.	4	5	6	7	8	9	10
Piez. reading	--	9.177	8.709	8.249	7.807	7.373	6.884
Piez. reading for C_t data							
Piez. reading at check sta.							

Concentration and Velocity Profile Data

Sampler sta (y/D)	0.06	0.16	0.26	0.36	0.46	0.56	0.66	0.76	0.86	0.96
Avg. Conc. (C %)	2.35	2.07	1.98	2.07	1.94	1.98	1.97	2.05	2.19	2.32
Velocity (u fps)	--	--	--	--	11.53	11.21	10.90	9.73	8.60	7.18

Boundary Type: Hel-Cor Run No. 74 H Q = 5.90 cfs V = 7.52 fps
Profile Traverse: Vertical C_t = 2.21 percent T = 24.2 °C

Average Piezometer Reading

Piez. No.	4	5	6	7	8	9	10
Piez. reading	--	8.707	8.343	7.980	7.634	7.289	6.907
Piez. reading for C_t data							
Piez. reading at check sta.							

Concentration and Velocity Profile Data

Sampler sta (y/D)	0.06	0.16	0.26	0.36	0.46	0.56	0.66	0.76	0.86	0.96
Avg. Conc. (C %)	2.34	2.16	2.12	2.21	2.13	2.13	2.12	2.24	2.21	2.43
Velocity (u fps)										

Boundary Type: Hel-Cor Run No. 76 H Q = 6.60 cfs V = 8.40 fps
Profile Traverse: Vertical C_t = 0.919 percent T = 21.2 °C

Average Piezometer Reading

Piez. No.	4	5	6	7	8	9	10
Piez. reading	--	9.151	8.710	8.270	7.854	7.436	6.981
Piez. reading for C_t data							
Piez. reading at check sta.							

Concentration and Velocity Profile Data

Sampler sta (y/D)	0.06	0.16	0.26	0.36	0.46	0.56	0.66	0.76	0.86	0.96
Avg. Conc. (C %)	1.06	0.864	0.849	0.870	0.897	0.870	0.870	0.903	0.960	1.04
Velocity (u fps)	--	8.86	10.00	10.85	11.50	11.45	10.80	9.80	8.80	7.36

Boundary Type: Hel-Cor Run No. 77 H Q = 5.80 cfs V = 7.25 fps
Profile Traverse: Vertical C_t = 0.854 percent T = 22.3 °C

Average Piezometer Reading

Piez. No.	4	5	6	7	8	9	10
Piez. reading	--	8.608	8.282	7.969	7.661	7.358	7.025
Piez. reading for C_t data							
Piez. reading at check sta.							

Concentration and Velocity Profile Data

Sampler sta (y/D)	0.06	0.16	0.26	0.36	0.46	0.56	0.66	0.76	0.86	0.96
Avg. Conc. (C %)	0.855	0.825	0.810	0.845	0.820	0.865	0.820	0.840	0.840	0.990
Velocity (u fps)	5.95	7.57	8.57	9.31	9.72	9.80	9.29	8.34	7.40	6.21

Boundary Type: Hel-Cor Run No. 78 H Q = 6.63 cfs V = 8.45 fps
Profile Traverse: Horizontal C_t = 0.758 percent T = 21.8 °C

Average Piezometer Reading

Piez. No.	4	5	6	7	8	9	10
Piez. reading	--	9.304	8.849	8.400	7.970	7.543	7.069
Piez. reading for C_t data							
Piez. reading at check sta.	•						

Concentration and Velocity Profile Data

Sampler sta (y/D)	0.06	0.16	0.26	0.36	0.46	0.56	0.66	0.76	0.86	0.96
Avg. Conc. (C %)	0.883	0.715	0.705	0.730	0.730	0.740	0.730	0.750	0.763	0.820
Velocity (u fps)	7.54	8.75	9.81	10.90	11.50	11.50	10.90	10.00	8.82	7.45

Boundary Type: Hel-Cor Run No. 79 H Q = 6.63 cfs V = 8.45 fps
Profile Traverse: Horizontal C_t = 0.748 percent T = 22.3 °C

Average Piezometer Reading

Piez. No.	4	5	6	7	8	9	10
Piez. reading	--	9.295	8.841	8.390	7.959	7.533	7.061
Piez. reading for C_t data							
Piez. reading at check sta.							

Concentration and Velocity Profile Data

Sampler sta (y/D)	0.06	0.16	0.26	0.36	0.46	0.56	0.66	0.76	0.86	0.96
Avg. Conc. (C %)	--	0.730	--	0.750	--	0.725	--	0.715	--	0.820
Velocity (u fps)	7.45	8.75	9.81	10.90	11.50	11.50	10.90	10.00	8.82	7.45

Boundary Type: Hel-Cor Run No. 80 H Q = 5.85 cfs V = 7.45 fps
Profile Traverse: Horizontal C_t = 0.870 percent T = 25.3 °C

Average Piezometer Reading

Piez. No.	4	5	6	7	8	9	10
Piez. reading	--	8.610	8.312	7.993	7.681	7.375	7.037
Piez. reading for C_t data							
Piez. reading at check sta.							

Concentration and Velocity Profile Data

Sampler sta (y/D)	0.06	0.16	0.26	0.36	0.46	0.56	0.66	0.76	0.86	0.96
Avg. Conc. (C %)	--	0.835	--	0.845	--	0.865	--	0.885	--	0.920
Velocity (u fps)	6.01	7.70	8.39	9.29	9.71	9.70	9.32	8.26	7.36	6.26

Boundary Type: Hel-Cor Run No. 81 H Q = 5.85 cfs V = 7.45 fps
Profile Traverse: Horizontal C_t = 0.872percent T = 25.8 °C

Average Piezometer Reading

Piez. No.	4	5	6	7	8	9	10
Piez. reading	--	8.639	8.311	7.994	7.686	7.380	7.044
Piez. reading for C_t data							
Piez. reading at check sta.							

Concentration and Velocity Profile Data

Sampler sta (y/D)	0.06	0.16	0.26	0.36	0.46	0.56	0.66	0.76	0.86	0.96
Avg. Conc. (C %)	1.050	0.820	0.825	0.825	0.839	0.839	0.850	0.865	0.905	0.899
Velocity (u fps)	6.01	7.70	8.39	9.29	9.71	9.70	9.32	8.26	7.36	6.26

Boundary Type: Hel-Cor Run No. 82 H Q = 7.63 cfs V = 9.72 fps
Profile Traverse: Horizontal C_t = percent T = 17.0 °C

Average Piezometer Reading

Piez. No.	4	5	6	7	8	9	10
Piez. reading	9.557	9.069	8.499	7.943	7.408	6.880	6.295
Piez. reading for C_t data							
Piez. reading at check sta.							

Concentration and Velocity Profile Data

Sampler sta (y/D)	0.06	0.16	0.26	0.36	0.46	0.56	0.66	0.76	0.86	0.96
Avg. Conc. (C %)										
Velocity (u fps)	--	--	11.24	12.25	12.80	12.78	12.13	11.00	9.76	8.30

Boundary Type: Hel-Cor Run No. 83 H Q = 7.70 cfs V = 9.80 fps
Profile Traverse: Horizontal C_t = 0.0 percent T = 20.7 °C

Average Piezometer Reading

Piez. No.	4	5	6	7	8	9	10
Piez. reading	9.451	8.996	8.418	7.853	7.319	6.795	6.202
Piez. reading for C_t data							
Piez. reading at check sta.							

Concentration and Velocity Profile Data

Sampler sta (y/D)	0.06	0.16	0.26	0.36	0.46	0.56	0.66	0.76	0.86	0.96
Avg. Conc. (C %)										
Velocity (u fps)	--	9.90	11.18	12.25	12.89	12.90	12.20	11.16	9.80	8.50

Boundary Type: Hel-Cor Run No. 84 H Q = 6.60 cfs V = 8.40 fps
Profile Traverse: Horizontal C_t = 0.0 percent T = 21.3 °C

Average Piezometer Reading

Piez. No.	4	5	6	7	8	9	10
Piez. reading	9.512	9.143	8.698	8.264	7.837	7.430	6.971
Piez. reading for C_t data							
Piez. reading at check sta.							

Concentration and Velocity Profile Data

Sampler sta (y/D)	0.06	0.16	0.26	0.36	0.46	0.56	0.66	0.76	0.86	0.96
Avg. Conc. (C %)	trace	trace	trace	trace	trace	trace	trace	trace	trace	trace
Velocity (u fps)	7.27	8.83	9.86	10.82	11.35	11.40	10.85	9.83	8.67	7.40

Boundary Type: Hel-Cor Run No. 85 H Q = 5.78 cfs V = 7.39 fps
Profile Traverse: Horizontal C_t = 0.0 percent T = 22.5 °C

Average Piezometer Reading

Piez. No.	4	5	6	7	8	9	10
Piez. reading	8.857	8.607	8.307	8.006	7.720	7.433	7.121
Piez. reading for C_t data							
Piez. reading at check sta.							

Concentration and Velocity Profile Data

Sampler sta (y/D)	0.06	0.16	0.26	0.36	0.46	0.56	0.66	0.76	0.86	0.96
Avg. Conc. (C %)		trace		trace		trace		trace		trace
Velocity (u fps)	6.06	7.23	8.22	9.00	9.50	9.51	9.00	8.20	7.05	6.17

Boundary Type: Hel-Cor Run No. 86 H Q = 5.80 cfs V = 7.23 fps
Profile Traverse: Horizontal C_t = 0.0 percent T = 26.2 °C

Average Piezometer Reading

Piez. No.	4	5	6	7	8	9	10
Piez. reading	9.112	8.830	8.484	8.144	7.819	7.501	7.146
Piez. reading for C_t data							
Piez. reading at check sta.							

Concentration and Velocity Profile Data

Sampler sta (y/D)	0.06	0.16	0.26	0.36	0.46	0.56	0.66	0.76	0.86	0.96
Avg. Conc. (C %)										
Velocity (u fps)	6.57	7.60	9.00	9.40	10.00	9.96	9.50	9.00	7.60	6.57

Boundary Type: Hel-Cor Run No. 87 H Q = 6.60 cfs V = 8.21 fps
Profile Traverse: Horizontal C_t = 0.0percent T = 27.0 °C

Average Piezometer Reading

Piez. No.	4	5	6	7	8	9	10
Piez. reading	9.575	9.219	8.774	8.331	7.910	7.502	7.021
Piez. reading for C_t data							
Piez. reading at check sta.							

Concentration and Velocity Profile Data

Sampler sta (y/D)	0.06	0.16	0.26	0.36	0.46	0.56	0.66	0.76	0.86	0.96
Avg. Conc. (C %)										
Velocity (u fps)	--	8.64	9.74	10.70	11.33	11.33	10.70	9.65	8.62	7.63

Boundary Type: Hel-Cor Run No. 88 H Q = 6.70 cfs V = 8.40 fps
Profile Traverse: Horizontal C_t = 0.0 percent T = 28.5 °C

Average Piezometer Reading

Piez. No.	4	5	6	7	8	9	10
Piez. reading	9.596	9.232	8.772	8.320	7.896	7.469	6.991
Piez. reading for C_t data							
Piez. reading at check sta.							

Concentration and Velocity Profile Data

Sampler sta (y/D)	0.06	0.16	0.26	0.36	0.46	0.56	0.66	0.76	0.86	0.96
Avg. Conc. (C %)										
Velocity (u fps)	--	8.68	9.76	10.91	11.39	11.39	10.80	9.86	8.72	7.65

Boundary Type: Hel-Cor Run No. 89 H Q = 3.53 cfs V = 4.45 fps
Profile Traverse: Horizontal C_t = 0.0 percent T = 27.0 °C

Average Piezometer Reading

Piez. No.	4	5	6	7	8	9	10
Piez. reading	8.357	8.242	8.112	7.985	7.858	7.730	7.597
Piez. reading for C_t data							
Piez. reading at check sta.							

Concentration and Velocity Profile Data

Sampler sta (y/D)	0.06	0.16	0.26	0.36	0.46	0.56	0.66	0.76	0.86	0.96
Avg. Conc. (C %)										
Velocity (u fps)	3.93	4.60	5.39	6.00	6.31	6.32	6.00	5.39	4.68	3.85

Boundary Type: Hel-Cor Run No. 90 H Q = 4.78 cfs V = 6.00 fps
Profile Traverse: Horizontal C_t = 0.0 percent T = 27.1 °C

Average Piezometer Reading

Piez. No.	4	5	6	7	8	9	10
Piez. reading	8.976	8.789	8.566	8.347	8.137	7.931	7.702
Piez. reading for C_t data							
Piez. reading at check sta.							

Concentration and Velocity Profile Data

Sampler sta (y/D)	0.06	0.16	0.26	0.36	0.46	0.56	0.66	0.76	0.86	0.96
Avg. Conc. (C %)										
Velocity (u fps)	4.68	5.67	6.67	7.31	7.70	7.74	7.40	6.67	5.64	4.68

Boundary Type: Hel-Cor Run No. 91 H Q = 1.63 cfs V = 2.08 fps
Profile Traverse: Horizontal C_t = 0.0 percent T = 26.4 °C

Average Piezometer Reading

Piez. No.	4	5	6	7	8	9	10
Piez. reading	7.983	7.960	7.932	7.905	7.870	7.842	7.812
Piez. reading for C_t data							
Piez. reading at check sta.							

Concentration and Velocity Profile Data

Sampler sta (y/D)	0.06	0.16	0.26	0.36	0.46	0.56	0.66	0.76	0.86	0.96
Avg. Conc. (C %)										
Velocity (u fps)	--	--	2.41	2.78	2.90	2.90	2.78	2.41	2.27	1.60

Boundary Type: Smooth Run No. 1 S Q = 1.83 cfs V = 2.36 fps
Profile Traverse: C_t = 0.0 percent T = 16.0 °C

Average Piezometer Reading

Piez. No.	4	5	6	7	8	9	10
Piez. reading	0.288	0.267	0.251	0.234	0.219	0.191	0.185
Piez. reading for C_t data							
Piez. reading at check sta.							

Concentration and Velocity Profile Data

Sampler sta (y/D)	0.06	0.16	0.26	0.36	0.46	0.56	0.66	0.76	0.86	0.96
Avg. Conc. (C %)										
Velocity (u fps)	1.80	2.41	2.41	2.78	2.76	2.90	2.76	2.54	2.27	1.80

Boundary Type: Smooth Run No. 2 S Q = 5.83 cfs V = 7.30 fps
Profile Traverse: Vertical C_t = 0.0 percent T = 18.0 °C

Average Piezometer Reading

Piez. No.	4	5	6	7	8	9	10
Piez. reading	9.100	8.947	8.874	8.775	8.696	8.568	8.471
Piez. reading for C_t data							
Piez. reading at check sta.							

Concentration and Velocity Profile Data

Sampler sta (y/D)	0.06	0.16	0.26	0.36	0.46	0.56	0.66	0.76	0.86	0.96
Avg. Conc. (C %)										
Velocity (u fps)	6.82	7.48	8.03	8.26	8.37	8.50	8.07	7.62	7.18	6.12

Boundary Type: Smooth Run No. 3 S Q = 4.78 cfs V = 6.00 fps
Profile Traverse: Vertical C_t = 0.0 percent T = 18.5 °C

Average Piezometer Reading

Piez. No.	4	5	6	7	8	9	10
Piez. reading	8.747	8.674	8.550	8.491	8.422	8.364	8.230
Piez. reading for C_t data							
Piez. reading at check sta.							

Concentration and Velocity Profile Data

Sampler sta (y/D)	0.06	0.16	0.26	0.36	0.46	0.56	0.66	0.76	0.86	0.96
Avg. Conc. (C %)										
Velocity (u fps)	5.74	6.33	6.63	7.00	6.95	7.05	6.77	6.48	6.06	5.50

Boundary Type: Smooth Run No. 4 S Q = 3.65 cfs V = 4.52 fps
Profile Traverse: Vertical C_t = 0.0 percent T = 18.8 °C

Average Piezometer Reading

Piez. No.	4	5	6	7	8	9	10
Piez. reading	0.367	0.284	0.242	0.200	0.151	0.110	0.059
Piez. reading for C_t data							
Piez. reading at check sta.							

Concentration and Velocity Profile Data

Sampler sta (y/D)	0.06	0.16	0.26	0.36	0.46	0.56	0.66	0.76	0.86	0.96
Avg. Conc. (C %)										
Velocity (u fps)	4.47	5.02	5.02	5.33	5.63	5.39	5.27	5.08	4.69	4.02

Boundary Type: Smooth Run No. 5 S Q = 6.62 cfs V = 8.30 fps
Profile Traverse: Vertical C_t = 0.0 percent T = 18.1 °C

Average Piezometer Reading

Piez. No.	4	5	6	7	8	9	10
Piez. reading	8.869	8.584	8.514	8.391	8.299	8.162	8.008
Piez. reading for C_t data							
Piez. reading at check sta.							

Concentration and Velocity Profile Data

Sampler sta (y/D)	0.06	0.16	0.26	0.36	0.46	0.56	0.66	0.76	0.86	0.96
Avg. Conc. (C %)										
Velocity (u fps)	8.03	9.00	9.47	9.94	10.10	9.97	9.70	9.24	8.56	7.40

Boundary Type: Smooth Run No. 6 S Q = 7.32 cfs V = 9.17 fps
Profile Traverse: Vertical C_t = 0.0 percent T = 18.9 °C

Average Piezometer Reading

Piez. No.	4	5	6	7	8	9	10
Piez. reading	8.995	8.664	8.591	8.447	8.347	8.194	8.019
Piez. reading for C_t data							
Piez. reading at check sta.							

Concentration and Velocity Profile Data

Sampler sta (y/D)	0.06	0.16	0.26	0.36	0.46	0.56	0.66	0.76	0.86	0.96
Avg. Conc. (C %)										
Velocity (u fps)	7.40	9.67	10.32	10.58	10.70	10.60	10.31	9.85	9.05	8.00

Boundary Type: Smooth Run No. 7 S Q = 7.400 cfs V = 9.17 fps
Profile Traverse: Vertical C_t = 0.261 percent T = 21.7 °C

Average Piezometer Reading

Piez. No.	4	5	6	7	8	9	10
Piez. reading	7.764	7.472	7.346	7.199	7.100	6.942	6.767
Piez. reading for C_t data	7.761	7.469	7.347	7.205	7.106	6.949	6.772
Piez. reading at check sta.							

Concentration and Velocity Profile Data

Sampler sta (y/D)	0.06	0.16	0.26	0.36	0.46	0.56	0.66	0.76	0.86	0.96
Avg. Conc. (C %)	1.39	0.630	0.379	0.286	0.210	0.165	0.134	0.106	0.078	0.059
Velocity (u fps)	8.07	9.25	10.00	10.50	10.80	10.80	10.50	9.86	9.16	8.07

Boundary Type: Smooth Run No. 8 S Q = 6.60 cfs V = 8.40 fps
Profile Traverse: Vertical C_t = 0.195 percent T = 22.7 °C

Average Piezometer Reading

Piez. No.	4	5	6	7	8	9	10
Piez. reading	7.568	7.333	7.214	7.096	7.010	6.871	6.725
Piez. reading for C_t data	7.574	7.336	7.220	7.098	7.010	6.874	6.721
Piez. reading at check sta.							

Concentration and Velocity Profile Data

Sampler sta (y/D)	0.06	0.16	0.26	0.36	0.46	0.56	0.66	0.76	0.86	0.96
Avg. Conc. (C %)	1.130	0.429	0.266	0.190	0.148	0.120	0.082	0.059	0.045	trace
Velocity (u fps)	7.52	8.62	9.21	9.70	10.00	9.95	9.70	9.16	8.45	7.50

Boundary Type: Smooth Run No. 9 S Q = 5.80 cfs V = 7.39 fps
Profile Traverse: Vertical C_t = 0.125 percent T = 23.5 °C

Average Piezometer Reading

Piez. No.	4	5	6	7	8	9	10
Piez. reading	7.203	7.019	6.929	6.831	6.761	6.654	6.534
Piez. reading for C_t data	7.204	7.032	6.935	6.836	6.776	6.660	6.541
Piez. reading at check sta.							

Concentration and Velocity Profile Data

Sampler sta (y/D)	0.06	0.16	0.26	0.36	0.46	0.56	0.66	0.76	0.86	0.96
Avg. Conc. (C %)	0.885	0.300	0.163	0.121	0.078	0.064	0.046	0.03	0.02	0.01
Velocity (u fps)	6.61	7.60	8.15	8.60	8.90	8.90	8.60	8.15	7.57	6.61

Boundary Type: Smooth Run No. 10 S Q = 7.50 cfs V = 9.55 fps
Profile Traverse: Horizontal C_t = 0.332 percent T = 24.5 °C

Average Piezometer Reading

Piez. No.	4	5	6	7	8	9	10
Piez. reading	7.641	7.365	7.243	7.117	6.995	6.854	6.683
Piez. reading for C_t data	7.649	7.375	7.240	7.114	7.001	6.855	6.679
Piez. reading at check sta.							

Concentration and Velocity Profile Data

Sampler sta (y/D)	0.06	0.16	0.26	0.36	0.46	0.56	0.66	0.76	0.86	0.96
Avg. Conc. (C %)	0.224	0.210	0.195	0.195	0.182	0.182	0.176	0.186	0.190	0.190
Velocity (u fps)	---	9.90	10.40	10.70	11.00	11.00	10.90	10.40	9.64	8.71

Boundary Type: Smooth Run No. 11 S Q = 6.60 cfs V = 8.40 fps
Profile Traverse: Horizontal C_t = 0.175 percent T = 21.7 °C

Average Piezometer Reading

Piez. No.	4	5	6	7	8	9	10
Piez. reading	7.529	7.254	7.186	7.070	6.984	6.855	6.706
Piez. reading for C_t data	7.521	7.248	7.182	7.068	6.985	6.858	6.708
Piez. reading at check sta.							

Concentration and Velocity Profile Data

Sampler sta (y/D)	0.06	0.16	0.26	0.36	0.46	0.56	0.66	0.76	0.86	0.96
Avg. Conc. (C %)	0.115	0.106	0.110	0.101	0.110	0.101	0.106	0.110	0.110	0.115
Velocity (u fps)	8.17	8.95	9.55	9.87	10.10	10.25	9.94	9.55	8.88	7.84

Boundary Type: Smooth Run No. 12 S Q = 5.80 cfs V = 7.37 fps
Profile Traverse: Horizontal C_t = 0.151 percent T = 24.2 °C

Average Piezometer Reading

Piez. No.	4	5	6	7	8	9	10
Piez. reading	7.424	7.305	7.152	7.065	6.987	6.879	6.761
Piez. reading for C_t data	7.425	7.307	7.155	7.069	6.990	6.885	6.763
Piez. reading at check sta.							

Concentration and Velocity Profile Data

Sampler sta (y/D)	0.06	0.16	0.26	0.36	0.46	0.56	0.66	0.76	0.86	0.96
Avg. Conc. (C %)	0.073	0.068	--	0.068	--	0.068	0.068	0.068	0.068	0.073
Velocity (u fps)	6.90	8.080	8.50	8.85	8.94	8.90	8.79	8.50	7.95	6.76

Boundary Type: Smooth Run No. 13 S Q = 8.75 cfs V = 11.1 fps
Profile Traverse: C_t = 0.386 percent T = 23.5 °C

Average Piezometer Reading

Piez. No.	4	5	6	7	8	9	10
Piez. reading							
Piez. reading for C_t data	8.740	8.499	--	8.106	7.909	7.699	7.465
Piez. reading at check sta.							

Concentration and Velocity Profile Data

Sampler sta (y/D)	0.06	0.16	0.26	0.36	0.46	0.56	0.66	0.76	0.86	0.96
Avg. Conc. (C %)	---									
Velocity (u fps)	--	--	12.00	12.33	12.56	12.48	12.30	11.92	11.18	5.91

Boundary Type: Smooth Run No. 14 S δ Q = 4.80 cfs V = 6.11 fps
Profile Traverse: Horizontal C_t = 0.383 percent T = 20.8 °C

Average Piezometer Reading

Piez. No.	4	5	6	7	8	9	10
Piez. reading	8.532	8.445	8.330	8.289	8.202	8.139	8.056
Piez. reading for C_t data	8.519	8.437	8.331	8.284	8.198	8.126	8.045
Piez. reading at check sta.							

Concentration and Velocity Profile Data

Sampler sta (y/D)	0.06	0.16	0.26	0.36	0.46	0.56	0.66	0.76	0.86	0.96
Avg. Conc. (C %)	0.167	0.153	0.144	0.134	0.125	0.120	0.115	0.110	0.115	0.110
Velocity (u fps)	5.85	6.52	7.26	7.50	7.65	7.65	7.50	7.26	6.52	5.85

Boundary Type: Smooth Run No. 15 S δ Q = 4.85 cfs V = 6.18 fps
Profile Traverse: Vertical C_t = 0.374 percent T = 23.8 °C

Average Piezometer Reading

Piez. No.	4	5	6	7	8	9	10
Piez. reading	8.532	8.446	8.335	8.277	8.201	8.125	8.042
Piez. reading for C_t data	8.519	8.432	8.324	8.278	8.196	8.116	8.036
Piez. reading at check sta.							

Concentration and Velocity Profile Data

Sampler sta (y/D)	0.06	0.16	0.26	0.36	0.46	0.56	0.66	0.76	0.86	0.96
Avg. Conc. (C %)	7.60	0.960	0.349	0.200	0.115	0.077	0.059	trace	trace	trace
Velocity (u fps)	4.39	6.02	6.80	7.18	7.50	7.52	7.25	6.82	6.32	5.25

Boundary Type: Smooth Run No. 16 S Q = 4.86 cfs V = 6.18 fps
Profile Traverse: Vertical C_t = 0.116 percent T = 25.7 °C

Average Piezometer Reading

Piez. No.	4	5	6	7	8	9	10
Piez. reading	8.475	8.396	8.286	8.255	8.181	8.106	8.035
Piez. reading for C_t data	8.484	8.401	8.290	8.226	8.184	8.104	8.020
Piez. reading at check sta.							

Concentration and Velocity Profile Data

Sampler sta (y/D)	0.06	0.16	0.26	0.36	0.46	0.56	0.66	0.76	0.86	0.96
Avg. Conc. (C %)	1.65	0.415	0.187	0.127	0.080	0.059	0.045	trace	trace	trace
Velocity (u fps)	5.21	6.02	6.87	7.10	7.37	7.33	7.05	6.68	6.43	5.45

Boundary Type: Smooth Run No. 17 S Q = 3.40 cfs V = 4.33 fps
Profile Traverse: Vertical C_t = 0.081 percent T = 20.5 °C

Average Piezometer Reading

Piez. No.	4	5	6	7	8	9	10
Piez. reading	8.129	8.091	8.027	7.999	7.957	7.916	7.874
Piez. reading for C_t data	8.116	8.081	8.016	7.990	7.950	7.901	7.858
Piez. reading at check sta.							

Concentration and Velocity Profile Data

Sampler sta (y/D)	0.06	0.16	0.26	0.36	0.46	0.56	0.66	0.76	0.86	0.96
Avg. Conc. (C %)	0.810	0.165	0.073	0.054	trace	trace	--	--	--	--
Velocity (u fps)	3.60	4.47	4.78	5.20	5.39	5.39	5.20	4.95	4.54	4.02

Boundary Type: Smooth Run No. 18 S δ Q = 2.20 cfs V = 2.80 fps
Profile Traverse: Vertical C_t = 0.040 percent T = 21.4 °C

Average Piezometer Reading

Piez. No.	4	5	6	7	8	9	10
Piez. reading	0.789	0.769	0.745	0.732	0.714	0.698	0.679
Piez. reading for C_t data							
Piez. reading at check sta.							

Concentration and Velocity Profile Data

Sampler sta (y/D)	0.06	0.16	0.26	0.36	0.46	0.56	0.66	0.76	0.86	0.96
Avg. Conc. (C %)	0.465	trace	trace	trace	--	--	--	--	--	--
Velocity (u fps)	--	2.27	2.66	2.90	3.11	3.22	3.11	3.01	2.54	2.41

Boundary Type: Smooth Run No. 19 S Q = 4.80 cfs V = 6.11 fps
Profile Traverse: Vertical C_t = 0.010 percent T = 23.0 °C

Average Piezometer Reading

Piez. No.	4	5	6	7	8	9	10
Piez. reading	8.472	8.391	8.293	8.243	8.170	8.094	8.013
Piez. reading for C_t data	0.466	0.386	0.285	0.238	0.170	0.093	0.014
Piez. reading at check sta.							

Concentration and Velocity Profile Data

Sampler sta (y/D)	0.06	0.16	0.26	0.36	0.46	0.56	0.66	0.76	0.86	0.96
Avg. Conc. (C %)	0.163	0.059	trace	--	--	--	--	--	--	--
Velocity (u fps)	5.32	6.30	6.51	6.90	7.12	7.12	6.90	6.57	6.10	5.20

Boundary Type: Smooth — Run No. 30 S δ — Q = 5.82 cfs — V = 7.41 fps
Profile Traverse: Horizontal — C_t = 0.609 percent — T = 26.4 °C

Average Piezometer Reading

Piez. No.	4	5	6	7	8	9	10
Piez. reading	8.263	8.155	8.026	7.959	7.854	7.753	7.641
Piez. reading for C_t data	8.271	8.161	8.028	7.960	7.856	7.756	7.640
Piez. reading at check sta.							

Concentration and Velocity Profile Data

Sampler sta (y/D)	0.06	0.16	0.26	0.36	0.46	0.56	0.66	0.76	0.86	0.96
Avg. Conc. (C %)	0.210	0.200	--	0.205	--	0.186	0.177	0.177	0.171	0.167
Velocity (u fps)	6.90	7.57	8.26	8.45	8.69	8.69	8.40	7.98	7.52	6.51

Boundary Type: Smooth — Run No. 31 S δ — Q = 5.80 cfs — V = 7.38 fps
Profile Traverse: Vertical — C_t = 0.613 percent — T = 22.0 °C

Average Piezometer Reading

Piez. No.	4	5	6	7	8	9	10
Piez. reading	8.224	8.117	7.983	7.915	7.809	7.705	7.586
Piez. reading for C_t data	8.247	8.135	7.999	7.935	7.829	7.727	7.610
Piez. reading at check sta.							

Concentration and Velocity Profile Data

Sampler sta (y/D)	0.06	0.16	0.26	0.36	0.46	0.56	0.66	0.76	0.86	0.96
Avg. Conc. (C %)	9.50	1.63	0.730	0.430	0.267	0.172	0.129	0.092	0.068	--
Velocity (u fps)	5.26	7.26	7.95	8.27	8.82	8.82	8.27	7.90	7.25	6.37

Boundary Type: Smooth — Run No. 32 S — Q = 6.70 cfs — V = 8.53 fps
Profile Traverse: Vertical — C_t = 0.624 percent — T = 23.7 °C

Average Piezometer Reading

Piez. No.	4	5	6	7	8	9	10
Piez. reading	8.514	8.355	8.166	8.054	7.937	7.800	7.642
Piez. reading for C_t data	8.514	8.362	8.168	8.086	7.940	7.796	7.642
Piez. reading at check sta.							

Concentration and Velocity Profile Data

Sampler sta (y/D)	0.06	0.16	0.26	0.36	0.46	0.56	0.66	0.76	0.86	0.96
Avg. Conc. (C %)	5.79	1.58	0.850	0.557	0.378	0.252	0.172	0.134	0.100	--
Velocity (u fps)	7.13	8.42	9.31	10.00	10.20	10.20	9.81	9.31	8.69	7.70

Boundary Type: Smooth — Run No. 33 S — Q = 7.50 cfs — V = 9.55 fps
Profile Traverse: Vertical — C_t = 0.731 percent — T = 21.7 °C

Average Piezometer Reading

Piez. No.	4	5	6	7	8	9	10
Piez. reading	8.790	8.576	8.328	8.221	8.035	7.861	7.664
Piez. reading for C_t data	8.737	8.548	8.323	8.232	8.057	7.893	7.707
Piez. reading at check sta.							

Concentration and Velocity Profile Data

Sampler sta (y/D)	0.06	0.16	0.26	0.36	0.46	0.56	0.66	0.76	0.86	0.96
Avg. Conc. (C %)	4.60	1.840	1.040	0.719	0.500	0.352	0.256	0.190	0.499	0.092
Velocity (u fps)	8.45	9.78	10.30	10.50	10.70	10.70	10.40	10.00	9.50	8.45

Boundary Type: Smooth — Run No. 34 S $\bar{\delta}$ — Q = 5.83 cfs — V = 7.43 fps
Profile Traverse: Vertical — C_t = 1.17 percent — T = 20.0 °C

Average Piezometer Reading

Piez. No.	4	5	6	7	8	9	10
Piez. reading	8.334	8.216	8.072	7.990	7.866	7.747	7.616
Piez. reading for C_t data	8.327	8.210	8.063	7.987	7.866	7.751	7.624
Piez. reading at check sta.							

Concentration and Velocity Profile Data

Sampler sta (y/D)	0.06	0.16	0.26	0.36	0.46	0.56	0.66	0.76	0.86	0.96
Avg. Conc. (C %)	10.70	4.70	1.70	0.909	0.545	0.351	0.256	0.190	0.129	0.092
Velocity (u fps)	4.34	6.72	7.96	8.62	9.15	9.15	8.86	8.34	7.65	6.57

Boundary Type: Smooth — Run No. 36 S — Q = 6.60 cfs — V = 8.41 fps
Profile Traverse: Vertical — C_t = 1.16 percent — T = 22.2 °C

Average Piezometer Reading

Piez. No.	4	5	6	7	8	9	10
Piez. reading	8.558	8.404	8.221	8.135	7.989	7.847	7.690
Piez. reading for C_t data	8.568	8.411	8.226	8.141	7.994	7.854	7.696
Piez. reading at check sta.							

Concentration and Velocity Profile Data

Sampler sta (y/D)	0.06	0.16	0.26	0.36	0.46	0.56	0.66	0.76	0.86	0.96
Avg. Conc. (C %)	13.20	3.48	1.14	0.990	0.644	0.415	--	0.234	0.162	0.120
Velocity (u fps)	7.61	8.42	9.42	10.00	10.45	10.35	9.35	8.72	7.65	--

Boundary Type: Smooth — Run No. 37 S — Q = 7.60 cfs — V = 9.68 fps
Profile Traverse: Vertical — C_t = 1.19 percent — T = 20.5 °C

Average Piezometer Reading

Piez. No.	4	5	6	7	8	9	10
Piez. reading	8.851	8.634	8.386	8.280	8.096	7.919	7.725
Piez. reading for C_t data	8.799	8.608	8.384	8.289	8.111	7.945	7.756
Piez. reading at check sta.							

Concentration and Velocity Profile Data

Sampler sta (y/D)	0.06	0.16	0.26	0.36	0.46	0.56	0.66	0.76	0.86	0.96
Avg. Conc. (C %)	9.40	3.23	1.71	1.20	1.12	1.03	0.920	0.763	0.530	0.405
Velocity (u fps)	7.82	9.35	9.86	10.60	10.70	10.70	10.60	10.00	9.34	8.19

Boundary Type: Smooth — Run No. 38 S — Q = 5.84 cfs — V = 7.44 fps
Profile Traverse: Horizontal — C_t = 1.16 percent — T = 24.6 °C

Average Piezometer Reading

Piez. No.	4	5	6	7	8	9	10
Piez. reading	8.334	8.195	8.051	7.981	7.854	7.735	7.607
Piez. reading for C_t data	8.320	8.190	8.041	7.965	7.841	7.724	7.594
Piez. reading at check sta.							

Concentration and Velocity Profile Data

Sampler sta (y/D)	0.06	0.16	0.26	0.36	0.46	0.56	0.66	0.76	0.86	0.96
Avg. Conc. (C %)	0.354	--	0.339	--	0.358	0.364	0.314	0.376	0.395	0.400
Velocity (u fps)	7.31	8.30	8.81	9.30	9.35	9.41	9.15	8.67	8.08	7.12

Boundary Type: Smooth — Run No. 39 S — Q = 6.63 cfs — V = 8.45 fps
Profile Traverse: Horizontal — C_t = 1.15 percent — T = 27.0 °C

Average Piezometer Reading

Piez. No.	4	5	6	7	8	9	10
Piez. reading	8.494	8.334	8.155	8.074	7.927	7.792	7.636
Piez. reading for C_t data	8.479	8.323	8.141	8.065	7.920	7.789	7.634
Piez. reading at check sta.							

Concentration and Velocity Profile Data

Sampler sta (y/D)	0.06	0.16	0.26	0.36	0.46	0.56	0.66	0.76	0.86	0.96
Avg. Conc. (C %)	0.430	0.439	--	0.439	--	0.465	0.439	0.459	0.459	0.498
Velocity (u fps)	8.02	9.30	9.90	10.30	10.40	10.40	10.20	9.74	8.97	7.78

Boundary Type: Smooth — Run No. 40 S — Q = 7.70 cfs — V = 9.80 fps
Profile Traverse: Horizontal — C_t = 1.29 percent — T = 24.0 °C

Average Piezometer Reading

Piez. No.	4	5	6	7	8	9	10
Piez. reading	8.699	8.507	8.285	8.196	8.026	7.865	7.680
Piez. reading for C_t data	8.698	8.504	8.281	8.195	8.023	7.861	7.676
Piez. reading at check sta.							

Concentration and Velocity Profile Data

Sampler sta (y/D)	0.06	0.16	0.26	0.36	0.46	0.56	0.66	0.76	0.86	0.96
Avg. Conc. (C %)	0.665	--	0.649	--	0.630	0.610	0.665	0.685	0.649	0.715
Velocity (u fps)	9.12	10.30	10.90	11.40	11.60	11.60	11.30	10.80	10.10	8.82

Boundary Type: Smooth Run No. 41 S Q = 8.80 cfs V = 11.2 fps
Profile Traverse: Horizontal C_t = 1.54 percent T = 22.4 °C

Average Piezometer Reading

Piez. No.	4	5	6	7	8	9	10
Piez. reading	8.486	8.236	7.957	7.854	7.654	7.441	7.212
Piez. reading for C_t data	8.448	8.198	7.950	7.820	7.606	7.407	7.177
Piez. reading at check sta.							

Concentration and Velocity Profile Data

Sampler sta (y/D)	0.06	0.16	0.26	0.36	0.46	0.56	0.66	0.76	0.86	0.96
Avg. Conc. (C %)										
Velocity (u fps)	10.10	10.70	12.20	12.50	12.66	12.75	12.55	12.02	11.20	9.84

Boundary Type: Smooth Run No. 42 S Q = 8.81 cfs V = 11.25 fps
Profile Traverse: Horizontal C_t = 2.51 percent T = 26.0 °C

Average Piezometer Reading

Piez. No.	4	5	6	7	8	9	10
Piez. reading	8.401	8.160	7.886	7.781	7.570	7.369	7.136
Piez. reading for C_t data	8.405	8.165	7.892	7.784	7.574	7.374	7.143
Piez. reading at check sta.							

Concentration and Velocity Profile Data

Sampler sta (y/D)	0.06	0.16	0.26	0.36	0.46	0.56	0.66	0.76	0.86	0.96
Avg. Conc. (C %)										
Velocity (u fps)	7.41	9.68	10.10	10.84	11.00	10.80	10.45	9.85	9.05	7.71

Boundary Type: Smooth Run No. 43 S Q = 7.58 cfs V = 9.66 fps
Profile Traverse: Vertical C_t = 1.93 percent T = 28.2 °C

Average Piezometer Reading

Piez. No.	4	5	6	7	8	9	10
Piez. reading	8.754	8.566	8.353	8.261	8.094	7.935	7.753
Piez. reading for C_t data	8.750	8.570	8.355	8.261	8.095	7.933	7.742
Piez. reading at check sta.							

Concentration and Velocity Profile Data

Sampler sta (y/D)	0.06	0.16	0.26	0.36	0.46	0.56	0.66	0.76	0.86	0.96
Avg. Conc. (C %)	19.00	5.75	2.75	1.54	0.965	0.610	0.405	0.285	0.200	0.129
Velocity (u fps)	7.04	9.08	10.20	11.00	11.50	11.50	11.00	10.20	9.55	8.15

Boundary Type: Smooth Run No. 44 S δ Q = 6.65 cfs V = 8.46 fps
Profile Traverse: Vertical C_t = 2.08 percent T = 23.7 °C

Average Piezometer Reading

Piez. No.	4	5	6	7	8	9	10
Piez. reading	8.632	8.472	8.294	8.209	8.062	7.921	7.760
Piez. reading for C_t data	8.611	8.455	8.273	8.194	8.044	7.901	7.742
Piez. reading at check sta.							

Concentration and Velocity Profile Data

Sampler sta (y/D)	0.06	0.16	0.26	0.36	0.46	0.56	0.66	0.76	0.86	0.96
Avg. Conc. (C %)	21.70	8.890	3.15	1.67	1.00	0.610	0.435	0.300	0.224	0.144
Velocity (u fps)	5.55	7.95	9.30	10.20	10.60	10.60	10.20	9.56	8.71	7.70

Boundary Type: Smooth Run No. 45 S δ Q = 5.85 cfs V = 7.45 fps
Profile Traverse: Vertical C_t = 2.35 percent T = 22.0 °C

Average Piezometer Reading

Piez. No.	4	5	6	7	8	9	10
Piez. reading	8.502	8.352	8.187	8.098	7.954	7.827	7.687
Piez. reading for C_t data	8.505	8.355	8.186	8.097	7.956	7.827	7.686
Piez. reading at check sta.							

Concentration and Velocity Profile Data

Sampler sta (y/D)	0.06	0.16	0.26	0.36	0.46	0.56	0.66	0.76	0.86	0.96
Avg. Conc. (C %)	21.00	13.00	4.19	1.60	0.844	0.500	0.300	0.214	0.148	0.110
Velocity (u fps)	4.74	6.57	7.85	8.88	9.50	9.56	9.15	8.53	8.04	7.04

Boundary Type: Smooth Run No. 46 S δ Q = 6.70 cfs V = 8.53 fps
Profile Traverse: Vertical C_t = 3.00 percent T = 24.2 °C

Average Piezometer Reading

Piez. No.	4	5	6	7	8	9	10
Piez. reading	8.667	8.500	8.307	8.216	8.054	7.902	7.733
Piez. reading for C_t data	8.667	8.499	8.305	8.213	8.049	7.896	7.724
Piez. reading at check sta.							

Concentration and Velocity Profile Data

Sampler sta (y/D)	0.06	0.16	0.26	0.36	0.46	0.56	0.66	0.76	0.86	0.96
Avg. Conc. (C %)	24.60	13.70	5.56	2.53	1.52	0.955	0.644	0.46	0.330	0.214
Velocity (u fps)	---	2.27	2.66	2.90	3.11	3.22	3.11	3.01	2.54	2.41

Boundary Type: Smooth Run No. 47 S Q = 7.60 cfs V = 9.67 fps
Profile Traverse: Vertical C_t = 3.01 percent T = 22.2 °C

Average Piezometer Reading

Piez. No.	4	5	6	7	8	9	10
Piez. reading	7.909	7.719	7.500	7.408	7.231	7.061	7.876
Piez. reading for C_t data	7.909	7.726	7.502	7.406	7.230	7.066	7.879
Piez. reading at check sta.							

Concentration and Velocity Profile Data

Sampler sta (y/D)	0.06	0.16	0.26	0.36	0.46	0.56	0.66	0.76	0.86	0.96
Avg. Conc. (C %)	22.80	11.80	5.20	2.70	1.65	1.090	0.770	0.555	0.410	0.280
Velocity (u fps)	6.05	9.08	10.40	11.20	11.73	11.70	11.30	10.50	9.72	8.52

Boundary Type: Smooth Run No. 48 S δ Q = 6.65 cfs V = 8.46 fps
Profile Traverse: Horizontal C_t = 3.19 percent T = 21.0 °C

Average Piezometer Reading

Piez. No.	4	5	6	7	8	9	10
Piez. reading	7.764	7.600	7.411	7.316	7.156	7.000	6.830
Piez. reading for C_t data	7.759	7.595	7.406	7.311	7.149	6.997	6.827
Piez. reading at check sta.							

Concentration and Velocity Profile Data

Sampler sta (y/D)	0.06	0.16	0.26	0.36	0.46	0.56	0.66	0.76	0.86	0.96
Avg. Conc. (C %)	1.340	1.270	--	1.360	--	1.380	1.350	1.365	1.340	1.360
Velocity (u fps)	8.30	9.20	10.10	10.56	11.00	11.00	10.50	10.08	9.20	8.07

Boundary Type: Smooth Run No. 49 S δ Q = 5.80 cfs V = 7.38 fps
Profile Traverse: Horizontal C_t = 2.65 percent T = 20.7 °C

Average Piezometer Reading

Piez. No.	4	5	6	7	8	9	10
Piez. reading	7.691	7.526	7.344	7.241	7.087	6.941	6.786
Piez. reading for C_t data	7.671	7.502	7.317	7.219	7.062	6.920	6.766
Piez. reading at check sta.							

Concentration and Velocity Profile Data

Sampler sta (y/D)	0.06	0.16	0.26	0.36	0.46	0.56	0.66	0.76	0.86	0.96
Avg. Conc. (C %)	1.150	--	1.060	--	1.130	1.120	1.120	1.090	1.170	1.100
Velocity (u fps)	5.90	6.90	8.30	7.95	8.15	8.19	7.95	7.47	6.90	5.90

Boundary Type: Smooth Run No. 50 S Q = 7.70 cfs V = 9.80 fps
Profile Traverse: Horizontal C_t = 3.04 percent T = 25.0 °C

Average Piezometer Reading

Piez. No.	4	5	6	7	8	9	10
Piez. reading	7.978	7.786	7.561	7.462	7.286	7.115	6.927
Piez. reading for C_t data	7.990	7.799	7.570	7.474	7.299	7.130	6.936
Piez. reading at check sta.							

Concentration and Velocity Profile Data

Sampler sta (y/D)	0.06	0.16	0.26	0.36	0.46	0.56	0.66	0.76	0.86	0.96
Avg. Conc. (C %)	1.380	--	1.380	--	1.420	1.440	1.460	1.440	1.430	1.410
Velocity (u fps)	9.08	10.20	11.10	11.60	11.90	11.90	11.60	11.10	10.20	9.13

Boundary Type: Corrugated Run No. 2 C Q = 3.54 cfs V = 4.45 fps
Profile Traverse: Vertical C_t = 0.0 percent T = 22.1 °C

Average Piezometer Reading

Piez. No.	4	5	6	7	8	9	10
Piez. reading	9.017	8.581	8.142	7.815	7.447	7.058	6.670
Piez. reading for C_t data							
Piez. reading at check sta.	9.224	8.845	8.434	--	--	7.280	6.893

Concentration and Velocity Profile Data

Sampler sta (y/D)	0.06	0.16	0.26	0.36	0.46	0.56	0.66	0.76	0.86	0.96
Avg. Conc. (C %)										
Velocity (u fps)	4.16	4.73	5.06	5.42	5.97	5.97	5.77	5.18	4.13	3.48

Boundary Type: Corrugated Run No. 3 C Q = 4.78 cfs V = 5.98 fps
Profile Traverse: Vertical C_t = 0.0 percent T = 23.3 °C

Average Piezometer Reading

Piez. No.	4	5	6	7	8	9	10
Piez. reading	--	9.101	8.395	7.840	7.249	6.569	5.935
Piez. reading for C_t data							
Piez. reading at check sta.	--	9.640	8.944	--	--	6.988	6.341

Concentration and Velocity Profile Data

Sampler sta (y/D)	0.06	0.16	0.26	0.36	0.46	0.56	0.66	0.76	0.86	0.96
Avg. Conc. (C %)										
Velocity (u fps)	5.14	5.78	6.86	7.18	7.70	7.60	7.34	6.53	5.78	5.26

Boundary Type: Corrugated Run No. 4 C Q = 5.82 cfs V = 7.23 fps
Profile Traverse: Vertical C_t = 0.0 percent T = 25.3 °C

Average Piezometer Reading

Piez. No.	4	5	6	7	8	9	10
Piez. reading	--	9.800	8.845	8.079	7.249	6.295	5.380
Piez. reading for C_t data							
Piez. reading at check sta.	--	--	9.601	--	--	6.914	6.025

Concentration and Velocity Profile Data

Sampler sta (y/D)	0.06	0.16	0.26	0.36	0.46	0.56	0.66	0.76	0.86	0.96
Avg. Conc. (C %)										
Velocity (u fps)	6.42	7.10	7.78	8.37	8.97	8.97	8.46	8.27	7.04	6.33

Boundary Type: Corrugated Run No. 5 C Q = 1.84 cfs V = 2.38 fps
Profile Traverse: Vertical C_t = 0.0 percent T = 27.1 °C

Average Piezometer Reading

Piez. No.	4	5	6	7	8	9	10
Piez. reading	8.094	7.985	7.873	7.785	7.686	7.581	7.483
Piez. reading for C_t data							
Piez. reading at check sta.	8.126	8.030	7.924	--	--	7.622	7.524

Concentration and Velocity Profile Data

Sampler sta (y/D)	0.06	0.16	0.26	0.36	0.46	0.56	0.66	0.76	0.86	0.96
Avg. Conc. (C %)										
Velocity (u fps)	1.80	2.25	2.60	2.74	2.74	2.75	2.71	2.66	2.41	--

Boundary Type: Corrugated Run No. 6 C Q = 3.50 cfs V = 4.52 fps
Profile Traverse: Vertical C_t = 0.183 percent T = 31.9 °C

Average Piezometer Reading

Piez. No.	4	5	6	7	8	9	10
Piez. reading	8.991	8.501	8.060	7.736	7.376	7.011	6.594
Piez. reading for C_t data							
Piez. reading at check sta.	9.206	8.820	8.412	--	--	7.241	6.857

Concentration and Velocity Profile Data

Sampler sta (y/D)	0.06	0.16	0.26	0.36	0.46	0.56	0.66	0.76	0.86	0.96
Avg. Conc. (C %)	0.520	0.370	0.305	0.225	0.176	0.150	0.110	0.100	0.072	0.068
Velocity (u fps)	3.50	4.10	4.48	5.39	5.91	5.96	5.80	5.08	4.25	3.11

Boundary Type: Corrugated Run No. 7 C c Q = 4.80 cfs V = 6.12 fps
Profile Traverse: Vertical C_t = 0.334 percent T = 30.7 °C

Average Piezometer Reading

Piez. No.	4	5	6	7	8	9	10
Piez. reading	--	9.064	8.354	7.796	7.214	6.626	5.950
Piez. reading for C_t data							
Piez. reading at check sta.	--	9.640	8.962	--	--	7.021	6.376

Concentration and Velocity Profile Data

Sampler sta (y/D)	0.06	0.16	0.26	0.36	0.46	0.56	0.66	0.76	0.86	0.96
Avg. Conc. (C %)	0.680	0.605	0.473	0.420	0.364	0.300	0.234	0.195	0.181	0.158
Velocity (u fps)	5.09	5.56	6.37	7.10	7.78	7.86	7.45	6.62	5.51	4.68

Boundary Type: Corrugated Run No. 8 C Q = 5.80 cfs V = 7.20 fps
Profile Traverse: Vertical C_t = 0.448 percent T = 25.7 °C

Average Piezometer Reading

Piez. No.	4	5	6	7	8	9	10
Piez. reading	--	9.950	8.960	8.179	7.317	6.442	5.450
Piez. reading for C_t data							
Piez. reading at check sta.	--	--	9.83	--	--	7.030	6.112

Concentration and Velocity Profile Data

Sampler sta (y/D)	0.06	0.16	0.26	0.36	0.46	0.56	0.66	0.76	0.86	0.96
Avg. Conc. (C %)	0.735	0.670	0.565	0.535	0.460	0.420	0.315	0.290	0.276	0.248
Velocity (u fps)	6.06	7.05	8.20	8.94	9.15	9.11	8.94	8.20	7.12	6.22

Boundary Type: Corrugated Run No. 9C $\frac{F}{O}$ Q = 1.63 cfs V = 2.08 fps
Profile Traverse: Vertical C_t = 0.046 percent T = 26.9 °C

Average Piezometer Reading

Piez. No.	4	5	6	7	8	9	10
Piez. reading	8.031	7.940	7.848	7.754	7.687	7.606	7.521
Piez. reading for C_t data							
Piez. reading at check sta.	8.101	7.996	7.885	--	--	7.639	7.556

Concentration and Velocity Profile Data

Sampler sta (y/D)	0.06	0.16	0.26	0.36	0.46	0.56	0.66	0.76	0.86	0.96
Avg. Conc. (C %)	0.300	0.144	0.093	--	--	--	--	--	--	--
Velocity (u fps)	1.80	2.12	2.27	2.66	2.84	2.84	2.66	2.27	2.12	--

Boundary Type: Corrugated Run No. 10 C Q = 3.55 cfs V = 4.52 fps
Profile Traverse: Horizontal C_t = 0.250 percent T = 24.7 °C

Average Piezometer Reading

Piez. No.	4	5	6	7	8	9	10
Piez. reading	9.078	8.608	8.169	7.843	7.459	7.101	6.683
Piez. reading for C_t data							
Piez. reading at check sta.	9.270	8.887	8.481	--	--	7.310	6.930

Concentration and Velocity Profile Data

Sampler sta (y/D)	0.06	0.16	0.26	0.36	0.46	0.56	0.66	0.76	0.86	0.96
Avg. Conc. (C %)	0.220	0.220	0.229	0.234	0.234	0.234	0.267	0.248	0.267	0.265
Velocity (u fps)	4.48	4.68	5.33	5.80	5.91	5.91	5.73	5.02	4.75	4.02

Boundary Type: Corrugated Run No. 11 C Q = 4.70 cfs V = 5.98 fps
Profile Traverse: Horizontal C_t = 0.320 percent T = 26.1 °C

Average Piezometer Reading

Piez. No.	4	5	6	7	8	9	10
Piez. reading	--	9.114	8.367	7.851	7.275	6.704	6.010
Piez. reading for C_t data							
Piez. reading at check sta.	--	9.650	8.976	--	--	7.065	6.438

Concentration and Velocity Profile Data

Sampler sta (y/D)	0.06	0.16	0.26	0.36	0.46	0.56	0.66	0.76	0.86	0.96
Avg. Conc. (C %)	0.281	0.290	0.295	0.295	0.315	0.305	0.335	0.330	0.340	0.330
Velocity (u fps)	5.45	6.22	6.67	7.22	7.49	7.49	6.95	6.42	5.85	5.09

Boundary Type: Corrugated Run No. 12 C Q = 5.80cfs V = 7.38 fps
Profile Traverse: Horizontal C_t = 0.340percent T = 28.5 °C

Average Piezometer Reading

Piez. No.	4	5	6	7	8	9	10
Piez. reading	--	9.730	8.769	8.017	7.211	6.396	5.420
Piez. reading for C_t data							
Piez. reading at check sta.	--	--	9.556	--	--	6.915	6.041

Concentration and Velocity Profile Data

Sampler sta (y/D)	0.06	0.16	0.26	0.36	0.46	0.56	0.66	0.76	0.86	0.96
Avg. Conc. (C %)	0.315	0.310	0.315	0.310	0.330	0.330	0.345	0.359	0.350	0.369
Velocity (u fps)	6.43	7.73	8.27	8.98	8.98	9.04	8.50	7.62	7.10	6.17

Boundary Type: Corrugated Run No. 13 C Q = 3.58 cfs V = 4.56 fps
Profile Traverse: Horizontal C_t = 0.385percent T = 31.5 °C

Average Piezometer Reading

Piez. No.	4	5	6	7	8	9	10
Piez. reading	8.936	8.458	8.019	7.669	7.292	6.931	6.509
Piez. reading for C_t data							
Piez. reading at check sta.	9.169	8.767	8.364	--	--	--	--

Concentration and Velocity Profile Data

Sampler sta (y/D)	0.06	0.16	0.26	0.36	0.46	0.56	0.66	0.76	0.86	0.96
Avg. Conc. (C %)	0.315	0.305	0.340	0.320	0.369	0.345	0.365	0.330	0.335	0.335
Velocity (u fps)	4.25	4.54	5.33	5.68	6.07	6.12	5.80	5.08	4.61	4.02

Boundary Type: Corrugated Run No. 14 C Q = 4.80 cfs V = 6.11 fps
Profile Traverse: Horizontal C_t = 0.720percent T = 30.4 °C

Average Piezometer Reading

Piez. No.	4	5	6	7	8	9	10
Piez. reading	--	9.007	8.284	7.729	7.114	6.558	5.920
Piez. reading for C_t data							
Piez. reading at check sta.	--	9.556	8.892	--	--	6.926	6.313

Concentration and Velocity Profile Data

Sampler sta (y/D)	0.06	0.16	0.26	0.36	0.46	0.56	0.66	0.76	0.86	0.96
Avg. Conc. (C %)	0.590	0.590	0.590	0.625	0.650	0.649	0.640	0.650	0.625	0.630
Velocity (u fps)	5.73	6.37	7.36	7.62	7.82	7.82	7.58	7.10	6.22	5.33

Boundary Type: Corrugated Run No. 15 C Q = 5.78 cfs V = 7.37 fps
Profile Traverse: Horizontal C_t = 1.06 percent T = 29.2 °C

Average Piezometer Reading

Piez. No.	4	5	6	7	8	9	10
Piez. reading	--	9.800	8.761	8.000	7.132	6.249	5.380
Piez. reading for C_t data							
Piez. reading at check sta.	--	--	9.621	--	--	6.865	5.999

Concentration and Velocity Profile Data

Sampler sta (y/D)	0.06	0.16	0.26	0.36	0.46	0.56	0.66	0.76	0.86	0.96
Avg. Conc. (C %)	0.859	0.865	0.860	0.885	0.935	0.970	0.995	0.989	1.000	0.980
Velocity (u fps)	6.16	7.45	8.15	8.75	8.98	8.98	8.45	7.75	6.81	6.16

Boundary Type: Corrugated Run No. 16 C Q = 3.58 cfs V = 4.56 fps
Profile Traverse: Vertical C_t = 0.455percent T = 29.6 °C

Average Piezometer Reading

Piez. No.	4	5	6	7	8	9	10
Piez. reading	8.974	8.471	8.043	7.594	7.312	6.959	6.538
Piez. reading for C_t data							
Piez. reading at check sta.	9.187	8.782	8.331	--	--	7.185	6.790

Concentration and Velocity Profile Data

Sampler sta (y/D)	0.06	0.16	0.26	0.36	0.46	0.56	0.66	0.76	0.86	0.96
Avg. Conc. (C %)	1.050	0.899	0.720	0.570	0.425	0.340	0.248	0.190	0.144	0.120
Velocity (u fps)	3.84	4.17	4.88	5.62	6.21	6.32	5.62	4.88	4.56	4.17

Boundary Type: Corrugated Run No. 17 C Q = 4.80 cfs V = 6.11 fps
Profile Traverse: Vertical C_t = 0.688percent T = 30.6 °C

Average Piezometer Reading

Piez. No.	4	5	6	7	8	9	10
Piez. reading	--	9.011	8.249	7.714	7.101	6.536	5.870
Piez. reading for C_t data							
Piez. reading at check sta.	--	9.575	8.904	--	--	6.936	6.301

Concentration and Velocity Profile Data

Sampler sta (y/D)	0.06	0.16	0.26	0.36	0.46	0.56	0.66	0.76	0.86	0.96
Avg. Conc. (C %)										
Velocity (u fps)	5.00	5.38	6.41	7.05	7.76	7.82	7.36	6.72	5.84	5.13

Boundary Type: Corrugated Run No. 18 C Q = 5.80 cfs V = 7.25 fps
Profile Traverse: Vertical C_t = 0.881percent T = 32.3 °C

Average Piezometer Reading

Piez. No.	4	5	6	7	8	9	10
Piez. reading	--	--	8.672	7.902	7.018	6.263	--
Piez. reading for C_t data							
Piez. reading at check sta.	--	--	9.592	--	--	6.818	5.950

Concentration and Velocity Profile Data

Sampler sta (y/D)	0.06	0.16	0.26	0.36	0.46	0.56	0.66	0.76	0.86	0.96
Avg. Conc. (C %)	1.700	1.370	1.199	1.070	0.900	0.800	0.660	0.590	0.520	0.475
Velocity (u fps)	6.06	6.71	7.61	8.42	8.95	9.32	9.00	8.02	7.95	6.74

Boundary Type: Corrugated Run No. 19 C Q = 6.30 cfs V = 8.02 fps
Profile Traverse: Vertical C_t = 0.868percent T = 28.3 °C

Average Piezometer Reading

Piez. No.	4	5	6	7	8	9	10
Piez. reading	--	--	8.906	7.940	6.809	5.812	4.550
Piez. reading for C_t data							
Piez. reading at check sta.	--	--	--	--	--	6.468	5.350

Concentration and Velocity Profile Data

Sampler sta (y/D)	0.06	0.16	0.26	0.36	0.46	0.56	0.66	0.76	0.86	0.96
Avg. Conc. (C %)	1.200	1.090	1.050	0.945	0.870	0.765	0.685	0.645	0.585	0.570
Velocity (u fps)	7.12	8.22	8.83	9.80	10.40	10.40	10.20	9.42	8.63	7.70

Boundary Type: Corrugated Run No. 20 C Q = 6.30 cfs V = 8.02 fps
Profile Traverse: Vertical C_t = 1.20 percent T = 32.7 °C

Average Piezometer Reading

Piez. No.	4	5	6	7	8	9	10
Piez. reading	--	--	8.965	7.968	6.859	4.750	4.550
Piez. reading for C_t data							
Piez. reading at check sta.	--	--	--	--	--	6.586	5.400

Concentration and Velocity Profile Data

Sampler sta (y/D)	0.06	0.16	0.26	0.36	0.46	0.56	0.66	0.76	0.86	0.96
Avg. Conc. (C %)	1.740	1.590	1.440	1.340	1.190	1.040	0.920	0.845	0.765	0.719
Velocity (u fps)	7.12	7.71	8.50	9.35	10.30	10.40	10.20	9.42	8.56	7.71

Boundary Type: Corrugated Run No. 21 C Q = 4.78 cfs V = 6.09 fps
Profile Traverse: Vertical C_t = 1.09 percent T = 28.6 °C

Average Piezometer Reading

Piez. No.	4	5	6	7	8	9	10
Piez. reading	--	9.162	8.441	7.898	7.271	6.667	6.002
Piez. reading for C_t data							
Piez. reading at check sta.	--	9.658	9.032	--	--	7.089	6.445

Concentration and Velocity Profile Data

Sampler sta (y/D)	0.06	0.16	0.26	0.36	0.46	0.56	0.66	0.76	0.86	0.96
Avg. Conc. (C %)	2.260	1.900	1.660	1.360	1.170	0.950	0.770	0.685	0.595	0.550
Velocity (u fps)	4.47	5.26	6.16	7.09	7.65	7.78	7.35	6.72	6.00	5.07

Boundary Type: Corrugated Run No. 22 C Q = 5.78 cfs V = 7.37 fps
Profile Traverse: Vertical C_t = 1.32 percent T = 30.2 °C

Average Piezometer Reading

Piez. No.	4	5	6	7	8	9	10
Piez. reading	--	--	8.968	8.168	7.241	6.391	--
Piez. reading for C_t data							
Piez. reading at check sta.	--	--	9.839	--	--	7.004	6.147

Concentration and Velocity Profile Data

Sampler sta (y/D)	0.06	0.16	0.26	0.36	0.46	0.56	0.66	0.76	0.86	0.96
Avg. Conc. (C %)	2.410	2.200	1.790	1.620	1.320	1.140	0.995	0.889	0.800	0.765
Velocity (u fps)	5.32	6.46	7.44	8.57	9.25	9.55	8.97	8.51	7.65	6.21

Boundary Type: Corrugated Run No. 23 C Q = 3.55 cfs V = 4.43 fps
Profile Traverse: Vertical C_t = 0.845 percent T = 27.0 °C

Average Piezometer Reading

Piez. No.	4	5	6	7	8	9	10
Piez. reading	9.056	8.584	8.148	7.832	7.436	7.091	6.596
Piez. reading for C_t data							
Piez. reading at check sta.	9.258	8.871	8.469	---	---	7.315	6.932

Concentration and Velocity Profile Data

Sampler sta (y/D)	0.06	0.16	0.26	0.36	0.46	0.56	0.66	0.76	0.86	0.96
Avg. Conc. (C %)	2.000	1.720	1.360	1.080	0.840	0.670	0.530	0.415	0.320	0.258
Velocity (u fps)	3.32	4.01	4.33	5.39	6.11	6.17	5.68	6.01	4.54	3.68

Boundary Type: Corrugated Run No. 24 C Q = 5.80 cfs V = 7.38 fps
Profile Traverse: Horizontal C_t = 0.46 percent T = 27.8 °C

Average Piezometer Reading

Piez. No.	4	5	6	7	8	9	10
Piez. reading	---	---	8.985	8.189	7.245	6.350	5.492
Piez. reading for C_t data							
Piez. reading at check sta.	---	---	9.882	---	---	7.002	6.048

Concentration and Velocity Profile Data

Sampler sta (y/D)	0.06	0.16	0.26	0.36	0.46	0.56	0.66	0.76	0.86	0.96
Avg. Conc. (C %)	1.240	1.200	1.230	1.240	1.280	1.340	1.400	1.340	1.360	1.360
Velocity (u fps)	6.62	7.80	8.17	9.08	9.52	9.40	8.80	8.26	7.18	6.52

Boundary Type: Corrugated Run No. 25 C Q = 4.78 cfs V = 6.09 fps
Profile Traverse: Horizontal C_t = 1.16 percent T = 28.9 °C

Average Piezometer Reading

Piez. No.	4	5	6	7	8	9	10
Piez. reading	----	9.078	8.363	7.835	7.189	6.596	5.940
Piez. reading for C_t data							
Piez. reading at check sta.	---	9.640	8.960	--	--	7.014	6.365

Concentration and Velocity Profile Data

Sampler sta (y/D)	0.06	0.16	0.26	0.36	0.46	0.56	0.66	0.76	0.86	0.96
Avg. Conc. (C %)	0.930	0.920	0.960	0.945	1.040	1.040	1.060	1.030	0.990	0.990
Velocity (u fps)	5.38	6.36	6.95	7.57	7.61	7.61	7.40	6.71	5.78	5.21

Boundary Type: Corrugated Run No. 26 C Q = 3.50 cfs V = 4.45 fps
Profile Traverse: Horizontal C_t = 0.610 percent T = 31.0 °C

Average Piezometer Reading

Piez. No.	4	5	6	7	8	9	10
Piez. reading	8.886	8.429	8.002	7.704	7.319	6.980	6.620
Piez. reading for C_t data							
Piez. reading at check sta.	9.122	8.719	8.341	--	--	7.227	6.856

Concentration and Velocity Profile Data

Sampler sta (y/D)	0.06	0.16	0.26	0.36	0.46	0.56	0.66	0.76	0.86	0.96
Avg. Conc. (C %)	0.475	0.450	0.530	0.540	0.535	0.580	0.570	0.570	0.485	0.550
Velocity (u fps)	4.21	4.94	5.56	5.84	5.96	5.96	5.44	5.26	4.66	3.71

Boundary Type: Corrugated Run No. 27 C δ Q = 3.43 cfs V = 4.36 fps
Profile Traverse: Horizontal C_t = 1.00 percent T = 29.1 °C

Average Piezometer Reading

Piez. No.	4	5	6	7	8	9	10
Piez. reading	8.949	8.501	8.090	7.760	7.389	7.060	6.685
Piez. reading for C_t data							
Piez. reading at check sta.	9.148	8.775	8.390	--	--	7.280	6.921

Concentration and Velocity Profile Data

Sampler sta (y/D)	0.06	0.16	0.26	0.36	0.46	0.56	0.66	0.76	0.86	0.96
Avg. Conc. (C %)	0.850	0.915	0.850	0.920	0.920	0.910	0.925	0.924	0.895	0.910
Velocity (u fps)	4.17	4.81	5.50	5.90	6.11	6.11	5.73	5.20	4.46	3.93

Boundary Type: Corrugated Run No. 28 C Q = 4.76 cfs V = 6.06 fps
Profile Traverse: Horizontal C_t = 1.82 percent T = 29.8 °C

Average Piezometer Reading

Piez. No.	4	5	6	7	8	9	10
Piez. reading	--	9.096	8.390	7.855	7.226	6.641	5.951
Piez. reading for C_t data							
Piez. reading at check sta.	--	9.612	8.959	--	--	7.056	6.424

Concentration and Velocity Profile Data

Sampler sta (y/D)	0.06	0.16	0.26	0.36	0.46	0.56	0.66	0.76	0.86	0.96
Avg. Conc. (C %)	1.560	1.590	1.570	1.560	1.630	1.660	1.660	1.560	1.580	1.530
Velocity (u fps)	5.62	6.37	7.05	7.70	7.98	7.98	7.61	6.80	6.06	5.00

Boundary Type: Corrugated Run No. 29 C Q = 5.78 cfs V = 7.37 fps
Profile Traverse: Horizontal C_t = 2.47 percent T = 31.3 °C

Average Piezometer Reading

Piez. No.	4	5	6	7	8	9	10
Piez. reading	--	--	8.904	8.119	7.194	6.344	--
Piez. reading for C_t data							
Piez. reading at check sta.	--	--	9.732	--	6.932	6.012	--

Concentration and Velocity Profile Data

Sampler sta (y/D)	0.06	0.16	0.26	0.36	0.46	0.56	0.66	0.76	0.86	0.96
Avg. Conc. (C %)	1.990	2.100	2.100	2.120	2.210	2.290	2.250	2.260	2.200	2.230
Velocity (u fps)	7.44	8.15	8.90	9.35	9.70	9.59	8.96	8.41	7.35	6.37

Boundary Type: Corrugated Run No. 30 C δ Q = 3.53 cfs V = 4.50 fps
Profile Traverse: Vertical C_t = 0.972 percent T = 30.5 °C

Average Piezometer Reading

Piez. No.	4	5	6	7	8	9	10
Piez. reading	8.939	8.480	8.058	7.737	7.339	6.999	6.607
Piez. reading for C_t data							
Piez. reading at check sta.	9.158	8.769	8.382	--	--	7.238	6.854

Concentration and Velocity Profile Data

Sampler sta (y/D)	0.06	0.16	0.26	0.36	0.46	0.56	0.66	0.76	0.86	0.96
Avg. Conc. (C %)	2.600	2.160	1.750	1.350	0.963	0.742	0.520	0.420	0.350	0.300
Velocity (u fps)	3.11	3.59	4.60	5.25	6.10	6.10	5.62	5.13	4.17	3.32

Boundary Type: Corrugated Run No. 31 C Q = 4.80 cfs V = 6.05 fps
Profile Traverse: Vertical C_t = 1.56 percent T = 31.6 °C

Average Piezometer Reading

Piez. No.	4	5	6	7	8	9	10
Piez. reading	--	9.117	8.395	7.873	7.220	6.638	5.991
Piez. reading for C_t data							
Piez. reading at check sta.	--	9.648	8.988	--	--	7.053	6.414

Concentration and Velocity Profile Data

Sampler sta (y/D)	0.06	0.16	0.26	0.36	0.46	0.56	0.66	0.76	0.86	0.96
Avg. Conc. (C %)	3.550	2.860	2.500	2.000	1.650	1.340	1.090	0.905	0.820	0.735
Velocity (u fps)	4.47	5.08	6.21	7.09	7.90	8.19	7.39	6.86	5.83	5.08

Boundary Type: Corrugated Run No. 32 C Q = 5.70 cfs V = 7.25 fps
Profile Traverse: Vertical C_t = 2.17 percent T = 32.2 °C

Average Piezometer Reading

Piez. No.	4	5	6	7	8	9	10
Piez. reading	--	9.852	8.836	8.072	7.161	6.325	5.422
Piez. reading for C_t data							
Piez. reading at check sta.	--	--	9.647	--	--	6.929	6.016

Concentration and Velocity Profile Data

Sampler sta (y/D)	0.06	0.16	0.26	0.36	0.46	0.56	0.66	0.76	0.86	0.96
Avg. Conc. (C %)	3.740	3.430	2.890	2.470	2.200	1.850	1.570	1.340	1.180	1.130
Velocity (u fps)	6.06	6.85	7.70	8.55	9.55	9.66	9.25	8.39	7.52	6.55

Boundary Type: Corrugated Run No. 33 C Q = 6.28 cfs V = 7.85 fps
Profile Traverse: Vertical C_t = 2.47 percent T = 28.4 °C

Average Piezometer Reading

Piez. No.	4	5	6	7	8	9	10
Piez. reading	--	--	9.058	8.060	6.936	5.802	4.598
Piez. reading for C_t data							
Piez. reading at check sta.	--	--	--	--	--	6.554	5.395

Concentration and Velocity Profile Data

Sampler sta (y/D)	0.06	0.16	0.26	0.36	0.46	0.56	0.66	0.76	0.86	0.96
Avg. Conc. (C %)	3.460	3.290	3.010	2.770	2.480	2.200	1.950	1.700	1.610	1.460
Velocity (u fps)	6.71	7.40	8.51	9.56	10.40	10.60	10.20	9.40	8.42	7.48

Boundary Type: Corrugated Run No. 34 C Q = 6.32 cfs V = 8.04 fps
Profile Traverse: Vertical C_t = 3.86 percent T = 31.6 °C

Average Piezometer Reading

Piez. No.	4	5	6	7	8	9	10
Piez. reading	--	--	8.989	8.000	6.830	5.690	4.360
Piez. reading for C_t data							
Piez. reading at check sta.	--	--	--	--	--	6.400	5.305

Concentration and Velocity Profile Data

Sampler sta (y/D)	0.06	0.16	0.26	0.36	0.46	0.56	0.66	0.76	0.86	0.96
Avg. Conc. (C %)	5.50	5.10	4.75	4.30	3.80	3.25	2.80	2.40	2.27	2.17
Velocity (u fps)	6.02	6.45	7.50	8.90	10.10	10.50	10.40	9.80	8.70	7.48

Boundary Type: Corrugated Run No. 35 C δ^E Q = 3.58 cfs V = 4.56 fps
Profile Traverse: Vertical C_t = 2.09 percent T = 29.7 °C

Average Piezometer Reading

Piez. No.	4	5	6	7	8	9	10
Piez. reading	9.089	8.638	8.206	7.895	7.501	7.154	6.748
Piez. reading for C_t data							
Piez. reading at check sta.	9.300	8.920	8.535	--	--	7.404	7.028

Concentration and Velocity Profile Data

Sampler sta (y/D)	0.06	0.16	0.26	0.36	0.46	0.56	0.66	0.76	0.86	0.96
Avg. Conc. (C %)	7.550	4.900	3.340	2.460	1.880	1.358	0.990	0.785	0.645	0.545
Velocity (u fps)	3.11	4.24	5.07	5.90	6.37	6.56	6.10	5.20	4.39	3.67

Boundary Type: Corrugated Run No. 36 C Q = 4.75 cfs V = 6.03 fps
Profile Traverse: Vertical C_t = 2.97 percent T = 30.6 °C

Average Piezometer Reading

Piez. No.	4	5	6	7	8	9	10
Piez. reading	--	9.164	8.626	7.971	7.361	6.790	6.115
Piez. reading for C_t data							
Piez. reading at check sta.	--	9.632	8.990	--	--	7.164	6.554

Concentration and Velocity Profile Data

Sampler sta (y/D)	0.06	0.16	0.26	0.36	0.46	0.56	0.66	0.76	0.86	0.96
Avg. Conc. (C %)	6.750	5.800	4.700	3.810	3.000	2.360	1.880	1.600	1.480	1.280
Velocity (u fps)	4.10	5.08	6.06	7.26	7.85	8.02	7.52	6.86	5.79	5.28

Boundary Type: Corrugated Run No. 37 C Q = 5.80 cfs V = 7.27 fps
Profile Traverse: Vertical C_t = 3.69 percent T = 30.8 °C

Average Piezometer Reading

Piez. No.	4	5	6	7	8	9	10
Piez. reading	--	--	9.305	8.460	7.491	6.514	5.451
Piez. reading for C_t data							
Piez. reading at check sta.	--	--	--	--	--	4.128	6.132

Concentration and Velocity Profile Data

Sampler sta (y/D)	0.06	0.16	0.26	0.36	0.46	0.56	0.66	0.76	0.86	0.96
Avg. Conc. (C %)	6.001	5.590	4.830	4.060	3.600	3.080	2.490	2.380	2.190	2.050
Velocity (u fps)	5.55	6.31	7.65	8.85	9.80	10.00	9.61	8.82	7.77	6.70

Boundary Type: Corrugated Run No. 38 C δ^E Q = 3.54 cfs V = 4.51 fps
Profile Traverse: Horizontal C_t = 2.30 percent T = 28.3 °C

Average Piezometer Reading

Piez. No.	4	5	6	7	8	9	10
Piez. reading	8.990	8.557	8.147	7.836	7.452	7.111	6.711
Piez. reading for C_t data							
Piez. reading at check sta.	9.195	8.835	8.454	--	--	7.356	6.982

Concentration and Velocity Profile Data

Sampler sta (y/D)	0.06	0.16	0.26	0.36	0.46	0.56	0.66	0.76	0.86	0.96
Avg. Conc. (C %)	1.570	1.660	1.740	1.750	1.740	1.760	1.650	1.600	1.504	1.501
Velocity (u fps)	4.83	5.51	6.03	6.73	7.11	7.11	7.00	6.40	5.51	4.70

Boundary Type: Corrugated Run No. 39 C Q = 4.70 cfs V = 6.08 fps
Profile Traverse: Horizontal C_t = 3.10 percent T = 29.4 °C

Average Piezometer Reading

Piez. No.	4	5	6	7	8	9	10
Piez. reading	--	9.097	8.418	7.882	7.266	6.664	6.002
Piez. reading for C_t data							
Piez. reading at check sta.	--	9.562	8.910	--	---	7.058	6.429

Concentration and Velocity Profile Data

Sampler sta (y/D)	0.06	0.16	0.26	0.36	0.46	0.56	0.66	0.76	0.86	0.96
Avg. Conc. (C %)	2.710	2.680	2.740	2.760	2.860	2.80	2.840	2.640	2.600	2.500
Velocity (u fps)	5.52	6.33	7.33	7.85	8.21	8.05	7.85	7.11	6.13	5.33

Boundary Type: Corrugated Run No. 40 C Q = 5.75 cfs V = 7.32 fps
Profile Traverse: Horizontal C_t = 4.07 percent T = 30.3 °C

Average Piezometer Reading

Piez. No.	4	5	6	7	8	9	10
Piez. reading	--	--	9.212	8.374	7.401	6.395	5.330
Piez. reading for C_t data							
Piez. reading at check sta.	--	--	--	--	---	7.006	5.992

Concentration and Velocity Profile Data

Sampler sta (y/D)	0.06	0.16	0.26	0.36	0.46	0.56	0.66	0.76	0.86	0.96
Avg. Conc. (C %)	3.380	3.420	3.610	3.690	3.600	3.700	3.800	3.740	3.580	3.480
Velocity (u fps)	6.97	8.05	9.32	9.62	9.95	9.95	9.42	8.71	7.55	6.38

Boundary Type: Corrugated Run No. 41 C δ Q = 4.75 cfs V = 6.10 fps
Profile Traverse: Horizontal C_t = 5.05 percent T = 24.8 °C

Average Piezometer Reading

Piez. No.	4	5	6	7	8	9	10
Piez. reading							
Piez. reading for C_t data							
Piez. reading at check sta.							

Concentration and Velocity Profile Data

Sampler sta (y/D)	0.06	0.16	0.26	0.36	0.46	0.56	0.66	0.76	0.86	0.96
Avg. Conc. (C %)	3.990	4.250	4.410	4.400	4.600	4.600	4.500	4.390	4.120	3.990
Velocity (u fps)										

Boundary Type: **Corrugated** Run No. 42 C Q = 5.75 cfs V = 7.32 fps
Profile Traverse: **Horizontal** C_t = 5.55 percent T = 27.0 °C

Average Piezometer Reading

Piez. No.	4	5	6	7	8	9	10
Piez. reading	--	--	9.255	8.385	7.364	6.354	5.270
Piez. reading for C_t data							
Piez. reading at check sta.	--	--	--	--	--	6.890	5.962

Concentration and Velocity Profile Data

Sampler sta (y/D)	0.06	0.16	0.26	0.36	0.46	0.56	0.66	0.76	0.86	0.96
Avg. Conc. (C %)	4.520	4.550	5.000	5.060	5.010	5.090	5.110	5.000	4.750	4.750
Velocity (u fps)										

Boundary Type: **Corrugated** Run No. 43 C Q = 5.78 cfs V = 7.37 fps
Profile Traverse: **Vertical** C_t = 4.72 percent T = 27.1 °C

Average Piezometer Reading

Piez. No.	4	5	6	7	8	9	10
Piez. reading	--	--	9.261	8.416	7.400	6.419	5.360
Piez. reading for C_t data	--	--	--	--	--	6.969	5.960
Piez. reading at check sta.							

Concentration and Velocity Profile Data

Sampler sta (y/D)	0.06	0.16	0.26	0.36	0.46	0.56	0.66	0.76	0.86	0.96
Avg. Conc. (C %)	7.600	6.750	6.050	5.390	4.800	4.150	3.550	3.310	2.800	2.640
Velocity (u fps)	5.80	6.67	7.73	8.98	9.86	10.15	9.830	8.61	7.79	6.72

Boundary Type: **Corrugated** Run No. 44 C δ Q = 4.83 cfs V = 6.15 fps
Profile Traverse: **Vertical** C_t = 4.53 percent T = 28.7 °C

Average Piezometer Reading

Piez. No.	4	5	6	7	8	9	10
Piez. reading	--	9.126	8.452	7.909	7.281	6.684	6.005
Piez. reading for C_t data							
Piez. reading at check sta.	--	9.556	8.912	--	--	7.064	6.426

Concentration and Velocity Profile Data

Sampler sta (y/D)	0.06	0.16	0.26	0.36	0.46	0.56	0.66	0.76	0.86	0.96
Avg. Conc. (C %)	10.040	8.800	6.800	5.580	4.11	3.75	3.03	2.450	2.10	--
Velocity (u fps)	4.75	5.63	6.76	7.66	8.22	8.41	8.10	7.00	5.91	4.40

Boundary Type: **Corrugated** Run No. 45 C Q = 5.95 cfs V = 7.58 fps
Profile Traverse: **Vertical** C_t = 6.87 percent T = 26.5 °C

Average Piezometer Reading

Piez. No.	4	5	6	7	8	9	10
Piez. reading	--	--	9.412	8.016	7.507	6.504	5.545
Piez. reading for C_t data							
Piez. reading at check sta.	--	--	--	--	--	6.976	5.960

Concentration and Velocity Profile Data

Sampler sta (y/D)	0.06	0.16	0.26	0.36	0.46	0.56	0.66	0.76	0.86	0.96
Avg. Conc. (C %)	10.60	9.50	9.10	7.80	7.25	6.10	5.20	4.65	4.30	4.10
Velocity (u fps)	5.62	7.10	8.21	9.40	10.40	10.60	10.10	9.05	7.90	6.61

Boundary Type: **Corrugated** Run No. 46 C δ Q = 4.82 cfs V = 6.06 fps
Profile Traverse: **Vertical** C_t = 8.72 percent T = 28.7 °C

Average Piezometer Reading

Piez. No.	4	5	6	7	8	9	10
Piez. reading	9.910	9.139	8.459	7.920	7.215	6.686	6.010
Piez. reading for C_t data							
Piez. reading at check sta.	--	9.515	8.865	--	--	7.027	6.388

Concentration and Velocity Profile Data

Sampler sta (y/D)	0.06	0.16	0.26	0.36	0.46	0.56	0.66	0.76	0.86	0.96
Avg. Conc. (C %)	13.90	11.40	9.65	8.25	6.78	5.60	4.38	3.65	3.03	2.29
Velocity (u fps)	6.80	7.83	8.56	9.53	9.90	10.20	9.65	8.75	7.85	6.80

Boundary Type: **Corrugated** Run No. 47 C δ Q = 4.75 cfs V = 5.95 fps
Profile Traverse: **Vertical** C_t = 10.9 percent T = 32.5 °C

Average Piezometer Reading

Piez. No.	4	5	6	7	8	9	10
Piez. reading	9.800	9.106	8.438	7.902	7.286	6.708	6.021
Piez. reading for C_t data							
Piez. reading at check sta.	--	9.458	8.809	--	--	7.016	6.375

Concentration and Velocity Profile Data

Sampler sta (y/D)	0.06	0.16	0.26	0.36	0.46	0.56	0.66	0.76	0.86	0.96
Avg. Conc. (C %)	17.30	15.02	12.30	10.02	8.25	6.80	5.39	4.45	3.83	2.95
Velocity (u fps)										

Boundary Type: **Corrugated** Run No. 48 C Q = 6.00 cfs V = 7.50 fps
Profile Traverse: **Vertical** C_t = 8.16 percent T = 34.0 °C

Average Piezometer Reading

Piez. No.	4	5	6	7	8	9	10
Piez. reading	--	--	9.282	8.396	7.376	6.368	5.300
Piez. reading for C_t data							
Piez. reading at check sta.	--	--	9.875	--	--	6.840	5.820

Concentration and Velocity Profile Data

Sampler sta (y/D)	0.06	0.16	0.26	0.36	0.46	0.56	0.66	0.76	0.86	0.96
Avg. Conc. (C %)	13.70	12.30	11.20	9.50	8.30	7.00	6.20	5.52	5.00	4.46
Velocity (u fps)										

Boundary Type: Run No. Q = cfs V = fps
Profile Traverse: C_t = percent T = °C

Average Piezometer Reading

Piez. No.	4	5	6	7	8	9	10
Piez. reading							
Piez. reading for C_t data							
Piez. reading at check sta.							

Concentration and Velocity Profile Data

Sampler sta (y/D)	0.06	0.16	0.26	0.36	0.46	0.56	0.66	0.76	0.86	0.96
Avg. Conc. (C %)										
Velocity (u fps)										

SUMMARY OF SEDIMENT SIEVE ANALYSIS

Run No	Date of Taking Sample 1954	Traverse Direct.	Station No. (y/D)	Sample Number	Mean Sieve Diameter (mm) (Avg = 0.20)	Std. Dev. of Sieve Diameter (mm) (Avg = 0.051)
--	Jan. 23	integrated		--	0.175	0.0493
--	Feb. 5	integrated		--	0.175	0.0472
--	Feb. 13	integrated		--	0.195	0.0470
--	Mar. 2	integrated		--	0.155	0.0563
--	Mar. 25	integrated		--	0.215	0.0512
--	Mar. 23	integrated		--	0.198	0.0478
40H	Mar. 24	horz.	0.06	8,10	0.195	0.0564
51H	Mar. 26	vert.	0.16	13,15	0.193	0.0455
52H	Mar. 27	integrated		18,20	0.202	0.0527
56H	Mar. 29	vert.	0.06	25	0.205	0.0564
58H	Mar. 30	horz.	0.06	27	0.205	0.0564
67H	Apr. 3	horz.	0.06	34,35	0.205	0.0498
68H	Apr. 3	horz.	0.06	37	0.205	0.0498
71H	Apr. 16	horz.	0.06	40	0.251	0.075
76H	Apr. 19	vert.	0.06	48	0.250	0.065
77H	Apr. 19	vert.	0.06	50	0.250	0.065
84H	Apr. 21	horz.	0.96	55,56	0.183	0.058
85H	Apr. 21	horz.	0.06	57,59	0.183	0.055
22S	May 11	integrated		61,62	0.215	0.060
32S	May 14	vert.	0.06	70	0.195	0.031
33S	May 15	vert.	0.66	76,78	0.195	0.073
33S	May 15	vert.	0.26	80	0.195	0.052
--	--	integrated		--	0.182	0.042
34S	May 17	vert.	0.16	84	0.183	0.030
44S	May 22	vert.	0.96	86	0.143	0.041
44S	May 22	vert.	0.86	103	0.143	0.041
44S	May 22	vert.	0.76	104	0.143	0.041
44S	May 22	vert.	0.26	109	0.174	0.031
45S	May 24	vert.	0.56	124	0.157	0.041
45S	May 24	vert.	0.46	125	0.157	0.041
45S	May 24	vert.	0.26	127	0.178	0.029
47S	May 26	vert.	0.06	141	0.198	0.027

DIFFERENTIAL HEAD BETWEEN CORRUGATION CRESTS AND TROUGHS

Run No.	$\delta\pi$ (ft)	Run No.	$\delta\pi$ (ft)	Run No.	$\delta\pi$ (ft)	Run No.	$\delta\pi$ (ft)	Run No.	$\delta\pi$ (ft)	Run No.	$\delta\pi$ (ft)
1C	0.34	9C	0.06	17C	0.54	27C	0.26	35C	0.28	44C	0.40
2C	0.23	10C	0.26	18C	0.60	28C	0.49	36C	0.40	45C	0.40
3C	0.48	11C	0.47	21C	0.50	29C	0.62	37C	0.70	46C	0.38
4C	0.66	12C	0.63	22C	0.69	30C	0.25	38C	0.23	47C	0.30
5C	0.05	13C	0.30	23C	0.25	31C	0.44	39C	0.44	48C	0.48
6C	0.26	14C	0.50	24C	0.60	32C	0.60	40C	0.61		
7C	0.43	15C	0.60	25C	0.46	33C	0.74	42C	0.54		
8C	0.53	16C	0.28	26C	0.26	34C	0.80	43C	0.54		

HP AND Q AS FUNCTIONS OF G (Fig. 14)

$Jx10^2$	V (fps)	C_t	Q (cfs)	$Gx10^2$ (cfs)	$HPx10^3$
			Hel-Cor		
0.157	1.60	0.10	1.25	0.125	0.222
0.245	2.00	0.14	1.57	0.220	0.436
0.550	3.00	0.32	2.35	0.752	1.46
0.98	4.00	0.73	3.14	2.29	3.48
1.52	5.00	1.70	3.92	6.66	6.75
2.17	6.00	3.90	4.71	18.4	11.6
2.95	7.00	10.50	5.48	57.5	18.4
3.84	8.00	20.0	6.27	125.4	26.3
			Corrugated		
1.45	2.85	0.100	2.24	0.224	3.68
1.60	3.00	0.124	2.35	0.291	4.15
2.85	4.00	0.42	3.14	1.32	10.2
4.50	5.00	1.40	3.92	5.48	20.0
6.40	6.00	4.90	4.71	23.1	33.5
8.70	7.00	16.5	5.48	90.5	54.1
			Smooth		
0.56	5.02	0.10	3.93	0.393	2.50
0.76	6.00	0.21	4.71	0.990	4.06
0.98	7.00	0.48	5.48	2.63	6.11
1.25	8.00	1.02	6.27	6.40	8.89
1.52	9.00	2.27	7.06	16.0	12.1
1.82	10.00	5.00	7.85	39.2	16.2

CONCENTRATION AT 10-IN. ORIFICE
(FIG. 6)

Run No.	c/C', NS Traverse, at x/r_1					c/C', EW Traverse at x/r_1					Total Load
	-0.96	-0.72	-0.24	+0.24	0.48	-0.96	-0.72	-0.24	+0.24	0.48	C_t
50H	0.968	1.084	1.018	0.913	0.855	1.200	0.960	1.042	0.960	1.000	6.04
54H	0.967	1.073	1.000	1.041	0.993	1.247	1.024	1.068	0.836	0.673	12.2
55H	1.033	1.025	1.081	0.896	0.904	1.147	0.952	1.010	0.961	0.961	12.4
56H	0.985	1.050	1.018	1.000	0.908	1.173	1.082	1.075	0.917	0.769	12.1
57H	1.037	1.086	1.008	0.997	0.890	1.086	1.000	1.023	1.000	0.897	12.7
58H	0.942	1.067	1.067	0.943	0.976	1.067	0.853	0.943	1.017	1.131	12.2
61H	0.792	0.993	1.008	1.000	0.975	1.192	0.976	0.975	1.041	1.047	6.25
63H	0.845	1.051	0.986	1.005	1.068	1.051	0.931	1.005	1.051	1.068	6.56
64H	0.923	1.115	1.060	0.959	0.877	1.115	0.928	1.004	0.977	1.042	5.47
66H	0.873	1.035	1.284	1.051	1.058	1.149	0.907	0.985	1.051	1.051	4.44
68H	1.204	1.146	1.014	0.903	0.760	1.205	0.976	0.983	1.041	1.022	4.30
72H	0.777	1.031	1.005	1.052	1.085	1.196	0.889	0.947	0.941	1.052	1.88
11S	0.926	0.978	1.005	1.063	1.040	1.230	0.926	0.973	1.115	1.005	0.175
20S	1.005	1.311	1.050	0.728	0.728	1.433	1.101	1.008	0.773	0.813	0.360
21S	0.829	1.010	1.010	0.963	1.022	1.262	0.883	0.940	1.021	1.055	0.374
22S	0.684	1.010	1.042	1.010	0.994	1.351	1.025	0.994	0.944	0.920	0.307
23S	0.673	1.128	1.010	0.976	0.961	1.281	1.010	0.991	0.991	0.957	0.312
24S	0.795	0.990	1.057	1.040	1.040	1.126	0.860	0.990	1.057	1.040	0.293
28S	1.054	0.985	0.948	0.948	0.948	1.285	0.984	0.957	0.970	0.920	0.778
29S	0.790	0.995	1.010	1.045	1.024	1.256	0.871	0.965	1.024	1.031	0.684
32S	0.803	1.010	1.035	1.019	1.025	1.283	0.833	0.930	1.035	1.035	0.624
33S	0.943	1.047	0.943	0.695	0.950	1.205	1.018	0.979	0.985	0.979	0.731
36S	0.863	0.975	1.020	1.008	1.020	1.209	0.870	0.975	1.033	1.033	1.16
37S	0.705	1.050	0.992	1.009	1.033	1.183	1.033	0.975	0.992	1.009	1.19
39S	0.87	1.027	1.027	0.975	0.956	1.278	0.87	0.947	0.983	1.061	1.15
40S	0.783	0.993	1.009	1.009	0.971	1.296	1.102	0.932	0.977	0.932	1.29
41S	1.123	1.070	0.934	0.942	0.953	1.181	0.925	0.927	0.987	0.973	1.54
44S	0.933	1.009	1.033	0.933	0.962	1.134	0.890	0.994	1.050	1.050	2.08
48S	0.877	1.056	0.971	0.965	0.960	1.256	0.877	0.940	1.033	1.060	3.19
49S	0.823	0.970	1.087	0.935	0.930	1.408	0.930	0.981	0.955	0.981	2.65

KARMAN k IN $z_1 = w/k u_*$

Smooth Pipe			Corrugated Pipe			
Run No.	k	C_t	Run No.	k	k'	C_t
7	0.332	0.261	6	0.440	0.473	0.183
8	0.339	0.195	8	1.33	1.43	0.449
9	0.292	0.125	9	0.436	0.468	0.046
15	0.230	0.374	16	0.824	0.885	0.455
16	0.353	0.166	17	0.767	0.825	0.689
17	0.305	0.081	18	0.530	0.570	0.881
18	0.298	0.040	19	0.950	1.022	0.768
19	0.309	0.010	20	0.807	0.753	1.20
20	0.224	0.360	21	0.645	0.600	1.09
21	0.252	0.374	22	0.537	0.577	1.32
22	0.303	0.307	30	0.625	0.673	0.972
31	0.217	0.613	31	0.560	0.603	1.56
32	0.247	0.624	32	0.725	0.778	2.17
33	0.236	0.731	33	1.05	1.13	2.47
34	0.209	1.17	34	0.960	1.035	3.56
36	0.229	1.16	35	0.338	0.363	2.09
37	0.247	1.19	36	0.525	0.565	2.97
43	0.221	1.93	37	0.646	0.694	3.69
44	0.253	2.08	43	0.605	0.649	4.72
45	0.313	2.35	44	0.554	0.595	4.53
46	0.287	3.00	45	0.804	0.865	6.87
47	0.279	3.01	46	0.555	0.596	8.72
			47	0.643	0.674	10.9
			48	0.603	0.648	8.16

DIMENSIONLESS CONCENTRATION PROFILES --HORIZONTAL
(Fig. 16)

Run No.	c/C' at station z/D 0.06	0.16	0.26	0.36	0.46	0.56	0.66	0.76	0.86	0.96
10S	1.160	1.088	1.010	1.010	0.943	0.943	0.912	0.963	0.985	0.985
11S	1.065	0.981	1.020	0.935	1.020	0.925	0.981	1.020	1.020	1.065
12S	1.059	0.985	--	0.985	--=	0.985	0.985	0.985	0.985	1.059
14S	1.294	1.185	1.115	1.038	0.970	0.930	0.891	0.852	0.891	0.852
23S	0.995	0.941	--	0.974	--	0.974	0.995	1.042	0.995	1.070
24S	1.018	0.987	--	0.987	--	1.018	1.018	1.043	0.957	0.957
25S	1.140	1.049	--	0.993	--	0.993	0.950	0.950	0.950	0.993
28S	1.159	1.077	--	1.031	--	0.969	0.957	0.957	0.923	0.923
29S	1.125	1.138	--	1.021	--	0.946	0.915	0.976	0.946	0.930
30S	1.123	1.070	--	1.097	--	0.994	0.947	0.947	0.914	0.893
38S	0.975	--	0.934	--	0.986	1.000	0.865	1.035	1.089	1.102
39S	0.947	0.967	--	0.967	--	1.022	0.967	1.010	1.010	1.100
40S	1.010	--	0.985	--	0.957	0.926	0.926	1.010	1.040	1.086
48S	1.181	1.119	--	1.200	--	1.217	1.189	1.202	1.181	1.200
49S	0.954	--	0.879	--	0.937	0.930	0.930	0.905	0.871	0.913
50S	0.973	--	0.973	--	1.001	1.013	1.029	1.013	1.008	0.993
10C	0.905	0.905	0.942	0.963	0.963	1.000	1.100	1.020	1.100	1.090
11C	0.901	0.930	0.945	0.945	1.010	0.978	1.072	1.058	1.089	1.058
12C	0.946	0.930	0.946	0.930	0.990	0.990	0.990	1.079	1.052	1.109
13C	0.937	0.907	1.010	0.952	1.098	1.027	1.085	0.983	0.995	0.995
14C	0.945	0.945	0.945	1.002	1.042	1.040	1.027	1.042	1.002	1.010
15C	0.920	0.925	0.921	0.947	1.001	1.039	1.065	1.059	1.071	1.048
24C	0.955	0.925	0.947	0.955	0.985	1.031	1.079	1.031	1.047	1.047
25C	0.957	0.967	0.952	1.048	1.048	1.067	1.067	1.038	0.997	0.997
26C	0.897	0.850	1.001	1.020	1.012	1.097	1.078	1.078	0.917	1.040
27C	0.843	1.014	0.843	1.019	1.019	1.010	1.024	1.022	0.993	1.010
28C	0.980	1.000	0.987	0.980	1.023	1.042	1.042	0.980	0.993	0.963
29C	0.915	0.965	0.965	0.975	1.015	1.051	1.033	1.039	1.011	1.023
38C	0.954	1.009	1.057	1.062	1.057	1.069	1.002	0.972	0.914	0.910
39C	0.998	0.990	1.010	1.019	1.055	1.032	1.048	0.973	0.959	0.922
40C	0.938	0.950	1.001	1.023	1.000	1.028	1.056	1.039	0.994	0.968
41C	0.920	0.982	1.018	1.014	1.061	1.061	1.040	1.013	0.951	0.920
42C	0.925	0.931	1.022	1.025	1.024	1.041	1.042	1.022	0.972	0.972

VELOCITY PARAMETER AT 10-IN. ORIFICE
(Fig. 6)

Run No.	Direct Trav.	Magnitude of $\delta h/\delta h'$ at Position x/r_1							Mean Value ($\delta h'$)
		-0.84	-0.72	-0.48	-0.24	0.00	0.24	0.48	
1S′	NS	0.887	0.999	1.064	1.056	0.999	1.008	0.997	1.241
1S′	EW	0.980	0.987	0.963	0.972	1.020	1.069	1.078	1.237
2S′	NS	0.980	1.031	0.990	0.990	0.980	1.000	1.031	0.990
2S′	EW	1.028	1.047	1.038	1.009	0.977	0.947	0.947	0.983
3S′	NS	1.055	1.113	1.113	1.040	0.967	0.893	0.820	0.683
3S′	EW	1.124	1.150	1.110	0.987	0.918	0.835	0.863	0.730
4S′	NS	0.743	0.876	1.040	1.081	1.081	1.081	1.104	1.416
4S′	EW	0.915	0.962	0.975	0.995	1.001	1.070	1.082	1.488
5S′	NS	0.963	1.005	1.021	1.030	1.030	0.963	0.980	1.193
5S′	EW-	0.875	0.978	0.987	0.987	1.048	1.064	1.073	1.167
6S′	NS	1.000	1.050	1.010	0.980	0.980	0.990	1.010	1.000
6S′	EW	0.720	0.780	0.770	0.750	0.670	0.620	0.560	1.000
7S′	NS	1.033	1.121	1.106	1.077	0.963	0.890	0.804	0.696
7S′	EW	1.120	1.148	1.092	1.012	0.904	0.877	0.850	0.741
8S′	NS	0.875	1.005	1.043	1.043	1.043	1.018	0.966	0.766
8S′	EW	1.049	1.072	1.072	1.010	0.953	0.940	0.892	0.830
9S′	NS	0.995	1.005	1.005	1.005	1.005	1.015	0.975	1.016
9S′	EW	1.030	1.040	1.040	1.000	0.950	0.940	0.940	1.000
10S′	NS	0.743	0.895	1.039	1.080	1.080	1.080	1.080	1.453
10S′	EW	--	--	--	--	--	--	--	--
11S′	NS	0.914	0.972	0.977	1.001	1.022	1.060	1.060	1.567
11S′	EW	0.689	0.923	1.032	1.079	1.085	1.092	1.100	1.464
12S′	NS	0.886	1.090	1.098	1.048	0.979	0.946	0.954	1.187
12S′	EW	0.911	0.929	0.973	0.998	1.033	1.070	1.087	1.131
13S′	NS	0.954	1.075	1.013	0.954	0.954	1.013	1.035	0.986
13S′	EW	1.040	1.071	1.040	1.020	0.969	0.937	0.937	0.971

SUPPLEMENTARY DATA -- 12-IN. HEL-COR
(without sediment)

Run No.	Q cfs	V fps	T °C	f x 10^2	Re x 10^{-5}
1	4.10	5.17	17.0	3.91	4.45
2	4.30	5.41	17.0	3.82	4.70
3	4.32	5.45	17.0	4.12	4.72
4	3.80	4.80	17.1	4.19	4.20
5	3.60	4.52	17.2	4.04	3.95
6	3.40	4.29	17.3	3.85	3.75
7	3.25	4.10	17.3	3.60	3.58
8	2.70	3.43	17.4	3.84	2.98
9	1.70	2.16	17.4	3.97	1.90
10	1.40	1.77	17.4	3.90	1.55
11	6.80	8.46	17.4	3.96	7.40
12	6.30	7.95	17.5	4.33	7.00
13	5.82	7.24	17.5	3.97	6.35
14	5.23	6.61	17.5	3.91	5.80
15	4.60	5.80	17.5	3.83	5.10
16	7.63	9.51	13.0	3.92	7.35
17	7.35	9.20	13.1	3.96	7.20
18	6.95	8.68	13.3	4.09	6.75
19	6.42	8.10	13.4	4.22	6.40
20	5.90	7.40	13.6	3.76	5.80
21	5.43	6.80	13.8	3.90	5.48
22	4.95	6.23	14.0	3.97	5.00
23	1.92	2.45	14.0	4.00	1.97
24	1.73	2.22	14.2	4.12	1.77
25	1.47	1.88	14.4	3.75	1.53
26	1.27	1.63	14.6	4.01	1.32
27	1.13	1.46	14.8	3.68	1.02
28	0.84	1.10	15.0	3.94	0.910
29	0.75	0.98	15.2	4.13	0.820
30	0.80	1.05	15.4	3.96	0.890

VALUES OF ϵ_s/w = cdy/dc

Run No.	ϵ_s/w at Location y/D									
	0.96	0.86	0.76	0.66	0.56	0.46	0.36	0.26	0.16	0.06
6C	0.355	0.700	0.667	0.385	0.350	0.386	0.400	0.390	0.365	0.260
7C	0.960	0.840	0.700	0.510	0.520	0.544	0.580	0.582	0.682	0.755
8C	1.385	0.780	0.700	0.690	0.724	0.690	0.710	0.810	0.910	1.010
9C	--	--	--	--	--	0.050	0.150	0.225	0.154	0.110
16C	0.645	0.410	0.378	0.340	0.343	0.362	0.350	0.450	0.550	0.650
17C	0.800	0.910	0.400	0.476	0.525	0.530	0.585	0.685	0.785	0.885
18C	0.840	0.910	0.690	0.655	0.620	0.610	0.710	0.638	0.580	0.446
19C	1.650	1.320	1.245	1.050	0.890	0.990	1.090	1.190	1.290	1.390
20C	1.350	1.200	1.190	0.810	0.765	0.865	0.965	1.065	1.165	1.265
21C	1.650	0.912	0.710	0.500	0.500	0.510	0.550	0.585	0.620	0.615
22C	1.955	1.090	0.986	0.790	0.672	0.500	0.600	0.700	0.800	0.900
23C	0.470	0.468	0.435	0.400	0.400	0.395	0.420	0.455	0.520	0.615
30C	0.500	0.545	0.480	0.350	0.305	0.336	0.355	0.430	0.515	0.580
31C	0.900	0.875	0.660	0.515	0.475	0.434	0.460	0.532	0.590	0.675
32C	1.650	0.800	0.690	0.635	0.620	0.620	0.620	0.720	0.820	0.920
33C	1.350	0.985	0.905	0.714	0.785	0.915	1.015	1.115	1.650	3.410
34C	3.960	1.075	0.895	0.565	0.665	0.765	0.865	1.200	1.275	1.980
35C	0.707	0.585	0.480	0.327	0.300	0.328	0.340	0.280	0.245	0.295
36C	0.743	0.825	0.680	0.520	0.390	0.415	0.425	0.460	0.560	0.660
37C	2.500	1.390	1.080	0.600	0.590	0.570	0.670	0.770	0.870	0.970
43C	1.850	1.065	0.456	0.710	0.720	0.755	0.780	0.880	0.920	0.880
44C	--	0.770	0.540	0.500	0.510	0.500	0.455	0.420	0.440	1.000
45C	2.195	1.555	0.985	0.780	0.700	0.800	0.900	1.000	1.100	1.200
48C	1.158	1.000	0.985	0.710	0.710	0.710	0.650	0.750	0.850	1.220

VALUES OF ϵ_s/w = cdy/dc

Run No.	ϵ_s/w at Location y/D									
	0.96	0.86	0.76	0.66	0.56	0.46	0.36	0.26	0.16	0.06
7S	0.420	0.450	0.360	0.324	0.390	0.341	0.360	0.272	0.230	0.060
8S	0.180	0.280	0.340	0.380	0.380	0.375	0.337	0.248	0.160	0.088
9S	0.120	0.220	0.300	0.240	0.295	0.280	0.240	0.232	0.105	0.100
15S	0.050	0.100	0.110	0.210	0.280	0.134	0.154	0.140	0.092	0.078
16S	0.140	0.194	0.294	0.296	0.300	0.260	0.210	0.156	0.131	0.104
17S	0.100	0.025	0.125	0.120	0.220	0.200	0.240	0.183	0.040	0.010
18S	--	--	--	--	--	--	0.100	0.080	0.074	0.010
19S	--	--	--	--	0.030	0.130	0.118	0.154	0.100	0.070
20S	0.220	0.320	0.420	0.280	0.210	0.190	0.205	0.140	0.072	0.066
21S	0.300	0.360	0.340	0.255	0.280	0.245	0.210	0.170	0.094	0.142
22S	0.410	0.510	0.525	0.540	0.440	0.456	0.230	0.184	0.155	0.130
31S	0.140	0.240	0.340	0.190	0.292	0.218	0.200	0.190	0.092	0.060
32S	0.300	0.206	0.230	0.245	0.250	0.262	0.240	0.208	0.115	0.060
33S	0.160	0.194	0.230	0.265	0.300	0.295	0.280	0.230	0.145	0.085
34S	--	--	0.080	0.120	0.120	0.155	0.190	0.090	0.088	0.080
36S	0.057	0.080	0.250	0.278	0.245	0.220	0.210	0.168	0.111	0.132
37S	0.200	0.245	0.340	0.230	0.200	0.800	0.76	0.180	0.124	0.076
43S	0.100	0.200	0.200	0.205	0.250	0.236	0.200	0.140	0.085	0.150
44S	0.100	0.100	0.084	0.058	0.190	0.272	0.165	0.120	0.105	0.138
45S	0.080	0.120	0.146	0.170	0.225	0.260	0.158	0.086	0.090	0.180
46S	0.050	0.100	0.180	0.195	0.230	0.236	0.145	0.124	0.120	0.220
47S	0.100	0.125	0.200	0.210	0.235	0.245	0.150	0.132	0.110	0.208

TOTAL LOAD DATA AT 10-IN. ORIFICE

Nomenclature:
r_1 - radius of orifice
x^1 - distance along diameter from centerline

Note: Orifice is located in a vertical section of the circulation system.

Run No.	Mixture Discharge Q cfs	Avg. Temp T °C	Trav. Direct.	Local mean concentration c at station location x/r_1 -0.96	-0.72	-0.24	0.24	0.48
50H	6.60	24.0	NS	55.85	6.55	6.15	5.52	5.17
50H	6.60	24.0	EW	7.25	5.80	6.30	5.80	6.05
54H	5.80	18.4	NS	11.8	13.1	12.2	12.7	12.1
54H	5.80	18.4	EW	15.2	12.5	13.0	10.2	9.50
55H	6.50	22.1	NS	12.8	12.7	13.4	11.1	11.2
55H	6.50	22.1	EW	14.2	11.8	12.5	11.9	11.9
56H	5.85	21.0	NS	11.9	12.7	13.3	12.1	11.0
56H	5.85	21.0	EW	14.2	13.1	13.0	11.1	9.3
57H	6.35	16.2	NS	13.2	13.8	12.8	12.4	11.3
57H	6.35	16.2	EW	13.8	12.7	13.0	12.7	11.4
58H	7.02	20.3	NS	11.5	13.0	13.0	11.5	11.9
58H	7.02	20.3	EW	13.0	10.4	11.5	12.4	13.8
61H	6.93	18.9	NS	4.95	6.20	6.30	6.25	6.08
61H	6.93	18.9	EW	7.45	6.10	6.08	6.50	6.55
63H	6.20	18.6	NS	5.55	6.90	6.35	6.60	7.00
63H	6.20	18.6	EW	6.90	6.10	6.35	6.90	7.00
64H	6.05	15.0	NS	5.05	6.10	5.80	5.25	4.80
64H	6.05	15.0	EW	6.10	5.08	5.50	5.35	5.70
66H	6.93	18.5	NS	3.88	4.60	3.70	4.67	4.70
66H	6.93	18.5	EW	5.10	4.03	4.37	4.67	4.67
68H	5.95	21.6	NS	4.03	4.93	4.36	3.88	3.27
68H	5.95	21.6	EW	5.18	4.20	4.23	4.48	4.40
72H	6.73	21.4	NS	1.46	1.94	1.89	1.98	2.04
72H	6.73	21.4	EW	2.25	1.67	1.78	1.77	1.98
11S	6.60	21.7	NS	0.162	0.172	0.176	0.186	0.182
11S	6.60	21.7	EW	0.215	0.162	0.172	0.195	0.176
20S	5.80	21.5	NS	0.362	0.472	0.378	0.262	0.262
20S	5.80	21.5	EW	0.520	0.400	0.366	0.280	0.295
21S	6.60	22.7	NS	0.310	0.378	0.378	0.360	0.382
21S	6.60	22.7	EW	0.472	0.330	0.352	0.382	0.395

TOTAL LOAD DATA AT 10-IN. ORIFICE --Continued

Nomenclature:
r_i - radius of orifice
x - distance along diameter from centerline

Note: Orifice is locate in a vertical section of the circulation system.

Run No.	Mixture Discharge Q cfs	Avg. Temp T °C	Trav. Direct.	Local mean concentration c at station location x/r_1 -0.96	-0.72	-0.24	0.24	0.48
22S	7.50	19.2	NS	0.210	0.310	0.320	0.310	0.305
22S	7.50	19.2	EW	0.415	0.315	0.305	0.290	0.288
23S	7.80	22.7	NS	0.210	0.353	0.315	0.305	0.300
23S	7.80	22.7	EW	0.400	0.315	0.310	0.310	0.300
24S	6.64	24.0	NS	0.233	0.290	0.310	0.305	0.305
24S	6.64	24.0	EW	0.330	0.252	0.290	0.310	0.305
28S	7.62	22.9	NS	0.820	0.765	0.737	0.737	0.737
28S	7.62	22.9	EW	1.00	0.765	0.745	0.755	0.715
29S	6.75	25.2	NS	0.540	0.680	0.715	0.690	0.700
29S	6.75	25.2	EW	0.860	0.595	0.660	0.700	0.705
32S	6.70	24.4	NS	0.500	0.630	0.645	0.635	0.640
32S	6.70	24.4	EW	0.800	0.520	0.580	0.645	0.645
33S	7.63	22.7	NS	0.690	0.765	0.690	0.695	0.695
33S	7.63	22.7	EW	0.880	0.743	0.715	0.720	0.715
36S	6.65	23.2	NS	1.00	1.13	1.18	1.17	1.18
36S	6.65	23.2	EW	1.40	1.01	1.13	1.20	1.20
37S	7.62	21.5	NS	0.84	1.25	1.18	1.20	1.23
37S	7.62	21.5	EW	1.41	1.23	1.16	1.18	1.20
39S	6.63	27.6	NS	1.00	1.18	1.18	1.12	1.10
39S	6.63	27.6	EW	1.47	1.00	1.09	1.13	1.22
40S	7.70	24.5	NS	1.01	1.28	1.30	1.30	1.25
40S	7.70	24.5	EW	1.67	1.42	1.20	1.26	1.20
41S	8.78	23.5	NS	1.73	1.65	1.44	1.45	1.47
41S	8.78	23.5	EW	1.82	1.41	1.43	1.52	1.50
44S	6.62	25.1	NS	1.94	2.10	2.15	1.94	2.00
44S	6.62	25.1	EW	2.36	1.85	2.07	2.18	2.18
48S	6.65	21.0	NS	2.80	3.37	3.10	3.08	3.06
48S	6.65	21.0	EW	4.02	2.80	3.00	3.30	3.38
49S	5.80	21.7	NS	2.18	2.57	2.88	2.48	2.47
49S	5.80	21.7	EW	3.73	2.46	2.60	2.58	2.60

DIMENSIONLESS CONCENTRATION PROFILE
COMPUTATIONS

Run No.	c/C_t at station y/D 0.96	0.86	0.76	0.66	0.56	0.46	0.36	0.26	0.16	0.06
1 H	1.099	1.099	0.947	1.023	1.00	0.985	0.970	0.932	0.932	1.023
4 H	0.934	0.997	0.994	1.005	0.997	1.000	0.963	1.005	0.957	1.162
17 Hδ	0.843	1.121	1.213	1.098	1.181	0.897	1.213	1.034	0.636	0.757
18 Hδ	0.987	1.213	1.147	0.853	1.213	1.147	1.021	0.987	0.987	0.454
19 H	1.075	1.019	1.000	1.025	0.983	0.968	0.975	0.975	0.987	0.996
20 H	1.093	1.006	0.989	0.981	0.948	0.967	0.987	0.981	0.993	1.040
21 H	1.035	1.070	1.038	1.000	1.000	1.035	1.000	0.983	0.905	0.934
22 H	1.010	1.057	1.032	1.010	0.991	1.003	0.980	0.944	0.944	1.032
31 H	1.127	1.008	1.019	0.973	1.034	0.973	1.010	0.893	0.953	1.008
32 H	1.103	0.998	1.017	0.961	0.923	0.998	0.961	0.922	0.926	0.998
41 H	1.127	0.995	0.993	1.015	1.015	0.952	0.993	0.937	0.963	1.020
42 H	1.101	1.034	1.002	1.009	0.992	0.917	1.053	0.889	1.009	0.987
43 H	1.058	1.036	1.004	1.009	0.961	1.009	0.952	0.993	0.934	1.058
44 H	1.000	1.000	1.023	0.986	0.995	0.995	0.995	0.977	1.027	1.013
47 Hδ	--	0.477	0.493	0.503	0.630	0.801	1.158	1.241	1.797	1.931
48 H	1.073	0.988	0.980	0.990	1.029	1.021	1.010	--	0.973	0.988
49 H	1.120	1.066	0.992	0.974	0.972	0.995	0.956	0.955	0.953	1.034
50 H	1.143	1.020	0.962	0.970	0.970	1.002	0.953	0.965	0.953	1.053
51 H	1.098	0.965	0.970	0.953	0.965	0.975	0.965	0.953	1.025	1.130
53 H	1.046	1.019	1.028	1.005	0.983	0.955	1.000	0.947	1.019	1.028
54 Hδ	0.573	0.553	0.787	0.757	0.800	0.942	0.942	1.190	1.176	1.140
55 H	1.009	1.023	1.009	1.023	1.031	1.023	0.968	0.921	1.011	0.968
56 Hδ	0.630	0.797	0.743	0.877	0.877	1.058	1.080	1.309	1.210	1.243
62 H	1.056	0.986	0.964	1.056	0.985	0.971	0.952	0.940	0.971	1.109
73 H	1.110	1.048	0.982	0.943	0.947	0.928	0.990	0.947	0.990	1.124
74 H	1.100	1.000	1.014	0.959	0.964	0.964	1.000	0.960	0.977	1.059
76 H	1.129	1.043	0.983	0.947	0.947	0.978	0.947	0.923	0.941	1.153
77 H	1.159	0.973	0.973	0.961	1.013	0.961	0.990	0.949	0.967	1.035

DIMENSIONLESS CONCENTRATION PROFILE
COMPUTATIONS --
Continued

Run No.	c/C_t at station y/D or z/D									
	0.96	0.86	0.76	0.66	0.56	0.46	0.36	0.26	0.16	0.06
6H	1.015	1.060	0.985	0.930	1.000	0.965	0.970	0.930	0.970	1.100
7H	0.967	0.978	0.978	0.973	0.978	0.989	0.962	0.978	0.978	1.218
8H	1.041	1.008	1.016	0.992	0.992	0.987	0.987	0.973	0.975	1.150
9H	1.039	1.023	1.023	0.948	0.962	0.967	0.953	0.995	1.009	1.103
10H	1.049	0.943	1.023	0.954	0.941	0.954	0.941	0.943	0.978	1.160
13H	1.034	0.991	0.997	0.984	0.963	0.977	0.991	0.984	1.010	1.101
14H	1.057	0.997	0.946	0.963	0.946	0.997	1.026	0.967	0.986	1.128
15Hδ	0.700	0.875	1.063	1.108	1.152	1.031	0.943	1.031	1.031	1.063
16Hδ	0.695	0.869	0.935	0.972	1.109	1.006	1.319	1.006	0.869	1.211
23H	0.985	1.000	1.008	1.008	0.978	0.993	0.953	0.985	0.985	1.085
24H	1.000	1.000	1.008	0.960	0.984	1.008	1.000	0.960	0.984	1.134
26Hδ	0.808	0.907	0.992	1.055	1.077	1.040	0.887	1.045	0.977	1.220
28H	0.984	1.000	1.202	0.984	1.002	0.980	0.953	0.951	0.947	1.171
29H	0.853	0.993	1.046	1.010	1.065	0.993	0.973	0.945	0.973	1.130
34H	0.994	0.997	1.019	0.994	0.997	0.923	1.039	0.967	0.967	1.121
35H	0.973	1.047	0.973	0.993	1.057	0.973	0.982	0.934	0.973	1.112
57H	0.883	0.883	1.008	0.938	0.993	1.038	1.030	1.046	1.060	1.090
58H	1.009	1.009	0.984	0.993	0.983	0.967	0.983	0.993	1.000	1.105
63H	1.038	1.009	1.015	0.986	1.001	0.965	0.943	0.947	1.001	1.099
64H	0.987	1.022	1.005	0.983	0.970	0.983	0.973	0.973	0.994	1.109
67H	1.011	1.033	1.022	0.990	0.945	0.967	0.954	0.943	1.012	1.133
68H	1.000	1.012	1.001	0.976	0.980	0.980	0.943	0.982	0.955	1.171
71H	1.034	1.029	1.005	1.034	0.943	0.943	0.976	0.928	0.976	1.134
79H	1.097	--	0.956	--	0.970	--	1.002	--	0.977	--
81H	1.030	1.037	0.990	0.974	0.962	0.962	0.945	0.945	0.939	1.200

DIMENSIONLESS CONCENTRATION PROFILE
COMPUTATIONS --
Continued

Run No.	c/C_t at station y/D or z/D 0.96	0.86	0.76	0.66	0.56	0.46	0.36	0.26	0.16	0.06
7S	0.226	0.299	0.406	0.514	0.632	0.805	1.100	1.451	2.416	5.330
8S	--	0.231	0.303	0.421	0.616	0.759	0.975	1.365	2.200	5.800
9S	0.080	0.160	0.240	0.368	0.513	0.624	0.969	1.302	2.400	7.085
15Sδ	--	--	--	0.153	0.206	0.307	0.535	0.927	2.570	20.350
16S	--	--	--	0.271	0.356	0.482	0.759	1.127	2.500	9.940
17S	--	--	--	--	--	--	0.667	0.901	2.038	10.00
18Sδ	--	--	--	--	--	--	--	--	--	11.620
19S	--	--	--	--	--	--	--	--	5.900	16.300
20Sδ	--	--	0.164	0.203	0.295	0.453	0.703	1.167	2.620	15.830
21S	--	0.144	0.209	0.259	0.358	0.561	0.843	1.390	2.650	8.630
22S	0.147	0.254	0.300	0.358	0.424	0.557	0.667	1.156	2.048	4.915
32S	--	0.161	0.215	0.276	0.406	0.606	0.894	1.363	2.536	9.290
33S	0.126		0.260	0.350	0.482	0.685	0.984	1.423	2.520	6.290
34Sδ	0.079	0.111	0.163	0.219	0.300	0.466	0.777	1.451	4.020	16.850
36S	0.104	0.140	0.202	--	0.358	0.555	0.855	1.585	3.000	11.40
37S	--	--	--	--	--	--	--	1.437	2.762	7.90
43S	0.067	0.104	0.148	0.210	0.316	0.500	0.799	1.425	3.500	9.850
44Sδ	0.069	0.108	0.144	0.209	0.294	0.481	0.804	1.518	4.275	10.42
45Sδ	0.049	0.066	0.095	0.133	0.222	0.376	0.712	1.865	5.780	9.330
46Sδ	0.071	0.110	0.153	0.213	0.318	0.506	0.843	1.853	4.567	8.200
47Sδ	0.093	0.136	0.184	0.256	0.362	0.547	0.897	1.729	3.920	7.570
31Sδ	--	0.111	0.150	0.210	0.281	0.436	0.702	1.190	2.660	15.600
10S	0.573	0.573	0.560	0.630	0.548	0.548	0.587	0.587	0.633	0.675
11S	0.657	0.628	0.628	0.605	0.577	0.628	0.577	0.628	0.605	0.657
12S	0.484	0.451	0.451	0.451	0.451	--	0.451	--	0.451	0.484
14Sδ	0.280	0.293	0.280	0.293	0.307	0.318	0.341	0.367	0.389	0.425
23S	0.640	0.596	0.625	0.596	0.583	--	0.583	--	0.563	0.596
24S	0.522	0.522	0.570	0.556	0.556	--	0.540	--	0.540	0.556
25S	0.426	0.408	0.408	0.408	0.426	--	0.426	--	0.451	0.490
28S	0.520	0.520	0.540	0.540	0.545	--	0.582	--	0.609	0.655
29S	0.446	0.453	0.467	0.438	0.453	--	0.490	--	0.545	0.539
30Sδ	0.274	0.281	0.291	0.291	0.305	--	0.337	--	0.329	0.345
38S	0.345	0.341	0.324	0.314	0.314	0.308	--	0.292	--	0.305
39S	0.433	0.399	0.399	0.382	0.404	--	0.382	--	0.382	0.374
40S	0.555	0.503	0.531	0.515	0.474	0.489	--	0.502	--	0.515
48Sδ	0.426	0.420	0.428	0.423	0.433	--	0.426	--	0.404	0.420
49Sδ	0.415	0.403	0.411	0.423	0.423	0.427	--	0.417	--	0.434
50S	0.464	0.470	0.474	0.481	0.474	0.467	--	0.454	--	0.454

DIMENSIONLESS CONCENTRATION PROFILE
COMPUTATIONS --
Continued

Run No.	c/C_t at station y/D or z/D									
	0.96	0.86	0.76	0.66	0.56	0.46	0.36	0.26	0.16	0.06
6C	0.372	0.394	0.547	0.601	0.820	0.963	1.229	1.667	2.020	2.840
7C	0.473	0.542	0.584	0.700	0.897	1.090	1.259	1.417	1.811	2.038
8C	0.553	0.616	0.647	0.704	0.938	1.027	1.195	1.261	1.491	1.640
9C§	--	--	--	--	--	--	--	1.955	3.300	6.515
16C	0.264	0.316	0.417	0.545	0.747	0.934	1.254	1.583	1.975	2.310
17C	0.472	0.516	0.581	0.704	0.864	1.045	1.250	1.401	1.673	1.931
18C	0.538	0.590	0.669	0.749	0.907	1.021	1.213	1.359	1.554	1.930
19C	0.656	0.674	0.693	0.749	0.882	1.00	1.089	1.209	1.255	1.383
20C	0.600	0.637	0.704	0.767	0.867	0.993	1.117	1.200	1.337	1.451
21C	0.505	0.519	0.639	0.707	0.873	1.075	1.249	1.525	1.745	2.076
22C	0.580	0.607	0.674	0.754	0.863	1.00	1.227	1.356	1.668	1.827
23C	0.306	0.379	0.491	0.627	0.793	0.993	1.276	1.610	2.041	2.390
30C§	0.309	0.360	0.432	0.535	0.763	0.99	1.389	1.800	2.220	2.675
31C	0.471	0.526	0.581	0.700	0.860	1.059	1.281	1.600	1.835	2.275
32C	0.521	0.544	0.617	0.723	0.853	1.015	1.129	1.333	1.581	1.725
33C	0.591	0.653	0.689	0.790	0.891	1.005	1.122	1.220	1.332	1.400
34C	0.561	0.587	0.623	0.725	0.842	0.985	1.115	1.230	1.321	1.425
35C§	0.261	0.309	0.376	0.474	0.650	0.900	1.177	1.600	2.348	3.618
36C	0.431	0.497	0.539	0.633	0.794	1.009	1.282	1.583	1.951	2.272
37C	0.555	0.593	0.645	0.675	0.835	0.975	1.100	1.310	1.516	1.628
43C	0.560	0.594	0.702	0.753	0.878	1.018	1.143	1.283	1.430	1.610
44C	--	0.463	0.540	0.668	0.827	0.907	1.232	1.500	1.945	2.220
45C	0.596	0.654	0.677	0.757	0.887	1.055	1.136	1.324	1.383	1.541
48C	0.546	0.613	0.675	0.760	0.857	1.017	1.163	1.372	1.508	1.679
10C	--	--	--	--	0.935	0.900	0.900	0.881	0.847	0.847
11C	--	--	--	--	0.953	0.985	0.921	0.921	0.905	0.877
12C	--	--	--	--	0.970	0.970	0.911	0.926	0.911	0.926
13C	0.870	0.870	0.857	0.947	0.896	0.958	0.832	0.883	0.792	0.817
14C	0.875	0.868	0.903	0.889	0.900	0.903	0.868	0.819	0.819	0.819
15C	0.925	0.943	0.933	0.937	0.915	0.883	0.835	0.812	0.817	0.810
24C	0.931	0.931	0.918	0.959	0.918	0.877	0.850	0.843	0.823	0.850
25C	0.855	0.855	0.889	0.916	0.897	0.897	0.816	0.830	0.795	0.820
26C	0.903	0.795	0.935	0.935	0.951	0.877	0.885	0.869	0.738	0.778
27C§	0.910	0.895	0.924	0.925	0.910	0.920	0.920	0.850	0.915	0.850
38C§	0.900	0.891	0.916	0.911	0.927	0.895	0.859	0.851	0.851	0.805
40C	0.805	0.837	0.849	0.916	0.900	0.920	0.890	0.883	0.863	0.873
41C§	0.856	0.881	0.920	0.935	0.912	0.887	0.910	0.888	0.842	0.831
42C	0.791	0.817	0.871	0.892	0.912	0.912	0.873	0.874	0.842	0.791

ONE-DIMENSIONAL ANALYSIS

Note: V and J rounded to three figures after f was computed.

Note: Subscript t on a run number denotes it is the total load portion of a run.

Run No.	Direct. Trav.	Q cfs	V fps	T °C	C_t	$V/\sqrt{gD}$	$fx10^2$	$Rex10^{-5}$	$Jx10^2$
1H	vert.	5.20	6.62	16.4	1.32	1.17	3.83	5.60	2.55
2H	vert.	5.20	6.62	15.6	1.35	1.17	3.68	5.55	2.55
3H	vert.	5.30	6.75	15.0	1.90	1.19	3.73	5.60	2.65
4H	vert.	5.21	6.63	18.4	1.85	1.17	3.90	5.85	2.58
6H	horz.	6.50	8.28	18.9	2.00	1.46	4.00	7.50	4.10
7H	horz.	6.50	8.28	22.5	1.83	1.46	3.98	8.20	4.10
8H	horz.	6.60	8.40	28.6	2.21	1.48	3.86	9.42	4.25
9H	horz.	6.60	8.40	29.0	2.13	1.48	3.80	9.60	4.25
10H	horz.	6.45	8.22	17.5	2.87	1.45	4.02	7.20	4.08
11H	horz.	6.65	8.47	20.0	2.70	1.49	3.77	7.85	4.30
12H	horz.	6.45	8.22	21.5	2.43	1.45	4.07	8.10	4.08
13H	horz.	6.45	8.22	21.3	3.17	1.45	4.00	8.00	4.08
14H	horz.	6.45	8.22	22.8	3.01	1.45	4.00	8.20	4.08
15Hδ	horz.	1.64	2.09	19.8	0.157	0.369	4.90	1.93	0.260
16Hδ	horz.	1.55	1.97	24.7	0.138	0.347	4.93	2.05	0.235
17Hδ	vert.	1.61	2.06	25.6	0.165	0.36	4.60	2.17	0.244
18Hδ	vert.	1.63	2.08	26.1	0.141	0.37	5.00	2.25	0.260
19H	vert.	4.70	5.98	20.0	1.59	1.05	3.96	5.52	2.08
20H	vert.	4.70	5.98	22.5	1.52	1.05	3.96	5.78	2.08
21H	vert.	3.53	4.50	27.1	0.840	0.79	4.45	5.00	1.23
22H	vert.	3.53	4.50	27.7	0.837	0.79	4.13	5.00	1.20
23H	horz.	4.80	6.11	26.5	1.30	1.08	3.96	6.60	2.20
24H	horz.	4.80	6.11	27.6	1.28	1.08	3.83	6.75	2.20
25H	horz.	3.45	4.40	31.8	0.756	0.776	4.38	5.35	1.16
26Hδ	horz.	3.45	4.40	32.3	0.711	0.776	4.65	5.40	1.16
27H	horz.	4.80	6.12	21.1	2.06	1.08	3.74	5.80	2.20
28H	horz.	4.75	6.05	22.9	1.93	1.07	4.05	6.00	2.16
29H	horz.	3.53	4.50	26.5	1.08	1.26	4.27	4.95	1.23
30H	horz.	3.53	4.50	26.7	1.08	1.26	4.27	4.95	1.20
31H	vert.	4.82	6.08	19.1	0.515	1.07	3.72	5.98	2.18
32H	vert.	4.81	6.12	20.6	0.520	1.08	3.75	5.75	2.20
33H	vert.	3.57	4.55	24.1	0.295	1.25	5.40	4.70	1.23
34H	horz.	4.78	6.10	22.0	0.564	1.08	3.67	5.90	2.19
35H	horz.	4.78	6.10	22.9	0.535	1.08	3.81	6.10	2.19
36H	horz.	3.43	4.37	24.8	0.402	0.77	6.07	4.52	1.13
37H	horz.	4.73	6.03	28.0	2.39	1.06	4.18	6.80	2.13

ONE-DIMENSIONAL ANALYSIS --Continued

Run No.	Direct. Trav.	Q cfs	V fps	T °C	C_t	$V/\sqrt{gD}$	$fx10^2$	$Rex10^{-5}$	$Jx10^2$
38H	horz.	4.73	6.03	28.8	2.36	1.06	4.14	6.90	2.13
39H	horz.	4.00	5.10	31.0	1.83	0.90	5.53	6.10	1.55
40H	horz.	3.82	4.87	31.5	1.81	0.86	5.00	5.85	1.43
41H	vert.	4.73	6.03	24.3	3.48	1.06	5.01	6.20	2.13
42H	vert.	4.73	5.93	25.9	3.27	1.05	4.77	5.65	2.08
43H	vert.	4.36	5.55	29.2	2.27	0.98	4.63	6.40	1.78
44H	vert.	4.35	5.54	29.6	2.21	0.98	4.78	6.40	1.78
45H	--	4.82	6.14	22.0	4.45	1.08	4.67	5.95	2.22
$45H_t$	--	4.90	6.24	23.7	4.45	1.10	4.45	4.90	2.30
$46H_t\delta$	--	5.10	6.60	26.9	3.48	1.16	4.53	7.22	3.45
$47H\ \delta$	vert.	5.10	6.60	28.3	3.73	1.16	4.53	7.22	3.45
$48H_t$	--	5.80	7.39	19.0	5.87	1.30	3.74	6.70	3.24
48H	vert.	5.80	7.39	21.1	5.87	1.30	3.74	7.10	3.24
49H	vert.	5.80	7.39	22.3	5.65	1.30	3.72	7.35	3.24
$50H_t$	--	6.60	8.41	24.0	6.03	1.48	3.92	8.60	4.25
50H	vert.	6.60	8.41	24.8	6.03	1.48	3.96	8.60	4.25
51H	vert.	6.60	8.41	25.5	6.00	1.48	4.00	8.90	4.25
$52H_t$	--	5.78	7.37	20.0	10.3	1.30	4.15	6.84	3.22
$53H_t\delta$	--	6.50	8.28	22.4	11.1	1.46	3.81	8.20	4.10
$53H\ \delta$	vert.	6.53	8.32	23.2	12.2	1.46	3.78	8.40	4.13
$54H_t\delta$	--	5.80	7.38	18.4	12.2	1.30	5.73	6.62	3.24
$54H\ \delta$	vert.	5.72	7.27	19.0	12.2	1.28	5.84	6.60	3.12
$55H_t$	--	6.50	8.27	22.1	12.7	1.30	4.02	7.90	4.09
55H	vert.	6.55	8.20	22.6	12.7	1.32	4.21	8.10	4.08
$56H_t\delta$	--	5.85	7.45	21.0	12.3	1.31	5.63	7.10	3.32
$56H\ \delta$	vert.	5.90	7.52	21.5	12.3	1.32	5.58	7.25	3.40
$57H_t$	--	6.35	8.09	16.2	13.2	1.43	4.19	6.95	3.92
57H	horz.	6.35	8.09	17.2	13.2	1.43	4.28	7.10	3.92
$58H_t$	--	7.02	8.94	20.3	12.2	1.57	4.14	8.40	4.90
58H	horz.	7.10	9.05	21.3	12.2	1.60	4.04	8.65	5.00
$59H_t$	--	8.45	10.77	17.8	12.2	1.90	3.62	9.30	--
$60H_t$	--	8.00	10.20	17.0	6.25	1.80	3.86	8.70	--
$61H_t$	--	6.93	8.82	18.9	6.25	1.55	3.76	8.00	4.60
62H	vert.	7.00	8.92	19.5	6.48	1.57	3.76	8.10	4.80
$63H_t$	--	6.20	7.89	18.6	6.74	1.39	4.18	7.10	3.75
63H	horz.	6.20	7.89	19.8	6.74	1.39	4.19	7.25	3.75
$64H_t$	--	6.05	7.70	15.0	5.37	1.36	4.23	6.40	3.55
64H	horz.	6.10	7.70	16.1	5.37	1.36	4.34	6.55	3.55
$65H_t$	--	8.00	10.20	23.5	4.44	1.80	3.59	10.2	7.54

ONE-DIMENSIONAL ANALYSIS --Continued

Run No.	Direct Trav.	Q cfs	V fps	T °C	C_t	$V/\sqrt{gD}$	$fx10^2$	$Rex10^{-5}$	$Jx10^2$
$66H_t$	--	6.93	8.82	18.5	4.44	1.55	3.94	7.90	4.60
67H	horz.	6.90	8.80	19.1	4.55	1.55	3.96	8.00	4.59
$68H_t$	--	5.95	7.58	21.6	4.40	1.34	4.17	7.40	3.47
68H	horz.	6.00	7.64	22.0	4.40	1.35	4.19	7.43	3.50
$69H_t$	--	7.90	10.05	18.7	1.98	1.77	3.31	9.10	6.15
70H	horz.	5.85	7.45	20.5	2.13	1.31	4.15	6.95	3.32
71H	horz.	5.90	7.52	21.5	2.09	1.32	4.01	7.30	3.40
$70H_t$	--	5.80	7.39	22.5	2.13	1.30	4.27	7.28	3.24
$72H_t$	--	6.73	8.58	21.4	1.80	1.51	4.03	8.30	4.40
72H	horz.	6.73	8.58	21.9	1.80	1.51	3.89	8.43	4.40
73H	vert.	6.75	8.48	23.3	2.09	1.49	4.12	8.60	4.30
74H	vert.	5.90	7.52	24.2	2.21	1.32	4.10	7.70	3.40
76H	vert.	6.60	8.40	21.2	0.919	1.48	4.05	8.15	4.25
77H	vert.	5.82	7.25	22.3	0.854	1.28	3.85	7.20	3.10
78H	horz.	6.63	8.45	21.8	0.758	1.49	3.97	8.15	4.27
79H	horz.	6.63	8.45	22.3	0.748	1.49	4.33	8.40	4.27
80H	horz.	5.85	7.45	25.3	0.870	1.31	3.87	7.90	3.32
81H	horz.	5.85	7.45	25.8	0.872	1.31	3.71	8.00	2.02
$82H_t$	--	7.63	9.72	17.0	--	1.71	4.56	8.40	5.60
83H	vert.	7.70	9.80	20.7	--	1.73	4.38	9.25	5.80
84H	horz.	6.60	8.40	21.3	--	1.48	3.92	8.20	4.20
85H	horz.	5.80	7.39	22.5	--	1.30	3.50	7.35	3.24
86H	horz.	5.70	7.23	26.2	--	1.28	4.18	7.65	3.15
87H	horz.	6.60	8.21	27.0	--	1.45	4.11	9.00	4.09
88H	horz.	6.70	8.40	28.5	--	1.48	4.06	9.50	4.20
89H	horz.	3.53	4.45	27.0	--	0.78	4.22	4.85	1.18
90H	horz.	4.78	6.00	27.1	--	1.06	3.82	6.60	2.15
91H	horz.	1.63	2.08	26.4	--	0.37	4.46	2.27	0.262
1S	--	1.87	2.36	16.0	--	0.42	1.76	2.00	0.643
2S	--	5.83	7.30	18.0	--	1.28	1.28	6.50	1.60
3S	--	4.78	6.00	18.5	--	1.06	1.14	5.35	0.75
4S	--	3.56	4.52	18.8	--	0.80	1.50	4.15	0.51
5S	--	6.62	8.30	18.1	--	1.46	1.35	7.40	1.44
6S	--	7.32	9.17	18.9	--	1.61	1.24	8.30	1.58
7S	vert.	7.20	9.17	21.7	0.261	1.61	1.26	8.85	1.64
8S	vert.	6.60	8.40	22.7	0.195	1.48	1.24	8.30	1.36
9S	vert.	5.80	7.39	23.5	0.125	1.30	1.31	7.50	1.12

ONE-DIMENSIONAL ANALYSIS --Continued

Run No.	Direct. Trav.	Q cfs	V fps	T °C	C_t	$V/\sqrt{gD}$	$fx10^2$	$Rex10^{-5}$	$Jx10^2$
10S	horz.	7.50	9.55	24.5	0.332	1.68	1.13	9.90	1.60
$10S_t$	--	7.42	9.44	25.0	0.332	1.66	1.11	9.90	1.54
11S	horz.	6.60	8.40	21.7	0.175	1.48	1.22	8.10	1.34
12S	horz.	5.78	7.37	24.2	0.151	1.30	1.35	7.60	1.14
$12S_t$	--	5.80	7.38	24.4	0.151	1.30	1.33	7.60	1.14
$13S_t$	--	8.75	11.1	23.5	0.386	1.96	1.11	11.0	2.12
14S δ	horz.	4.80	6.11	20.8	0.393	1.08	1.51	5.75	0.88
$14S_t$ δ	--	4.80	6.11	22.2	0.393	1.08	1.37	5.95	0.80
15S δ	vert.	4.85	6.18	23.8	0.374	1.09	1.36	6.30	0.82
$15S_t$ δ	--	4.90	6.23	24.5	0.374	1.10	1.39	6.45	0.84
16S	vert.	4.86	6.18	25.7	0.166	1.09	1.28	6.60	0.76
$16S_t$	--	4.86	6.18	26.0	0.166	1.09	1.31	6.70	0.78
17S	vert.	3.40	4.33	20.5	0.081	0.76	1.43	3.90	0.426
$17S_t$	--	3.35	4.26	20.8	0.081	0.75	1.56	3.90	0.44
18S δ	vert.	2.20	2.80	21.4	0.040	0.49	1.48	2.70	0.18
19S	vert	4.80	6.11	23.0	0.010	1.08	1.31	6.20	0.76
$19S_t$	--	4.81	6.12	23.2	0.010	1.08	1.30	6.20	0.76
20S δ	vert.	5.83	7.42	20.7	0.360	1.30	1.24	7.00	1.06
$20S_t$ δ	--	5.80	7.38	21.5	0.360	1.30	1.23	7.05	1.04
21S	vert.	6.62	8.42	22.2	0.374	1.48	1.27	9.30	1.40
$21S_t$	--	6.60	8.40	22.7	0.374	1.48	1.28	9.30	1.40
22S	vert.	7.45	9.47	18.8	0.307	1.66	1.19	8.60	1.66
$22S_t$	--	7.50	9.55	19.2	0.307	1.68	1.21	8.70	--
23S	horz.	7.80	9.92	22.5	0.312	1.75	1.15	7.80	1.76
$23S_t$	--	7.80	9.92	22.7	0.312	1.75	1.14	7.80	1.74
24S	horz.	6.62	8.42	23.8	0.293	1.48	1.33	8.55	1.46
$24S_t$	--	6.64	8.45	24.0	0.293	1.49	1.32	8.70	1.46
25S	horz.	5.80	7.38	19.7	0.235	1.30	1.25	6.70	1.06
$25S_t$	--	5.60	7.13	20.7	0.235	1.26	1.31	6.70	1.04
$26S_t$	--	8.60	10.95	21.7	0.323	1.93	1.13	10.00	2.10
$27S_t$	--	8.70	11.10	23.5	0.720	1.96	1.13	11.0	2.16
28S	horz.	7.65	9.74	22.2	0.778	1.72	1.18	9.50	1.74
$28S_t$	--	7.62	9.70	22.9	0.778	1.71	1.25	9.60	1.74
29S	horz.	6.65	8.46	24.9	0.684	1.49	1.33	8.85	1.48
$29S_t$	--	6.75	8.60	25.2	0.684	1.52	1.26	9.15	1.44
30S δ	horz.	5.82	7.41	26.4	0.609	1.31	1.22	8.05	1.04
$30S_t$ δ	--	5.70	7.26	26.7	0.609	1.28	1.27	7.90	1.04
31S δ	vert.	5.80	7.38	22.0	0.613	1.30	1.23	7.20	1.04
$31S_t$ δ	--	5.65	7.20	23.0	0.613	1.27	1.27	7.25	1.02

ONE-DIMENSIONAL ANALYSIS --Continued

Run No.	Direct. Trav.	Q cfs	V fps	T °C	C_t	$V/\sqrt{gD}$	$fx10^2$	$Rex10^{-5}$	$Jx10^2$
32S	vert.	6.70	8.53	23.7	0.624	1.50	1.31	8.60	1.48
$32S_t$	--	6.70	8.53	24.4	0.624	1.50	1.31	8.80	1.48
33S	vert.	7.50	9.55	21.7	0.731	1.68	1.33	9.20	1.88
$33S_t$	--	7.63	9.72	22.7	0.731	1.71	1.17	9.60	1.72
34S δ	vert.	5.83	7.43	20.0	1.17	1.31	1.40	6.90	1.20
35S δ	--	5.80	7.39	21.4	1.17	1.30	1.37	7.05	1.16
36S	vert.	6.60	8.41	22.2	1.16	1.48	1.34	8.19	1.46
$36S_t$	--	6.65	8.47	23.2	1.16	1.49	1.33	8.50	1.48
37S	vert.	7.60	9.68	20.5	1.19	1.70	1.33	9.05	1.92
$37S_t$	--	7.62	9.70	21.5	1.19	1.71	1.19	9.30	1.74
38S	horz.	5.84	7.44	24.6	1.16	1.31	1.40	7.70	1.20
$38S_t$	--	5.87	7.47	26.0	1.16	1.31	1.34	8.00	1.16
39S	horz.	6.63	8.45	27.0	1.15	1.49	1.30	9.25	1.42
$39S_t$	--	6.63	8.45	27.6	1.15	1.49	1.28	9.35	1.42
40S	horz.	7.70	9.80	24.0	1.29	1.73	1.14	10.20	1.70
$40S_t$	--	7.70	9.80	24.5	1.29	1.73	1.14	10.30	1.70
$41S_t$	--	8.80	11.2	22.4	1.54	1.96	1.08	10.8	2.12
$41S_t$	--	8.78	11.18	23.5	1.54	1.96	1.10	11.2	2.14
42S	--	8.84	11.25	26.0	2.51	2.00	1.08	11.6	2.12
$42S_t$	--	8.84	11.25	26.8	2.51	2.00	1.05	11.7	2.06
43S	vert.	7.58	9.66	28.2	1.93	1.70	1.15	10.9	1.66
$43S_t$	--	7.60	9.67	26.7	1.93	1.70	1.17	10.7	1.70
44S δ	vert.	6.65	8.46	23.7	2.08	1.49	1.31	8.55	1.46
$44S_t$ δ	--	6.62	8.42	25.1	2.08	1.48	1.29	9.00	1.42
45S δ	vert.	5.85	7.45	22.0	2.35	1.31	1.56	7.25	1.3
$45S_t$ δ	--	5.80	7.38	23.1	2.35	1.30	1.61	7.35	1.36
46S δ	vert.	6.70	8.53	24.2	3.00	1.50	1.38	8.75	1.56
$46S_t$ δ	--	6.70	8.53	23.4	3.00	1.50	1.40	8.50	1.58
47S	vert.	7.60	9.67	22.2	3.01	1.70	1.17	9.40	1.70
$47S_t$	--	7.60	9.67	23.4	3.01	1.70	1.20	9.60	1.62
48S δ	horz.	6.65	8.46	21.0	3.19	1.49	1.42	8.00	1.58
$48S_t$ δ	horz.	6.65	8.46	22.0	3.19	1.49	1.40	8.20	1.56
49S δ	horz.	5.80	7.38	20.7	2.65	1.30	1.75	6.95	1.48
49S δ	--	5.80	7.38	21.7	2.65	1.30	1.77	7.10	1.50
50S	horz.	7.70	9.80	25.0	3.04	1.73	1.17	10.3	1.74
$50S_t$	--	7.70	9.80	24.5	3.04	1.73	1.18	10.1	1.76

ONE-DIMENSIONAL ANALYSIS --Continued

Run No.	Direct. Trav.	Q cfs	V fps	T °C	C_t	$V/\sqrt{gD}$	$fx10^2$	$Rex10^{-5}$	$Jx10^2$
1C	--	4.32	5.30	21.6	--	0.93	1.21	51.0	5.20
2C	--	3.54	4.45	22.1	--	0.78	1.25	4.30	3.80
3C	--	4.78	5.98	23.3	--	1.05	1.12	6.05	6.24
4C	--	5.80	7.23	25.3	--	1.28	1.11	7.70	9.00
5C	--	1.87	2.38	27.1	--	0.42	1.14	2.63	1.00
6C	vert.	3.55	4.52	31.9	0.183	0.80	1.27	5.50	4.04
7C	vert.	4.80	6.12	30.7	0.334	1.08	1.07	7.30	6.02
8C	vert.	5.75	7.20	25.7	0.448	1.27	1.055	7.70	8.50
9C[δ]	vert.	1.63	2.08	26.9	0.462	0.37	0.125	2.27	0.84
10C	horz.	3.55	4.52	24.7	0.260	0.80	1.21	4.67	3.84
11C	horz.	4.70	5.98	26.1	0.320	1.05	1.11	6.42	6.18
12C	horz.	5.80	7.38	28.5	0.340	1.30	0.99	8.15	8.40
13C	horz.	3.58	4.56	31.5	0.385	0.80	1.22	5.98	3.96
14C	horz.	4.80	6.11	30.4	0.720	1.08	1.04	8.25	6.00
15C	horz.	5.78	7.37	29.2	1.06	1.30	1.03	8.40	8.58
16C	vert.	3.58	4.56	29.6	0.455	0.80	1.24	5.50	4.02
17C	vert.	4.80	6.11	30.6	0.688	1.08	1.02	8.25	5.92
18C	vert.	5.80	7.25	32.3	0.881	1.28	0.99	8.75	8.10
19C	vert.	6.30	8.02	28.3	0.868	1.42	1.02	9.15	10.24
20C	vert.	6.30	8.02	32.7	1.20	1.42	1.10	10.1	10.96
21C	vert.	4.78	6.09	28.6	1.09	1.08	1.10	6.95	6.32
22C	vert.	5.78	7.37	30.2	1.32	1.30	1.02	8.75	8.64
23C	vert.	3.55	4.43	27.0	0.845	1.28	1.24	4.60	3.80
24C	horz.	5.80	7.38	27.8	1.46	1.30	1.12	8.25	8.74
25C	horz.	4.78	6.09	28.9	1.16	1.08	1.08	7.00	6.24
26C	horz.	3.50	4.45	31.0	0.610	1.27	1.23	5.30	3.80
27C[δ]	horz.	3.43	4.36	29.1	1.00	0.77	1.20	4.85	3.56
28C	horz.	4.76	6.06	29.8	1.82	1.07	1.09	8.07	6.20
29C	horz.	5.78	7.37	31.3	2.47	1.30	1.05	8.80	8.84
30C[δ]	vert.	3.53	4.50	30.5	0.972	0.80	1.15	5.35	3.76
31C	vert.	4.80	6.05	31.6	1.56	1.07	1.09	7.30	6.20
32C	vert.	5.70	7.25	32.5	2.17	1.28	1.08	8.90	8.84
33C	vert.	6.28	7.85	28.4	2.47	1.38	1.20	8.90	11.50
34C	vert.	6.32	8.04	31.6	3.86	1.42	1.16	9.75	11.70
35C[δ]	vert.	3.60	4.56	29.7	3.09	0.80	1.17	5.27	3.76
36C	vert.	4.70	6.03	30.6	2.97	1.07	1.06	7.20	6.04
37C	vert.	5.80	7.27	30.8	3.69	1.28	1.16	8.70	9.54
38C[δ]	horz.	3.54	4.51	28.3	2.30	0.80	1.17	5.20	3.90
39C	horz.	4.78	6.08	29.4	3.10	1.07	1.11	6.90	6.20
40C	horz.	5.75	7.32	30.3	4.07	1.29	1.21	8.70	10.10

ONE-DIMENSIONAL ANALYSIS --Continued

Run No.	Direct. Trav.	Q cfs	V fps	T ^{o}C	C_t	$V/\sqrt{gD}$	$fx10^{2}$	$Rex10^{-5}$	$Jx10^{2}$
41Cδ	horz.	4.80	6.10	24.8	5.05	1.08	1.12	6.92	---
42C	horz.	5.75	7.32	27.0	5.55	1.29	1.19	8.00	9.90
43C	vert.	5.78	7.37	27.1	4.72	1.30	1.17	8.05	9.88
44Cδ	vert.	4.83	6.15	28.7	4.53	1.08	1.07	7.05	6.30
45C	vert.	5.95	7.58	26.5	6.87	1.34	1.08	8.25	9.68
46Cδ	vert.	4.82	6.06	28.7	8.72	1.07	1.10	6.85	6.30
47Cδ	vert.	4.75	5.95	32.5	10.9	1.05	1.10	7.30	6.06
48C	vert.	6.00	7.50	34.0	8,16	1.32	1.13	9.43	9.92